INVESTIGATING THE ROLE OF THE APICOPLAST IN *PLASMODIUM FALCIPARUM* GAMETOCYTE STAGES

Jessica D. Wiley

Dissertation submitted to the faculty of the Virginia Polytechnic Institute and State University in partial fulfillment of the requirements for the degree of

Doctor of Philosophy
In
Biochemistry

Maria B. Cassera
Carla V. Finkielstein
Michael W. Klemba
Glenda E. Gillaspy
Jinsong Zhu

April 25, 2014
Blacksburg, VA

Keywords: *Plasmodium falciparum*, malaria, gametocytogenesis, apicoplast, drug discovery, natural products

INVESTIGATING THE ROLE OF THE APICOPLAST IN *PLASMODIUM FALCIPARUM* GAMETOCYTE STAGES

Jessica D. Wiley

ABSTRACT

Malaria continues to be a global health burden that affects millions of people worldwide each year. Increasing demand for malaria control and eradication has led research to focus on sexual development of the malaria parasite. Sexual development is initiated when pre-destined intraerythrocytic ring stage parasites leave asexual reproduction and develop into gametocytes. A mosquito vector will ingest mature gametocytes during a blood meal. Sexual reproduction will occur in the midgut, leading to the production of sporozoites that will migrate to the salivary gland. The sporozoites will be injected to another human host during the next blood meal consequently, transmitting malaria. Due to decreased drug susceptibility of mature gametocytes, more investigation of the biology and metabolic requirements of malaria parasites during gametocytogenesis, as well as during the mosquito stages, are urgently needed to reveal novel targets for development of transmission-blocking agents. Furthermore, increasing drug resistance of the parasites to current antimalarials, including slowed clearance rates to artemisinin, requires the discovery of innovative drugs against asexual intraerythrocytic stages with novel mechanisms of action. Here, we have investigated the role of the apicoplast during *Plasmodium falciparum* gametocytogenesis. In addition, we describe drug-screening studies that have elucidated a novel mode of action of one compound from the Malaria Box, as well as identified new natural product compounds that may be serve as starting molecules for antimalarial development.

ACKNOWLEDGEMENTS

Above all, I give God all of the glory for this achievement. I am very thankful to my loving husband, Michael Wiley, who has encouraged and supported me throughout this whole process. I am very blessed to have met you during this time and look forward to a lifetime together. I thank my parents, James and Carole Bowman, for raising me to be the woman I am today. You have loved me, supported me, encouraged me, and prayed for me in whatever avenue life has taken. Thanks to my grandparents, Bruce and Julia Smyser for loving me to no end. To my sister, Jennifer Bowman, thanks for encouraging me and being a great sister. I am glad that we will finally live close to each other. To my brother Matthew and his wife Karen, I am so glad to have you in my life. Thank you for the encouragement and prayer during this time. To Ana Lisa and Melissa, thank you ladies for all of the fun times and helping me get through this degree. I wish you all of the best in your endeavors and Mike and I hope to make it to Costa Rica soon. To Kiko and Isabel, thank you for your kindness, advice, AND your amazing culinary creations. Mike and I are very grateful to have you as friends. To Sanjay and Nicola, thank you for your encouragement and letting me live with you guys these past few months. You are great friends. To the Wileys, thank you so much for all of your prayer and support. I am very blessed to be a part of your family. Thank you to all of my other friends for so many good times and all of your support during this time. Thank you to Dr. Hemric for sparking my interest in biochemistry and helping me to pursue graduate school. Thank you to Christian for being a good lab mate to work with and I wish you good luck in your next chapter of life. Thanks to Fernando for suggestions and helping me with experiments and analysis. To my committee members, Dr. Finkielstein, Dr. Klemba, Dr. Gillaspy, and Dr. Zhu, I am very grateful for your instruction and guidance through my project. Thank you for giving of your time to listen and teach me throughout this time. Lastly, thank you to Dr. Maria Belen Cassera for mentoring me. It has been a pleasure working for you and with you and thank you for training me, and giving me the tools to have a successful career. I have learned so much in my time here and I will continue to be your “mini-me.” Thank you for giving of your time and resources to guide me, and our project, and helping me mature as a scientist.

This dissertation is dedicated to my loving parents James and Carole Bowman and to my loving husband Michael Wiley. Thanks for always being a blessing in my life and always being there for me.

TABLE OF CONTENTS

LIST OF FIGURES

LIST OF TABLES

ATTRIBUTION

The dissertation research discussed herein would not have been possible without the help of several individuals. Their names and contributions to each chapter are listed below. Each published chapter has the original work cited and is used with permission of the publishers. All work on this dissertation, unless noted, is original, and completed by Jessica D. Wiley.

Chapter 1: Literature review: *Plasmodium falciparum* Gametocytes: Metabolic Insights to Identify Potential Drug Targets.

1. **Christian D. Laourdakis, M.S.** (Fralin Life Science Institute, Department of Biochemistry and Virginia Tech Center for Drug Discovery, Virginia Polytechnic Institute and State University): Contributed to writing.
2. **Emilio F. Merino, Ph.D.** (Fralin Life Science Institute, Department of Biochemistry and Virginia Tech Center for Drug Discovery, Virginia Polytechnic Institute and State University): Contributed to writing and reviewing the manuscript.
3. **Maria B. Cassera, Ph.D.** (Fralin Life Science Institute, Department of Biochemistry and Virginia Tech Center for Drug Discovery, Virginia Polytechnic Institute and State University): Conceived the focus of this review, obtained funding, and contributed write the manuscript.

Chapter 2: Isoprenoid Precursor Biosynthesis is the Essential Role of the Apicoplast During Gametocytogenesis in *Plasmodium falciparum*.

1. **Emilio F. Merino, Ph.D.** (Fralin Life Science Institute, Department of Biochemistry and Virginia Tech Center for Drug Discovery, Virginia Polytechnic Institute and State University): Conceived the original idea, performed qPCR and LC-MS/MS experiments and analysis, conceived and designed the experiments, and helped write the manuscript.
2. **Priscilla Krai, Ph.D.** (Department of Biochemistry and Virginia Tech Center for Drug Discovery, Virginia Polytechnic Institute and State University): Contributed to experimental design, provided meaningful discussion, and reviewed manuscript.
3. **Kyle J. McLean** (Johns Hopkins Malaria Research Institute (JHMRI), Johns Hopkins Bloomberg School of Public Medicine): Contributed to experimental design, guided

mosquito infection experiments, provided meaningful interpretation of results, and reviewed the manuscript.

4. **Abhai K. Tripathi** (Johns Hopkins Malaria Research Institute (JHMRI), Gametocyte Core Facility, Johns Hopkins Bloomberg School of Public Medicine): Raised infectious gametocytes for mosquito infections, and reviewed the manuscript.
5. **Joel Vega-Rodríguez, Ph.D.** (Johns Hopkins Malaria Research Institute (JHMRI), Johns Hopkins Bloomberg School of Public Medicine): Contributed to experimental design, performed salivary gland dissection for sporozoites extraction, provided meaningful interpretation of results, and reviewed the manuscript.
6. **Michael Klemba, Ph.D.** (Department of Biochemistry and Virginia Tech Center for Drug Discovery, Virginia Polytechnic Institute and State University): Contributed reagents, provided meaningful discussions, and reviewed the manuscript.
7. **Marcelo Jacobs-Lorena, Ph.D.** (Johns Hopkins Malaria Research Institute (JHMRI), Johns Hopkins Bloomberg School of Public Medicine): Provided funding and contributed to experimental designed for mosquito infection, and reviewed the manuscript.
8. **Maria B. Cassera, Ph.D.** (Fralin Life Science Institute, Department of Biochemistry and Virginia Tech Center for Drug Discovery, Virginia Polytechnic Institute and State University): Conceived the original idea, obtained funding, conceived, designed and performed experiments, and helped writing the manuscript.

Chapter 3: Antiapicoplast and Gametocytocidal Screening to Identify the Mechanisms of Action of Compounds within the Malaria Box

1. **Emilio F. Merino, Ph.D.** (Fralin Life Science Institute, Department of Biochemistry and Virginia Tech Center for Drug Discovery, Virginia Polytechnic Institute and State University): Conceived the original idea, contributed to data analysis, figure design and reviewed the manuscript.
2. **Carrie F. Brooks, B.S.** (Department of Cellular Biology and Center for Tropical and Emerging Global Diseases, University of Georgia): Performed drug screening experiments with *Toxoplasma gondii* and reviewed the manuscript.

3. **Boris Striepen, Ph.D.** (Department of Cellular Biology and Center for Tropical and Emerging Global Diseases, University of Georgia): Provided funding and contributed to experimental designed for drug screening experiments in *Toxoplasma gondii* and reviewed the manuscript.
4. **Paul Carlier, Ph.D.** (Department of Chemistry and Virginia Tech Center for Drug Discovery, Virginia Polytechnic Institute and State University): Contributed structure-activity analysis, discussion, and helped writing the manuscript.
5. **Maria B. Cassera, Ph.D.** (Fralin Life Science Institute, Department of Biochemistry and Virginia Tech Center for Drug Discovery, Virginia Polytechnic Institute and State University): Conceived the original idea, obtained funding, conceived, designed and performed experiments, and helped write the manuscript.

CHAPTER 1 LITERATURE REVIEW: *Plasmodium falciparum* GAMETOCYTES: METABOLIC INSIGHTS TO IDENTIFY POTENTIAL DRUG TARGETS

J. D. Wiley, C. D. Laourdakis, E. F. Merino, and M. B. Cassera

Manuscript Unpublished

ABSTRACT

Most of the *Plasmodium falciparum* malaria research has been focused mainly in the asexual intraerythrocytic stages while the sexual intraerythrocytic stages, gametocytes, have been neglected. In the last several years, laboratories around the world have improved the *in vitro* culture of *P. falciparum* gametocytes allowing medium-throughput drug screening as well as studies of its particular biology. Today, with increasing drug resistance development to almost all current antimalarials, there is clear need to expand our knowledge of the gametocyte stages to develop more effective drugs that will cure malaria and reduce its transmission. While finding the "magic bullet" may still be a dream, revealing the nutritional needs and key cellular process of the *P. falciparum* gametocytogenesis will aid in the identification of common targets in asexual and sexual intraerythrocytic stages for drug development.

Introduction

Malaria remains a significant infectious disease in tropical and subtropical regions causing millions of clinical cases and more than 800,000 deaths per year, with most of the death occurring in children under the age of five (*1*). Malaria is caused by apicomplexan parasites of the genus *Plasmodium* and *P. falciparum* is the deadliest of the species that infect humans. *Plasmodium* species possess a complex life cycle that involves the human host and its vector, the *Anopheles* mosquitoes. During the blood infection stage, *Plasmodium* is an intracellular parasite with a complex intraerythrocytic life cycle. The asexual intraerythrocytic cycle of *P. falciparum* lasts 48 hrs, during which the parasite progresses through four morphologically different stages: ring, trophozoite, and schizont stages, ending with the rupture of the erythrocyte and release of the new merozoites, which reinvade new erythrocytes. Transmission of the malaria parasite requires the development of different parasite forms, called male and female gametocytes, which are ingested by female mosquitoes during a blood meal and undergo sexual reproduction in the mosquito's midgut. Gametocytes develop during intraerythrocytic stages when an asexual schizont is committed to sexual reproduction triggered by factors that still remain unclear. *P. falciparum* gametocytes take between 10 and 14 days to mature and progress through five morphologically distinct forms (stages I to V), which are different from other *Plasmodium* species (*2-4*). Recently, the gene *Plasmodium falciparum* Gametocyte Development 1 (*Pfgdv1*) has been identified as a key gene for early sexual differentiation in the malaria parasite (*5*); however, what controls or triggers the expression of *Pfgdv1* remains unexplored. Other factors influencing the commitment to gametocyte development have been reviewed elsewhere (*6*). Transcriptomics and proteomics analyses indicated that several genes are specific for sexual differentiation (*7, 8*); however, almost no metabolomics data have been reported.

Current malaria drug development requires a comprehensive study of a candidate's effect on multiple parasite stages (i.e. asexual and sexual intraerythrocytic, liver and mosquito stages) to develop resilient treatments (*9*). Artemisinin-based combination therapies (ACTs) are currently the preferred first-line antimalarial against asexual *P. falciparum* infection but remain inactive against mature gametocytes (*10*). Clinical trials demonstrated that ACTs help reduce gametocyte load that while this does not lead to malaria elimination, it does lessen the transmissibility of parasites (*11, 12*). A recent study by Peatey and colleagues investigated the activity of 44 compounds (comprised of currently used and experimental anti-malarial drugs)

against gametocytes (*10*). Only a few compounds showed activity against this parasite's stage probably because drugs are not transported by the gametocytes; however, this possibility has not been investigated. The inactivity of these compounds during gametocytogenesis may also result from translational repression mediated by DOZI where mRNA is stored in messenger ribonucleoprotein particles (mRNPs) and translated only when needed (*13*). If the message is not being translated into protein, the drug target is not around to be inhibited. DOZI-mediated translational repression will be discussed in more detail herein as a potential drug target. Other antimalarial molecules demonstrated encouraging activity against *P. falciparum* gametocytes and has been reviewed elsewhere (*14*). Recently, two reviews on *in vitro* screening for gametocytocidal compounds and strategies for the development of transmission blocking therapies have summarized the current research in transmission blocking strategies (*15, 16*). This review aims to debate the prospect of validating metabolic drug targets in the sexual stages of *P. falciparum* gametocytes, to identify new potential drug targets.

Gametocytes must be prepared for drastic environmental alterations in the mosquito vector

While gametocytes inflict no clinical symptoms in humans, they cause forward transmission (*17, 18*). A female *Anopheline* mosquito ingests gametocytes during a blood meal and sexual reproduction occurs in the midgut. In the blood meal, gametocytes experience a dramatic change in environment and must adapt adequately (*4, 19, 20*). A decrease in temperature from 37˚C to ambient temperature and the presence of xanthurenic acid triggers gametogenesis, in which both male (microgametocyte) and female (macrogametocyte) forms egress from infected red blood cells (RBCs) (*20-27*). The mature microgametocyte rapidly replicates its genome three times forming eight copies of the genome for exflagellation, a process in which each genome is linked to an axoneme (flagella-like appendage) and releasing the microgametes to find a macrogamete (*20, 28, 29*). The structural proteins needed for axoneme formation and the multiple genome copies must be pre-synthesized prior to exflagellation because of the speed required in the fertilization process (*20, 29*).

Macrogametes, which differ greatly from microgametes, contain well-developed endoplasmic reticulum, mitochondrion, and apicoplast in preparation for rapid development as a zygote (*20, 29*). During macrogametocyte development, mitochondrial cristate are increased

significantly in preparation for increased metabolic activity and protein synthesis (*20, 26*). The macrogamete utilizes numerous osmiophilic bodies within the female parasite that apparently disrupt the cell membrane of the erythrocyte (*20, 30, 31*). Once the macrogamete escapes the RBC, it translates stored mRNA (DOZI-mediated translational repression) that encodes essential proteins for zygote development and mosquito midgut invasion, such as *p25* and *p28* (*13, 32*).

Gametogenesis occurs within 12 minutes post blood meal in the mosquito. A motile microgamete, fueled through glycolysis, will fertilize a macrogamete and the formation of the zygote is usually complete within 30 minutes (*19, 20, 28, 30, 31*). The formed ookinete secretes a chitinase that allows the parasite to penetrate the peritrophic membrane surrounding the blood meal (*26, 33*). The ookinete will then migrate through the midgut epithelium to the basal lamina, where it will develop into an oocyst (*26, 34*). The oocyst generates sporozoites that travel to the salivary glands of the mosquito and will be injected into another human host upon the mosquito's next blood meal. Because gametocytes are metabolically active, identification of their essential metabolism involved in maintenance and differentiation during both gametocytogenesis and gametogenesis could reveal potential targets for drug development.

The apicoplast: a source of parasite-specific metabolic targets

Drugs targeting the apicoplast have been reviewed elsewhere and here we briefly describe them (*35, 36*). Most members of the phylum *Apicomplexan* contain a vestigial plastid called apicoplast. This peculiar organelle in *Plasmodium spp.* has been demonstrated to be essential to the parasites. The apicoplast contains its own 35 kb prokaryotic-like genome, yet is not self-sufficient, as it requires many proteins that are nuclear encoded and then targeted to the organelle. It is predicted that approximately 540 gene products in the *P. falciparum* nuclear genome are targeted to the apicoplast, representing about 10% of the total parasite predicted genes (*37*). Of the genes encoding anticipated apicoplast-targeted proteins, around 16% have unknown function and the majority are involved in housekeeping functions (~55%) (*37*).

The apicoplast cannot be generated *de novo* and must be maternally inherited (*2, 38*). Apicoplast-DNA replication, transcription, and translation are potential drug targets since inhibition of these functions prevent *de novo* generation of this organelle. Three drugs, ciprofloxacin (DNA replication), rifampicin (transcription), and doxycycline (translation), inhibit of *P. falciparum* growth by preventing elongation and segregation of the apicoplast to the newly

formed merozoites (*35*). Ciprofloxacin is of the fluoroquinolone drug class, which targets DNA replication in bacteria by inhibiting topoisomerases II and IV (*39, 40*). In *Plasmodium*, ciprofloxacin inhibits apicoplast-DNA replication by targeting the apicoplast gyrase (*35, 41, 42*). Rifampicin is an inhibitor of bacterial RNA polymerase (*43*) therefore blocking transcription. Due to the prokaryotic-like structure of the apicoplast, it is thought to have a similar mode of action in *P. falciparum* (*35*). A combination therapy of rifampicin, cotrimoxazole, and isoniazid exhibited a good safety profile and is in clinical trials (*35, 44, 45*). Apicoplast translation is inhibited by doxycycline, which is a tetracycline that binds to the 30S ribosomal subunit and blocks the attachment of charged aminoacyl-tRNA (*35*). Doxycycline specifically disturbs expression of apicoplast genes and consequently prevents apicoplast segregation for progeny (*46*). Clindamycin and chloramphenicol also inhibit apicoplast translation (*47*). Microscopic imaging demonstrated that compounds targeting the apicoplast-DNA replication, transcription, and translation resulted in loss of apicoplast division and segregation (*46, 48*), and a "delayed death" phenotype is observed in the treated parasites which is demonstrated by at least a 10-fold decrease in the half maximal inhibitory concentration (IC_{50}) values after 96 h of treatment versus 48 h of treatment (*49*). In contrast to asexual intraerythrocytic parasites, the function of the apicoplast during gametocytogenesis is poorly understood; however, it is known that it does not elongate or divide staying small and rounded during gametocytogenesis (*38*).

Azithromycin (AZM) is a macrolide compound that has been used for bacterial infections and targets the apicoplast as demonstrated by its "delayed death" phenotype and the fact that progeny parasites cannot develop due to abnormal apicoplast development (*48, 50, 51*). AZM is well tolerated in patients, including children and pregnant women, and has been used broadly for bacterial infections (*50, 52-55*). AZM as well as doxycycline and tetracycline had no effect on *P. falciparum* gametocytes (*10, 56*). The rodent malaria *P. berghei* was used to investigate AZMs effect on mosquito stages (*50*). While gametocyte development is different in *P. falciparum* gametocytes than in *P. berghei*, AZM is proposed to have a similar effect on parasite's development in the mosquito. AZM had no effect on male gametocyte exflagellation, but one dose of AZM (400 mg/kg) in mice was shown to subdue parasite development in the mosquito vector after blood feeding (50% reduction of ookinetes, 45% reduction in oocyst development in the midgut, 79% reduction of sporozoites in the midgut, and 50% reduction of sporozoites in the salivary glands) (*50*). Replication of the apicoplast during blood stages in AZM-treated mice was

not impaired after six days post-treatment, even though the dosage used in that study was over 13 times higher than the recommended dose in humans (30 mg/kg) (*57, 58*). Therefore, mosquito stages should be investigated when working with drugs targeting the apicoplast.

The apicoplast became a promising drug target in asexual intraerythrocytic stages because it houses biochemical pathways that are either absent from or are different from those found in humans such as fatty acids, isoprenoid precursors, iron-sulfur clusters assembly, and is involved in part of the heme synthesis pathway (*35, 37*). It has been demonstrated recently that isoprenoid precursor synthesis is the sole function of the apicoplast during asexual intraerythrocytic parasites (*59*). The methylerythritol phosphate (MEP) pathway provides isopentenyl diphosphate (IPP) and dimethylallyl diphosphate (DMAPP) in the malaria parasite which are the building blocks of isoprenoids (*60, 61*). Isoprenoids are a wide variety of molecules with diverse biological functions and in the parasite, only the synthesis of a few isoprenoid products had been confirmed to be present, such as synthesis of ubiquinones and menaquinone (*62-64*), carotenoids, dolichols (*61, 65, 66*), vitamin E (*67*), and prenylated proteins (*68-75*).

Fosmidomycin (FOS) is a specific inhibitor of the MEP pathway and is effective against several *P. falciparum* strains (*60, 76, 77*). FOS inhibits 1-deoxyxylulose-5-phosphate reductoisomerase (DXR), a key enzyme in the MEP pathway, has shown promising potential as an antimalarial when used in combination with other drugs (*60, 76, 78*) and had been already used in human clinical trials for the treatment of uncomplicated malaria (*76, 77, 79*). However, significant recrudescence occurred in some treated patients which may lead to parasite resistance therefore preventing FOS from being considered as a monotherapy (*76, 77, 80, 81*). One clinical trial revealed that patients treated with FOS showed increased gametocytemia by the end of the study compared with the same patients on the initial treatment day (*76*) indicating that FOS may not be active against gametocytes stages and also it may stimulate gametocytogenesis. In a recent study by Peatey and colleagues, FOS showed no activity against mature gametocytes (*10*) and at this moment it cannot be ruled out that FOS is not being transported leading to an "apparent resistance" in gametocytes similar to *Toxoplasma gondii* in which DXR is essential to its survival, but the "apparent resistance" to FOS is due to a lack of uptake in the parasite (*82*). In addition, it has been shown that FOS treatment in asexual intraerythrocytic stages of *P. falciparum* inhibited the apicoplast elongation similar to antibiotics targeting this organelle, but

do not display "delay death" phenotype (*82*). One potential mechanism of by which FOS could prevent the apicoplast development is through inhibition of the isoprenoid modification of the tRNA on the heterocyclic ring of purine bases which is essential for binding to the mRNA-ribosome complex and ensures translational integrity (*37, 83*). Four tRNAs in *Plasmodium* are predicted to be isoprenylated in the apicoplast (*37*), however, no studies have been reported demonstrating tRNA isoprenylation. While protein synthesis in the apicoplast has been demonstrated in asexual stage parasites (*84*), its activity during gametocytogenesis has yet to be established.

We have recently demonstrated that the apicoplast is required during gametocytogenesis by generating gametocytes lacking the apicoplast (manuscript in preparation). Gametocytes lacking the apicoplast were generated by treating asexual stages with doxycycline and IPP supplementation similar to the method reported by Yeh and DeRisi (*85*) before inducing gametocytogenesis. Our study revealed that IPP supplementation is required during the entire gametocytogenesis through stage I to V and that morphologically normal stage V gametocytes were formed in the absence of the apicoplast. Consequently, while the apicoplast does not elongate and divide during gametocytogenesis, as in asexual intraerythrocytic stages, synthesis of isoprenoid precursors IPP and DMAPP are the main function of this organelle during gametocytogenesis. Therefore, we propose that drugs targeting the apicoplast would prevent gametocytogenesis hence, blocking transmission. However, the role of the isoprenoid biosynthesis in the mosquito stages remains to be studied.

As mentioned above, several isoprenoid end products have been detected in *P. falciparum* and their biosynthesis may also represent potential drug targets. Despite the fact that isoprenoid products are synthesized outside the apicoplast, they will be discussed in this section since they are dependent on apicoplast precursors. Ubiquinones are synthesized in the mitochondria and play an important role on electron carriers (*68, 83*), therefore, its role as a drug target will be discussed in the next section.

Carotenoids have antioxidant properties and can regulate membrane fluidity (*68, 83*) however, their role in *P. falciparum* remains unknown. Increased carotenoid production was detected in parasites that were treated with chloroquine, which causes oxidative stress (OS), indicating that the main function of carotenoids may be as antioxidants in the parasites (*70, 83*). As asexual parasitemia increases, OS arises from erythrocyte rupture and various other sources,

such as the mitochondrial free heme and hydrogen peroxide (*86-88*). *Plasmodium* parasites compartmentalize their redox metabolism to adequately balance the redox flux throughout its lifecycle (*89*). Certain drugs such as usnic acid (*83, 90*), chloroquine and primaquine (*91*) can induce OS on the parasites, however, the redox metabolism in gametocyte stages has not been explored. Dolichols are important for the co- and post-translational modification of proteins in *Plasmodium*, such as *N*-linked glycosylation (*65, 83*), and are required for the coupling of glycosylphosphatidylinositol (GPI) anchors and carbohydrates in *P. falciparum* asexual intraerythrocytic parasites (*92*). The role of dolichols in gametocytes has not been yet addressed, however, because protein synthesis still occurs in this stage (*8, 93*), it is expected that dolichols may play an important role in post-translational modifications in gametocytes. Additionally, dolichols had been found as modification in proteins indicating that these isoprenoid products are involved in other processes beyond glycosylation but more research is needed to established the role of protein dolicholation in *P. falciparum* (*66*). Protein prenylation is another post-translational modification that involves the covalent attachment of farnesyl (C_{15}) or geranylgeranyl (C_{20}) moieties to cysteine residues *via* a thioether linkage and their respective isoprenoid diphosphate precursors performed by protein prenyl transferases (*94, 95*). Prenyl modification is relevant for several biological process such as membrane association and localization (*71, 72, 83*), signal-transduction pathways, regulation of DNA replication, cell cycle progression (*83, 96*), erythrocyte invasion (*83, 97*), vesicular trafficking *via* SNARE proteins (*83, 97*), GTPases (*68, 83*), and palmitoylation (*94, 95*). The isoprenylated cystine is part of a C-terminal CaaX box ("C" is cysteine, "a" is usually an aliphatic residue and "X" is usually Ser, Met, Cys, Ala, Gln or Leu) where the identity of this final amino acid determines if the protein becomes farnesylated or geranylgeranylated (*94, 95, 98, 99*). After prenylation, CaaX box processing involves in the proteolytic cleavage of the last three amino acids followed by the methylation of the free carboxyl group of the isoprenylated cysteine (*94, 100*). In isoprenylated proteins, this acylation is understood to encourage the interaction of the modified protein with cellular membranes so that a subsequent palmitoylation can occur in cysteine residues neighboring to the farnesylated or geranylgeranylated cysteine of the CaaX motif. Site-directed mutagenesis of the Cys residue from the CaaX box, consequently abolishing farneyslation or geranylgeranylation, results in the absence of palmitoylation (*94, 101, 102*). Post-prenylation-processing enzymes have been proposed as new targets in cancer (*100*) and it would be worth

investigating if the same mechanism occurs in *Plasmodium spp*. Taken together, it is possible several process during gametocytogenesis are dependent on prenylation and its inhibition would be effective in killing gametocytes as they have been shown to kill asexual parasites (*73, 74, 83, 103*). Further investigation into the role of isoprenoids during gametocytogenesis is needed.

Gametocyte transcriptomic studies indicated upregulation of genes for apicoplast type II fatty acid biosynthesis (*7*). Fatty acid biosynthesis had been demonstrated to be essential in liver stages but not during asexual intraerythrocytic stages (*104*). Type II fatty acid biosynthesis is markedly different from type I fatty acid biosynthesis that occurs in human cells and is a favorable drug target in *Plasmodium* (*35, 37, 38*). Membrane composition and transporters in asexual stage parasites facilitate the uptake of many solutes (*105, 106*); however, during gametocytogenesis the parasite undergoes drastic morphological changes which may include alterations in the transport of fatty acids explaining the upregulation of genes involved in this pathway, but these transport modifications still remain to be investigated.

The mitochondrion: an active organelle during gametocytogenesis

The mitochondrion is another attractive drug target in the malaria parasite. This organelle is in close association with the apicoplast, most likely for the exchange of metabolites (*37*). In asexual intraerythrocytic parasites, the mitochondrion is crescent-shaped in merozoites and branches during the trophozoite stage before segregation for schizogony (*107*). The mitochondrion is not well developed in asexual parasites, however, in gametocytes it showed increased cristae, which are needed for full mitochondrial function, as well as changes in its membrane potential and sensitivity to mitochondrial inhibitors (*26, 38, 108-111*). Female gametocytes show a marked increase in their cristate mitochondria from stage III which is also the point where drug sensitivity changes (*20, 112, 113*). In stage II gametocytes, the mitochondrion branches in a similar way as in the trophozoite stage but then forms a cluster around the apicoplast, more than the association observed in asexual parasites, and remains like this throughout gametocyte's development (*38*). Additional morphological changes in the mitochondrion occur as the gametocyte elongates during differentiation (*111*). These observations are consistent with increased mitochondrial metabolism in gametocytes (*114*). Moreover, measurement of mitochondrial activity using the oxidoreduction indicator alamarBlue became an low cost marker to evaluate gametocytocidal activity for drug screening (*115*).

P. falciparum and other *Plasmodium spp.* have a functional electron transport chain (ETC) (*26, 38, 111, 114*). The ETC is thought to serve as an electron sink for pyrimidine biosynthesis via dihyroorotate dehydrogenase (DHODase) (*26, 111, 114, 116*). The activity of DHODase and the respiratory mtETC complexes III and IV are on average 8-10 fold more active in gametocytes (*114*).

DHODase requires ubiquinone, an important electron carrier synthesized in the mitochondrion and localized to the inner mitochondrial membrane and serves as the junction of all the electron donations along the ETC (*62, 83, 88, 111, 114, 117*). Ubiquinone, also known as coenzyme Q, is an isoprenoid derivative and consists of two parts: a benzoquinone ring that participates in redox reaction and an isoprenoid tail for membrane association (*83, 88, 114*). The MEP pathway is the sole source of isoprene building blocks for ubiquinone synthesis and therefore indicates that though the apicoplast may not be replicating in gametocytes, isoprenoid precursor synthesis is required during gametocyte differentiation.

Electrons are donated by ubiquinone to complex III or cytochrome bc_1 complex to reduce cytochrome *c* (*83, 88, 114*). The ETC culminates in the net movement of protons from the mitochondrial matrix to the intermembrane space contributing to the proton gradient across the inner membrane, which maintains a negative membrane potential inside the intermembrane and a positive membrane potential outside the intermembrane in both asexual and sexual stages of the malaria parasites (*88, 114*). Asexual intraerythrocytic stages rely on cytosolic glycolysis for ATP production and do not employ the functional mitochondrial tricarboxylic acid (TCA) cycle (*26, 38, 88, 111, 114*). Transcriptomics, however, reveals that 15 of the 16 mitochondrial TCA cycle enzymes are upregulated in gametocytes (*38, 114*). A recent study indicates that both asexual and sexual blood stages employ a conventional TCA cycle to catabolize glucose and glutamine (*118*). The authors also observed an increased sensitivity of gametocytes to TCA-cycle inhibitors like sodium fluoroacetate (NaFAc), which is a potent and selective inhibitor of the TCA-cycle enzyme aconitase (*118, 119*). It should be noted that this increased inhibition was observed at millimolar concentrations of NaFAc (*118*). However, demonstrating a functional TCA cycle in gametocytes could indicate that the parasites switch energy generation pathways most likely to accommodate the reduced amounts of glucose in the mosquito vector (*88, 118*). Another way of obtaining sufficient energy levels in the mosquito is by use of phosphoenolpyruvate carboxykinase (PEPCK), which is known to fix CO_2 in *P. falciparum* (*120, 121*). PEPCK

expression is upregulated in gametocytes and can generate and employ free amino acids to create ATP for the significant morphological changes from zygotes to sporogony (*122*). Thus, PEPCK may be another attractive metabolic target that requires further investigation.

The current "gold standard" gametocytocidal compound is primaquine (PQ), an 8-aminoquinoline compound that was discovered in 1925 (*123*). PQ acts specifically on the mitochondria of *P. falciparum* most likely by generating reactive oxygen species (ROS) (*114, 123*). The disadvantages of PQ treatment are its side effects methemoglobinemia and hemolysis in people that suffer from a deficiency in their glucose-6-phosphate dehydrogenase (G6PD) (*91, 123, 124*). Evaluation of substituted PQ compounds have exhibited less hemolytic damage and continue to be investigated as to their effectiveness in gametocyte's clearance (*14, 123, 125*). PQ derivatives elubaquine and bulaquine have demonstrated gametocytocidal activity in *P. cynamolgi* infected rhesus monkeys and gametocytocidal activity against *P. falciparum*, respectively (*126, 127*). Elubaquine is three to four times less toxic than PQ and validates that chemical modification for safety profiles can be accomplished without abolishing antimalarial activity (*126*). Bulaquine was also less toxic than PQ and was more effective in maintaining long term gametocytocidal activity (*127*). PQ and artesunate, an artemisinin derivative, demonstrated high activity against gametocyte infectivity to the mosquito, however, the concerns with toxicity of PQ and the fast biological clearance of artesunate have caused these two molecules to remain in clinical trials to optimize the pharmacokinetics and pharmacodynamics of this promising combination (*114, 128, 129*). One group of antimalarial compounds derived from artemisinin, called trioxaquines, have exhibited potent activity against all gametocyte stages (*129*). Trioxaquines can be synthesized at low cost, have lower IC_{50} values than artesunate, and have a good safety profile (*129*). As artemisinin resistance continue to rise, especially in Thailand, any artemisinin derivative is also likely to become ineffective against asexual and sexual malaria stages (*130, 131*), thus, alternative antimalarials with different mode of action are urgently needed. Transcriptomics, proteomics, metabolomics and differential-drug susceptibility data of the mitochondrion in gametocytes supports increased metabolic activity in this organelle as compared to asexual intraerythrocytic parasites thus, is a strong drug target in gametocyte stages.

The food vacuole: into the great unknown

The food vacuole is essential for providing amino acids by digestion of the erythrocyte's hemoglobin during the asexual development. The internal compartment of this organelle is under low pH conditions and processes the majority of hemoglobin (50-80%) producing large amounts of heme. The parasite produces digestive enzymes, such as plasmepsins and falcipain, which release heme that in the presence of oxygen is oxidized to ferric-protoporphyrin IX forming α-hematin, which is toxic to the parasite inducing cell membrane disruption and ROS. To overcome this toxicity α-hematin is converted into β-hematin and mobilized into insoluble crystals called hemozoin (*132*). Hemozoin crystals are produced when two β-hematins form hydrogen bonds causing crystallization. This crystal is inert and is often referred to as "dark-pigment" when visualized by microscopy (*133*). Currently, a few drugs are known to target this organelle, and the process of hemozoin crystallization. Chloroquine has been used since the late 1940's and has been shown to accumulate in the digestive vacuoles. Recently, Chugh and colleagues showed that chloroquine reduces hemoglobin binding to falcipain 2 and alters the ability of hemozoin crystals to form by possible π-π bonding interactions between chloroquine and β-hematins, blocking further crystal growth (*132*). Under chloroquine drug pressure the parasite's digestive vacuole aggregates and the pigment forms clumps, which is implicit of disruption of hemozoin formation and hemoglobin digestion (*134*). Chloroquine has demonstrated inhibitory affects against asexual stages of *P. falciparum*, but it is inactive against gametocytes. Moreover, chloroquine may induce gametocytogenesis (*14, 135*). This finding may be similar to what was thought with FOS and its inactivity against stage V gametocytes most likely because the MEP pathway activity is reduced. However, gametocytes rely on hemoglobin digestion to obtain necessary amino acids for protein synthesis or for increasing biomass availability. The development and metabolic activity of the food vacuole during gametocytogenesis has not been studied, however, hemozoin crystals are present in late stage gmaetocytes where in some cases are stored in a peculiar compartment called Garnham bodies (G-bodies) (*136, 137*). G-bodies were proposed to be vestigial structures cast off by the growing gametocytes but their function remain unclear (*136, 137*). Further investigation is needed to assess the food vacuole development and metabolic role during gametocytogenesis to establish this organelle as drug target in sexual stages.

We recently discovered two new dimeric phloroglucinols (PGs) (Figure 1.1) from Madagascar rain forest that showed inhibitory effects against asexual chloroquine-resistant and sexual intraerythrocytic stages of the parasite (*138*). These new PGs were active not only in late stage gametocytes but also prevented gametocytogenesis at low nanomolar concentrations. The ability of an asexual-killing compound to prevent gametocytogenesis is not unusual, however; additional medicinal chemistry on PGs may increase their killing activity against mature gametocytes. PGs are hydroxylated benzene rings and the potential mode of action is likely to occur by affecting the hemozoin formation, but this needs to be confirmed (*138, 139*). As mentioned above, the role of the food vacuole during gametocytogenesis remains unknown and determination of the mode of action of these new PGs will aid to study the potential of this organelle as a target to block transmission.

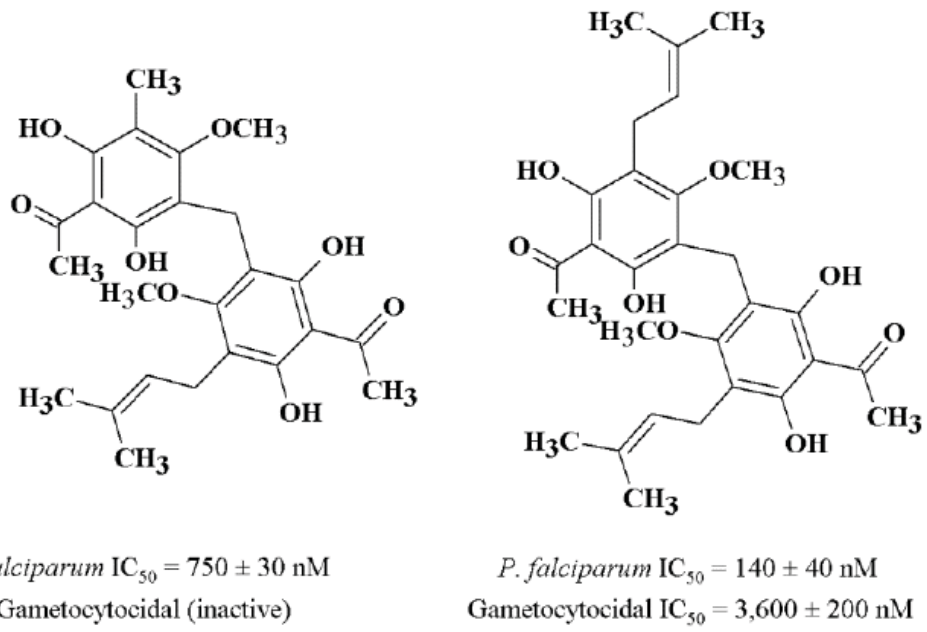

Figure 1. 1. Dimeric Phloroglucinols

Methylene blue (MB) has also shown inhibitory properties in both asexual and sexual stage parasites and was one of the first synthetic compounds to be shown to inhibit malaria (*14, 140*). It is postulated that MB has more than one target, making it a pleiotropic drug. The first postulated target is the ability of MB to interfere non-competitively with glutathione reductase which causes depletion of glutathione (*140, 141*). Low levels of glutathione in the parasite result in greater sensitivity to other antimalarials, such as chloroquine (*140, 141*). MB was shown to

interfere with heme degradation by lowering the amount of reducing compounds available (*140, 141*). The other possible mechanism of action is similar to that chloroquine, in which hemozoin crystallization is impeded by π-π interactions preventing characterization (*140, 142*), thus, the therapeutic effects are most likely a response to both mechanisms (*142*). MB exhibits low nanomolar IC_{50} against both early and late stage gametocytes (*143*). Adjalley and colleagues also showed that gametocytes pre-treated with MB produced a lower number of oocysts (*143*). Further studies are needed to elucidate if MB is active against the mosquito stages. The low cost of MB synthesis is advantageous for implementation in combination therapies in endemic countries. Combination therapy with MB was revisited since it has synergistic effects with chloroquine (*14, 141*). Combination therapy of MB and chloroquine was attempted but phase II clinical trials were halted due to not meeting the WHO 95% efficacy threshold (*143*). In addition, unwanted side effects such as urine and sclera turning blue/green and potential toxicity when used at higher doses than 2 mg/kg are a concern (*14, 141, 144*).

DOZI-mediated translational repression: a necessary mechanism during sexual development

Despite DNA synthesis does not occur during gametocytogenesis, RNA synthesis is still active (*26*), but decreases in late-stages, most likely due to translational repression (TR) which is essential for sexual development of the malaria parasite (*13, 145*). The defining characteristic of TR is the incorporation of certain mRNAs together with proteins into dormant messenger ribonucleoprotein particles (mRNPs or P bodies), where these transcripts are stored and stabilized for translation at a later point in development (*13, 145, 146*). TR is accomplished through an RNA helicase called DOZI (Development of Zygote Inhibited), which is a member of the DDX6 family of DEAD-box RNA helicases and has been identified in the sex-specific proteome of *P. berghei* and *P. falciparum* gametocytes (*13, 147, 148*). TR occurs in the cytoplasm and is also essential in the mitochondrion and apicoplast (*149*). This phenomenon could explain the lack of activity of most antimalarials during gametocytogenesis.

PbDOZI was demonstrated to form an mRNP complex with multiple mRNAs including *P25* and *P28* (essential for zygote development and mosquito midgut invasion) and was identified in female gametocytes where the transcripts for both proteins were present but not translated until a mosquito blood meal (*6, 13, 32*). In the absence of DOZI, transcripts are neither

stored in silent mRNPs nor transported to translating polysomes but instead are explicitly degraded (*13, 146*). Interestingly, deletion of *pbdozi* and *pbcith* (protein that interacts with DOZI) lead to the destabilization of *pbs28* mRNA instead of restoring translation of the P28 protein (*6, 146*), indicating that there are other factors involved in TR that have yet to be identified.

In depth analysis of the 3' UTRs of nine mRNAs known to be translationally repressed, identified that all *P. berghei* mRNAs contain a 47-base U-rich motif leading to TR (*6, 13, 145, 146*). Interestingly, this motif can be located in the 3' or 5' UTR and still stimulate repression (*6, 150*). This U-rich domain has not be identified in *P. falciparum* although TR still occurs (*6, 145, 148*). DOZI-mediated TR provides a potential mechanism for metabolic regulation during gametocytogenesis and further investigation will aid to identify novel molecular targets for drug development.

Microgametocyte's exflagellation: male gametes on the move

Microtubules have a wide variety of functions ranging from cellular skeletal support, motility, vesicular trafficking, and cell division. Microtubules are comprised of α and β-tubulin protein polymers. It has been shown that microtubule formation is critical for gametocytogenesis, and is involved with male gamete motility (*151*). Actin II is the pivotal protein for proper male gamete formation in the mosquito midgut (*151*). Two variants of actin are found in *Plasmodium*; actin I and actin II. Actin I is essential during the asexual life cycle and is understood to have roles in hemoglobin uptake and trafficking. Actin II was shown by Siden-Kiamos and colleagues to be only expressed during the sexual development using gene deletion (*151*). In order for the microgametocytes to become motile and eventually mate, exflagellation must occur in the mosquito midugt (*151, 152*). Exflagellation requires the synthesis of axonemes and components of the flagella, which must be accomplished quickly (*151*). The microgamete will then propel itself through the mosquito midgut until a female is located after which sexual fusion will occur. Therefore, microtubule formation during the exflagellation processes is a potential drug target to halt sexual reproduction of the parasites in the mosquito, therefore, blocking malaria transmission.

Currently there is one natural product, azadirachtin, a tetranortriterpenoid that has been isolated from the Neem tree (*Azadirachta indica*) and has been shown to disrupt microtubule

formation and exflagellation in gametocytes (*153*). The molecular target linked to the microtubule formation disruption is still unknown, but *in vitro* studies showed that azadirachtin disrupts exflagellation by interrupting endomitotic division, and axoneme formation (*153, 154*). Billker and colleagues demonstrated that azadirachtin disrupts cytoplasmic and axonenomal microtubule formation (*155*). Additional studies are needed to understand the direct implications of azadirachtin on development of the parasite's sexual stages, but these observations supports inhibition of microtubules formation as a potential target for combinatorial drug treatments.

Proteases as drugable targets during gametocyte development

Proteasomes contribute to many roles in malaria parasites including maintaining normal turnover of proteins (*156-158*), degradation of defective proteins (*159*), cell cycle progression (*160*), and transcription factor regulation (*161*); thus, affecting several metabolic pathways when its proper function is disrupted. Data-mining has revealed at least 25 protease genes in the *P. falciparum* genome, most of them remaining uncharacterized (*162*). Predicted proteasome genes are expressed throughout gametocytogenesis supporting the activity of the proteasome in these stages and providing promising drug targets (*162, 163*). Interestingly, proteases are one of the most abundant proteins in the parasitophorous vacuole of *P. falciparum* (*164*). Multiple studies have identified epoxomicin, an antitumor agent with nanomolar IC_{50} values in *P. falciparum*, to be an excellent inhibitor of asexual and sexual intraerythrocytic parasites, and oocyst development (*14, 158, 163*). Epoxomicin showed no signs of potential cross-resistance with partner drugs and is effective against chloroquine-resistant parasites (*158*). However, epoxomicin is very toxic to human cells (HepG2 cells) with an IC_{50} of 3 nM (*165*) which makes use in human treatment impossible. Medicinal chemistry may lower this cytotoxicity but that remains to be determined. Another promising drug is thiostrepton, which has been shown to target the parasites proteasome as well as the apicoplast showed modest gametocytocidal activity when tested with a conventional gametocytocidal assay which does not distinguish male and female activity (*49*). A recent study showed that thiostrepton is more potent on male gametocytes and less effective on female gametocytes (*166*). Thus, the proteasome is undoubtedly another potential drug target and further investigation of its role in gametocyte stages is needed.

Plasmodium nucleic acid metabolism in gametocytes: to target or not to target

P. falciparum cannot synthesize purines *de novo* for synthesis of DNA, RNA and cofactors, and must salvage them from the host by deamination of adenosine to inosine followed by the conversion of inosine to hypoxanthine by purine nucleoside phosphorylase (PNP) (*167*). Hypoxanthine, which can also be salvaged directly from the host, is then converted to inosine monophosphate (IMP) by hypoxanthine-guanine-xanthine phosphoribosyltransferase (HGXPRT). Hypoxanthine is commonly used as a nutritional supplement in malarial culture media and a key source of hypoxanthine *in vivo* is from the erythrocyte purine pool. Immucillins are picomolar transition state inhibitors of *P. falciparum* and human PNP (*168-170*) and are potent inhibitors of the parasites during the *P. falciparum* asexual intraerythrocytic stages both *in vitro* and *in vivo* (*171, 172*). Because PNP is also present in the host, in order to prevent purine salvage in the malaria parasite, human PNP must be also blocked. PNP knockout experiments had shown that parasites can still survive during intraerythrocytic stages and gametocytogenesis was not impaired (*173, 174*). However, PNP-knockout *P. berghei* were not able to develop oocysts in mosquitoes (*175*), thus, purine salvage is essential for the asexual intraerythrocytic stages and parasite development in the mosquito validating PNP as potential drug target. Since the mode of action of immucillins differ from the current antimalarials, this class of compounds are great candidates for combination therapies.

DNA replication is blocked leading to the formation of only one gametocyte after red blood cell invasion (*176*). Uptake by the female mosquito activates gametocytes immediately and within 10 minutes male gametocytes replicate their DNA three times leading to eight copies of the genome (*177*). The DNA-binding agent centanamycin is thought to act by covalently modifying DNA consequently, damaging the DNA and preventing replication. Centanamycin was investigated as potential transmission blocking agent and while it did not have an effect on *P. berghei* gametocyte development, it drastically reduced oocyst formation and surviving oocysts were unable to produce sporozoites in the mosquito vector (*178*). Centanamycin showed no significant chromosome aberrations through *in vitro* genotoxicity studies, but this concern has yet to be investigated in mutagenicity studies (*178*).

Another potential drug target is DNA topoisomerase II which is inhibited by 9-anilinoacridine derivatives (*179-182*). These compounds inhibited asexual intraerythrocytic *P. falciparum* growth *in vitro* with IC_{50} in the low nanomolar range but some derivatives may have

a different molecular target (revised in (*183*)). A modified 9-anilinoacridine was shown to have 10-fold increased gametocytocidal activity as compared to the parent compound despite DNA replication being halted during gametocytogenesis (*179*). DNA topoisomerase II also functions to stabilize chromosome organization (*184*). When stage I and stage IV treated-gametocytes were analyzed by electron microscopy a abnormal clumped nuclei was observed indicating that the acridine-based drugs affected chromosome organization (*184*). These studies indicate that drugs targeting DNA topoisomerases may have gametocytocidal activity by interfering with chromosome organization. In addition, some 9-anilinoacridine compounds were inactive against asexual intraerythrocytic stages of *P. berghei* and *P. yoelii* in mice and it has been postulated that a rapid metabolic inactivation may occur in mice and/or poor blood distribution may occur (*181, 183, 185*). Differences at the molecular target level as well as in the transport of the drugs between *Plasmodium* species cannot be ruled out.

Concluding remarks

The metabolism of malaria gametocytes has long been understudied. With new techniques to culture and isolate gametocyte stages, we are starting to reveal that several metabolic pathways are still active in gametocytes and may offer key targets for therapeutic intervention. To date, most of the information about gametocyte stages have come from genetic, transcriptomics and proteomics studies, and very little is known regarding the metabolic requirements during gametocytogenesis. In the present work, we have addressed the potential targets in gametocyte stages and highlighted the need to expand the knowledge of the gametocyte's metabolism, which remains largely unexplored. This knowledge will reveal common essential targets between asexual and sexual intraerythrocytic stages for future development of multi-satge antimalarials.

Acknowledgments

J.D.B. and C.D.L. are recipients of a scholarship from the National Science Foundation S-STEM project (DUE-0850198).

References

1. World Malaria Report 2012. Switzerland, World Health Organization, 2012.
2. D. A. Baker, Malaria gametocytogenesis. *Mol Biochem Parasitol* **172**, 57-65 (2010).
3. T. Bousema, C. Drakeley, Epidemiology and Infectivity of *Plasmodium falciparum* and *Plasmodium vivax* Gametocytes in Relation to Malaria Control and Elimination. *Clin. Microbiol. Rev.* **24**, 377-410 (2011).
4. A. M. Talman, O. Domarle, F. E. McKenzie, F. Ariey, V. Robert, Gametocytogenesis: the puberty of *Plasmodium falciparum*. *Malaria Journal* **3**, 1-14 (2004).
5. S. Eksi, B. J. Morahan, Y. Haile, T. Furuya, H. Jiang, O. Ali, H. Xu, K. Kiattibutr, A. Suri, B. Czesny, A. Adeyemo, T. G. Myers, J. Sattabongkot, X.-z. Su, K. C. Williamson, *Plasmodium falciparum* Gametocyte Development 1 (*Pfgdv1*) and Gametocytogenesis Early Gene Identification and Commitment to Sexual Development. *PLoS Pathog* **8**, e1002964 (2012).
6. Z. Liu, J. Miao, L. Cui, Gametocytogenesis in malaria parasite: commitment, development and regulation. *Future Microbiology* **6**, 1351-1369 (2011).
7. J. A. Young, Q. L. Fivelman, P. L. Blair, P. de la Vega, K. G. Le Roch, Y. Zhou, D. J. Carucci, D. A. Baker, E. A. Winzeler, The *Plasmodium falciparum* sexual development transcriptome: A microarray analysis using ontology-based pattern identification. *Molecular and Biochemical Parasitology* **143**, 67-79 (2005).
8. L. Florens, M. P. Washburn, J. D. Raine, R. M. Anthony, M. Grainger, J. D. Haynes, J. K. Moch, N. Muster, J. B. Sacci, D. L. Tabb, A. A. Witney, D. Wolters, Y. Wu, M. J. Gardner, A. A. Holder, R. E. Sinden, J. R. Yates, D. J. Carucci, A proteomic view of the *Plasmodium falciparum* life cycle. *Nature* **419**, 520-526 (2002).
9. M. Delves, D. Plouffe, C. Scheurer, S. Meister, S. Wittlin, E. A. Winzeler, R. E. Sinden, D. Leroy, The activities of current antimalarial drugs on the life cycle stages of *Plasmodium*: a comparative study with human and rodent parasites. *PLoS Med* **9**, e1001169 (2012).
10. C. Peatey, D. Leroy, D. Gardiner, K. Trenholme, Anti-malarial drugs: how effective are they against *Plasmodium falciparum* gametocytes? *Malaria Journal* **11**, 34 (2012).
11. R. N. Price, F. Nosten, Effects of artemisinin derivatives on malaria transmissibility. *Lancet* **347**, 1654 (1996).

12. C. J. Woodrow, R. K. Haynes, S. Krishna, Artemisinins. *Postgraduate medical journal* **81**, 71-78 (2005).
13. G. R. Mair, J. A. M. Braks, L. S. Garver, J. C. A. G. Wiegant, N. Hall, R. W. Dirks, S. M. Khan, G. Dimopoulos, C. J. Janse, A. P. Waters, Regulation of Sexual Development of *Plasmodium* by Translational Repression. *Science* **313**, 667-669 (2006).
14. O. Dechy-Cabaret, F. Benoit-Vical, Effects of Antimalarial Molecules on the Gametocyte Stage of *Plasmodium falciparum*: The Debate. *Journal of Medicinal Chemistry*, (2012).
15. M. J. Delves, Plasmodium cell biology should inform strategies used in the development of antimalarial transmission-blocking drugs. *Future Medicinal Chemistry* **4**, 2251-2263 (2012).
16. L. Lucantoni, V. Avery, Whole-cell *in vitro* screening for gametocytocidal compounds. *Future Medicinal Chemistry* **4**, 2337-2360 (2012).
17. C. A. Lobo, N. Kumar, Sexual Differentiation and Development in the Malaria Parasite. *Parasitology Today* **14**, 146-150 (1998).
18. P. Alano, *Plasmodium falciparum* gametocytes: still many secrets of a hidden life. *Molecular Microbiology* **66**, 291-302 (2007).
19. J. C. Beier, MALARIA PARASITE DEVELOPMENT IN MOSQUITOES. *Annual Review of Entomology* **43**, 519 (1998).
20. R. E. Sinden, in *Advances in Parasitology,* J. R. Baker, R. Muller, Eds. (Academic Press, 1983), vol. Volume 22, pp. 153-216.
21. R. Carter, M. M. Nijhout, Control of Gamete Formation (Exflagellation) in Malaria Parasites. *Science* **195**, 407-409 (1977).
22. M. M. Kariuki, J. K. Kiaira, F. K. Mulaa, J. K. Mwangi, M. K. Wasunna, S. K. Martin, Plasmodium falciparum: purification of the various gametocyte developmental stages from in vitro-cultivated parasites. *The American Journal of Tropical Medicine and Hygiene* **59**, 505-508 (1998).
23. Rodrı, amp, x, M. C. guez, G. Margos, H. Compton, M. Ku, H. Lanz, M. H. guez, R. E. Sinden, *Plasmodium berghei*: routine production of pure gametocytes, extracellular gametes, zygotes, and ookinetes. *Experimental Parasitology* **101**, 73-76 (2002).
24. C. Mendis, B. H. Noden, J. C. Beier, Exflagellation Responses for Cultured *Plasmodium falciparum* (Haemosporida: Plasmodiidae) Gametocytes to Human Sera and Midguts of

Anopheline Mosquitoes (Diptera: Culicidae). *Journal of Medical Entomology* **31**, 767-769 (1994).

25. J. E. Gerber, T. E. Ukena, L. Cote, J. M. Wyllie, W. C. Winn, Exflagellation of malarial parasites in human peripheral blood. *Journal of Clinical Microbiology* **13**, 236-237 (1981).
26. N. Lang-Unnasch, A. D. Murphy, Metabolic Changes of the Malaria Parasite During the Transition From the Human to the Mosquito. *Annual Review of Microbiology* **52**, 561 (1998).
27. M. K. Bhattacharyya, N. Kumar, Effect of xanthurenic acid on infectivity of *Plasmodium falciparum* to *Anopheles stephensi*. *International Journal for Parasitology* **31**, 1129-1133 (2001).
28. R. E. L. Paul, P. T. Brey, V. Robert, *Plasmodium* sex determination and transmission to mosquitoes. *Trends in Parasitology* **18**, 32-38 (2002).
29. R. E. Sinden, G. A. Butcher, O. Billker, S. L. Fleck, in *Advances in Parasitology,* R. M. J.R. Baker, D. Rollinson, Eds. (Academic Press, 1996), vol. Volume 38, pp. 53-117.
30. K. Hayton, T. J. Templeton, Osmiophilic bodies and the odd organelles of alveolates. *Molecular Microbiology* **67**, 236-240 (2008).
31. R. Sinden, R. Carter, C. Drakeley, D. Leroy, The biology of sexual development of *Plasmodium*: the design and implementation of transmission-blocking strategies. *Malaria Journal* **11**, 70 (2012).
32. I. Siden-Kiamos, D. Vlachou, G. Margos, A. Beetsma, A. P. Waters, R. E. Sinden, C. Louis, Distinct roles for pbs21 and pbs25 in the in vitro ookinete to oocyst transformation of *Plasmodium berghei*. *Journal of Cell Science* **113**, 3419-3426 (2000).
33. M. S. Ramasamy, R. Kulasekera, K. A. Srikrishnaraj, R. Ramasamy, Different effects of modulation of mosquito (Diptera:Culicidae) trypsin activity on the infectivity of two human malaria (Hemosporidia:Plasmodidae) parasites. *J Med Entomol* **33**, 777-782 (1996).
34. J. F. G. M. Meis, G. Pool, G. J. Gemert, A. H. W. Lensen, T. Ponnudurai, J. H. E. T. Meuwissen, *Plasmodium falciparum* ookinetes migrate intercellularly through Anopheles stephensi midgut epithelium. *Parasitology Research* **76**, 13-19 (1989).

35. C. Y. Botté, F. Dubar, G. I. MacFadden, E. Marechal, C. Biot, *Plasmodium falciparum* Apicoplast Drugs: Targets or Off-Targets? *Chemical reviews* **112**, 1269-1283 (2012).
36. C. D. Goodman, G. I. McFadden, Targeting apicoplasts in malaria parasites. *Expert Opin Ther Targets* **17**, 167-177 (2013).
37. S. A. Ralph, G. G. Van Dooren, R. F. Waller, M. J. Crawford, M. J. Fraunholz, B. J. Foth, C. J. Tonkin, D. S. Roos, G. I. McFadden, Tropical infectious diseases: Metabolic maps and functions of the *Plasmodium falciparum* apicoplast. *Nat Rev Microbiol* **2**, 203-216 (2004).
38. N. Okamoto, T. P. Spurck, C. D. Goodman, G. I. McFadden, Apicoplast and Mitochondrion in Gametocytogenesis of *Plasmodium falciparum*. *Eukaryotic Cell* **8**, 128-132 (2009).
39. K. Drlica, M. Malik, Fluoroquinolones: action and resistance. *Curr Top Med Chem* **3**, 249-282 (2003).
40. D. C. Hooper, Mechanisms of Action of Antimicrobials: Focus on Fluoroquinolones. *Clinical Infectious Diseases* **32**, S9-S15 (2001).
41. E. L. Dahl, P. J. Rosenthal, Apicoplast translation, transcription and genome replication: targets for antimalarial antibiotics. *Trends in Parasitology* **24**, 279-284 (2008).
42. M. E. Fichera, D. S. Roos, A plastid organelle as a drug target in apicomplexan parasites. *Nature* **390**, 407-409 (1997).
43. E. A. Campbell, N. Korzheva, A. Mustaev, K. Murakami, S. Nair, A. Goldfarb, S. A. Darst, Structural Mechanism for Rifampicin Inhibition of Bacterial RNA Polymerase. *Cell* **104**, 901-912 (2001).
44. B. Genton, I. Mueller, I. Betuela, G. Casey, M. Ginny, M. P. Alpers, J. C. Reeder, Rifampicin/Cotrimoxazole/Isoniazid Versus Mefloquine or Quinine + Sulfadoxine-Pyrimethamine for Malaria: A Randomized Trial. *PLOS Clin Trial* **1**, e38 (2006).
45. N. Aditya, S. Patankar, B. Madhusudhan, Assessment of in vivo antimalarial activity of rifampicin, isoniazide, and ethambutol combination therapy. *Parasitology Research* **106**, 1481-1484 (2010).
46. E. L. Dahl, J. L. Shock, B. R. Shenai, J. Gut, J. L. DeRisi, P. J. Rosenthal, Tetracyclines Specifically Target the Apicoplast of the Malaria Parasite *Plasmodium falciparum*. *Antimicrob Agents Chemother* **50**, 3124-3131 (2006).

47. T. N. Ramya, S. Mishra, K. Karmodiya, N. Surolia, A. Surolia, Inhibitors of nonhousekeeping functions of the apicoplast defy delayed death in *Plasmodium falciparum*. *Antimicrob Agents Chemother* **51**, 307-316 (2007).

48. E. L. Dahl, P. J. Rosenthal, Multiple antibiotics exert delayed effects against the *Plasmodium falciparum* apicoplast. *Antimicrob Agents Chemother* **51**, 3485-3490 (2007).

49. M. N. Aminake, S. Schoof, L. Sologub, M. Leubner, M. Kirschner, H. D. Arndt, G. Pradel, Thiostrepton and derivatives exhibit antimalarial and gametocytocidal activity by dually targeting parasite proteasome and apicoplast. *Antimicrob Agents Chemother* **55**, 1338-1348 (2011).

50. S. Shimizu, Y. Osada, T. Kanazawa, Y. Tanaka, M. Arai, Suppressive effect of azithromycin on *Plasmodium berghei* mosquito stage development and apicoplast replication. *Malaria Journal* **9**, 73-80 (2010).

51. H. Noedl, S. Krudsood, W. Leowattana, N. Tangpukdee, W. Thanachartwet, S. Looareesuwan, R. S. Miller, M. Fukuda, K. Jongsakul, K. Yingyuen, S. Sriwichai, C. Ohrt, C. Knirsch, In Vitro Antimalarial Activity of Azithromycin, Artesunate, and Quinine in Combination and Correlation with Clinical Outcome. *Antimicrob Agents Chemother* **51**, 651-656 (2007.

52. A. B. S. Sidhu, Q. Sun, L. J. Nkrumah, M. W. Dunne, J. C. Sacchettini, D. A. Fidock, In Vitro Efficacy, Resistance Selection, and Structural Modeling Studies Implicate the Malarial Parasite Apicoplast as the Target of Azithromycin. *Journal of Biological Chemistry* **282**, 2494-2504 (2007).

53. R. Carter, K. N. Mendis, L. H. Miller, L. Molineaux, A. Saul, Malaria transmission-blocking vaccines--how can their development be supported? *Nature Medicine* **6**, 241-244 (2000).

54. M. Sarkar, C. W. C, G. Koren, A. R. N. Einarson, Pregnancy outcome following gestational exposure to azithromycin. *BMC Pregnancy & Childbirth* **6**, 18-15 (2006).

55. G. Treadway, D. Pontani, Paediatric safety of azithromycin: worldwide experience. *Journal of Antimicrobial Chemotherapy* **37**, 143-149 (1996).

56. B. Rino, T. Van, F. Giovanni, M. Franco, Research letter. Azithromycin in the treatment of *Plasmodium falciparum* gametocytes: a preliminary observation. *Journal of Tropical Pediatrics* **46**, 56 (2000).

57. N. Lalak, D. Morris, Azithromycin Clinical Pharmacokinetics. *Clinical Pharmacokinetics* **25**, 370-374 (1993).

58. S. Nakornchai, P. Konthiang, Activity of azithromycin or erythromycin in combination with antimalarial drugs against multidrug-resistant *Plasmodium falciparum in vitro*. *Acta Tropica* **100**, 185-191 (2006).

59. E. Yeh, J. L. DeRisi, Chemical Rescue of Malaria Parasites Lacking an Apicoplast Defines Organelle Function in Blood-Stage *Plasmodium falciparum*. *PLoS Biol* **9**, e1001138 (2011).

60. H. Jomaa, J. Wiesner, S. Sanderbrand, B. Altincicek, C. Weidemeyer, M. Hintz, I. Türbachova, M. Eberl, J. Zeidler, H. K. Lichtenthaler, D. Soldati, E. Beck, Inhibitors of the Nonmevalonate Pathway of Isoprenoid Biosynthesis as Antimalarial Drugs. *Science* **285**, 1573-1576 (1999).

61. M. B. Cassera, F. C. Gozzo, F. L. D'Alexandri, E. F. Merino, H. A. del Portillo, V. J. Peres, I. C. Almeida, M. N. Eberlin, G. Wunderlich, J. Wiesner, H. Jomaa, E. A. Kimura, A. M. Katzin, The methylerythritol phosphate pathway is functionally active in all intraerythrocytic stages of *Plasmodium falciparum*. *J Biol Chem* **279**, 51749-51759 (2004).

62. C. S. de Macedo, M. L. Uhrig, E. A. Kimura, A. M. Katzin, Characterization of the isoprenoid chain of coenzyme Q in *Plasmodium falciparum*. *FEMS Microbiol Lett* **207**, 13-20 (2002).

63. R. Tonhosolo, F. L. D'Alexandri, F. A. Genta, G. Wunderlich, F. C. Gozzo, M. N. Eberlin, V. J. Peres, E. A. Kimura, A. M. Katzin, Identification, molecular cloning and functional characterization of an octaprenyl pyrophosphate synthase in intra-erythrocytic stages of *Plasmodium falciparum*. *Biochem J* **392**, 117-126 (2005).

64. R. Tonhosolo, H. B. Gabriel, M. Y. Matsumura, F. J. Cabral, M. M. Yamamoto, F. L. D'Alexandri, R. A. Sussmann, R. Belmonte, V. J. Peres, D. C. Crick, G. Wunderlich, E. A. Kimura, A. M. Katzin, Intraerythrocytic stages of *Plasmodium falciparum* biosynthesize menaquinone. *FEBS Letters* **584**, 4761-4768 (2010).

65. A. S. Couto, E. A. Kimura, V. J. Peres, M. L. Uhrig, A. M. Katzin, Active isoprenoid pathway in the intra-erythrocytic stages of *Plasmodium falciparum*: presence of dolichols of 11 and 12 isoprene units. *Biochem J* **341 (Pt 3)**, 629-637 (1999).

66. F. L. D'Alexandri, E. A. Kimura, V. J. Peres, A. M. Katzin, Protein dolichylation in *Plasmodium falciparum*. *FEBS Letters* **580**, 6343-6348 (2006).
67. R. A. Sussmann, C. B. Angeli, V. J. Peres, E. A. Kimura, A. M. Katzin, Intraerythrocytic stages of *Plasmodium falciparum* biosynthesize vitamin E. *FEBS Letters* **585**, 3985-3991 (2011).
68. F. M. Jordão, E. A. Kimura, A. M. Katzin, Isoprenoid biosynthesis in the erythrocytic stages of *Plasmodium falciparum*. *Memorias do Instituto Oswaldo Cruz* **106**, 134-141 (2011).
69. F. L. D'Alexandri, R. Tonhosolo, E. A. Kimura, A. M. Katzin, Mass spectrometry analysis of polyisoprenoids alcohols and carotenoids via ESI(Li(+))-MS/MS. *Methods Mol Biol* **580**, 109-128 (2009).
70. R. Tonhosolo, F. L. D'Alexandri, V. V. de Rosso, M. L. Gazarini, M. Y. Matsumura, V. J. Peres, E. F. Merino, J. M. Carlton, G. Wunderlich, A. Z. Mercadante, E. A. Kimura, A. M. Katzin, Carotenoid biosynthesis in intraerythrocytic stages of *Plasmodium falciparum*. *The Journal of biological chemistry* **284**, 9974-9985 (2009).
71. D. Chakrabarti, T. Da Silva, J. Barger, S. Paquette, H. Patel, S. Patterson, C. M. Allen, Protein farnesyltransferase and protein prenylation in *Plasmodium falciparum*. *J Biol Chem* **277**, 42066-42073 (2002).
72. R. Howe, M. Kelly, J. Jimah, D. Hodge, A. R. Odom, Isoprenoid biosynthesis inhibition disrupts Rab5 localization and food vacuolar integrity in *Plasmodium falciparum*. *Eukaryotic Cell* **12**, 215-223 (2013).
73. F. M. Jordao, A. Y. Saito, D. C. Miguel, V. de Jesus Peres, E. A. Kimura, A. M. Katzin, In Vitro and In Vivo Antiplasmodial Activities of Risedronate and Its Interference with Protein Prenylation in *Plasmodium falciparum*. *Antimicrob Agents Chemother* **55**, 2026-2031 (2011).
74. I. C. Moura, G. Wunderlich, M. L. Uhrig, A. S. Couto, V. J. Peres, A. M. Katzin, E. A. Kimura, Limonene arrests parasite development and inhibits isoprenylation of proteins in *Plasmodium falciparum*. *Antimicrob Agents Chemother* **45**, 2553-2558 (2001).
75. J. Wiesner, K. Kettler, J. Sakowski, R. Ortmann, A. M. Katzin, E. A. Kimura, K. Silber, G. Klebe, H. Jomaa, M. Schlitzer, Farnesyltransferase inhibitors inhibit the growth of malaria parasites *in vitro* and *in vivo*. *Angew Chem Int Ed Engl* **43**, 251-254 (2004).

76. M. A. Missinou, S. Borrmann, A. Schindler, S. Issifou, A. A. Adegnika, P. B. Matsiegui, R. Binder, B. Lell, J. Wiesner, T. Baranek, H. Jomaa, P. G. Kremsner, Fosmidomycin for malaria. *Lancet* **360**, 1941-1942 (2002).

77. J. Wiesner, S. Borrmann, H. Jomaa, Fosmidomycin for the treatment of malaria. *Parasitology Research* **90**, S71-S76 (2003).

78. T. Umeda, N. Tanaka, Y. Kusakabe, M. Nakanishi, Y. Kitade, K. T. Nakamura, Molecular basis of fosmidomycin's action on the human malaria parasite *Plasmodium falciparum*. *Scientific reports* **1**, 9 (2011).

79. J. Wiesner, D. Henschker, D. B. Hutchinson, E. Beck, H. Jomaa, In Vitro and In Vivo Synergy of Fosmidomycin, a Novel Antimalarial Drug, with Clindamycin. *Antimicrob Agents Chemother* **46**, 2889-2894 (2002).

80. S. Borrmann, A. A. Adegnika, F. Moussavou, S. Oyakhirome, G. Esser, P. B. Matsiegui, M. Ramharter, I. Lundgren, M. Kombila, S. Issifou, D. Hutchinson, J. Wiesner, H. Jomaa, P. G. Kremsner, Short-course regimens of artesunate-fosmidomycin in treatment of uncomplicated *Plasmodium falciparum* malaria. *Antimicrobial agents and chemotherapy* **49**, 3749-3754 (2005).

81. K. Na-Bangchang, R. Ruengweerayut, J. Karbwang, A. Chauemung, D. Hutchinson, Pharmacokinetics and pharmacodynamics of fosmidomycin monotherapy and combination therapy with clindamycin in the treatment of multidrug resistant falciparum malaria. *Malar J* **6**, 70 (2007).

82. S. C. Nair, C. F. Brooks, C. D. Goodman, A. Strurm, G. I. McFadden, S. Sundriyal, J. L. Anglin, Y. Song, S. N. J. Moreno, B. Striepen, Apicoplast isoprenoid precursor synthesis and the molecular basis of fosmidomycin resistance in *Toxoplasma gondii*. *The Journal of Experimental Medicine* **208**, 1547-1559 (2011).

83. J.-Y. van der Meer, A. K. H. Hirsch, The isoprenoid-precursor dependence of Plasmodium spp. *Natural Product Reports*, (2012).

84. S. Chaubey, A. Kumar, D. Singh, S. Habib, The apicoplast of *Plasmodium falciparum* is translationally active. *Molecular Microbiology* **56**, 81-89 (2005).

85. E. Yeh, J. L. DeRisi, Chemical Rescue of Malaria Parasites Lacking an Apicoplast Defines Organelle Function in Blood-Stage *Plasmodium falciparum*. *PLoS Biol* **9**, e1001138 (2011).

86. K. Becker, L. Tilley, J. L. Vennerstrom, D. Roberts, S. Rogerson, H. Ginsburg, Oxidative stress in malaria parasite-infected erythrocytes: host–parasite interactions. *International Journal for Parasitology* **34**, 163-189 (2004).

87. J. Noyola-Martinez, C. Shaw, B. Christian, G. Fox, M. Stevens, N. Garg, M. C. Gustin, R. Guerra, in *Methods of Microarray Data Analysis V,* P. McConnell, S. Lin, P. Hurban, Eds. (Springer US, 2007), chap. 4, pp. 45-58.

88. G. G. Van Dooren, L. M. Stimmler, G. I. McFadden, Metabolic maps and functions of the *Plasmodium* mitochondrion. *FEMS Microbiology Reviews* **30**, 596-630 (2006).

89. S. Kehr, N. Sturm, S. Rahlfs, J. M. Przyborski, K. Becker, Compartmentation of Redox Metabolism in Malaria Parasites. *PLoS Pathog* **6**, 1-12 (2010).

90. R. A. C. Sussmann, C. B. Angeli, V. J. Peres, E. A. Kimura, A. M. Katzin, Intraerythrocytic stages of *Plasmodium falciparum* biosynthesize vitamin E. *FEBS Letters* **585**, 3985-3991 (2011).

91. S. Ganesan, N. D. Chaurasiya, R. Sahu, L. A. Walker, B. L. Tekwani, Understanding the mechanisms for metabolism-linked hemolytic toxicity of primaquine against glucose 6-phosphate dehydrogenase deficient human erythrocytes: Evaluation of eryptotic pathway. *Toxicology* **294**, 54-60 (2012).

92. D. C. Gowda, P. Gupta, E. A. Davidson, Glycosylphosphatidylinositol Anchors Represent the Major Carbohydrate Modification in Proteins of Intraerythrocytic Stage *Plasmodium falciparum*. *Journal of Biological Chemistry* **272**, 6428-6439 (1997).

93. F. Silvestrini, E. Lasonder, A. Olivieri, G. Camarda, B. van Schaijk, M. Sanchez, S. Younis Younis, R. Sauerwein, P. Alano, Protein export marks the early phase of gametocytogenesis of the human malaria parasite *Plasmodium falciparum*. *Mol Cell Proteomics* **9**, 1437-1448 (2010).

94. C. Aicart-Ramos, R. A. Valero, I. Rodriguez-Crespo, Protein palmitoylation and subcellular trafficking. *Biochimica et Biophysica Acta (BBA) - Biomembranes* **1808**, 2981-2994 (2011).

95. P. J. Roberts, N. Mitin, P. J. Keller, E. J. Chenette, J. P. Madigan, R. O. Currin, A. D. Cox, O. Wilson, P. Kirschmeier, C. J. Der, Rho Family GTPase Modification and Dependence on CAAX Motif-signaled Posttranslational Modification. *Journal of Biological Chemistry* **283**, 25150-25163 (2008).

96. M. Sinensky, J. Logel, Defective macromolecule biosynthesis and cell-cycle progression in a mammalian cell starved for mevalonate. *Proc Natl Acad Sci U S A* **82**, 3257-3261 (1985).

97. L. Ayong, T. DaSilva, J. Mauser, C. M. Allen, D. Chakrabarti, Evidence for prenylation-dependent targeting of a Ykt6 SNARE in *Plasmodium falciparum*. *Molecular and Biochemical Parasitology* **175**, 162-168 (2011).

98. T. Scott Reid, K. L. Terry, P. J. Casey, L. S. Beese, Crystallographic Analysis of CaaX Prenyltransferases Complexed with Substrates Defines Rules of Protein Substrate Selectivity. *Journal of Molecular Biology* **343**, 417-433 (2004).

99. F. L. Zhang, P. J. Casey, Protein Prenylation: Molecular Mechanisms and Functional Consequences. *Annual Review of Biochemistry* **65**, 241-269 (1996).

100. A. M. Winter-Vann, P. J. Casey, Opinion: Post-prenylation-processing enzymes as new targets in oncogenesis. *Nature Reviews Cancer* **5**, 405-412 (2005).

101. I. Canobbio, P. Trionfini, G. F. Guidetti, C. Balduini, M. Torti, Targeting of the small GTPase Rap2b, but not Rap1b, to lipid rafts is promoted by palmitoylation at Cys176 and Cys177 and is required for efficient protein activation in human platelets. *Cellular Signalling* **20**, 1662-1670 (2008).

102. J. F. Hancock, A. I. Magee, J. E. Childs, C. J. Marshall, All ras proteins are polyisoprenylated but only some are palmitoylated. *Cell* **57**, 1167-1177 (1989).

103. J. H. No, F. de Macedo Dossin, Y. Zhang, Y.-L. Liu, W. Zhu, X. Feng, J. A. Yoo, E. Lee, K. Wang, R. Hui, L. H. Freitas-Junior, E. Oldfield, Lipophilic analogs of zoledronate and risedronate inhibit *Plasmodium* geranylgeranyl diphosphate synthase (GGPPS) and exhibit potent antimalarial activity. *Proceedings of the National Academy of Sciences* **109**, 4058-4063 (2012).

104. M. Yu, T. R. Kumar, L. J. Nkrumah, A. Coppi, S. Retzlaff, C. D. Li, B. J. Kelly, P. A. Moura, V. Lakshmanan, J. S. Freundlich, J. C. Valderramos, C. Vilcheze, M. Siedner, J. H. Tsai, B. Falkard, A. B. Sidhu, L. A. Purcell, P. Gratraud, L. Kremer, A. P. Waters, G. Schiehser, D. P. Jacobus, C. J. Janse, A. Ager, W. R. Jacobs, Jr., J. C. Sacchettini, V. Heussler, P. Sinnis, D. A. Fidock, The fatty acid biosynthesis enzyme FabI plays a key role in the development of liver-stage malarial parasites. *Cell host & microbe* **4**, 567-578 (2008).

105. K. Kirk, Membrane Transport in the Malaria-Infected Erythrocyte. *Physiol Rev* **81**, 495-537 (2001).

106. T. Spielmann, G. N. Montagna, L. Hecht, K. Matuschewski, Molecular make-up of the *Plasmodium* parasitophorous vacuolar membrane. *Int J Med Microbiol* **302**, 179-186 (2012).

107. G. G. van Dooren, M. Marti, C. J. Tonkin, L. M. Stimmler, A. F. Cowman, G. I. McFadden, Development of the endoplasmic reticulum, mitochondrion and apicoplast during the asexual life cycle of *Plasmodium falciparum*. *Molecular Microbiology* **57**, 405-419 (2005).

108. A. A. Divo, T. G. Geary, J. B. Jensen, H. Ginsburg, The mitochondrion of *Plasmodium falciparum* visualized by rhodamine 123 fluorescence. *The Journal of protozoology* **32**, 442-446 (1985).

109. M. Kato, K. Tanabe, A. Miki, K. Ichimori, S. Waki, Membrane potential of *Plasmodium falciparum* gametocytes monitored with rhodamine 123. *FEMS Microbiol Lett* **57**, 283-288 (1990).

110. I. K. Srivastava, H. Rottenberg, A. B. Vaidya, Atovaquone, a Broad Spectrum Antiparasitic Drug, Collapses Mitochondrial Membrane Potential in a Malarial Parasite. *Journal of Biological Chemistry* **272**, 3961-3966 (1997).

111. J. Krungkrai, P. Prapunwattana, S. R. Krungkrai, Ultrastructure and function of mitochondria in gametocytic stage of *Plasmodium falciparum*. *Parasite (Paris, France)* **7**, 19-26 (2000).

112. R. E. Sinden, Gametocytogenesis of *Plasmodium falciparum in vitro*: an electron microscopic study. *Parasitology* **84**, 1-11 (1982).

113. R. E. Sinden, M. E. Smalley, Gametocytogenesis of *Plasmodium falciparum* in vitro: the cell-cycle. *Parasitology* **79**, 277-296 (1979).

114. J. KrungkraI, The multiple roles of the mitochondrion of the malarial parasite. *Parasitology* **129**, 511-524 (2004).

115. T. Q. Tanaka, K. C. Williamson, A malaria gametocytocidal assay using oxidoreduction indicator, alamarBlue. *Mol Biochem Parasitol* **177**, 160-163 (2011).

116. W. E. Gutteridge, D. Dave, W. H. G. Richards, Conversion of dihydroorotate to orotate in parasitic protozoa. *Biochimica et Biophysica Acta (BBA) - General Subjects* **582**, 390-401 (1979).

117. J. Krungkrai, D. Burat, S. Kudan, S. Krungkrai, P. Prapunwattana, Mitochondrial oxygen consumption in asexual and sexual blood stages of the human malarial parasite, *Plasmodium falciparum*. *The Southeast Asian journal of tropical medicine and public health* **30**, 636-642 (1999).

118. J. MacRae, M. Dixon, M. Dearnley, H. Chua, J. Chambers, S. Kenny, I. Bottova, L. Tilley, M. McConville, Mitochondrial metabolism of sexual and asexual blood stages of the malaria parasite *Plasmodium falciparum*. *BMC Biology* **11**, 67 (2013).

119. E. C. Saunders, W. W. Ng, J. M. Chambers, M. Ng, T. Naderer, J. O. Krömer, V. A. Likić, M. J. McConville, Isotopomer Profiling of Leishmania mexicana Promastigotes Reveals Important Roles for Succinate Fermentation and Aspartate Uptake in Tricarboxylic Acid Cycle (TCA) Anaplerosis, Glutamate Synthesis, and Growth. *Journal of Biological Chemistry* **286**, 27706-27717 (2011).

120. I. W. Sherman, I. P. Ting, Carbon Dioxide Fixation in Malaria (Plasmodium lophurae). *Nature* **212**, 1387-1389 (1966).

121. I. W. Sherman, I. P. Ting, Carbon dioxide fixation in malaria—II. Plasmodium knowlesi (monkey malaria). *Comparative Biochemistry and Physiology* **24**, 639-642 (1968).

122. R. E. Hayward, *Plasmodium falciparum* phosphoenolpyruvate carboxykinase is developmentally regulated in gametocytes. *Molecular and Biochemical Parasitology* **107**, 227-240 (2000).

123. N. Vale, R. Moreira, P. Gomes, Primaquine revisited six decades after its discovery. *European Journal of Medicinal Chemistry* **44**, 937-953 (2009).

124. W. R. J. Taylor, N. J. White, Antimalarial Drug Toxicity. *Drug Safety* **27**, 25-61 (2004).

125. R. Capela, G. G. Cabal, P. J. Rosenthal, J. Gut, M. M. Mota, R. Moreira, F. Lopes, M. Prudencio, Design and Evaluation of Primaquine-Artemisinin Hybrids as a Multistage Antimalarial Strategy. *Antimicrob. Agents Chemother.* **55**, 4698-4706 (2011).

126. S. K. Puri, G. P. Dutta, Plasmodium cynomolgi: Gametocytocidal activity of the anti-malarial compound CDRI 80/53 (elubaquine) in rhesus monkeys. *Experimental Parasitology* **111**, 8-13 (2005).

127. N. J. Gogtay, K. D. Kamtekar, S. S. Dalvi, A. R. Chogle, U. Aigal, N. A. Kshirsagar, Preliminary report of the evaluation of the gametocytocidal action of bulaquine, in adult patients with acute, *Plasmodium falciparum* malaria. *Annals of Tropical Medicine & Parasitology* **98**, 525-528 (2004).

128. K. Chotivanich, J. Sattabongkot, R. Udomsangpetch, S. Looareesuwan, N. P. J. Day, R. E. Coleman, N. J. White, Transmission-Blocking Activities of Quinine, Primaquine, and Artesunate. *Antimicrob. Agents Chemother.* **50**, 1927-1930 (2006).

129. F. Benoit-Vical, J. Lelievre, A. Berry, C. Deymier, O. Dechy-Cabaret, J. Cazelles, C. Loup, A. Robert, J.-F. Magnaval, B. Meunier, Trioxaquines Are New Antimalarial Agents Active on All Erythrocytic Forms, Including Gametocytes. *Antimicrob. Agents Chemother.* **51**, 1463-1472 (2007).

130. A. M. Dondorp, F. Nosten, P. Yi, D. Das, A. P. Phyo, J. Tarning, K. M. Lwin, F. Ariey, W. Hanpithakpong, S. J. Lee, P. Ringwald, K. Silamut, M. Imwong, K. Chotivanich, P. Lim, T. Herdman, S. S. An, S. Yeung, P. Singhasivanon, N. P. Day, N. Lindegardh, D. Socheat, N. J. White, Artemisinin resistance in *Plasmodium falciparum* malaria. *New England Journal of Medicine* **361**, 455-467 (2009).

131. A. P. Phyo, S. Nkhoma, K. Stepniewska, E. A. Ashley, S. Nair, R. McGready, C. ler Moo, S. Al-Saai, A. M. Dondorp, K. M. Lwin, P. Singhasivanon, N. P. J. Day, N. J. White, T. J. C. Anderson, F. Nosten, Emergence of artemisinin-resistant malaria on the western border of Thailand: a longitudinal study. *The Lancet* **379**, 1960-1966 (2012).

132. M. Chugh, V. Sundararaman, S. Kumar, V. S. Reddy, W. A. Siddiqui, K. D. Stuart, P. Malhotra, Protein complex directs hemoglobin-to-hemozoin formation in *Plasmodium falciparum*. *Proc Natl Acad Sci U S A* **110**, 5392-5397 (2013).

133. M. E. Smalley, S. Abdalla, J. Brown, The distribution of *Plasmodium falciparum* in the peripheral blood and bone marrow of Gambian children. *Transactions of the Royal Society of Tropical Medicine and Hygiene* **75**, 103-105 (1981).

134. M. E. Smalley, *Plasmodium falciparum* gametocytes: the effect of chloroquine on their development. *Transactions of the Royal Society of Tropical Medicine and Hygiene* **71**, 526-529 (1977).

135. A. Buckling, L. C. Ranford-Cartwright, A. Miles, A. F. Read, Chloroquine increases *Plasmodium falciparum* gametocytogenesis in vitro. *Parasitology* **118 (Pt 4)**, 339-346 (1999).

136. P. C. C. Garnham, On some curious bodies found in erythrocytes containing immature crescents. *Transactions of the Royal Society of Tropical Medicine and Hygiene* **26**, 401-403 (1933).

137. A. U. Orjih, Hemozoin accumulation in Garnham bodies of *Plasmodium falciparum* gametocytes. *Parasitol Res* **111**, 2353-2359 (2012).

138. L. Harinantenaina, J. D. Bowman, P. J. Brodie, C. Slebodnick, M. W. Callmander, E. Rakotobe, R. Randrianaivo, V. E. Rasamison, A. Gorka, P. D. Roepe, M. B. Cassera, D. G. Kingston, Antiproliferative and Antiplasmodial Dimeric Phloroglucinols from *Mallotus oppositifolius* from the Madagascar Dry Forest (1). *J Nat Prod*, (2013).

139. L. Verotta, Are acylphloroglucinols lead structures for the treatment of degenerative diseases? *Phytochemistry Reviews* **1**, 389-407 (2002).

140. R. H. Schirmer, B. Coulibaly, A. Stich, M. Scheiwein, H. Merkle, J. Eubel, K. Becker, H. Becher, O. Müler, T. Zich, W. Schiek, B. Kouyaté, Methylene blue as an antimalarial agent. *Redox Report* **8**, 272-275 (2003).

141. K. Buchholz, R. H. Schirmer, J. K. Eubel, M. B. Akoachere, T. Dandekar, K. Becker, S. Gromer, Interactions of Methylene Blue with Human Disulfide Reductases and Their Orthologues from Plasmodium falciparum. *Antimicrob Agents Chemother* **52**, 183-191 (2008).

142. O. Blank, E. Davioud-Charvet, M. Elhabiri, Interactions of the antimalarial drug methylene blue with methemoglobin and heme targets in *Plasmodium falciparum*: a physico-biochemical study. *Antioxid Redox Signal* **17**, 544-554 (2012).

143. S. H. Adjalley, G. L. Johnston, T. Li, R. T. Eastman, E. H. Ekland, A. G. Eappen, A. Richman, B. K. L. Sim, M. C. S. Lee, S. L. Hoffman, D. A. Fidock, Quantitative assessment of *Plasmodium falciparum* sexual development reveals potent transmission-blocking activity by methylene blue. *Proceedings of the National Academy of Sciences* **108**, E1214–E1223 (2011).

144. P. R. Ginimuge, S. D. Jyothi, Methylene blue: revisited. *J Anaesthesiol Clin Pharmacol* **26**, 517-520 (2010).

145. N. Hall, M. Karras, J. D. Raine, J. M. Carlton, T. W. A. Kooij, M. Berriman, L. Florens, C. S. Janssen, A. Pain, G. K. Christophides, K. James, K. Rutherford, B. Harris, D. Harris, C. Churcher, M. A. Quail, D. Ormond, D. Jon, H. E. Trueman, J. Mendoza, L. B. Shelby, M.-A. Rajandream, D. J. Carucci, J. R. Y. Iii, F. C. Kafatos, C. J. Janse, B. Barrell, C. M. R. Turner, A. P. Waters, R. E. Sinden, A Comprehensive Survey of the Plasmodium Life Cycle by Genomic, Transcriptomic, and Proteomic Analyses. *Science* **307**, 82-86 (2005).

146. G. R. Mair, E. Lasonder, L. S. Garver, B. M. D. Franke-Fayard, C. K. Carret, J. C. A. G. Wiegant, R. W. Dirks, G. Dimopoulos, C. J. Janse, A. P. Waters, Universal Features of Post-Transcriptional Gene Regulation Are Critical for *Plasmodium* Zygote Development. *PLoS Pathog* **6**, e1000767 (2010)10.1371/journal.ppat.1000767).

147. S. M. Khan, B. Franke-Fayard, G. R. Mair, E. Lasonder, C. J. Janse, M. Mann, A. P. Waters, Proteome Analysis of Separated Male and Female Gametocytes Reveals Novel Sex-Specific Plasmodium Biology. *Cell* **121**, 675-687 (2005).

148. M. Tarique, M. Ahmad, A. Ansari, R. Tuteja, *Plasmodium falciparum* DOZI, an RNA helicase interacts with eIF4E. *Gene* **522**, 46-59 (2013).

149. M. Zhang, B. R. Joyce, W. J. Sullivan, V. Nussenzweig, Translational Control in *Plasmodium* and *Toxoplasma* Parasites. *Eukaryotic Cell* **12**, 161-167 (2013).

150. J. A. M. Braks, G. R. Mair, B. Franke-Fayard, C. J. Janse, A. P. Waters, A conserved U-rich RNA region implicated in regulation of translation in *Plasmodium female* gametocytes. *Nucleic Acids Research* **36**, 1176-1186 (2008).

151. E. Deligianni, R. N. Morgan, L. Bertuccini, T. W. A. Kooij, A. Laforge, C. Nahar, N. Poulakakis, H. Schüler, C. Louis, K. Matuschewski, I. Siden-Kiamos, Critical role for a stage-specific actin in male exflagellation of the malaria parasite. *Cellular Microbiology* **13**, 1714-1730 (2011).

152. O. Billker, V. Lindo, M. Panico, A. E. Etienne, et al., Identification of xanthurentic acid as the putative inducer of malaria development in the mosquito. *Nature* **392**, 289-292 (1998).

153. L. Lucantoni, R. Yerbanga, G. Lupidi, L. Pasqualini, F. Esposito, A. Habluetzel, Transmission blocking activity of a standardized neem (*Azadirachta indica*) seed extract

on the rodent malaria parasite *Plasmodium berghei* in its vector Anopheles stephensi. *Malaria Journal* **9**, 66 (2010).

154. I. W. Jones, A. A. Denholm, S. V. Ley, H. Lovell, A. Wood, R. E. Sinden, Sexual development of malaria parasites is inhibited in vitro by the neem extract azadirachtin, and its semi-synthetic analogues. *FEMS Microbiol Lett* **120**, 267-273 (1994)

155. O. Billker, M. K. Shaw, I. W. Jones, S. V. Ley, A. J. Mordue, R. E. Sinden, Azadirachtin Disrupts Formation of Organised Microtubule Arrays during Microgametogenesis of *Plasmodium berghei*. *Journal of Eukaryotic Microbiology* **49**, 489-497 (2002).

156. O. Coux, K. Tanaka, A. L. Goldberg, Structure and Functions of the 20S and 26S Proteasomes. *Annual Review of Biochemistry* **65**, 801-847 (1996).

157. W. Hilt, D. H. Wolf, Proteasomes: destruction as a programme. *Trends in Biochemical Sciences* **21**, 96-102 (1996).

158. A. Kreidenweiss, P. G. Kremsner, B. Mordmuller, Comprehensive study of proteasome inhibitors against *Plasmodium falciparum* laboratory strains and field isolates from Gabon. *Malar J* **7**, 187 (2008).

159. K. L. Rock, C. Gramm, L. Rothstein, K. Clark, R. Stein, L. Dick, D. Hwang, A. L. Goldberg, Inhibitors of the proteasome block the degradation of most cell proteins and the generation of peptides presented on MHC class I molecules. *Cell* **78**, 761-771 (1994).

160. R. W. King, R. J. Deshaies, J.-M. Peters, M. W. Kirschner, How Proteolysis Drives the Cell Cycle. *Science* **274**, 1652-1659 (1996).

161. H. L. Pahl, P. A. Baeurle, Control of gene expression by proteolysis. *Current Opinion in Cell Biology* **8**, 340-347 (1996).

162. Y. Wu, X. Wang, X. Liu, Y. Wang, Data-Mining Approaches Reveal Hidden Families of Proteases in the Genome of Malaria Parasite. *Genome Res.* **13**, 601-616 (2003).

163. B. Czesny, S. Goshu, J. L. Cook, K. C. Williamson, The proteasome inhibitor epoxomicin has potent *Plasmodium falciparum* gametocytocidal activity. *Antimicrob Agents Chemother* **53**, 4080-4085 (2009).

164. J. Nyalwidhe, K. Lingelbach, Proteases and chaperones are the most abundant proteins in the parasitophorous vacuole of *Plasmodium falciparum*-infected erythrocytes. *PROTEOMICS* **6**, 1563-1573 (2006).

165. J. Lelièvre, M. J. Almela, S. Lozano, C. Miguel, V. Franco, D. Leroy, E. Herreros, Activity of Clinically Relevant Antimalarial Drugs on *Plasmodium falciparum* Mature Gametocytes in an ATP Bioluminescence "Transmission Blocking" Assay. *PLoS One* **7**, e35019 (2012).

166. M. J. Delves, A. Ruecker, U. Straschil, J. Leliévre, S. Marques, M. J. López-Barragán, E. Herreros, R. E. Sinden, Male and female *P. falciparum* mature gametocytes show different responses to antimalarial drugs. *Antimicrob Agents Chemother*, (2013).

167. M. B. Cassera, Y. Zhang, K. Z. Hazleton, V. L. Schramm, Purine and pyrimidine pathways as targets in Plasmodium falciparum. *Curr Top Med Chem* **11**, 2103-2115 (2011).

168. G. A. Kicska, P. C. Tyler, G. B. Evans, R. H. Furneaux, K. Kim, V. L. Schramm, Transition state analogue inhibitors of purine nucleoside phosphorylase from *Plasmodium falciparum*. *J Biol Chem* **277**, 3219-3225 (2002).

169. A. Lewandowicz, V. L. Schramm, Transition state analysis for human and Plasmodium falciparum purine nucleoside phosphorylases. *Biochemistry* **43**, 1458-1468 (2004).

170. L. M. Ting, W. Shi, A. Lewandowicz, V. Singh, A. Mwakingwe, M. R. Birck, E. A. Ringia, G. Bench, D. C. Madrid, P. C. Tyler, G. B. Evans, R. H. Furneaux, V. L. Schramm, K. Kim, Targeting a novel *Plasmodium falciparum* purine recycling pathway with specific immucillins. *The Journal of biological chemistry* **280**, 9547-9554 (2005).

171. M. B. Cassera, K. Z. Hazleton, E. F. Merino, N. Obaldia, 3rd, M. C. Ho, A. S. Murkin, R. DePinto, J. A. Gutierrez, S. C. Almo, G. B. Evans, Y. S. Babu, V. L. Schramm, *Plasmodium falciparum* parasites are killed by a transition state analogue of purine nucleoside phosphorylase in a primate animal model. *PLoS One* **6**, e26916 (2011).

172. G. A. Kicska, P. C. Tyler, G. B. Evans, R. H. Furneaux, V. L. Schramm, K. Kim, Purine-less death in *Plasmodium falciparum* induced by immucillin-H, a transition state analogue of purine nucleoside phosphorylase. *The Journal of biological chemistry* **277**, 3226-3231 (2002).

173. D. C. Madrid, L. M. Ting, K. L. Waller, V. L. Schramm, K. Kim, P*lasmodium falciparum* purine nucleoside phosphorylase is critical for viability of malaria parasites. *The Journal of biological chemistry* **283**, 35899-35907 (2008).

174. M. Niikura, S. Inoue, S. Mineo, Y. Yamada, I. Kaneko, S. Iwanaga, M. Yuda, F. Kobayashi, Experimental cerebral malaria is suppressed by disruption of nucleoside transporter 1 but not purine nucleoside phosphorylase. *Biochemical and biophysical research communications* **432**, 504-508 (2013).

175. L. M. Ting, M. Gissot, A. Coppi, P. Sinnis, K. Kim, Attenuated *Plasmodium yoelii* lacking purine nucleoside phosphorylase confer protective immunity. *Nat Med* **14**, 954-958 (2008).

176. T. Q. Tanaka, K. C. Williamson, A malaria gametocytocidal assay using oxidoreduction indicator, alamarBlue. *Molecular and Biochemical Parasitology* **177**, 160-163 (2011)10.1016/j.molbiopara.2011.02.005).

177. C. J. Janse, P. F. Van der Klooster, H. J. Van der Kaay, M. Van der Ploeg, J. P. Overdulve, Rapid repeated DNA replication during microgametogenesis and DNA synthesis in young zygotes of *Plasmodium berghei*. *Trans R Soc Trop Med Hyg* **80**, 154-157 (1986).

178. S. K. Yanow, L. A. Purcell, G. Pradel, A. Sato, A. Rodriguez, M. Lee, T. W. Spithill, Potent Antimalarial and Transmission-Blocking Activities of Centanamycin, a Novel DNA-Binding Agent. *Journal of Infectious Diseases* **197**, 527-534 (2008).

179. P. Chavalitshewinkoon-Petmitr, G. Pongvilairat, R. K. Ralph, W. A. Denny, P. Wilairat, Inhibitory effects of 9-anilinoacridines on *Plasmodium falciparum* gametocytes. *Tropical Medicine & International Health* **6**, 42-45 (2001).

180. D. Figgitt, W. Denny, P. Chavalitshewinkoon, P. Wilairat, R. Ralph, In vitro study of anticancer acridines as potential antitrypanosomal and antimalarial agents. *Antimicrob Agents Chemother* **36**, 1644-1647 (1992).

181. S. A. Gamage, N. Tepsiri, P. Wilairat, S. J. Wojcik, D. P. Figgitt, R. K. Ralph, W. A. Denny, Synthesis and in vitro evaluation of 9-anilino-3,6-diaminoacridines active against a multidrug-resistant strain of the malaria parasite Plasmodium falciparum. *J Med Chem* **37**, 1486-1494 (1994).

182. S. Auparakkitanon, P. Wilairat, Cleavage of DNA induced by 9-anilinoacridine inhibitors of topoisomerase II in the malaria parasite Plasmodium falciparum. *Biochemical and biophysical research communications* **269**, 406-409 (2000).

183. A. F. Valdes, Acridine and acridinones: old and new structures with antimalarial activity. *Open Med Chem J* **5**, 11-20 (2011).
184. J. C. Wang, DNA Topoisomerases. *Annual Review of Biochemistry* **65**, 635-692 (1996).
185. A. Kumar, K. Srivastava, S. Raja Kumar, S. K. Puri, P. M. Chauhan, Synthesis of 9-anilinoacridine triazines as new class of hybrid antimalarial agents. *Bioorg Med Chem Lett* **19**, 6996-6999 (2009).

CHAPTER 2: ISOPRENOID PRECURSOR BIOSYNTHESIS IS THE ESSENTIAL ROLE OF THE APICOPLAST DURING GAMETOCYTOGENESIS IN *PLASMODIUM FALCIPARUM*

Jessica D. Wiley, Emilio F. Merino, Priscilla M. Krai, Kyle J. McLean, Abhai K. Tripathi, Joel Vega-Rodríguez, Michael Klemba, Marcelo Jacobs-Lorena, Maria B. Cassera

Manuscript in preparation for submission

ABSTRACT

Human malaria is a devastating disease that is caused by five species of *Plasmodium.* In the absence of an effective vaccine, drugs with novel mechanisms of action are urgently needed. Moreover, a renewed priority for malaria control and eradication has stimulated researchers to use multistage approaches to investigate and develop new therapies that will not only relieve malaria symptoms but stop its transmission. The malaria parasite harbors a relict plastid called the apicoplast and its discovery opened a new avenue for drug discovery and development due to its unusual and non-mammalian metabolism. This organelle is essential for intraerythrocytic and hepatic stages and there is strong evidence supporting its vital role during the mosquito stages. Moreover, the supply of the isoprenoid building blocks isopentenyl diphosphate (IPP) and dimethylallyl diphosphate (DMAPP) has been demonstrated to be the sole function of the apicoplast in the asexual intraerythrocytic stages. However, the metabolic role of the apicoplast during gametocyte development remains unknown. Here, we generated morphologically normal gametocytes lacking the apicoplast demonstrating that this organelle is essential during gametocytogenesis and its main role during these stages is to provide IPP for isoprenoid biosynthesis. Therefore, biosynthesis of isoprenoids remains as a valid drug target to develop transmission-blocking inhibitors.

Introduction

Human malaria is a devastating disease that is caused by five species of *Plasmodium*. Around 250 million cases of malaria occur every year with *Plasmodium falciparum* and *Plasmodium vivax* accounting for 95% of the infections (*1*). *P. falciparum*, the deadliest species, is resistant to most current antimalarials and emerging artemisinin-resistance, as marked by delayed clearance, has already been observed (*2*). In the absence of an effective vaccine, novel drugs with novel mechanism of action are urgently needed. Moreover, a renewed priority for malaria control and eradication has stimulated researchers to use multistage approaches to investigate and develop new therapies that will not only relieve malaria symptoms but stop its transmission (*3*).

All species of *Plasmodium* have a complex life cycle that is not very well understood at the metabolic level. *Plasmodium* parasites are transmitted from person to person during a blood meal of a female *Anopheles* mosquito. Mature female and male gametocytes, the transmission stages of the malaria parasite, are asymptomatic and non-replicating forms that can persist for weeks in the circulating blood. Different from other species of *Plasmodium*, *P. falciparum* gametocytes, develop through five morphologically distinct stages (I to V) and take 10 to 14 days to fully mature into stage V gametocytes that are released into the circulatory system (*4-6*). Additionally, mature stage V gametocytes require an additional two to three days to become infective to a mosquito (*7-10*). Immature gametocytes are often sensitive to schizonticides while mature gametocytes are insensitive, consequently, a person may have their clinical infection cleared but still can transmit the parasite to *Anopheles* mosquitoes for almost three weeks (*7, 9, 11*). Therefore, understanding the biology of the gametocytogenesis and revealing its metabolic requirements will expose novel drug targets offering new opportunities for development of therapeutic interventions.

The malaria parasite harbors a relict plastid called the apicoplast and its discovery opened a new avenue for drug discovery and development due to its unusual and non-mammalian metabolism (*12, 13*). This organelle is essential for intraerythrocytic and hepatic stages (*14, 15*), and there is strong evidence supporting its vital role during the mosquito stages (*16, 17*). To date, it is known that the apicoplast supports three metabolic functions: type II fatty acids, heme and isoprenoid biosynthesis. The *de novo* type II fatty acid biosynthesis has been demonstrated to be essential in liver stages and sporozoite development in the mosquito midgut but not in asexual

intraerythrocytic (*18-20*). During asexual blood stages, the parasite is able to salvage lipid from the host for apicoplast biogenesis (*21*). The *de novo* heme biosynthesis in the malaria parasite is unique since it encompasses several enzymes localized in three cellular compartments (mitochondria, apicoplast and cytosol) (*22, 23*). Recently, it has been demonstrated to be essential in the mosquito and liver stages while in the intraerythrocytic stages complement the host heme (*24*).

The supply of the isoprenoid precursors isopentenyl diphosphate (IPP) and dimethylallyl diphosphate (DMAPP) has been demonstrated to be the sole function of the apicoplast in the asexual intraerythrocytic stages (*15*). These building blocks used to synthesize all isoprenoid derivatives, occurs through the methylerythritol phosphate (MEP) pathway in the apicoplast and this pathway is absent in humans (*25, 26*). Isoprenoids represent the largest class of small molecules on earth with more than 40,000 compounds described. Isoprenoids are essential for life and are involved in a wide variety of biological functions, spanning from compartmentalization and stability to signaling and cell cycle control (*27*). Once IPP and DMAPP are transported out of the apicoplast, a myriad of isoprenoid products with different cellular localization and functions are synthesized in the malaria parasite.

At present, many isoprenoids products have been identified to be present in the intraerythrocytic asexual stages of *P. falciparum* such as dolichols (*28-30*), ubiquinones and menaquinone (*31-33*), carotenoids (*34, 35*), vitamin E (*36*), and prenylated proteins (*29, 37-40*). Ubiquinones are vital to the integrity of mitochondria election transport (*41*). Carotenoids have antioxidant properties and can regulate membrane fluidity (*41, 42*) and increased carotenoid production upon treatment with chloroquinine (which causes oxidative stress) indicated that, in *P. falciparum*, the main function of carotenoids may be as antioxidants (*34, 41*). Dolichols are important for co- and post-translational modifications of proteins in *Plasmodium*, such as *N*-linked glycosylation (*28, 41*), and are required for the coupling of glycosylphosphatidylinositol (GPI) anchors and carbohydrates in *P. falciparum* asexual intraerythrocytic parasites (*43*). Additionally, dolichols had been found as modifications in proteins but the role of protein dolicholation in *P. falciparum* remain unclear (*29*). Protein prenylation involves the covalent attachment of farnesyl (C_{15}) or geranylgeranyl (C_{20}) moieties to cysteine residues *via* a thioether linkage and their respective isoprenoid diphosphate precursors catalyzed by protein prenyl transferases (*44, 45*). Prenyl modification is relevant for several biological process such as

membrane association and localization (*37, 41, 46*), signal-transduction pathways, regulation of DNA replication, cell cycle progression (*41, 47*), erythrocyte invasion (*41, 48*), vesicular trafficking *via* SNARE proteins (soluble *N*-ethylmaleimide sensitive fusion attachement protein) (*41, 48*), GTPases (*41, 42, 46*), and palmitoylation (*44, 45*). Moreover, several inhibitors targeting different steps of isoprenoid biosynthesis, such as fosmidomycin (FOS), are lethal to the malaria parasite in the intraerythrocytic stages, supporting the biological relevance of isoprenoids as drug targets (*25, 26, 34, 38-40, 49-52*).

Metabolic requirements during gametocytogenesis still remains poorly understood. Recently, it was demonstrated that stage III gametocytes have increased glucose uptake as compared to mature asexual stages which is associated with an increased catabolism of glucose through the tricarboxylic acid (TCA) cycle in the mitochondria (*53*). Concurring with these findings, previous reports showed that gametocyte mitochondria are markedly different from asexual stages at morphological and electron transport activity levels (*54, 55*). The metabolic remodeling of the central carbon metabolism associated with gametocyte development is the first direct evidence that gametocyte stages are metabolically distinct from asexual stages and further investigation is needed to advance our understanding of other metabolisms.

FOS inhibits *P. falciparum* 1-deoxy-D-xylulose-5-phosphate reductoisomerase (DXR), the second enzyme of the MEP pathway, with an IC_{50} of 28 nM for the recombinant enzyme and between 300 and 1,200 nM for *P. falciparum* cell culture, depending on the strain (*25, 26*). A recent study indicated that FOS may also indirectly inhibit MEP cytidylyltransferase through accumulation of 2-*C*-methylerythrose 4-phosphate, a putative reaction intermediate (*52*). FOS and other antibiotics targeting the apicoplast do not affect late-stage gametocytes (*56, 57*) which could be expected since the apicoplast does not elongate and divide during gametocytogenesis (*55*). However, the metabolic role of the apicoplast during gametocyte development remains unknown.

During the early stages of the gametocytogenesis, parasites catabolized hemoglobin and no hemoglobin can be observed in the cytosol of the infected-erythrocyte by stage III. Mature gametocytes are insensitive to chloroquine while developing gametocytes are killed (*58, 59*) also supporting active hemoglobin digestion. In asexual stages, hemoglobin digestion occurs in the food vacuole where hemozoin crystals forms (*60*). However, very little is known about the food vacuole during gametocytogenesis. In addition, it has been shown that in gametocytes, hemozoin

accumulates in Garnham bodies (G-bodies) (*61, 62*). These G-bodies were originally described in 1933 as objects exhibiting a tendency to "form loops, ellipses and coils, and eventually appear to disintegrate" (*61*), and more recently, a protective role was suggested for them (*62*). However, if hemozoin crystals are transported to the G-bodies after formation or if vesicles transporting hemoglobin are accumulated in the G-bodies before crystals are formed, still remains unknown (*62*). Moreover, there is evidence supporting that proteins in the food vacuole may be prenylated (*46, 63*) and FOS treatment in asexual stages causes mislocalization of Rab5 as well as compromised the food vacuole integrity (*46*).

To investigate the role of the apicoplast and isoprenoid biosynthesis during gametocytogenesis, we generated asexual intraerythrocytic stages parasites lacking the apicoplast as described previously by Yeh and DeRisi (*15*) and induced gametocytogenesis. Using this approach, normal stage V gametocytes lacking the apicoplast were successfully generated. Our study revealed that the apicoplast is essential for *P. falciparum* gametocytogenesis and mosquito stages. Here, we demonstrate that the supply of isoprenoid precursors is the main role of the apicoplast during the sexual intraerythrocytic stages.

Results

P. falciparum asexual stages lacking the apicoplast present normal gametocytogenesis under continuous supply of IPP

Yeh and DeRisi demonstrated that isoprenoid biosynthesis is the main function of the apicoplast during the asexual intraerythrocytic stages by treating parasites with doxycycline (DOX), which inhibits translation in the apicoplast and irreversible loss of the organelle, and supplying IPP (chemical rescue) in the culture media (*15*). We hypothesized that the apicoplast may have a similar function in gametocyte stages and that isoprenoids may play a key role in

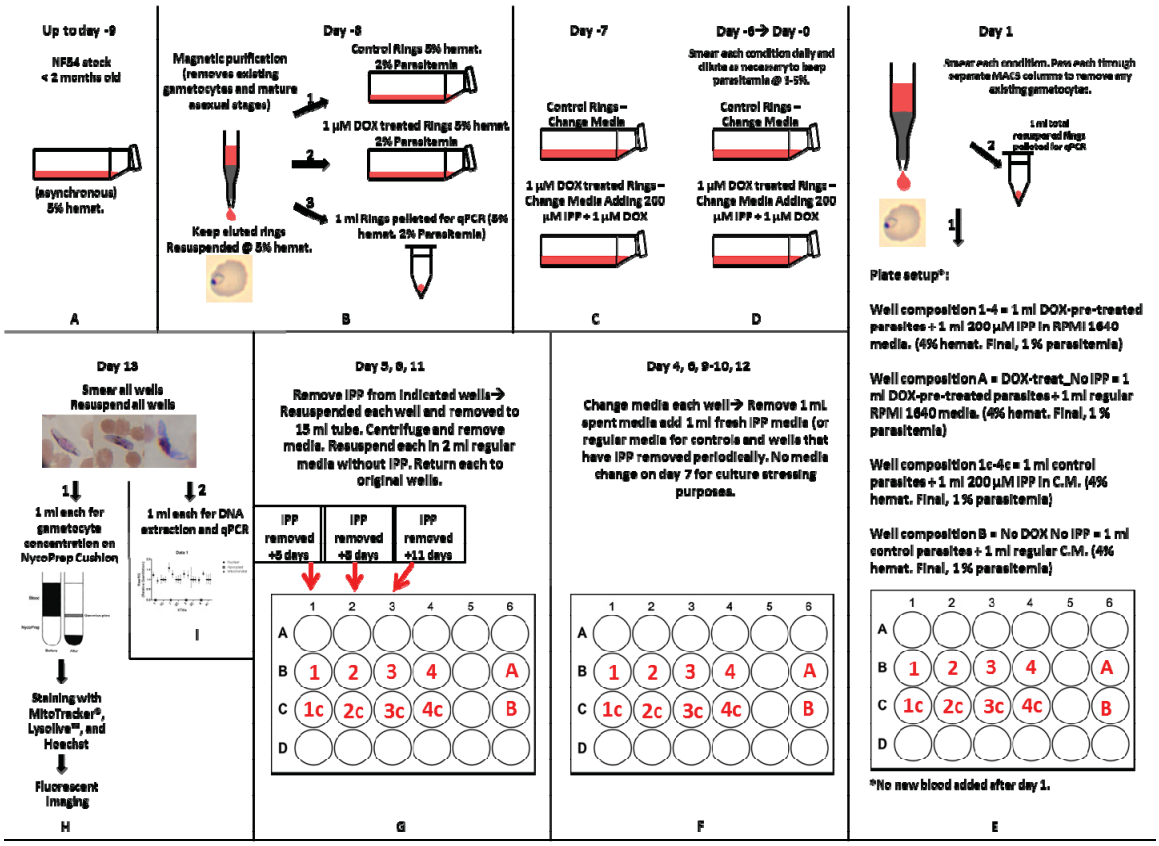

Figure 2. 1. Scheme of the procedure to generate API-minus *P. falciparum* gametocytes. *P. falciparum* API-minus generation previous inducing gametocytogenesis (panels A to D). After at least 8 days of DOX treatment, ring stages form DOX-treated and control cultures were recovered and subcultures for gametocytogenesis induction were set as indicated (panel E). IPP was sequentially removed as indicated on panel G. Smears where also performed before removing IPP. On day 13 post-gametocytogenesis induction, parasites were recovered for morphological evaluation (panel H).

gametocytogenesis. To test this hypothesis, highly synchronic ring stage parasites lacking the apicoplast (API-minus) were generated following the scheme outlined in Figure 2.1 (panels A to D) and as described in Materials and Methods. After one week of drug pressure, DOX pressure

was removed and four sub-cultures were set for gametocytogenesis induction (Figure 2.1E, conditions 1 to 4). Asexual parasites harboring the apicoplast (control cultures that were not exposed to DOX treatment) were processed in parallel and set under identical conditions as API-minus parasites. IPP was supplied to also control parasites to investigate the effect of excess IPP on control gametocytes (Figure 2.1, conditions 1C to 4C). A sub-culture from control parasites without IPP supplementation was included (Figure 2.1E). In order to test if isoprenoids may play a key role during gametocytogenesis, IPP was supplied to condition 1 and 1C for five days, to condition 2 and 2C for eight days, to condition 3 and 3C for 11 days, and to condition 4 and 4C for 12 days when all conditions were recovered for morphological evaluation and qPCR (Figure 2.1). For each condition, aliquots were processed for Giemsa-stained smears (Figure 2.2A), qPCR (Figure 2.2B) and fluorescence microscopy (Figure 2.3). Samples were also taken before and after DOX pre-treatment for qPCR analysis to ensure that asexual parasites were API-minus before inducing gametocytogenesis (data not shown). Giemsa-stained smears performed before removing IPP from each condition indicated that 5 days after setting the sub-cultures gametocytogenesis started (condition 1), after 8 days gametocytes were in stage II-III (condition 2), and after 11 days gametocytes were in stage IV (condition 3). Since sexually committed merozoites take 192-216 h to develop to stage V (*64*), parasites recovered on day 13 were mostly in stage V. Severe morphological defects were observed in Giemsa-stained API-minus gametocytes where IPP was removed early in development (conditions 1 and 2), when compared to controls and conditions 3 and 4 where IPP was supply until stages IV and V, respectively (Figure 2.2A). The qPCR analysis, using primers for genes tufA (apicoplast), cytb3 (mitochondria), CHT1 (nuclear), and tRNA synthase (reference primer) indicated that gametocytes from conditions 1-4 had effectively lost their apicoplast genome while the mitochondrial and nuclear DNA remained intact (Figure 2B). In addition, we did not observe any gametocyte or asexual stages in the subculture of ring stage API-minus parasites without IPP supplementation the end of the experiment.

To assess whether apicoplast minus gametocytes where IPP was supplemented during the entire experiment (condition 4) were alive at the time of collection, API-minus gametocytes were incubated with alamarBlue, an oxidoreduction indicator (*65*). AlamarBlue is a reporter of metabolic activity and the active ingredient (resazurin) is thought to be reduced by mitochondrial enzymes (*65-67*). AlamarBlue has been developed into gametocytocidal assays with great

success (*57, 65, 68*). API-minus mature gametocytes supplemented with IPP or control gametocytes were incubated with alamarBlue for 24 hours and then read with a microplate reader at 590 nm after excitation at 530 nm (Figure 2.2C). API-minus gametocytes presented high fluorescent similar to control gametocytes (Figure 2.2C). The higher fluorescence detected was due to differences in the parasite loading in the assay.

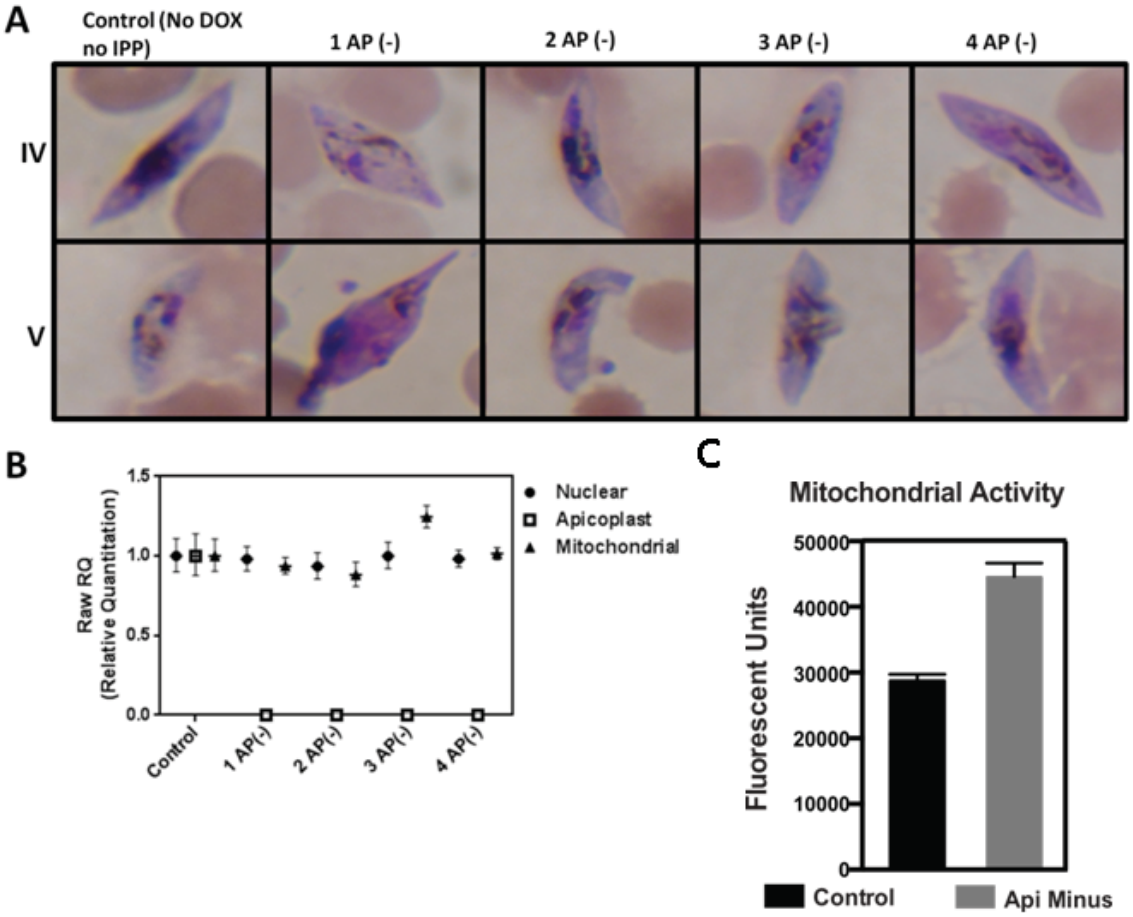

Figure 2. 2. Giemsa staining and qPCR of control and API-minus gametocytes. (A) Representative Giemsa stains of stages IV and V *P. falciparum* gametocytes. Nucleus is observed in dark pink and pigments in brown. Abnormal morphogenesis was observed when IPP was removed early in the gametocytogenesis while parasites maintained under continuous IPP supplementation developed morphologically normal gametocytes. (B) qPCR analysis showing that API-minus gametocytes have lost their apicoplast DNA while maintaining mitochondrial and nuclear DNA. (C) AlamarBlue assay demonstrating mitochondrial activity of API-minus gametocytes.

We also calculated the gametocytes stage distribution for all conditions and found that removing IPP early in development changed the stage distribution during gametocytogenesis

where, after 13 days, the population was in general younger than control (Figure 2.3). The excess of IPP in control gametocytes did not significantly change the stage distribution. Taking together, our results support the hypothesis that asexual parasites require isoprenoid biosynthesis to start and sustain gametocytogenesis and supply of isoprenoid precursors is the main role of the apicoplast during gametocytogenesis.

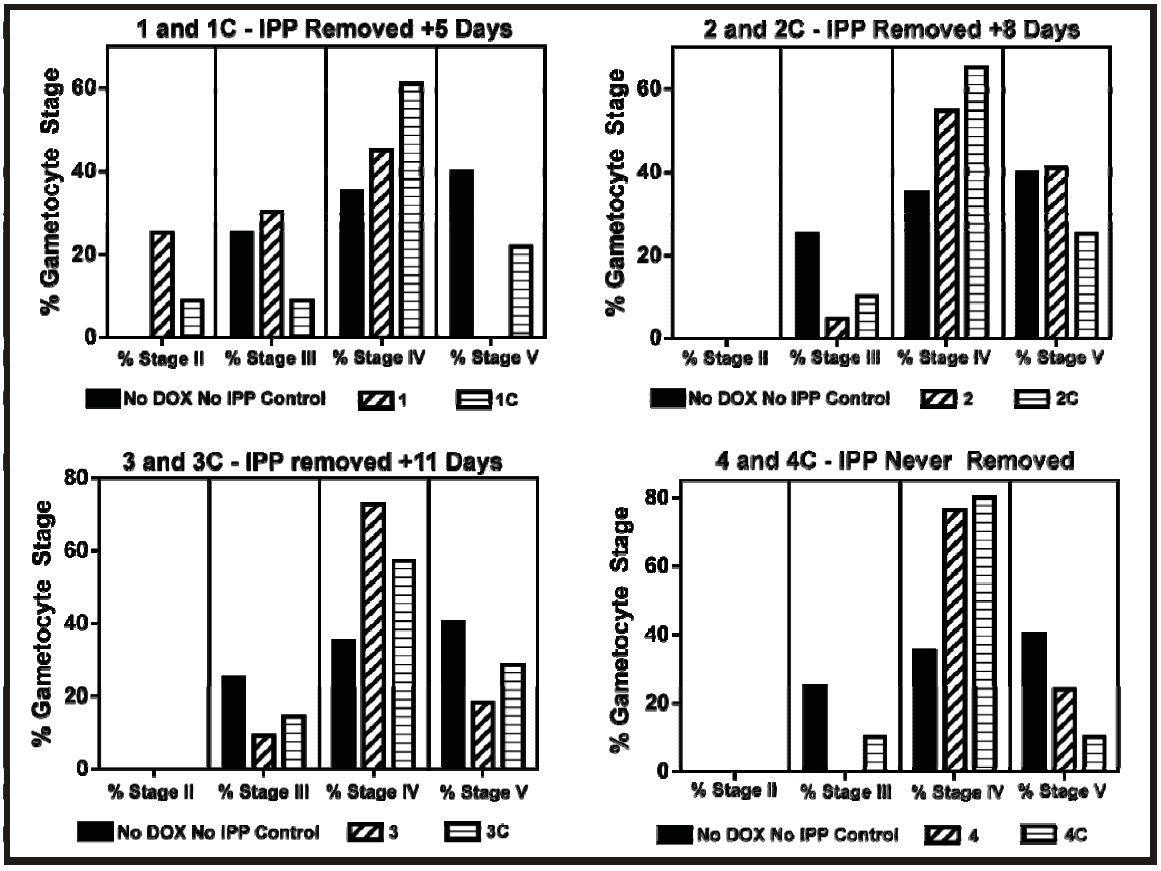

Figure 2. 3. Stage distribution from API-minus and control gametocytes. Gametocytes where IPP was removed early in development presented a younger overall population at the end of 13 days as measured by Giemsa and fluorescent imaging.

Isoprenoid precursors are essential for normal food vacuole-like system formation and mitochondrial membrane potential.

Early stages of the gametocytogenesis catabolized hemoglobin; however, very little is known about the food vacuole during gametocytes stages. A previous report showed that FOS treatment causes mislocalization of Rab5 and compromised the food vacuole integrity in asexual

stages (*46*). Moreover, isoprenoid precursors are necessary to assemble the isoprenic side-chain of ubiquinones (*31, 32*) and are vital to the integrity of mitochondria election transport (*41*). Therefore, we hypothesized that if a food vacuole-like system is present in early stage gametocytes and isoprenoids are involved in its biogenesis, API-minus parasites may also present a defective food vacuole-like system as well as a reduced mitochondria election transport. To address this hypothesis, gametocytes generated as describe in Figure 2.1 were stained with LysoLive™ to observe at the lysosomal or acidic vesicle formation and MitoTracker® to examine the mitochondrial membrane potential (Figure 2.4). In asexual intraerythrocytic stages of the parasites, LysoLive™ is co-localized to the food vacuole where hemoglobin digestion occurs (Figure 2.5); however, has never been used in gametocyte stages. LysoLive™ contains a sensitive substrate for esterase activity, an enzyme ubiquitous to all normal lysosomes. Fluorescence is increased upon cleavage by the esterase indicating lysosomes with metabolic health of the organelle. LysoLive™ also labels the parasitophorous vacuole membrane for still an unknown reason.

Control gametocytes exhibited a robust mitochondrial membrane potential as evidenced by strong MitoTracker® signal (Figure 2.4, panel No DOX No IPP). The endocytic vesicle formation in control gametocytes, as marked by LysoLive™, demonstrates a punctate network of endocytic vesicles formed up until stage IV (Figure 2.4) and was also observed in stage V gametocytes (data not shown). We are terming this punctate endocytic network a food vacuole-like system. In gametocytes where IPP was removed after five days of development, mitochondrial membrane potential appears severely reduced as there was only a faint MitoTracker® labeling (Figure 2.4, panel 1). Additionally, those gametocytes demonstrate a total lack of the food vacuole-like system that was present in control gametocytes (Figure 2.4, panel 1). API-minus gametocytes where IPP was removed early in development show vast morphological defects

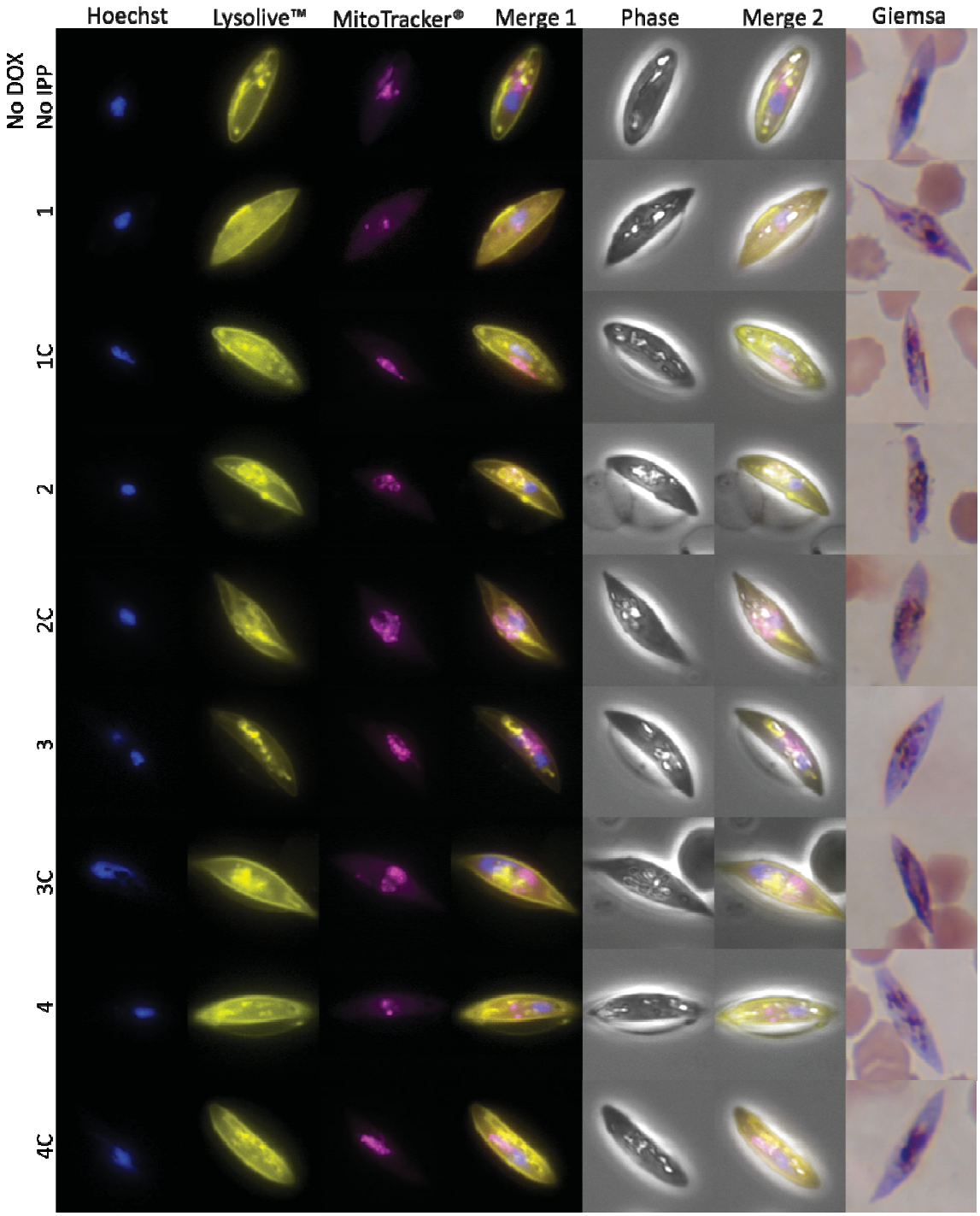

Figure 2. 4. Lack of defined internal organelles and mitochondrial membrane potential in API-minus gametocytes with earlier IPP removal. Representative Giemsa-stained microscopy and widefield epifluorescence for nucleus (Hoechst), PVM and endocytic vesicles (Lysolive™), and mitochondria (MitoTracker®) comparing control gametocytes (denoted by C after number) and API-minus gametocytes (denoted by numbers only). IPP was removed after 5 days (1 and 1C), after 8 days (2 and 2C), after 11 days (3 and 3C). Conditions 4 and 4C were supplemented until the end of the experiment.

visualized by Giemsa stains (Figure 2.4, Giemsa panels). These morphological defects were not present when IPP was supplemented until the end of the experiment (Figure 2.4, panels 2, 3, 4). Control gametocytes where IPP was also supplied, did not show abnormalities compared to the control without IPP supplementation (Figure 2.4, panels 1C, 2C, 3C, 4C). The longer IPP was supplemented to the API-minus gametocytes, the more intact food vacuole-like system and mitochondrial potential recovery were observed (Figure 2.4, panels 2, 3, 4). Taken together, our results supports isoprenoid precursors are essential for normal food vacuole-like network and mitochondria development during gametocytogenesis.

Co-localization of LysoLive™ and Dextran Texas Red® supports the presence of tubular food vacuole-like system in gametocyte stages

The use of LysoLive™ has not been reported previously with malaria parasites. Therefore, to verify that we were visualizing food vacuole-like system during gametocytogenesis, we performed a co-localization study with LysoLive™ and Dextran Texas Red® (DTR). Dextrans contain unique α-1,6-poly-glucose linkages which are resistant to proteolytic cleavage by most endogenous cellular glycosidases; therefore,

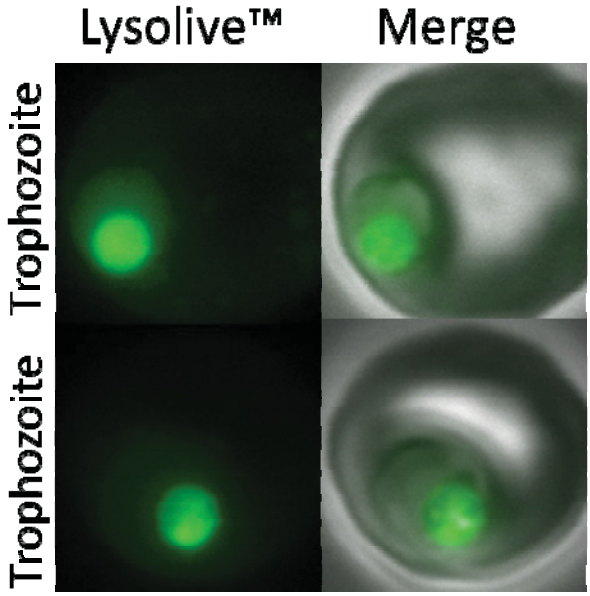

Figure 2. 5. LysoLive™ stain the food vacuole of asexual *P. falciparum* parasites. Asexual trophozoites demonstrating LysoLive™ accumulates in the food vacuole, therefore, serving as a metabolic marker for organelle localization.

dextran conjugates make ideal long-term markers for live cells. Fluorescent dextrans, such as DTR, is a valuable tracer for the uptake and internal processing of exogenous material by phagocytotic and endocytic pathways (*69*). In asexual parasites, DTR is ingested by the cytostome (specialized parasite organelle for endocytosis) in early stages of the parasites development and transported to the food vacuole allowing to visualize trafficking and localization of vesicles and organelles containing hemoglobin (*70*). We found that LysoLive™ localized in the food vacuole in trophozoite stages (Figure 2.5).

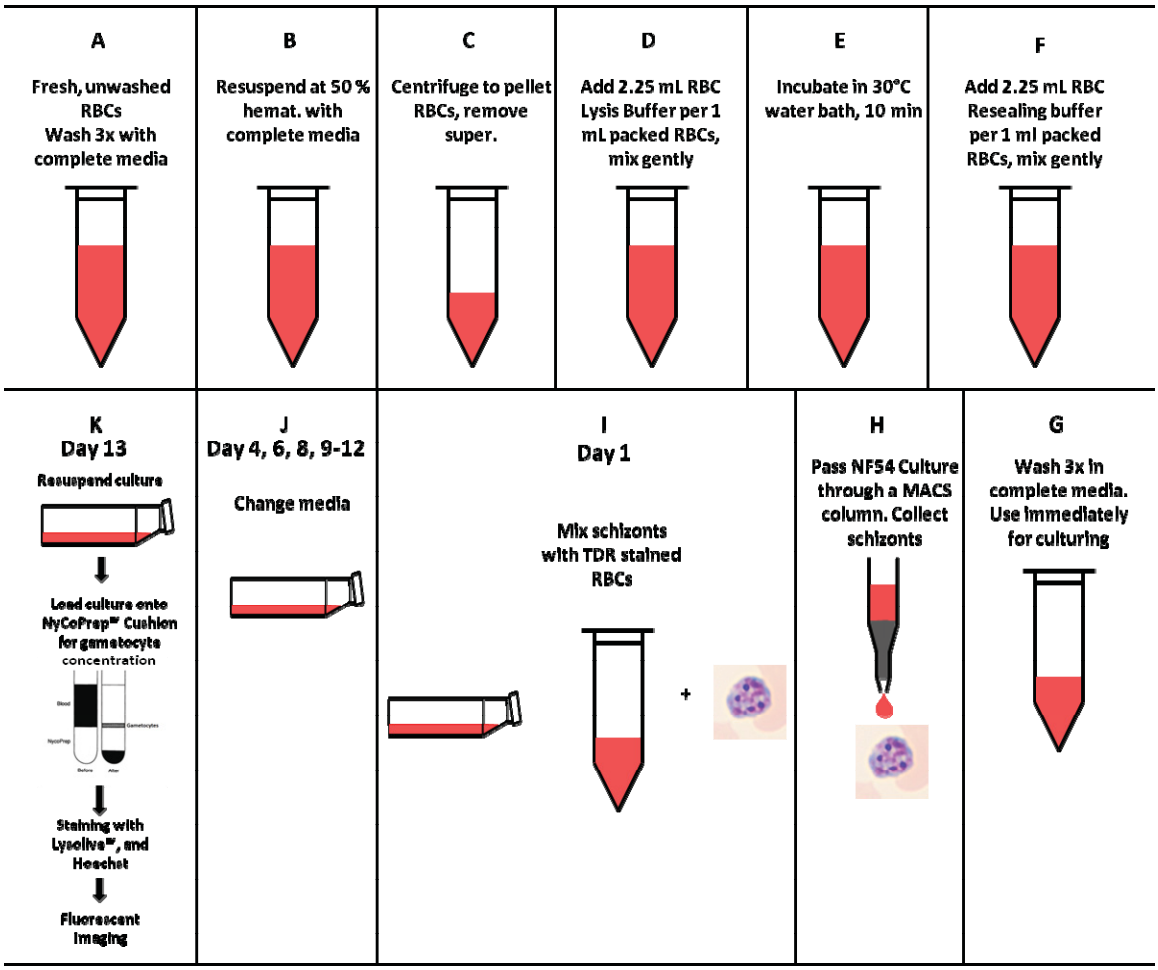

Figure 2. 6. Scheme for Dextran Texas Red® labeling of RBCs and gametocyte generation.

For this purpose, red blood cells (RBCs) were labelled with DTR based on a method from Saliba and colleagues with modifications (Figure 2.6) (*60*). MACS purified mature schizont stage NF54 strain were mixed with DTR stained RBCs to allow invasion of the stained RBCs.

Parasites were cultured under gametocytes inducing conditions for 13 days, labeled with LysoLive™, and imaged (Figure 2.7). Co-localization was observed between LysoLive™ and DTR confirming that LysoLive™ is indeed marking food vacuole-like structures (Figure 2.7). This is the first time that a food vacuole-like system is shown in gametocytes stages.

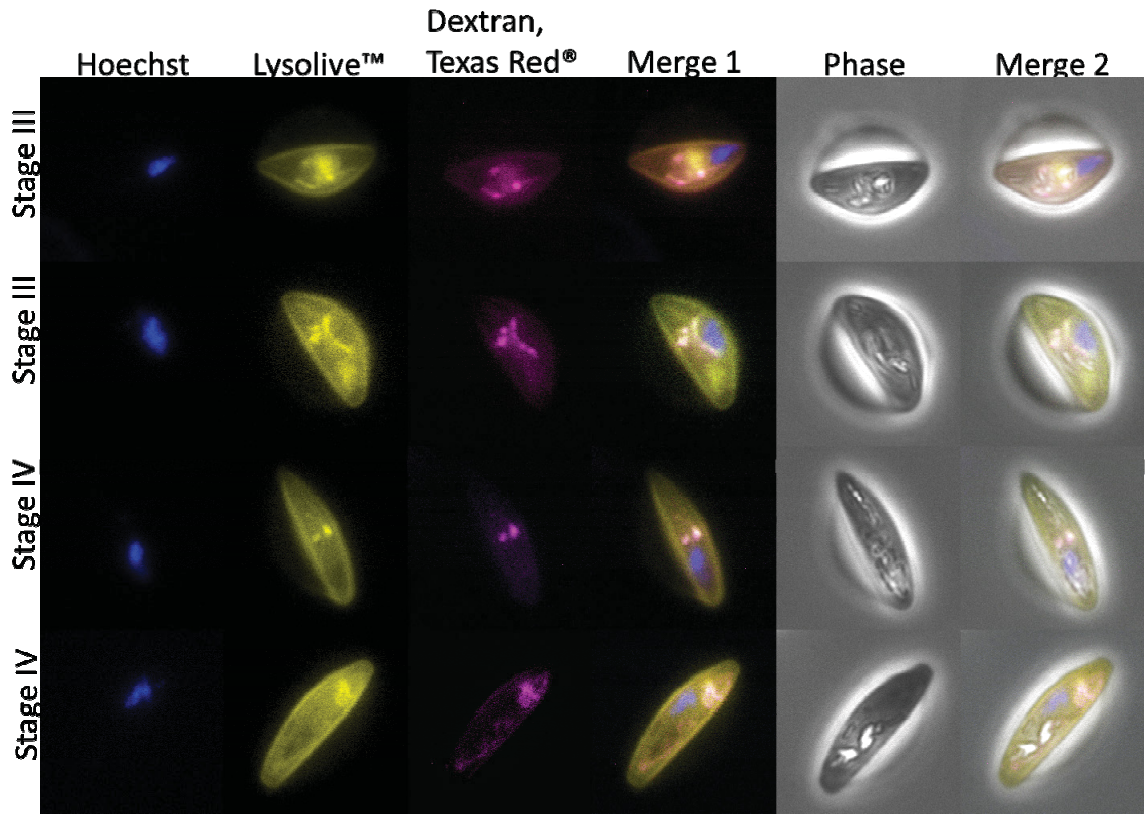

Figure 2. 7. Co-localization of LysoLive™ and Dextran Texas Red®. Co-localization was observed between LysoLive™ and Dextran Texas Red® after 13 days of gametocyte development in RBCs containing Dextran Texas Red® before invasion and gametocyte development indicating that tubular-vesicular structure stained by LysoLive™ correspond to food vacuole-like structures.

API-minus gametocytes present normal formation of vesicles and Garnham bodies

As mentioned above, gametocytes appear to place hemozoin into G-bodies and push these vesicles out from their body (*61, 62*). Recently, it was demonstrated that *P. falciparum* gametocytes could form "exosome-like vesicles" and erythrocyte-derived microvesicles that are involved in mediating communication between cells and with the host immune system and potentially as a response to environmental changes (*71, 72*). It was also shown that these vesicles are internalized by neighboring parasitized cells and induce gametocytogenesis (*71, 72*). We

observe both what appear to be “exosome-like vesicles” (Figure 2.8, white arrows, column 2) and G-bodies (Figure 2.8, black arrows, column 4). Further experimentation is needed to determine the true nature of the bodies; however, we can conclude that the API-minus gametocytes are still capable of producing these vesicles and G-bodies even when IPP was removed early during gametocyte development.

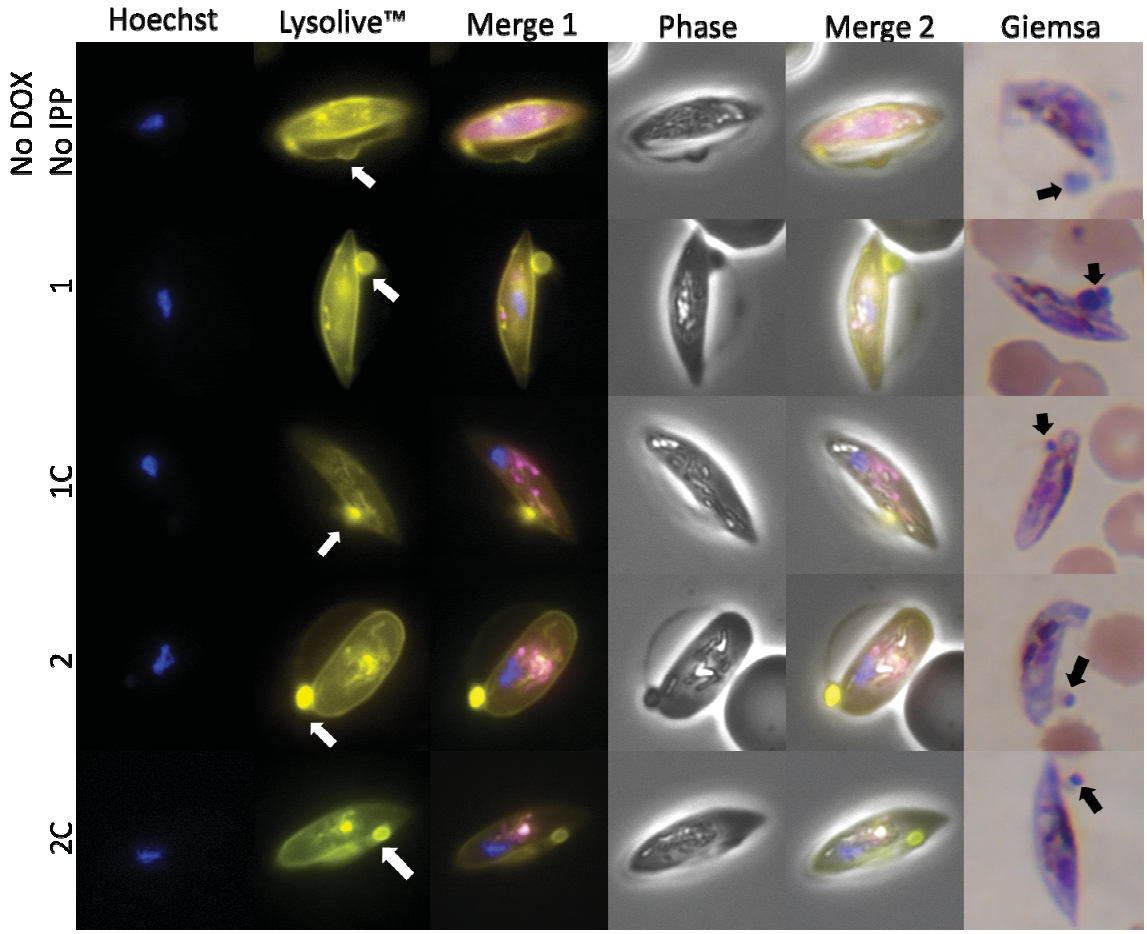

Figure 2. 8. Vesicles and G-Bodies formation is not affected by the lack of apicoplast. We observed these structures both on gametocytes control and API-minus gametocytes regardless if IPP was continuously supplemented or not.

The MEP pathway intermediates are present in stage IV and V gametocytes

FOS and other antibiotics targeting the apicoplast do not affect late-stage gametocytes (*56, 57*) as we also observed here (Figure 2.9A). A small study in 32 patients treated only with FOS revealed a significant increase in gametocyte carriers by the end of the study compared with the same patients on the initial treatment day (*73*). Therefore, we investigated if FOS triggers gametocytogenesis *in vitro* (Figure 2.9B). To study if FOS triggers gametocytogenesis, we set highly synchronic ring stage NF54 strain cultures for 13 days with or without 10 µM FOS under gametocyte inducing conditions (Figure 2.9B). Media alone or supplemented with FOS was replaced six times during the 13-day period. After 13 days, the cultures were recovered and the parasitemia of asexual and sexual stages was assessed from Giemsa-stained smears. At 10 µM FOS, both asexual and gametocyte stages were cleared, indicating that FOS does not induce gametocytogenesis *in vitro* after 13 days of treatment.

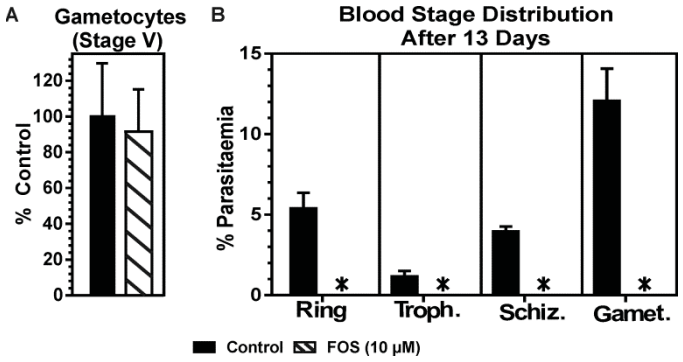

Figure 2. 9. FOS does not induce gametocytogenesis. FOS treatment does not affect stage V *P. falciparum* gametocytes (A) and does not gametocytogenesis *in vitro* (B). Blood distribution was assessed by Giemsa-stained smears.

All together our results showed that isoprenoid biosynthesis is essential for gametocytogenesis, especially during early stages of the development. However, lack of FOS inhibition in late stage gametocytes (Figure 2.9A) raised the question of whether the MEP pathway is still active through gametocyte stages IV to V or whether FOS is not transported in late gametocyte stages. The presence and activity of the MEP pathway has not been investigated in gametocytes. In fact, we detected the MEP pathway intermediates in mature gametocytes (stages IV-V) (Figure 2.10). Since API-minus gametocytes where IPP supply was removed at stage II-IV presented normal morphological development (Figures 2.2 and 2.4) and MEP intermediates are present in late stages but FOS treatment do not affect late stages, all together,

our results indicates that all the necessary isoprenoid products for gametocytogenesis are mostly synthesized during early stages (I to III).

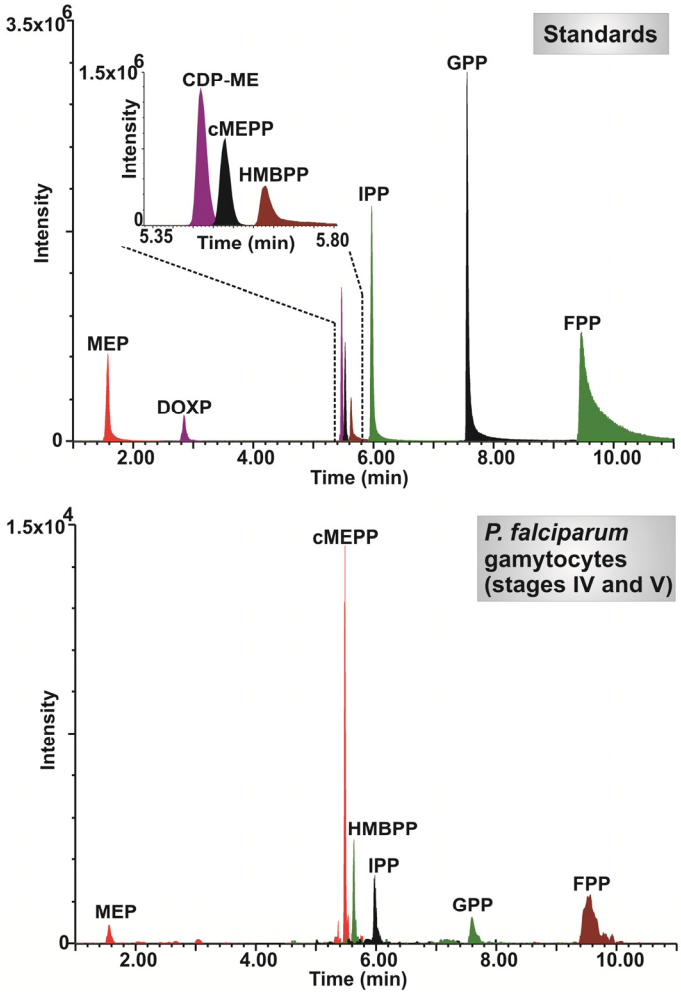

Figure 2. 10. Detection of MEP pathway intermediates by IP-RP-UPLC-MS/MS in *P. falciparum* gametocytes. MEP pathway intermediates standards (top panel) and stage IV and V gametocytes combined extracted ion chromatogram of each MRM channels for the indicated metabolites detected as follows (precursor ion mass > product ion mass): MEP (215.1 > 78.8), DOXP (213.1 > 96.8), CDP-ME (520.3 > 322.0), cMEPP (277.1 > 78.8), HMBPP (261.1 > 78.8), IPP (245.1 > 78.8), GPP (313.2 > 78.8), FPP (381.3 > 78.8).

Discussion

The apicoplast has been established as an excellent drug target in asexual intraerythrocytic stage *P. falciparum* due to its unusual and non-mammalian metabolism (*12, 13*). The apicoplast contains its own 35 kb prokaryotic-like genome, yet is not self-sufficient, as it requires many proteins that are nuclear encoded and then targeted to the organelle. Apicoplast protein targeting has also been suggested as a potential drug target in *P. falciparum* (*74*). It is predicted that approximately 540 gene products in the *P. falciparum* nuclear genome are targeted to the apicoplast, representing about 10% of the total parasite predicted genes (*75*). Of the genes encoding anticipated apicoplast-targeted proteins, around 16% have unknown function and the majority are involved in housekeeping functions (~55%) (*75*).

Here, we demonstrated that the apicoplast is essential during gametocytogenesis and that the sole role of the apicoplast during gametocyte development is to provide IPP for isoprenoid biosynthesis by generating morphologically normal API-minus gametocytes. In addition, API-minus gametocytes where IPP was removed early in development presented severe morphological defects. The apicoplast is the sole source of isoprenoid precursors through the MEP pathway, and while the apicoplast does not elongate and divide, as in asexual intraerythrocytic *P. falciparum*, it is metabolically active. Moreover, API-minus gametocytes where IPP supply was removed at stage II-IV presented normal morphological development (Figures 2.2 and 2.4) and MEP intermediates are present in late stages but FOS treatment does not affect late stages. Altogether, our results suggest that all the necessary isoprenoid products for gametocytogenesis are mostly synthesized during early stages (I to III).

In addition, our results supports that the changes in apicoplast metabolism during gametocytogenesis could be responsible for changes in FOS sensitivity. Comprehensive analysis of apicoplast targeting drugs should be followed through sexual development to gain insight on their effect in these stages. A drug may not have an apparent effect on gametocytes but may prevent sexual development in the mosquito stages due to apicoplast inhibition, as appears to be the case of Azithromycin (AZM). AZM is a macrolide compound that has been used for bacterial infections and targets the apicoplast as demonstrated by its "delayed death" phenotype and the fact that progeny parasites cannot develop due to abnormal apicoplast development (*16, 76, 77*). AZM is well tolerated in patients, including children and pregnant women, and has been used broadly for bacterial infections (*16, 78-81*). AZM as well as DOX and tetracycline had no effect

on *P. falciparum* gametocytes (*82, 83*). The rodent malaria *P. berghei* was used to investigate AZMs effect on mosquito stages (*16*). While gametocyte development is different in *P. falciparum* gametocytes than in *P. berghei*, the effects of AZM on mosquito stages is proposed to have a similar effect. AZM had no effect on male gametocyte exflagellation, but one dose of AZM (400 mg/kg) was shown to subdue parasite development in all four stages in the mosquito vector supporting the essential role of the apicoplast also during the mosquito stages (*16*).

It is known that early stages of the gametocytogenesis catabolized hemoglobin, very little is known about the food vacuole during gametocytes stages. Here, we reported the use of LysoLive™ to visualize the food vacuole-like system during gametocytogenesis. A co-localization study with LysoLive™ and Dextran Texas Red® revealed for the first time a food vacuole-like system in gametocytes stages. This system appeared as in a tubular-vesicular shape different from asexual stages where a single vacuole can be observed. In addition, FOS treatment in asexual stages causes defective formation of the food vacuole (*46*). We observed a defective food vacuole-like system in API-minus gametocytes where IPP supplementation was removed earlier during gametocytogenesis indicating the role of isoprenoid products in their biogenesis.

Isoprenoids represent the largest class of small molecules essential for life and are involved in a wide variety of biological functions, spanning from compartmentalization and stability to signaling and cell cycle control (*27*). Here, we demonstrated the essential role of isoprenoid products during gametocytogenesis validating their biosynthesis as potential drug targets to develop transmission-blocking inhibitors.

Materials and Methods

Cell Cultures

P. falciparum strain NF54, MRA-1000, deposited by M. Dowler, Walter Reed Army Institute of Research, was obtained through the MR4 Malaria Reagent Repository (ATCC, Manassas, VA) as part of the BEI Resources Repository, NIAID, NIH. NF54 is chloroquine-sensitive strain and is capable of producing gametocytes. As with all gametocyte-producing strains, NF54 loses the ability of producing gametocytes after continuous *in vitro* culturing. Therefore, a new aliquot of NF54 was used every two months to keep gametocyte production high. *P. falciparum* NF54 were cultured in O-positive red blood cells (RBCs) (Interstate Blood Bank Inc., Memphis, Tennessee) at 4% hematocrit in RPMI 1640 medium supplemented with 5 g/L Albumax I (GIBCO Life Technologies) 2 g/L glucose (Sigma-Aldrich), 2.3 g/L sodium bicarbonate (Sigma-Aldrich), 370 µM hypoxanthine (Sigma-Aldrich), 25 mM HEPES, and 20 mg/L gentamycin (GIBCO Life Technologies). Parasites were kept at 37˚C under reduced oxygen conditions (5.06% CO_2, 4.99% O_2, and 89.95% N_2).

Fosmidomycin treatment of late stage gametocytes

To verify that fosmidomycin (FOS) was active in killing *P. falciparum* late stage gametocytes, *P. falciparum* NF54 late stage gametocytes (stage IV-V) were generated as previously reported (*84*) . Briefly, asexual stage parasites were synchronized by sorbitol treatment two days before setting sub-cultures to induce gametocytogenesis (*85*). On day nine of the sub-cultures, parasites were treated with 5% sorbitol for 10 min at 37 °C to remove asexual stages. Sorbitol treatment was repeated for four consecutive days which effectively removes >99% of asexual parasites. Gametocyte recovery and concentration was achieved on day 13 using a NycoPrep 1.077 cushion (*59*), and the number of gametocytes was calculated using a Neubauer chamber. About 30,000-50,000 gametocytes per well were added to black flat-bottom half-area 96-well plates containing serially diluted FOS (highest concentration 10 µM final) in a 100 µl final volume. The plate was incubated in a humidified chamber at 37 °C and reduced oxygen conditions (5.06% CO_2, 4.99% O_2, and 89.95% N_2) for 72 h. Alamar Blue was added on day 16 post induction at 10% of the well volume (*65*). The plate was incubated for an additional 24 h and then was read in a microplate reader at 585 nm after excitation at 540 nm. The IC_{50} values were calculated using a dose-response curved fitting with GraFit. The reported IC_{50} values

are the average of two independent experiments where each experiment was performed in duplicate and are expresses ± S.D. Epoxomicin was used as a positive control.

Fosmidomycin treatment during gametocytogenesis

To determine if FOS was effective in preventing gametocytogenesis, low (500 nM) and high concentrations (10 μM) of FOS were added to NF54 asexual stages and gametocytogenesis was induced by nutrient stress as described previously (*84*). Briefly, 24-well plates were set at 0.75% parasitemia and 1% hematocrit and incubated with either 500 nM FOS, 10 μM FOS, or regular medium for 13 days. Medium or medium with FOS was replaced on day 4, 6, 8, and 9-12. Parasitemia (sexual and asexual stages) was calculated from Giemsa-stained smears on day 13. Figure was prepared using GraphPad Prism 6 and Coral Draw software.

Generating apicoplast minus gametocytes

P. falciparum NF54 strain culture that was less than two months was maintain under normal culturing conditions described above (4% hematocrit, parasitemia <10%) (Figure 2.1A). On day -8, the culture was passed through a MACS column to remove any existing gametocytes, trophozoites, and schizonts (Figure 2.1B). The ring stages were saved, adjusted to 5% hematocrit, then 1 mL was taken out and pelleted for qPCR (Figure 2.1B). The remaining culture was split into two 25 cm^2 (5 mL) flasks each containing 5% hematocrit and 2% parasitemia (Figure 2.1B). One of the 5 mL cultures was treated with 1 μM doxycycline (DOX) added to remove the apicoplast (Figure 2.1B). On day -7, 1 μM DOX and 200 μM IPP in fresh medium was added to the DOX treated cultures and fresh medium without DOX was added to the control cultures (Figure 2.1C). Day -6 to day 0, medium or medium with DOX and IPP were replaced in both cultures (Figure 2.1D). On day +1, each culture was passed again through MACS columns to remove any gametocytes and mature asexual stages (Figure 2.1E). NF54 ring stages were recovered and then plated (Figure 2.1E). One mL was removed and pelleted for qPCR to confirmed loss of the apicoplast (Figure 2.1E). DOX treatment was stopped at this point and those parasites were only treated with 200 μM IPP for the duration of the experiment or as indicated (Figure 2.1E). Control parasites were suppletmented with 200 μM IPP to assess if IPP alone has no adverse effects (Figure 2.1E). On days +4, +6, +9-10, and +12, one mL of spent medium was removed from each well. One mL of medium or medium supplemented with 200

μM IPP was added to each well as indicated (Figure 2.1F). On days +5, +8, and +11, IPP was removed from the indicated wells by resuspsending each well, centrifuging 5 min at 2,500 rpm, and adding fresh medium without IPP supplementation (Figure 2.1G). On day +13, each well was smeared and morphological changes of API-minus gametocytes were observed in Giemsa stained smears. One mL was removed from each well for qPCR analysis (Figure 2.1I). The remaining gametocytes were concentrated on a NycoPrep cushion and stained with MitoTracker®, Lysolive™, and Hoechst fluorescent dyes for imaging (Figure 2.1H). Adobe Photoshop CS2 was used to prepare final figures.

Quantitative Real-Time PCR

Each gametocyte pellet was resuspended in 180 μl PBS before DNA extraction DNA was purified using a QiaAMP blood kit (Qiagen) following manufacturer's protocol. Target primers were as described previously (*15*) were used as follows: tufA (apicoplast, PFC10_API0028): 5′-GATATTGATTCAGCTCCAGAAGAAA-3′ (forward) and 5′-ATATCCATTTGTGTGGCTCCTATAA-3′ (reverse); cytb3 (mitochondria, mal_mito_3): 5′-AGATACATGCACGCAACAGG-3′ (forward) and 5′-TCATTTGACCCCATGGTAAGA-3′ (reverse); CHT1 (nuclear, PF3D7_1252200): 5′-TGTTTCCTTCAACCCCTTTT-3′ (forward) and 5′- TAATCCAAACCCGTCTGCTC-3′ (reverse). We also used the following reference primers for tRNA synthase (PF3D7_0717700): 5′-AAGTAGCAGGTCATCGTGGTT-3′ (forward) and 5′- GTTCGGCACATTCTTCCATAA-3′ (reverse). Reactions contained template DNA, 0.1 μM of each primer, 1X GoTaq qPCR Master Mix, and 0.2 μl CXR reference dye in a final volume of 20 μL. PCR reactions were performed on an Applied Biosystems 7300 Real Time PCR System. Relative quantification of target genes was determined using the comparative method ($2^{-\Delta\Delta Ct}$) (Figure 2B).

Fluorescence microscopy

Potential changes in mitochondria membrane potential (MitoTracker®) and endocytic vesicles (Lysolive™) were tracked in API-minus gametocytes; DNA (Hoechst) was used for reference. Following gametocyte concentration (Figure 1H), gametocytes were incubated with 10 μM Lysolive™ (Marker Gene Technologies) in complete media for 2 hours at 37 °C protected from light. Each sample was washed one time with PBS followed by the addition of 100 nM

Mitotracker®Red CM-H2XRos (Life Technologies) in complete media for 15 min at 37 °C protected from light. Each sample was washed again one time with PBS and resuspended in 100 µl complete media. Hoechst 33342 at 0.25 µg/mL was added to each sample right before imaging. A Zeiss Axioimager M1 microscope with a 100x/1.4NA oil immersion objective and an Axiocam MRm digital camera was used to obtain fluorescent images as reported previously (*57*). Adobe Photoshop CS2 was used to prepare final figures.

Texas Red Dextran® staining of red blood cells

Because the use of LysoLive™ has not been reported to be used for food vacuole localization in the malaria parasites and very little is known about food vacuole development (or endocytic trafficking) in gametocyte stages, we verified that LysoLive™ was indeed staining an endocytic vesicle network by co-localization with Texas Red Dextran® (Life Technologies) based on a previous report (*60*) with the following modifications (Figure 2.6). Fresh red blood cells (RBCs) were resuspended at 50% hematocrit. RBC lysis buffer (5 mM HEPES pH 7.4, 11 mM glucose, 2 mM $MgCl_2$, 2 mM ATP, 100 µM Texas Red Dextran) was added slowly to the packed RBCs and incubated in a 30 °C water bath (protected from light) for 10 minutes (Figure 2.6A-5E). The RBCs were centrifuged and the supernatant was removed. Resealing buffer (1 mM HEPES pH 7.4, 280 mM NaCl, 40 mM KCl, 11 mM glucose) was then added and slowly mixed (Figure 2.6F). The RBCs were centrifuged and the supernatant was removed and then the RBCs were washed three times in complete media (Figure 2.6G). The RBCs were checked on the fluorescence microscope to verify that the cells contain the dye. *P. falciparum* schizont NF54 strain were collected on a MACS column and resuspended with RBCs containing Texas Red Dextran® and gametocytogenesis was induced by nutrient stress as described above (Figure 2.6H-5J). After 13 days, gametocytes were concentrated on a NycoPrep Cushion 1.077 (*86-88*) and stained with LysoLive™ (10 µM) for 1.5 hours at 37 °C protected from light. Cells were washed with PBS and 0.25 µg/ml Hoechst 33342 was added to the sample right before imaging as described above (Figure 2.6K).

MEP intermediates analysis by IP-UPLC-MS/MS analysis

Control gametocytes and API-minus gametocytes were generated as described above (Figure 2.1). Metabolite extraction was performed as described previously for asexual stages (*25*)

from lyophilized cell pellets stored at -80 °C until extraction. Briefly, isopentenyl *S*-thiolodiphosphate (ISPP) was used as internal standard at a final concentration of 100 mM. ISPP was diluted in water and 1 mL was added to each sample and sonicated for 10 minutes in water bath sonicator following by incubation at 60 °C for 1.5 hours. Samples were chilled on ice and centrifuged 10 minutes at 10,000 rpm at 4 °C. Supernatant was transferred to a 10 kDa centricom tube and centrifuged 10 minutes at 10,000 rpm at 4 °C. Filtered samples were dried in a speed vac with heat and samples were stored at -80 °C until analysis.

Ion pair reversed phase ultra-performance liquid chromatography in tandem with mass spectrometry (IP-UPLC-MS/MS) was used for analyses of intermediates. Standards and samples were separated using a gradient mobile phase consisting of 1.25 mM DBAA, 10 mM ammonium formate in water, and 1% formic acid to adjust the pH to 5.2 (A), and 1.25mM DBAA in acetonitrile (B). The flow rate was set at 0.3 mL/min and the gradient conditions were: 0-2 min (100% A); 2-7 min (100% A to 60% A); 7-9 min (60% A to 50% A); 9-11 min (50% A to 100% A); 11-15 min (100% A). The autosampler was set at 10 ^{0}C. The following MS conditions were used for the MEP intermediates analysis. Capillary voltage was set at 3.17 kV for negative ion mode. The source and desolvation gas temperatures of the mass spectrometer were set at 150 ^{0}C and 450 ^{0}C, respectively. The desolvation gas (nitrogen) was set at 700 L/h. The ion transitions, cone voltage, and collision energy used for ESI-MS/MS analysis were determined using MassLynx V4.1 intellistart software.

Samples were resuspended in 110 µL of water, centrifuged 10 minutes at 10,000 rpm at 4 °C, filtered, transferred to microplate and 40 µL of each sample was injected for LC-MS analysis. Two technical replicates were analyzed for each sample. Data acquisition and analysis were performed using MassLynx V4.1 software (Waters).

Acknowledgement

This work was supported by the National Institute of Allergy and Infectious Diseases of the National Institutes of Health under award number R01AI108819 to M.B.C. J.D.W. is recipient of a scholarship from the National Science Foundation S-STEM project under award number DUE-0850198. We thank Ryan C. Smith for helpful discussion. We would like to thank Dr. Janet Webster for comments and corrections.

References

1. World malaria report 2010. Geneva, World Health Organization, 2010 (WHO/HTM/GMP/2010.1).
2. A. M. Dondorp, S. Yeung, L. White, C. Nguon, N. P. Day, D. Socheat, L. von Seidlein, Artemisinin resistance: current status and scenarios for containment. *Nat Rev Microbiol* **8**, 272-280 (2010).
3. E. L. Flannery, A. K. Chatterjee, E. A. Winzeler, Antimalarial drug discovery - approaches and progress towards new medicines. *Nat Rev Microbiol* **11**, 849-862 (2013).
4. D. A. Baker, Malaria gametocytogenesis. *Mol Biochem Parasitol* **172**, 57-65 (2010).
5. T. Bousema, C. Drakeley, Epidemiology and Infectivity of Plasmodium falciparum and Plasmodium vivax Gametocytes in Relation to Malaria Control and Elimination. *Clin. Microbiol. Rev.* **24**, 377-410 (2011).
6. C. A. Lobo, N. Kumar, Sexual Differentiation and Development in the Malaria Parasite. *Parasitology Today* **14**, 146-150 (1998).
7. M. J. Delves, Plasmodium cell biology should inform strategies used in the development of antimalarial transmission-blocking drugs. *Future Medicinal Chemistry* **4**, 2251-2263 (2012).
8. A. Lensen, A. Bril, M. van de Vegte, G. J. van Gemert, W. Eling, R. Sauerwein, *Plasmodium falciparum*:Infectivity of Cultured, Synchronized Gametocytes to Mosquitoes. *Experimental Parasitology* **91**, 101-103 (1999).
9. R. E. Sinden, M. E. Smalley, Gametocytogenesis of *Plasmodium falciparum* in vitro: the cell-cycle. *Parasitology* **79**, 277-296 (1979).
10. A. M. Talman, O. Domarle, F. E. McKenzie, F. Ariey, V. Robert, Gametocytogenesis: the puberty of *Plasmodium falciparum*. *Malaria Journal* **3**, 1-14 (2004).
11. M. Delves, D. Plouffe, C. Scheurer, S. Meister, S. Wittlin, E. A. Winzeler, R. E. Sinden, D. Leroy, The activities of current antimalarial drugs on the life cycle stages of Plasmodium: a comparative study with human and rodent parasites. *PLoS Med* **9**, e1001169 (2012).
12. G. I. McFadden, M. E. Reith, J. Munholland, N. Lang-Unnasch, Plastid in human parasites. *Nature* **381**, 482 (1996).

13. G. I. McFadden, D. S. Roos, Apicomplexan plastids as drug targets. *Trends Microbiol* **7**, 328-333 (1999).
14. E. L. Dahl, J. L. Shock, B. R. Shenai, J. Gut, J. L. DeRisi, P. J. Rosenthal, Tetracyclines specifically target the apicoplast of the malaria parasite. *Antimicrob Agents Chemother* **50**, 3124-3131 (2006).
15. E. Yeh, J. L. DeRisi, Chemical Rescue of Malaria Parasites Lacking an Apicoplast Defines Organelle Function in Blood-Stage *Plasmodium falciparum*. *PLoS Biol* **9**, e1001138 (2011).
16. S. Shimizu, Y. Osada, T. Kanazawa, Y. Tanaka, M. Arai, Suppressive effect of azithromycin on *Plasmodium berghei* mosquito stage development and apicoplast replication. *Malaria Journal* **9**, 73-80 (2010).
17. M. Sullivan, J. Li, S. Kumar, M. J. Rogers, T. F. McCutchan, Effects of interruption of apicoplast function on malaria infection, development, and transmission. *Molecular and Biochemical Parasitology* **109**, 17-23 (2000).
18. A. M. Vaughan, M. T. O'Neill, A. S. Tarun, N. Camargo, T. M. Phuong, A. S. Aly, A. F. Cowman, S. H. Kappe, Type II fatty acid synthesis is essential only for malaria parasite late liver stage development. *Cell Microbiol* **11**, 506-520 (2009).
19. M. Yu, T. R. Kumar, L. J. Nkrumah, A. Coppi, S. Retzlaff, C. D. Li, B. J. Kelly, P. A. Moura, V. Lakshmanan, J. S. Freundlich, J. C. Valderramos, C. Vilcheze, M. Siedner, J. H. Tsai, B. Falkard, A. B. Sidhu, L. A. Purcell, P. Gratraud, L. Kremer, A. P. Waters, G. Schiehser, D. P. Jacobus, C. J. Janse, A. Ager, W. R. Jacobs, Jr., J. C. Sacchettini, V. Heussler, P. Sinnis, D. A. Fidock, The fatty acid biosynthesis enzyme FabI plays a key role in the development of liver-stage malarial parasites. *Cell host & microbe* **4**, 567-578 (2008).
20. B. C. van Schaijk, T. R. Kumar, M. W. Vos, A. Richman, G. J. van Gemert, T. Li, A. G. Eappen, K. C. Williamson, B. J. Morahan, M. Fishbaugher, M. Kennedy, N. Camargo, S. M. Khan, C. J. Janse, K. L. Sim, S. L. Hoffman, S. H. Kappe, R. W. Sauerwein, D. A. Fidock, A. M. Vaughan, Type II fatty acid biosynthesis is essential for *Plasmodium falciparum* sporozoite development in the midgut of Anopheles mosquitoes. *Eukaryot Cell*, (2013).

21. C. Y. Botte, Y. Yamaryo-Botte, T. W. Rupasinghe, K. A. Mullin, J. I. MacRae, T. P. Spurck, M. Kalanon, M. J. Shears, R. L. Coppel, P. K. Crellin, E. Marechal, M. J. McConville, G. I. McFadden, Atypical lipid composition in the purified relict plastid (apicoplast) of malaria parasites. *Proc Natl Acad Sci U S A* **110**, 7506-7511 (2013).
22. L. Koreny, M. Obornik, J. Lukes, Make it, take it, or leave it: heme metabolism of parasites. *PLoS Pathog* **9**, e1003088 (2013).
23. L. Sheiner, A. B. Vaidya, G. I. McFadden, The metabolic roles of the endosymbiotic organelles of Toxoplasma and Plasmodium spp. *Curr Opin Microbiol* **16**, 452-458 (2013).
24. V. A. Nagaraj, B. Sundaram, N. M. Varadarajan, P. A. Subramani, D. M. Kalappa, S. K. Ghosh, G. Padmanaban, Malaria parasite-synthesized heme is essential in the mosquito and liver stages and complements host heme in the blood stages of infection. *PLoS Pathog* **9**, e1003522 (2013).
25. M. B. Cassera, F. C. Gozzo, F. L. D'Alexandri, E. F. Merino, H. A. del Portillo, V. J. Peres, I. C. Almeida, M. N. Eberlin, G. Wunderlich, J. Wiesner, H. Jomaa, E. A. Kimura, A. M. Katzin, The methylerythritol phosphate pathway is functionally active in all intraerythrocytic stages of *Plasmodium falciparum*. *J Biol Chem* **279**, 51749-51759 (2004).
26. H. Jomaa, J. Wiesner, S. Sanderbrand, B. Altincicek, C. Weidemeyer, M. Hintz, I. Turbachova, M. Eberl, J. Zeidler, H. K. Lichtenthaler, D. Soldati, E. Beck, Inhibitors of the nonmevalonate pathway of isoprenoid biosynthesis as antimalarial drugs. *Science* **285**, 1573-1576 (1999).
27. S. A. Holstein, R. J. Hohl, Isoprenoids: remarkable diversity of form and function. *Lipids* **39**, 293-309 (2004).
28. A. S. Couto, E. A. Kimura, V. J. Peres, M. L. Uhrig, A. M. Katzin, Active isoprenoid pathway in the intra-erythrocytic stages of *Plasmodium falciparum*: presence of dolichols of 11 and 12 isoprene units. *Biochem J* **341 (Pt 3)**, 629-637 (1999).
29. F. L. D'Alexandri, E. A. Kimura, V. J. Peres, A. M. Katzin, Protein dolichylation in *Plasmodium falciparum*. *FEBS Letters* **580**, 6343-6348 (2006).

30. H. Shams-Eldin, C. S. de Macedo, S. Niehus, C. Dorn, J. Kimmel, N. Azzouz, R. T. Schwarz, *Plasmodium falciparum* dolichol phosphate mannose synthase represents a novel clade. *Biochem Biophys Res Commun* **370**, 388-393 (2008).

31. C. S. de Macedo, M. L. Uhrig, E. A. Kimura, A. M. Katzin, Characterization of the isoprenoid chain of coenzyme Q in *Plasmodium falciparum*. *FEMS Microbiol Lett* **207**, 13-20 (2002).

32. R. Tonhosolo, F. L. D'Alexandri, F. A. Genta, G. Wunderlich, F. C. Gozzo, M. N. Eberlin, V. J. Peres, E. A. Kimura, A. M. Katzin, Identification, molecular cloning and functional characterization of an octaprenyl pyrophosphate synthase in intra-erythrocytic stages of *Plasmodium falciparum*. *Biochem J* **392**, 117-126 (2005).

33. R. Tonhosolo, H. B. Gabriel, M. Y. Matsumura, F. J. Cabral, M. M. Yamamoto, F. L. D'Alexandri, R. A. Sussmann, R. Belmonte, V. J. Peres, D. C. Crick, G. Wunderlich, E. A. Kimura, A. M. Katzin, Intraerythrocytic stages of *Plasmodium falciparum* biosynthesize menaquinone. *FEBS Letters* **584**, 4761-4768 (2010).

34. R. Tonhosolo, F. L. D'Alexandri, V. V. de Rosso, M. L. Gazarini, M. Y. Matsumura, V. J. Peres, E. F. Merino, J. M. Carlton, G. Wunderlich, A. Z. Mercadante, E. A. Kimura, A. M. Katzin, Carotenoid biosynthesis in intraerythrocytic stages of *Plasmodium falciparum*. *The Journal of biological chemistry* **284**, 9974-9985 (2009).

35. F. L. D'Alexandri, R. Tonhosolo, E. A. Kimura, A. M. Katzin, Mass spectrometry analysis of polyisoprenoids alcohols and carotenoids via ESI(Li(+))-MS/MS. *Methods Mol Biol* **580**, 109-128 (2009).

36. R. A. Sussmann, C. B. Angeli, V. J. Peres, E. A. Kimura, A. M. Katzin, Intraerythrocytic stages of *Plasmodium falciparum* biosynthesize vitamin E. *FEBS Letters* **585**, 3985-3991 (2011).

37. D. Chakrabarti, T. Da Silva, J. Barger, S. Paquette, H. Patel, S. Patterson, C. M. Allen, Protein farnesyltransferase and protein prenylation in *Plasmodium falciparum*. *J Biol Chem* **277**, 42066-42073 (2002).

38. F. M. Jordao, A. Y. Saito, D. C. Miguel, V. de Jesus Peres, E. A. Kimura, A. M. Katzin, In Vitro and In Vivo Antiplasmodial Activities of Risedronate and Its Interference with Protein Prenylation in *Plasmodium falciparum*. *Antimicrob Agents Chemother* **55**, 2026-2031 (2011).

39. J. Wiesner, K. Kettler, J. Sakowski, R. Ortmann, A. M. Katzin, E. A. Kimura, K. Silber, G. Klebe, H. Jomaa, M. Schlitzer, Farnesyltransferase inhibitors inhibit the growth of malaria parasites *in vitro* and *in vivo*. *Angew Chem Int Ed Engl* **43**, 251-254 (2004).
40. R. Howe, M. Kelly, J. Jimah, D. Hodge, A. R. Odom, Isoprenoid biosynthesis inhibition disrupts Rab5 localization and food vacuolar integrity in *Plasmodium falciparum*. *Eukaryot Cell*, (2012).
41. J.-Y. van der Meer, A. K. H. Hirsch, The isoprenoid-precursor dependence of Plasmodium spp. *Natural Product Reports*, (2012).
42. F. M. Jordão, E. A. Kimura, A. M. Katzin, Isoprenoid biosynthesis in the erythrocytic stages of *Plasmodium falciparum*. *Memorias do Instituto Oswaldo Cruz* **106**, 134-141 (2011).
43. D. C. Gowda, P. Gupta, E. A. Davidson, Glycosylphosphatidylinositol Anchors Represent the Major Carbohydrate Modification in Proteins of Intraerythrocytic Stage *Plasmodium falciparum*. *Journal of Biological Chemistry* **272**, 6428-6439 (1997).
44. C. Aicart-Ramos, R. A. Valero, I. Rodriguez-Crespo, Protein palmitoylation and subcellular trafficking. *Biochimica et Biophysica Acta (BBA) - Biomembranes* **1808**, 2981-2994 (2011).
45. P. J. Roberts, N. Mitin, P. J. Keller, E. J. Chenette, J. P. Madigan, R. O. Currin, A. D. Cox, O. Wilson, P. Kirschmeier, C. J. Der, Rho Family GTPase Modification and Dependence on CAAX Motif-signaled Posttranslational Modification. *Journal of Biological Chemistry* **283**, 25150-25163 (2008).
46. R. Howe, M. Kelly, J. Jimah, D. Hodge, A. R. Odom, Isoprenoid biosynthesis inhibition disrupts Rab5 localization and food vacuolar integrity in *Plasmodium falciparum*. *Eukaryotic Cell* **12**, 215-223 (2013).
47. M. Sinensky, J. Logel, Defective macromolecule biosynthesis and cell-cycle progression in a mammalian cell starved for mevalonate. *Proc Natl Acad Sci U S A* **82**, 3257-3261 (1985).
48. L. Ayong, T. DaSilva, J. Mauser, C. M. Allen, D. Chakrabarti, Evidence for prenylation-dependent targeting of a Ykt6 SNARE in *Plasmodium falciparum*. *Molecular and Biochemical Parasitology* **175**, 162-168 (2011).

49. M. B. Cassera, E. F. Merino, V. J. Peres, E. A. Kimura, G. Wunderlich, A. M. Katzin, Effect of fosmidomycin on metabolic and transcript profiles of the methylerythritol phosphate pathway in *Plasmodium falciparum*. *Memorias do Instituto Oswaldo Cruz* **102**, 377-383 (2007).

50. I. C. Moura, G. Wunderlich, M. L. Uhrig, A. S. Couto, V. J. Peres, A. M. Katzin, E. A. Kimura, Limonene arrests parasite development and inhibits isoprenylation of proteins in *Plasmodium falciparum*. *Antimicrob Agents Chemother* **45**, 2553-2558 (2001).

51. H. Rodrigues Goulart, E. A. Kimura, V. J. Peres, A. S. Couto, F. A. Aquino Duarte, A. M. Katzin, Terpenes arrest parasite development and inhibit biosynthesis of isoprenoids in *Plasmodium falciparum*. *Antimicrob Agents Chemother* **48**, 2502-2509 (2004).

52. B. Zhang, K. M. Watts, D. Hodge, L. M. Kemp, D. A. Hunstad, L. M. Hicks, A. R. Odom, A second target of the antimalarial and antibacterial agent fosmidomycin revealed by cellular metabolic profiling. *Biochemistry* **50**, 3570-3577 (2011).

53. J. MacRae, M. Dixon, M. Dearnley, H. Chua, J. Chambers, S. Kenny, I. Bottova, L. Tilley, M. McConville, Mitochondrial metabolism of sexual and asexual blood stages of the malaria parasite *Plasmodium falciparum*. *BMC Biology* **11**, 67 (2013).

54. J. Krungkrai, P. Prapunwattana, S. R. Krungkrai, Ultrastructure and function of mitochondria in gametocytic stage of *Plasmodium falciparum*. *Parasite (Paris, France)* **7**, 19-26 (2000).

55. N. Okamoto, T. P. Spurck, C. D. Goodman, G. I. McFadden, Apicoplast and mitochondrion in gametocytogenesis of *Plasmodium falciparum*. *Eukaryot Cell* **8**, 128-132 (2009).

56. C. L. Peatey, D. Leroy, D. L. Gardiner, K. R. Trenholme, Anti-malarial drugs: how effective are they against *Plasmodium falciparum* gametocytes? *Malar J* **11**, 34 (2012).

57. J. D. Bowman, E. F. Merino, C. F. Brooks, B. Striepen, P. R. Carlier, M. B. Cassera, Antiapicoplast and Gametocytocidal Screening To Identify the Mechanisms of Action of Compounds within the Malaria Box. *Antimicrob Agents Chemother* **58**, 811-819 (2014).

58. M. E. Smalley, *Plasmodium falciparum* gametocytes: the effect of chloroquine on their development. *Transactions of the Royal Society of Tropical Medicine and Hygiene* **71**, 526-529 (1977).

59. J. Lelièvre, M. J. Almela, S. Lozano, C. Miguel, V. Franco, D. Leroy, E. Herreros, Activity of Clinically Relevant Antimalarial Drugs on *Plasmodium falciparum* Mature Gametocytes in an ATP Bioluminescence "Transmission Blocking" Assay. *PLoS One* **7**, e35019 (2012).

60. K. J. Saliba, R. J. W. Allen, S. Zissis, P. G. Bray, S. A. Ward, K. Kirk, Acidification of the Malaria Parasite's Digestive Vacuole by a H+-ATPase and a H+-pyrophosphatase. *Journal of Biological Chemistry* **278**, 5605-5612 (2003).

61. P. C. C. Garnham, On some curious bodies found in erythrocytes containing immature crescents. *Transactions of the Royal Society of Tropical Medicine and Hygiene* **26**, 401-403 (1933).

62. A. U. Orjih, Hemozoin accumulation in Garnham bodies of *Plasmodium falciparum* gametocytes. *Parasitol Res* **111**, 2353-2359 (2012).

63. P. R. Pendyala, L. Ayong, J. Eatrides, M. Schreiber, C. Pham, R. Chakrabarti, D. A. Fidock, C. M. Allen, D. Chakrabarti, Characterization of a PRL protein tyrosine phosphatase from *Plasmodium falciparum*. *Molecular and Biochemical Parasitology* **158**, 1-10 (2008).

64. K. S. Saliba, M. Jacobs-Lorena, Production of *Plasmodium falciparum gametocytes* in vitro. *Methods Mol Biol* **923**, 17-25 (2013).

65. T. Q. Tanaka, K. C. Williamson, A malaria gametocytocidal assay using oxidoreduction indicator, alamarBlue. *Molecular and Biochemical Parasitology* **177**, 160-163 (2011).

66. R. De Fries, M. Mitsuhashi, Quantification of mitogen induced human lymphocyte proliferation: Comparison of alamarbluetm assay to 3h-thymidine incorporation assay. *Journal of Clinical Laboratory Analysis* **9**, 89-95 (1995).

67. J. O'Brien, I. Wilson, T. Orton, F. Pognan, Investigation of the Alamar Blue (resazurin) fluorescent dye for the assessment of mammalian cell cytotoxicity. *European Journal of Biochemistry* **267**, 5421-5426 (2000).

68. W. Sun, T. Q. Tanaka, C. T. Magle, W. Huang, N. Southall, R. Huang, S. J. Dehdashti, J. C. McKew, K. C. Williamson, W. Zheng, Chemical signatures and new drug targets for gametocytocidal drug development. *Scientific reports* **4**, 3743 (2014).

69. S. Ohkuma, B. Poole, Fluorescence Probe Measurement of the Intralysosomal pH in Living Cells and the Perturbation of pH by Various Agents. *Proc Natl Acad Sci U S A* **75**, 3327-3331 (1978).

70. I. D. Goodyer, B. Pouvelle, T. G. Schneider, D. P. Trelka, T. F. Taraschi, Characterization of macromolecular transport pathways in malaria-infected erythrocytes. *Molecular and Biochemical Parasitology* **87**, 13-28 (1997).

71. N. Regev-Rudzki, Danny W. Wilson, Teresa G. Carvalho, X. Sisquella, Bradley M. Coleman, M. Rug, D. Bursac, F. Angrisano, M. Gee, Andrew F. Hill, J. Baum, Alan F. Cowman, Cell-Cell Communication between Malaria-Infected Red Blood Cells via Exosome-like Vesicles. *Cell* **153**, 1120-1133 (2013).

72. P.-Y. Mantel, Anh N. Hoang, I. Goldowitz, D. Potashnikova, B. Hamza, I. Vorobjev, I. Ghiran, M. Toner, D. Irimia, Alexander R. Ivanov, N. Barteneva, M. Marti, Malaria-Infected Erythrocyte-Derived Microvesicles Mediate Cellular Communication within the Parasite Population and with the Host Immune System. *Cell Host & Microbe* **13**, 521-534 (2013).

73. M. A. Missinou, S. Borrmann, A. Schindler, S. Issifou, A. A. Adegnika, P. B. Matsiegui, R. Binder, B. Lell, J. Wiesner, T. Baranek, H. Jomaa, P. G. Kremsner, Fosmidomycin for malaria. *Lancet* **360**, 1941-1942 (2002).

74. C. D. Goodman, G. I. McFadden, Targeting apicoplasts in malaria parasites. *Expert Opin Ther Targets* **17**, 167-177 (2013).

75. S. A. Ralph, G. G. Van Dooren, R. F. Waller, M. J. Crawford, M. J. Fraunholz, B. J. Foth, C. J. Tonkin, D. S. Roos, G. I. McFadden, Tropical infectious diseases: Metabolic maps and functions of the *Plasmodium falciparum* apicoplast. *Nat Rev Microbiol* **2**, 203-216 (2004).

76. E. L. Dahl, P. J. Rosenthal, Multiple antibiotics exert delayed effects against the *Plasmodium falciparum* apicoplast. *Antimicrob Agents Chemother* **51**, 3485-3490 (2007).

77. H. Noedl, S. Krudsood, W. Leowattana, N. Tangpukdee, W. Thanachartwet, S. Looareesuwan, R. S. Miller, M. Fukuda, K. Jongsakul, K. Yingyuen, S. Sriwichai, C. Ohrt, C. Knirsch, In Vitro Antimalarial Activity of Azithromycin, Artesunate, and Quinine in Combination and Correlation with Clinical Outcome. *Antimicrob Agents Chemother* **51**, 651-656 (2007).

78. A. B. S. Sidhu, Q. Sun, L. J. Nkrumah, M. W. Dunne, J. C. Sacchettini, D. A. Fidock, In Vitro Efficacy, Resistance Selection, and Structural Modeling Studies Implicate the Malarial Parasite Apicoplast as the Target of Azithromycin. *Journal of Biological Chemistry* **282**, 2494-2504 (2007).

79. R. Carter, K. N. Mendis, L. H. Miller, L. Molineaux, A. Saul, Malaria transmission-blocking vaccines--how can their development be supported? *Nature Medicine* **6**, 241-244 (2000).

80. M. Sarkar, C. W. C, G. Koren, A. R. N. Einarson, Pregnancy outcome following gestational exposure to azithromycin. *BMC Pregnancy & Childbirth* **6**, 18-15 (2006).

81. G. Treadway, D. Pontani, Paediatric safety of azithromycin: worldwide experience. *Journal of Antimicrobial Chemotherapy* **37**, 143-149 (1996).

82. B. Rino, T. Van, F. Giovanni, M. Franco, Research letter. Azithromycin in the treatment of *Plasmodium falciparum* gametocytes: a preliminary observation. *Journal of Tropical Pediatrics* **46**, 56 (2000).

83. C. Peatey, D. Leroy, D. Gardiner, K. Trenholme, Anti-malarial drugs: how effective are they against *Plasmodium falciparum* gametocytes? *Malaria Journal* **11**, 34 (2012).

84. L. Harinantenaina, J. D. Bowman, P. J. Brodie, C. Slebodnick, M. W. Callmander, E. Rakotobe, R. Randrianaivo, V. E. Rasamison, A. Gorka, P. D. Roepe, M. B. Cassera, D. G. Kingston, Antiproliferative and antiplasmodial dimeric phloroglucinols from *Mallotus oppositifolius* from the Madagascar Dry Forest *Journal of natural products* **76**, 388-393 (2013)

85. C. Lambros, J. P. Vanderberg, Synchronization of *Plasmodium falciparum* Erythrocytic Stages in Culture. *The Journal of Parasitology* **65**, 418-420 (1979).

86. V. Carter, H. Cable, B. A. Underhill, J. Williams, H. Hurd, Isolation of Plasmodium berghei ookinetes in culture using Nycodenz density gradient columns and magnetic isolation. *Malaria Journal* **2**, 35 (2003).

87. T. C. Ford, D. Rickwood, Formation of isotonic Nycodenz gradients for cell separations. *Analytical Biochemistry* **124**, 293-298 (1982)10.1016/0003-2697(82)90041-0).

88. D. Rickwood, T. Ford, J. Graham, Nycodenz: A new nonionic iodinated gradient medium. *Analytical Biochemistry* **123**, 23-31 (1982).

CHAPTER 3: ANTIAPICOPLAST AND GAMETOCYTOCIDAL SCREENING TO IDENTIFY THE MECHANISMS OF ACTION OF COMPOUNDS WITHIN THE MALARIA BOX

Jessica D. Bowman, Emilio F. Merino, Carrie F. Brooks, Boris Striepen, Paul R. Carlier, and Maria B. Cassera

Manuscript published – Reprinted with permission from Antimicrobial Agents and Chemotherapy

ABSTRACT

Malaria remains a significant infectious disease causing millions of clinical cases and more than 800,000 deaths per year. The Malaria Box is a collection of 400 commercially available chemical entities having antimalarial activity. The collection contains 200 drug-like compounds, based on their oral absorption and the presence of known toxicophores, and 200 probe-like compounds, which are intended to represent a broad structural diversity. These compounds have confirmed activity against the asexual intraerythrocytic stages of *Plasmodium falciparum* and low cytotoxicity but their mechanisms of action and their activity in other stages of the parasite's life cycle remains to be determined. The apicoplast is considered to be a promising source of malaria-specific targets and its main function during intraerythrocytic stages is to provide the isoprenoid precursor isopentenyl diphosphate, which can be used for phenotypic-based screens to identify compounds targeting this organelle. We screened 400 compounds from the Malaria Box using apicoplast-targeting phenotypic assays to identify their potential mechanisms of action. We identified one compound that specifically targeted the apicoplast. Further analyses indicated that this compound's molecular target may differ from current anti-apicoplast drugs such as fosmidomycin. Moreover, in our efforts to elucidate the mechanisms of action of compounds from the Malaria Box, we evaluated their activity against other stages of the parasite's life cycle. Gametocytes are the transmission stage of the malaria parasite and are recognized as a priority target in efforts to eradicate malaria. We identified twelve compounds that were active against gametocytes with IC_{50} values below 1 μM.

Introduction

More than 40% of the world's population is at risk of contracting malaria and the continued emergence of drug resistance is a constant threat. As a result, the identification and characterization of new leads for development of antimalarial drugs with different mechanisms of action is of highest priority. Historically, antimalarial drug discovery and development has focused on the asexual intraerythrocytic stages of the parasite's life cycle since these stages are responsible for the pathology. Gametocytes are the sexual stage of the malaria parasite and are essential for transmission of the parasite to the mosquito. Most current antimalarials have little or no effect on gametocytes, thus, treated patients can still transmit malaria. Development of new drugs that have a broader spectrum of activity, including activity against gametocytes, is recognized as a highly favorable quality in the effort to eradicate malaria (*1*).

In order to catalyze the development of new antimalarials, the Medicines for Malaria Venture (MMV) and SCYNEXIS assembled the Malaria Box (*2*), an open access library composed of 400 compounds originally identified by phenotypic screening of over 4,000,000 compounds from the research libraries of Saint Jude Children's Research Hospital, Novartis, and GlaxoSmithKline (*3*). The *in vitro* antimalarial activity of the Malaria Box compounds span a range of half-maximum inhibitory concentration (IC_{50}) values from 30 nM to 4 μM (*2*). The 400 compounds in the Box were selected based on several factors including low toxicity, oral bioavailability, and chemical diversity; however, the primary selection was based on their commercial availability to assure accessibility for follow-up experiments (*2*). Substantial information about these compounds is available at the ChEMBL-NTD archive (https://www.ebi.ac.uk/chemblntd); this knowledgebase is expected to grow iteratively as more research is performed. The Malaria Box compounds were selected based on global phenotypic screening against asexual intraerythrocytic stages of *P. falciparum*; however, their mechanisms of action and their efficacy against gametocyte stages remain unknown.

Malaria parasites contain a vestigial plastid called the apicoplast, which performs vital functions such as the biosynthesis of isoprenoid precursors, fatty acids, and heme (*4, 5*). *Plasmodium* parasites utilize the methylerythritol phosphate (MEP) pathway to synthesize isopentenyl pyrophosphate (IPP) and dimethylallyl pyrophosphate (DMAPP), which is essential for parasite growth (*6, 7*). This pathway is absent in humans, who rely on the mevalonate pathway instead. Recently, it has been suggested that the MEP pathway and the biosynthesis of

the isoprenoid precursors IPP and DMAPP represent the sole essential function of this organelle during asexual intraerythrocytic development of the parasites (*8*). The strongest support for this stems from the observation that loss of the apicoplast can be chemically complemented by supplementing the growth medium with IPP. Therefore, the inhibitory effect of drugs that directly target biosynthesis of isoprenoid precursors or indirectly disrupt their biosynthesis by interfering with processes essential for apicoplast biogenesis, such as apicoplast DNA replication, transcription, and protein translation, may be reverted by IPP supplementation (*8*). As a result, the reversal of growth inhibition by IPP supplementation can be used as a phenotypic screening diagnostic to identify compounds within the Malaria Box that target the apicoplast, thus, identifying their mechanism of action and narrowing their potential molecular targets (*8*).

Several antibiotics such as doxycycline (DOX), azithromycin, solithromycin, chloramphenicol, and clindamycin, kill malaria parasites by interfering with apicoplast genome replication, transcription, protein translation, post-translation modification, or protein turnover (*9-14*). Parasites treated with these antibiotics initially present normal morphology and continue to grow and release daughter cells (merozoites) that are capable of invading new host cells. However, this progeny will not complete the following intraerythrocytic cycle since the apicoplast will fail to replicate and segregate; this phenomenon is known as delayed death phenotype (*15*). In contrast to those antibiotics, fosmidomycin (FOS) is an inhibitor that directly targets the metabolism of the apicoplast (*7, 16-18*). FOS shows a rapid onset of action with IC_{50} values between 300 and 1,200 nM for *P. falciparum in vitro* culture, depending on the strain (*17, 18*). FOS is a specific inhibitor of the second enzyme in the MEP pathway, 1-deoxy-D-xylulose 5-phosphate reductoisomerase (DXR), which is essential for *P. falciparum* survival (*6, 17, 18*). Therefore, reversal of growth inhibition can aid in the characterization of the mechanism of action to, ultimately, identify the molecular target among the Malaria Box compounds.

In the present work, we aimed to identify the mechanisms of action of the compounds of the Malaria Box. We identified one drug-like compound that targets the apicoplast using cell-based phenotypic assays. Further analyses revealed that the mechanism of action of this compound is more similar to FOS than to DOX. In addition, we probed the Malaria Box for compounds having activity against late-stage gametocytes, which is the most insensitive stage to the current antimalarials (*19, 20*). We identified twelve gametocytocidal compounds with IC_{50} values below 1 μM.

Materials and Methods

Parasites. The following *P. falciparum* strains were obtained through the MR4 Malaria Reagent Repository (ATCC, Manassas, VA) as part of the BEI Resources Repository, NIAID, NIH: D10-ACP_L(leader)-GFP, MRA-568, deposited by A.F. Cowman; NF54, MRA-1000, deposited by M. Dowler, Walter Reed Army Institute of Research; Dd2, MRA-150, deposited by D. Walliker. NF54 is sensitive to chloroquine. Dd2 is a pyrimethamine, chloroquine, and mefloquine-resistant strain. D10-ACP_L-GFP has been transfected with a plasmid containing the leader sequence of the acyl carrier protein (ACP), which is targeted to the apicoplast and fused to green fluorescent protein (GFP), allowing observation of apicoplast development during the parasite's intraerythrocytic cycle. D10-ACP_L-GFP plasmid is maintained by 0.1 μM pyrimethamine treatment (*21*). *P. falciparum* resistant to FOS was a generous gift from David Fidock (*22*) and was maintained by 1 μM FOS treatment.

Malaria Box. The Malaria Box compound collection was provided by SCYNEXIS, Inc. (Research Triangle Park, NC) for MMV and supplied at 10 mM in dimethyl sulfoxide (DMSO). Additional amounts of MMV008138 were purchased from Sigma-Aldrich and results were reproduced using this commercial source.

***P. falciparum* asexual stages culture and drug sensitivity.** Parasites were maintained in O^+ human erythrocytes (4% hematocrit) in RPMI 1640 media supplemented with 5 g/L Albumax I (GIBCO Life Technologies), 2 g/L glucose (Sigma-Aldrich), 2.3 g/L sodium bicarbonate (Sigma-Aldrich), 370 μM hypoxanthine (Sigma-Aldrich), 25 mM HEPES, and 20 mg/L gentamycin (GIBCO Life Technologies). Parasites were kept at 37˚C under reduced oxygen conditions (5.06% CO_2, 4.99% O_2, and 89.95% N_2).

The effect of each compound identified as gametocytocidal was further evaluated against *P. falciparum* strains NF54 and Dd2 asexual parasites using the SYBR green assay as described previously (*23, 24*). Ten-point dilutions were used to test dose-response at concentrations ranging from 5 μM to 0.002 μM. The IC_{50} calculation was performed with GraFit 5 (Erithacus Software Ltd.) using nonlinear regression curve fitting and represents the average of two independent experiments and the standard deviation (SD). We determined the IC_{50} value for

MMV008138, FOS, and DOX at 72 h and 96 h by SYBR green assay to assess delayed death phenotype. MMV008138 was also tested against FOS resistant parasites (FOS-R) by the SYBR green assay.

Reversal of growth inhibition by isopentenyl diphosphate (IPP) supplementation. Recently, it was demonstrated that parasites can survive *in vitro* without the apicoplast when IPP is supplied at 200 μM. A reversal of growth inhibition by IPP supplementation was proposed as a method to potentially identify compounds targeting apicoplast function (*8*). We assessed whether compounds from the Malaria Box were targeting the apicoplast by measuring the growth recovery in the presence of inhibitor and IPP as described previously (*8*). Briefly, Dd2 strain ring stages were cultured under the following conditions: control (no drug), 5 μM of Malaria Box compounds, and 5 μM of Malaria Box compounds with 200 μM IPP, which is the necessary concentration to achieve 100% growth recovery (*8*). FOS was used as a control drug for growth inhibition and reversal of growth inhibition by IPP. All conditions were set in 96-well plates (200 μL/well with 1% hematocrit and 1% parasitemia), incubated for 72 h, and analyzed by the SYBR green assay as described previously (*23, 24*). Percentage of growth was normalized to untreated control parasites. Since several compounds within the Malaria Box did not inhibit growth completely at 5 μM, we only considered reversal of growth inhibition when a compound alone exhibited over 95% growth inhibition and over 60% growth recovery in the presence of inhibitor and IPP. Uninfected erythrocytes were used for background determination. Two independent experiments were performed.

To establish dose-dependency for the reversal of growth inhibition, ring stage parasite cultures (200 μL/well, 1% hematocrit, and 1% parasitemia) were grown for 72 h in the presence of increasing concentrations of the inhibitor and in the presence or absence of 200 μM IPP. The parasite's growth was assessed by SYBR green as described previously (*23, 24*).

Activity of MMV008138 against *Toxoplasma gondii*. RH-HX-KO-YFP2-DHFR(m2m3) strain *T. gondii* tachyzoites were maintained in human fibroblasts and parasite growth was measured by fluorescence assay as described previously (*25*). Drug assays were performed by twofold serial dilutions of MMV008138 dissolved in 100% DMSO using concentrations ranging from 5 μM to 0.039 μM. DMSO was added to a final concentration of 0.05% for all doses. Six replicates were

used for all doses and controls.

Gametocytocidal activity assay. Malaria parasites do not replicate their genome during gametocytogenesis; however, they are metabolically active, especially their mitochondrial metabolism (*26*). Therefore, gametocyte viability was measured using AlamarBlue, a fluorescent oxidoreduction indicator, as a general measure of metabolic activity. In this assay, the fluorometric readings are proportional to the number of living gametocytes and correspond to their metabolic activity. Damaged and nonviable gametocytes have lower metabolic activity and, therefore, generate a proportionally lower signal (dose-dependent) than healthy gametocytes. We investigated whether the compounds from the Malaria Box were active in killing late-stage (stage V) gametocytes using the AlamarBlue viability assay described previously by Tanaka and Williamson (*27*). Gametocytes were developed from the *P. falciparum* NF54 strain (a chloroquine-sensitive strain). Asexual stages were synchronized by sorbitol treatment two days before gametocyte cultures were started. *P. falciparum* subcultures for the generation of gametocytes were set at 1% parasitemia and 4% hematocrit, and the culture media was not changed until day four after subculture. Parasite development was evaluated by Giemsa-stained thin blood smears on days 4, 8, 12, and 13 after the initial subculture. Starting on day nine of gametocyte culture, parasites were treated for four consecutive days with 5% sorbitol for 10 min at 37 ˚C to remove asexual stages. Sorbitol treatment effectively removed >99% of asexual parasites. Gametocyte recovery and concentration was achieved on day 13 using a NycoPrep™ 1.077 cushion and gametocytes were counted using a Neubauer chamber. About 30,000 to 50,000 gametocytes per well (100 µL final volume) were added to black, flat-bottom, half-area 96-well plates containing the drug candidates or 60 nM epoxomicin (*28*) (positive control) or DMSO (negative control). The plate was incubated in a humidified chamber at 37 °C and low oxygen conditions (5.06% CO_2, 4.99% O_2, and 89.95% N_2) for 72 h. AlamarBlue was added on day 16 post-induction at 10% of the well volume and plates were returned to the chamber for an additional 24 h. Fluorescence was determined at 585 nm after excitation at 540 nm. The initial screen was performed at 5 µM (DATA SET S1). Compounds exhibiting over 85% inhibition of metabolic activity as compared to control were selected for further dose-dependent analyses using 10 µM as the highest concentration (Figure 3.5). The IC_{50} calculation was determined from dose-response curves calculated from normalized percent activity values and log10-transformed

concentrations using GraFit 5 software. Only compounds that showed a sigmoidal response were selected to report their gametocytocidal activity (Table 3.2 and Figure 3.5). Final figures were prepared using GraphPad Prism 6 software (Figure 3.5).

Fluorescence microscopy. A Zeiss Axioimager M1 microscope with a 100x/1.4NA oil immersion objective and an Axiocam MRm digital camera was used to image live parasites as described previously with minor modifications (*8*). Briefly, control (untreated), IPP alone, drug-treated, and drug-treated supplemented with 200 μM IPP D10-ACP_L-GFP parasites were incubated with 100 nM MitoTracker®Red CM-H2XRos (Life Technologies) for 15 min at 37˚C. Parasites were washed once with complete media and 0.25 μg/mL Hoechst 33342 (Life Technologies) was added to each condition immediately before imaging. Final figures were prepared using Adobe Photoshop CS2.

Results

Identification of compounds that act on the apicoplast

We used reversal of growth inhibition by IPP supplementation to interrogate the Malaria Box to identify compounds having a mechanism of action that targets the apicoplast (*8*). From the 400 compounds tested, only the drug-like compound MMV008138 met our criteria of >95% growth inhibition at 5 μM for the compound alone and over 60% growth recovery in the presence of inhibitor and 200 μM IPP, as detailed in the methods section. MMV008138 showed at least 85% recovery of growth inhibition in the presence of IPP (Figure 3.1A) when retested at 2.5 μM, indicating that this compound interferes with the function of the apicoplast as its mechanism of action. As expected, growth inhibition by FOS was 100% reversed by IPP supplementation. The complete data set listing growth inhibition at 5 μM for all inhibitors tested as well as the respective growth recovery in the presence of IPP is available as supplemental material (Data Set S1).

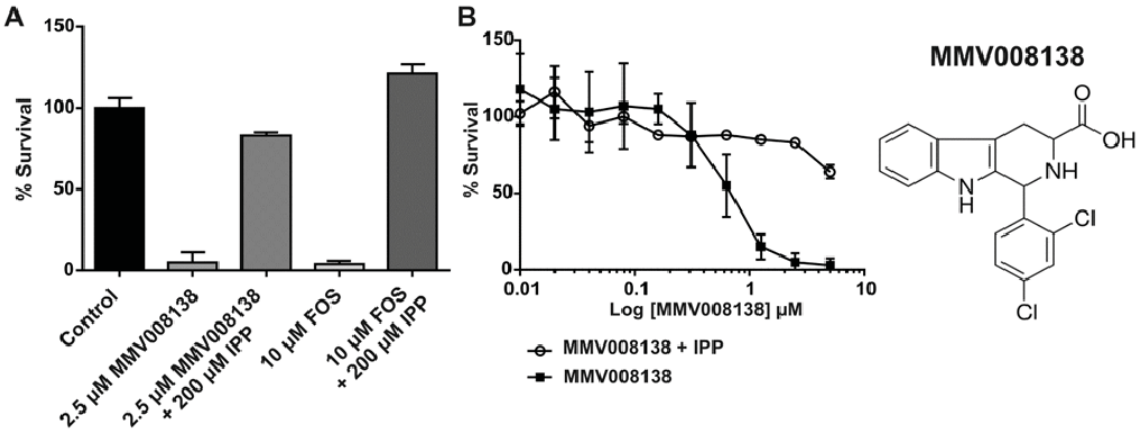

Figure 3. 1. ***In vitro*** **activity of MMV008138. A)** MMV008138 demonstrated at least 85% recovery of growth inhibition in the presence of 200 μM IPP. FOS was used as positive control as it is also rescued by IPP**. B)** MMV008138 concentration-dependent activity and growth recovery in the presence of 200 μM IPP after 72 h incubation.

We determined that MMV008138 has an IC_{50} value of 350 nM for the Dd2 strain (Table 3.1). We observed >85% growth recovery at concentrations up to 2.5 μM MMV008138 and 200 μM IPP but only ~70% growth recovery was observed at 5 μM MMV008138 and 200 μM IPP in the Dd2 strain (Figure 3.1B), which may indicate

Table 3. 1. *In vitro* activity (IC_{50}) of DOX, FOS, and MMV008138 against asexual stages in different *P. falciparum* strains.

	IC_{50} (nM) against:					
	Dd2 (nM)		NF54			
Compound	72 h	96 h	72 h	96 h	D10-ACP_L-GFP at 72 h	FOS^r Parasites at 72 h
DOX	>4,500	900 ± 180	2,370 ± 410	380 ± 60	N.D.	N.D.
FOS	880 ± 70	430 ± 50	980 ± 60	N.D.	1,610 ± 160	3,330 ± 150
MMV008138	350 ± 50	180 ± 30	300 ± 10	N.D.	370 ± 30	250 ± 10

[a] Data shown are mean ± SD
[b] ND, not determined

off-target effects at high concentrations. To avoid potential off-target effects, all of the following studies were performed at concentrations equal to or below 2.5 μM. We also noted that the kinetics of MMV008138 inhibition resembled that of FOS activity (Table 3.1, compare 72 and 96 h IC_{50} values) (*29-31*). For comparison, we used DOX, which blocks protein translation in the apicoplast and shows a pronounced delayed death phenotype (Table 3.1). Next, we decided to test MMV008138 against a FOS-resistant strain (FOS-R) to investigate DXR as the potential molecular target. The resistance in FOS-R is due to an increase in the copy number of the *Pfdxr* gene, which encodes for the enzyme targeted by FOS, allowing the parasite to overcome FOS-mediated inhibition of isoprenoid biosynthesis (*22*). Intriguingly, whereas FOS showed a four-fold increase in IC_{50} for the FOS-R, relative to its parental strain Dd2, MMV008138 exhibited no increase in its IC_{50} value against FOS-R (Table 3.1, compare Dd2 and FOS-R IC_{50} values at 72 h).

T. gondii is an apicomplexan parasite that, like *P. falciparum*, harbors an apicoplast that is essential for the parasite's survival. *T. gondii* causes toxoplasmosis in humans and can be life-threating for immunocompromised individuals. Currently, antifolates form the basis of chemotherapy against both primary and secondary (recurrent) infection by *T. gondii.* Antifolate therapy is effective in limiting the growth of the acute tachyzoite stage but does not cure chronic infection. New drugs with different modes of action are, therefore, highly desirable for this pathogen as well. We tested MMV008138 against *T. gondii* but no effect on the parasite's growth was observed (Figure 3.2). This lack of activity may be due to the lack of transport of MMV008138, similar to previous observations using FOS. While *T. gondii* relies on the MEP pathway for isoprenoid precursor biosynthesis, the parasite is insensitive to high concentrations

of FOS due to the lack of drug uptake at the level of the parasite plasma membrane (*7*).

Effect of MMV008138 on apicoplast development

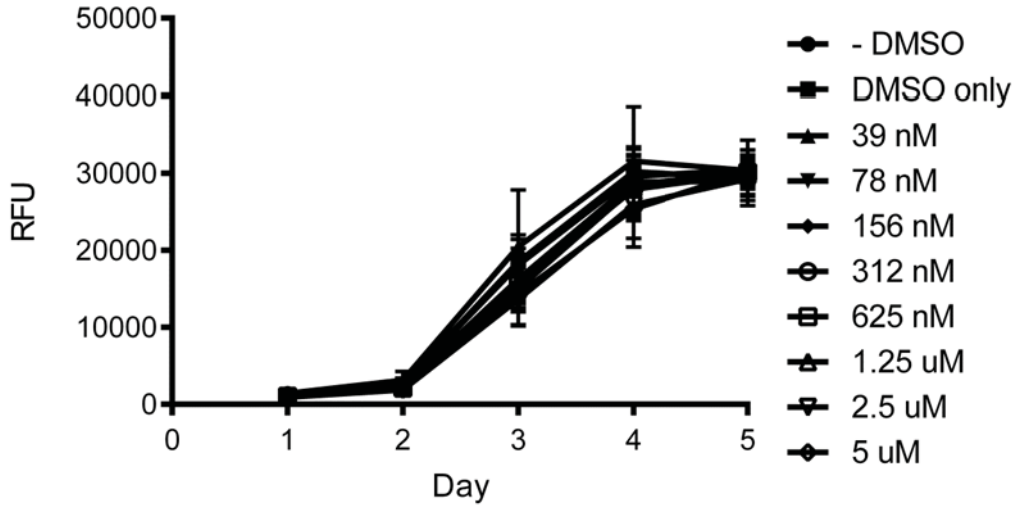

Figure 3. 2. *T. gondii* sensitivity to MMV008138. *T. gondii* parasite growth was not affected by MMV008138 treatment. This result could indicate that the molecular target is absent in this parasite or the drug is not transported.

To investigate the effect of MMV008138 on apicoplast development, we used a transgenic *P. falciparum* cell line D10-ACP_L-GFP to visualize the apicoplast (*21*). In this line, green fluorescent protein (GFP) is targeted to the lumen of the organelle and its developmental changes along the intraerythrocytic cycle are readily observed. Microscopic analysis showed that the apicoplast elongation and division process was arrested in MMV008138-treated parasites. A single stunted apicoplast was present at a point where controls showed a well-developed tubular apicoplast or an organelle that already had given rise to multiple daughters. This pattern was indistinguishable from parasites treated with FOS (Figure 3.3 and Figure 3.5). We also co-stained cells with MitoTracker®, which accumulates in the mitochondria of living cells and is dependent on the mitochondrial membrane potential. We noted diminished labeling of the mitochondrion in both FOS and MMV008138-treated parasites. A diminished membrane potential is consistent with the role of the apicoplast isoprenoid pathway in ubiquinone biosynthesis. It has been demonstrated that FOS inhibits ubiquinone biosynthesis (*17, 32*). Ubiquinones participate in the electron transport chain and their biosynthesis relies on the MEP pathway to provide precursors for the isoprene side chain that anchors them into the inner membrane of mitochondria. Importantly, the addition of 200 μM IPP rescued both apicoplast

development and mitochondrial membrane potential in FOS and MMV008138-treated parasites (Figure 3.2 and Figure 3.10) and this recovery was also observed at 1μM and 350 nM MMV008138 (Figure 3.4 and Figure 3.11). As mentioned above, the effect of DOX treatment on apicoplast development is not observed until the following intraerythrocytic cycle, explaining the slow action of this drug (*11*). As expected, 40 h of DOX treatment did not affect apicoplast development at this early time point (Figure 3.11) but inhibition of apicoplast elongation was observed after 120 h of treatment (Figure 3.2 and Figure 3.12). In contrast, IPP supplementation restored the mitochondrial membrane potential but not apicoplast morphology in DOX-treated parasites. The fact that MMV008138 is fully rescued by IPP suggests a metabolic function for its target, potentially in IPP biosynthesis.

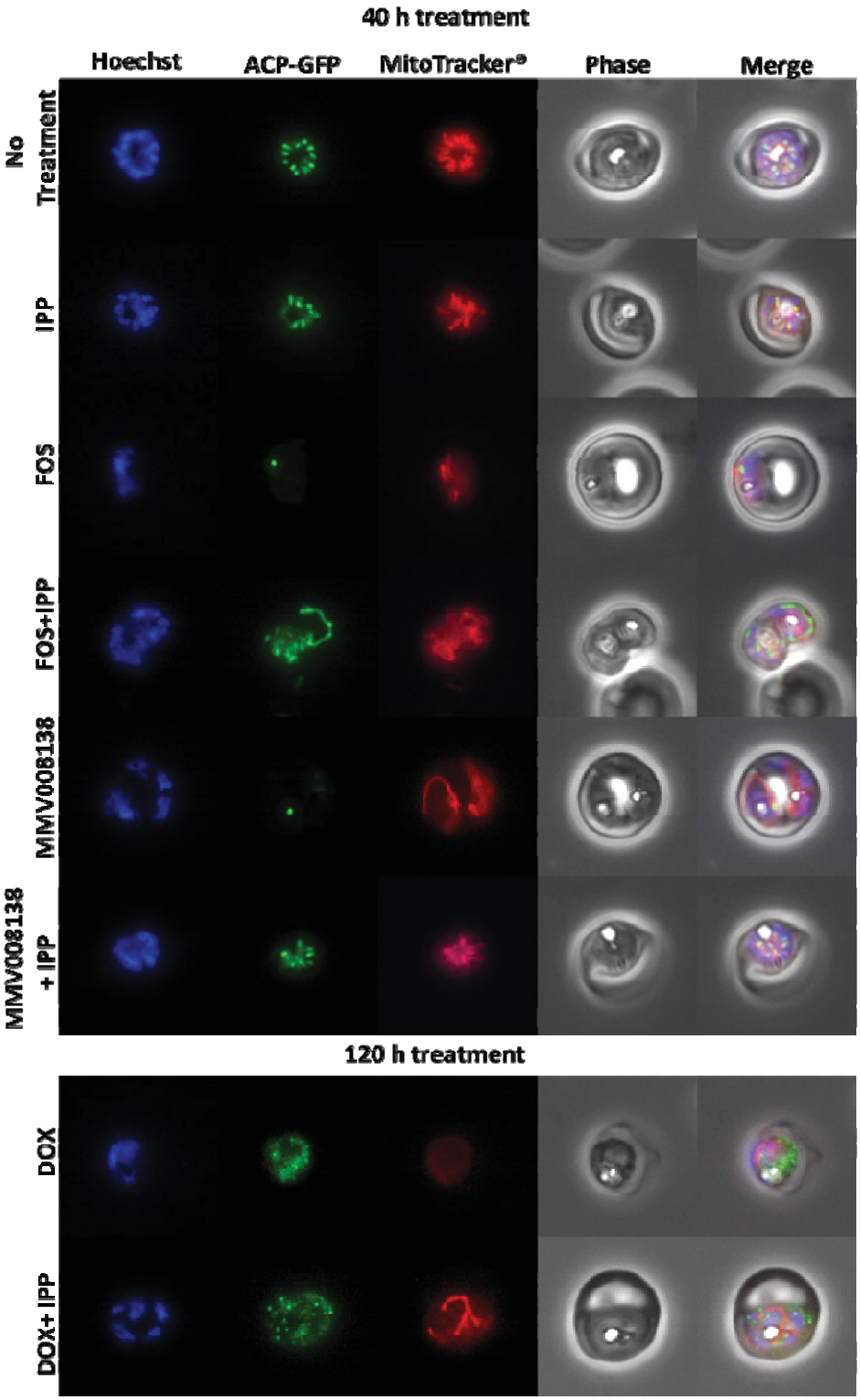

Figure 3. 3. Widefield epifluorescence microscopy for nucleus (Hoechst), apicoplast (ACP-GFP, and mitochondria (MitoTracker ®) of MMV008138 and IPP treated parasites. Comparison of schizonts in untreated control parasites, FOS-treated (10 µM), FOS-treated (10 µM) in the presence of IPP (200 µM), MMV008138-treated (2.5 µM), and MMV008138 (2.5 µM) in the presence of IPP (200 µM) after 40 h of treatment. Additional treatment with DOX (2 µM) and DOX (2 µM) with IPP (200 µM) after 120 h of treatment.

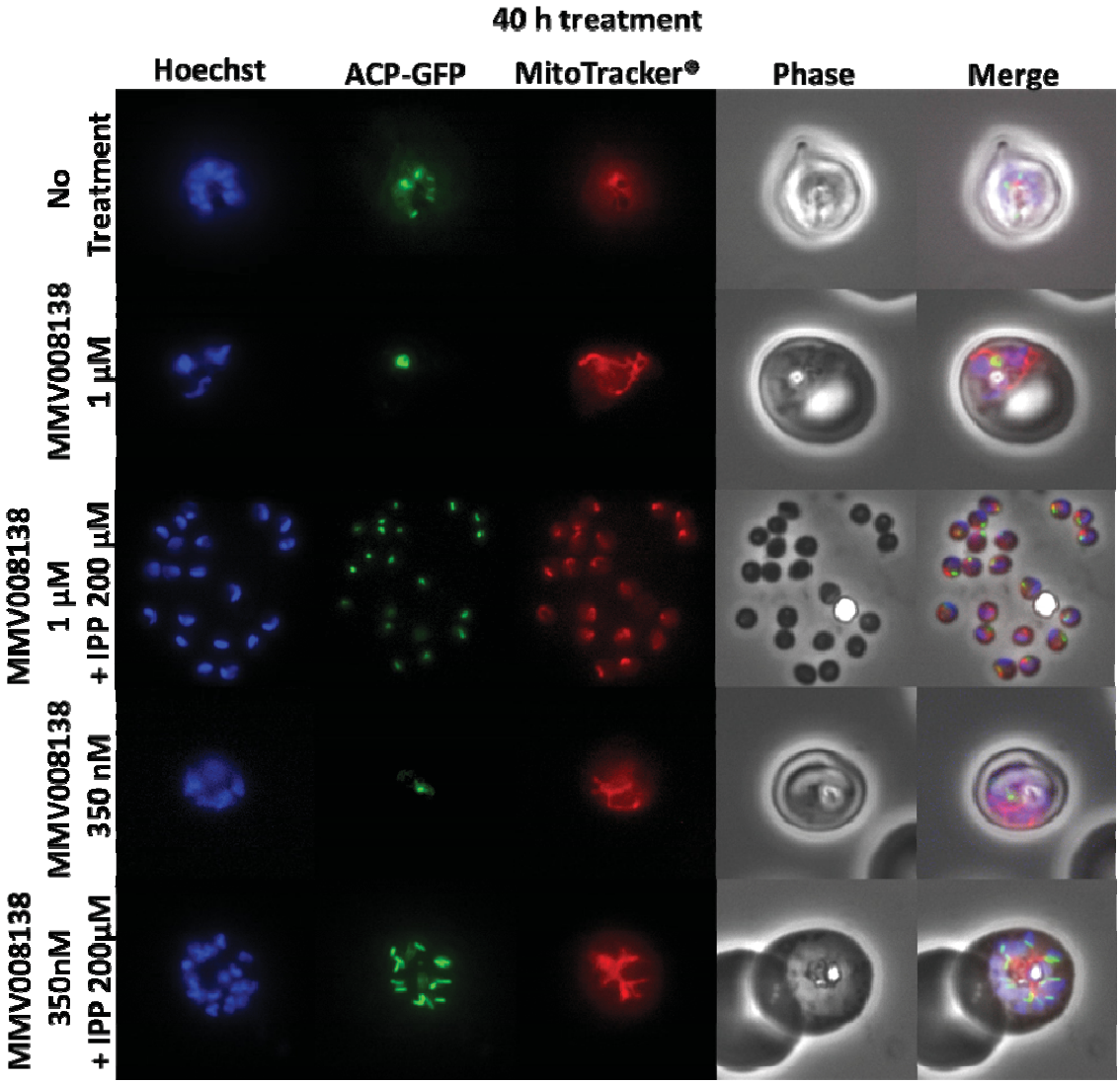

Figure 3. 4. Additional widefield epifluorescence microscopy for nucleus (Hoechst), apicoplast (ACP-GFP, and mitochondria (MitoTracker ®) of MMV008138 and IPP treated parasites. Comparison of schizonts in untreated control parasites, at the indicated concentrations, in the absence or presence of IPP (200 µM) after 40 h of treatment. We observed several microscopic fields of parasites treated with 350 nM (IC_{50} value) of MMV008138 and only ~ 50% of the treated parasites showed inhibition of apicoplast development in agreement with the mechanism of action.

Gametocytocidal activity among the Malaria Box compounds

In our efforts to elucidate the mechanisms of action of compounds within the Malaria Box, we also evaluated their activity against other stages of the parasite's life cycle. We decided to probe the Malaria Box collection for gametocytocidal activity since new transmission-blocking antimalarials are needed and the gametocytocidal potential of Malaria Box compounds has not been evaluated to date. We identified a set of 22 compounds that showed over 85% inhibition of gametocyte viability at 5 μM as assayed by AlamarBlue. The complete data for all compounds is available as supplemental material (Data Set S1). From the set of 22 active compounds, 18 compounds acted in a clear dose-dependent manner, and 12 showed IC_{50} values below 1 μM (Table 3.2 and Figure 3.5). At 5 μM concentration, MMV008138 did not have activity against late-stage gametocytes (Data Set S1). The set of 18 compounds was tested in asexual intraerythrocytic stages against drug resistant- and drug-sensitive parasites. Three compounds, MMV000248, MMV006172, and MMV019555, showed mid-nanomolar IC_{50} values in late stage gametocytes and low-nanomolar IC_{50} values in asexual stages (Table 3.2). An IC_{50} value of 3.8 nM was obtained for epoxomicin, a compound for which gametocytocidal activity had been reported previously (Table 3.2 and Figure 3.5) (*28*).

Figure 3.5

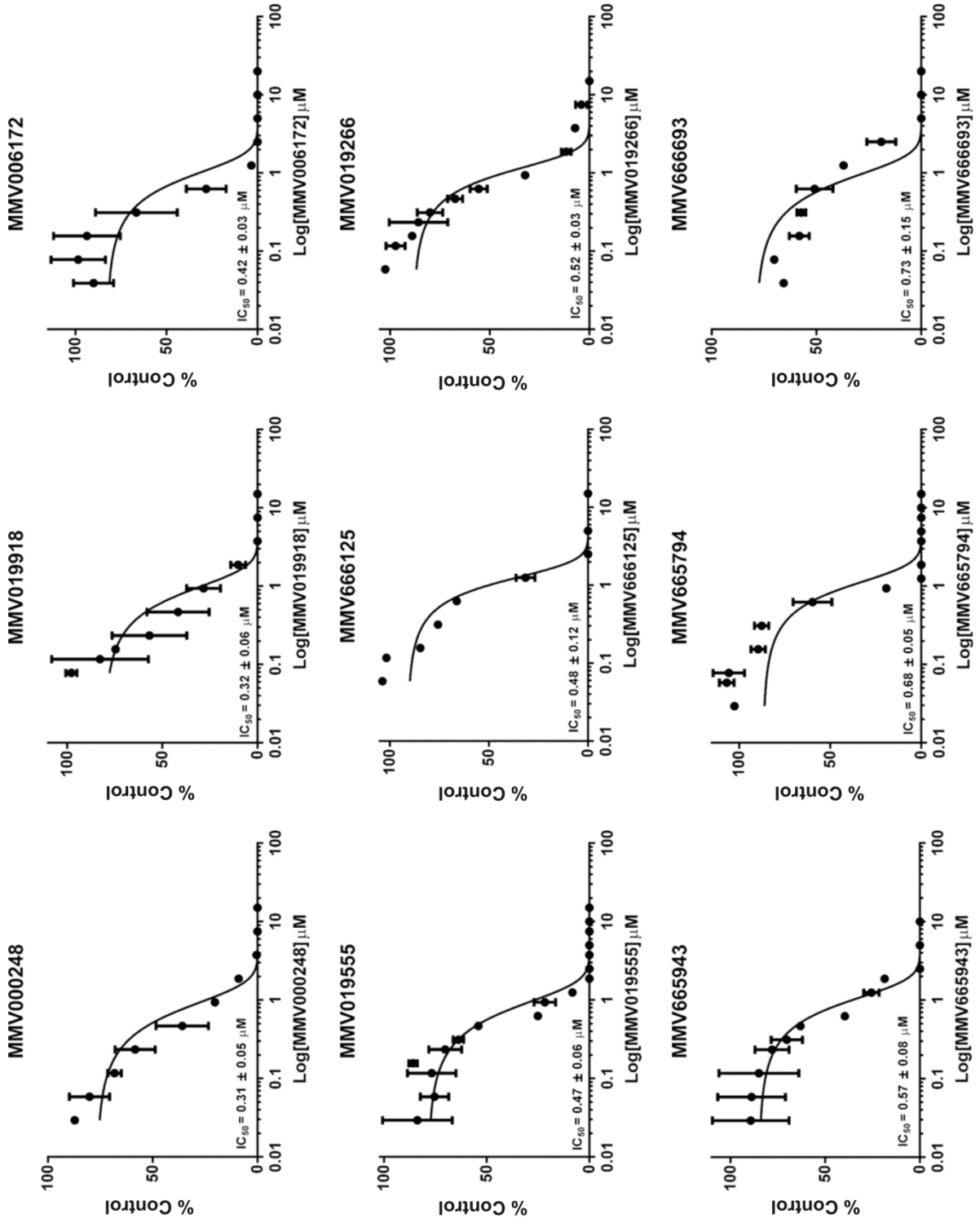
MMV006172
IC50 = 0.42 ± 0.03 µM
MMV019266
IC50 = 0.52 ± 0.03 µM
MMV666693
IC50 = 0.73 ± 0.15 µM
MMV019918
IC50 = 0.32 ± 0.06 µM
MMV666125
IC50 = 0.48 ± 0.12 µM
MMV665794
IC50 = 0.68 ± 0.05 µM
MMV000248
IC50 = 0.31 ± 0.05 µM
MMV019555
IC50 = 0.47 ± 0.06 µM
MMV665943
IC50 = 0.57 ± 0.08 µM
% Control
Log[MMV006172] µM
Log[MMV019266] µM
Log[MMV666693] µM
Log[MMV019918] µM
Log[MMV666125] µM
Log[MMV665794] µM
Log[MMV000248] µM
Log[MMV019555] µM
Log[MMV665943] µM

Figure 3.5

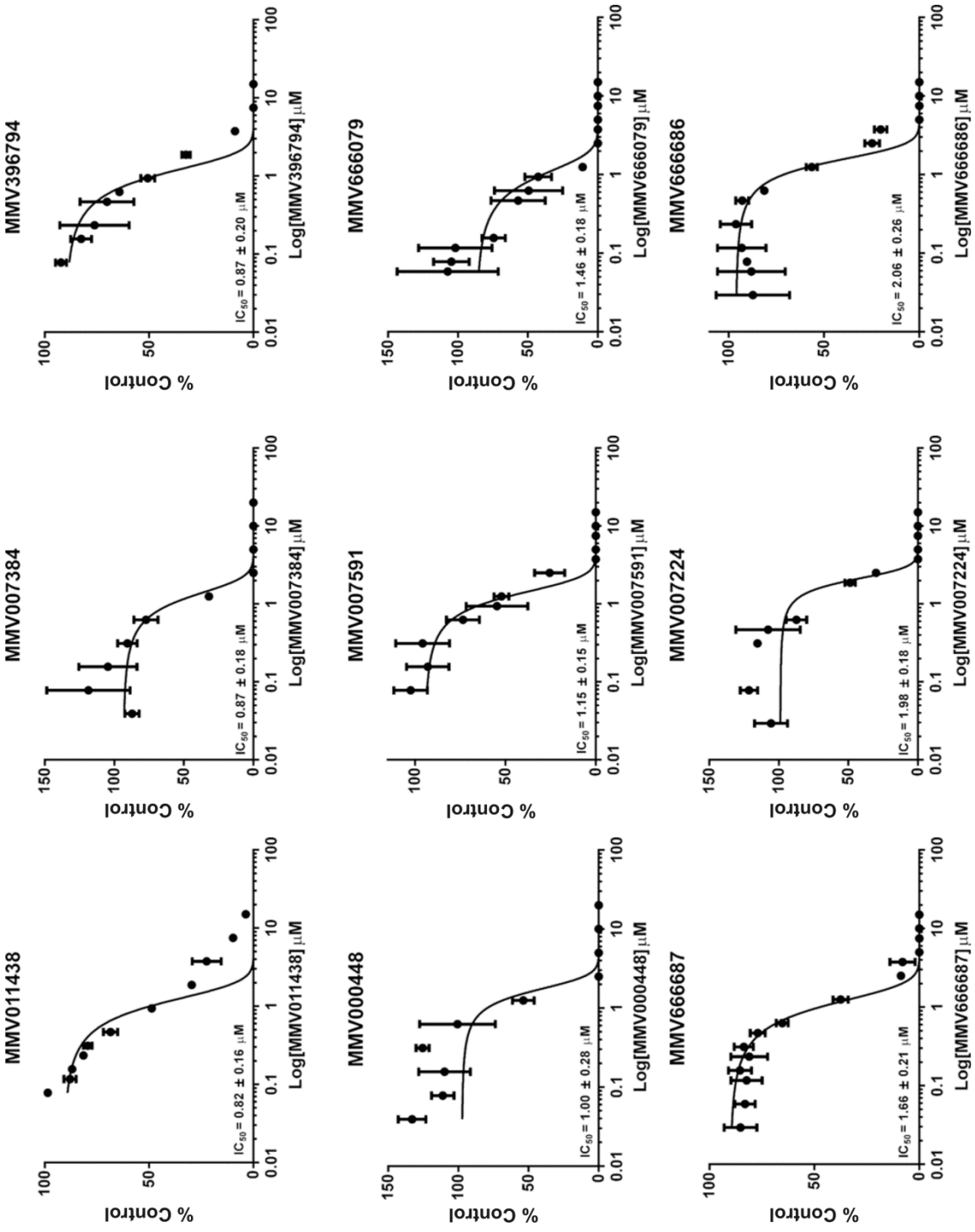
MMV396794
% Control
Log[MMV396794] µM
IC50 = 0.87 ± 0.20 µM
MMV007384
% Control
Log[MMV007384] µM
IC50 = 0.87 ± 0.18 µM
MMV666079
% Control
Log[MMV666079] µM
IC50 = 1.46 ± 0.18 µM
MMV666686
% Control
Log[MMV666686] µM
IC50 = 2.06 ± 0.26 µM
MMV011438
% Control
Log[MMV011438] µM
IC50 = 0.82 ± 0.16 µM
MMV007591
% Control
Log[MMV007591] µM
IC50 = 1.15 ± 0.15 µM
MMV007224
% Control
Log[MMV007224] µM
IC50 = 1.98 ± 0.18 µM
MMV000448
% Control
Log[MMV000448] µM
IC50 = 1.00 ± 0.28 µM
MMV666687
% Control
Log[MMV666687] µM
IC50 = 1.66 ± 0.21 µM

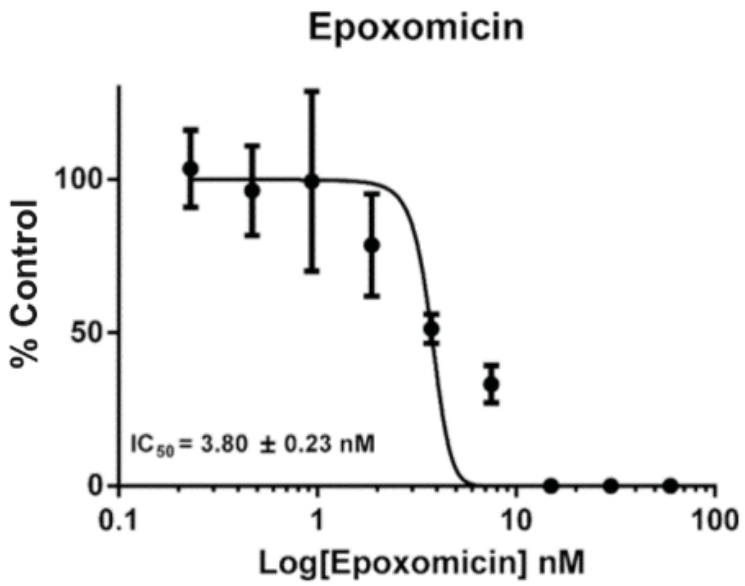

Figure 3. 5. Dose-response curves (gametocytocidal activity) for compounds shown in Table 3.2. Data were normalized (% control) as a percentage of the controls (no drug added). Epoxomicin was used as the control drug to evaluate gametocytocidal activity. Curves represent the average of two independent experiments performed in duplicate.

Table 3. 2. *In vitro* antimalarial activity (IC_{50}) against gametocytes (NF54 strain) and asexual stages (NF54 and Dd2 strain).

		IC_{50} (nM) (mean ± SD) against:		
			Parasites in asexual stages[b] in strain:	
MMV no.	Set	Gametocytes[a] NF54 (nM)	NF54 (nM)	Dd2 (nM)
MMV000248	Drug-like	310 ± 50	50 ± 6	90 ± 10
MMV019918	Drug-like	320 ± 60	280 ± 80	620 ± 280
MMV006172	Probe-like	420 ± 30	40 ± 3	60 ± 3
MMV019555	Probe-like	470 ± 60	20 ± 1	70 ± 5
MMV666125	Probe-like	480 ± 120	120 ± 20	50 ± 2
MMV019266	Drug-like	520 ± 30	310 ± 50	380 ± 20
MMV665943	Probe-like	570 ± 80	190 ± 30	190 ± 20
MMV665794	Probe-like	680 ± 50	90 ± 10	90 ± 5
MMV666693	Drug-like	730 ± 150	40 ± 6	20 ± 2
MMV011438	Probe-like	820 ± 160	50 ± 5	130 ± 20
MMV007384	Probe-like	870 ± 180	100 ± 7	190 ± 20
MMV396794	Drug-like	870 ± 200	180 ± 20	60 ± 6
MMV000448	Probe-like	1000 ± 280	50 ± 5	350 ± 40
MMV007591	Probe-like	1150 ± 150	920 ± 170	840 ± 400
MMV666079	Probe-like	1460 ± 180	210 ± 30	260 ± 20
MMV666687	Probe-like	1660 ± 210	270 ± 50	190 ± 8
MMV007224	Probe-like	1980 ± 180	320 ± 20	270 ± 20
MMV666686	Probe-like	2060 ± 260	450 ± 90	360 ± 30
Epoxomicin	(+) control	3.8 ± 0.2	N.D.[c]	N.D.

[a] Gametocytocidal activity was measured using alamarBlue, a fluorescent oxidoreduction indicator of gametocyte metabolic activity. The IC_{50} values were obtained from dose-response curves calculated from normalized percent activity values and log_{10}-transformed concentrations (see Figure 3.3S in the supplemental material). Epoxomicin and DMSO were used as positive and negative controls, respectively.

[b] *In vitro* antimalarial activity against parasites in asexual stages was evaluated using the SYBR green assay.

[c] ND, not determined

Discussion

MMV008138 inhibits apicoplast elongation

The apicoplast is indispensable for parasite survival and is unique to the parasite. The apicoplast is already a well-established and clinically used target for antibiotics in malaria and toxoplasmosis therapy (*4*). The apicoplast harbors hundreds of proteins and there are likely numerous additional targets to be identified and exploited (*4, 5, 33, 34*). Recently, it was demonstrated that parasites can survive *in vitro* without the apicoplast when IPP is supplied at 200 μM. A reversal of growth inhibition by IPP supplementation was proposed as a method to potentially identify compounds targeting apicoplast function (*8*). Here, we used the IPP supplementation assay to interrogate Malaria Box compounds targeting the apicoplast in order to establish their mechanisms of action and we identified MMV008138 as a new anti-apicoplast lead (Table 3.1). Interestingly, we noted that MMV008138's mechanism of action is more like FOS than DOX. In general, drugs like DOX, which target apicoplast genome replication, transcription, protein translation, post-translation modification, or protein turnover, exhibit a delayed death phenotype (*9-15*). The kinetics of MMV008138 provided circumstantial support for the hypothesis that this drug acts more directly on the metabolism of the organelle than through interference with its biogenesis.

More directly, we showed that MMV008138 inhibited apicoplast elongation and disturbed the mitochondrial membrane potential and that these phenotypes were reversed by the presence of IPP (Figure 3.2). FOS also showed inhibition of apicoplast elongation, as reported previously (*7*), and we reported here that this phenotype can be reversed by IPP supplementation. A potential mechanism by which FOS prevents apicoplast elongation could be through inhibition of the isoprenoid modification of the tRNA on the adenine bases, which is essential for binding to the mRNA-ribosome complex and ensures translational integrity (*33, 35*). Four tRNAs in *Plasmodium* are predicted to be isoprenylated in the apicoplast (*33*). However, no studies have been reported so far that directly demonstrate tRNA isoprenylation in *Plasmodium*. Furthermore, FOS also disrupted the mitochondrial membrane potential, which was expected as FOS inhibits ubiquinone biosynthesis (*17, 32*). Rescue of apicoplast elongation by IPP supplementation was not observed in parasites treated with DOX (Figure 3.2), similar to chloramphenicol (*8*) which inhibits protein synthesis in the apicoplast by targeting the ribosomes. This suggests that DOX and MMV008138 act on different targets and that MMV008138 does not interfere with protein

synthesis.

Altogether, our results are consistent with the hypothesis that MMV008138 may have its molecular target within the MEP pathway; therefore, we also tested this compound against FOS-R parasites. As mentioned above, the resistance in this parasite strain is due to an increase in the copy number of the *Pfdxr* gene (*22*). The FOS-R strain exhibited no change in its IC_{50} value for MMV008138 compared with its parental strain Dd2, suggesting that DXR is most likely not the molecular target (Table 3.1). Since the apicoplast is indispensable for apicomplexan parasites and an attractive drug target, we tested MMV008138 against *T. gondii,* another important human pathogen, but it was inactive, similar to FOS, perhaps due to poor transport (*7*). Our efforts to identify the potential molecular target(s) for MMV008138 in *P. falciparum* may also help to establish the basis of its lack of activity in *T. gondii.*

It has been shown that antibiotics targeting the apicoplast, including FOS, do not affect late-stage gametocytes (*20*), and we observed that MMV008138 also did not affect late-stage gametocytes. This lack of activity could be expected since the apicoplast does not grow during gametocytogenesis, but others have noted that the mitochondrion undergoes remarkable morphological development during gametocytogenesis (*36*), which requires an active MEP pathway to supply IPP and DMAPP for ubiquinone biosynthesis. The low activity of FOS and MMV008138 against late-stage gametocytes could then be attributed to either a) poor transport or b) prior biosynthesis and storage of the needed isoprenoids.

Due to its short half-life in plasma, FOS is not suitable for monotherapy; however, combination therapy studies in humans revealed success in maintaining total parasite clearance when FOS was used with artesunate or clindamycin (*37-43*). Thus far, our results indicate that MMV008138 affects apicoplast function and that its molecular target may differ from current anti-apicoplast drugs like FOS. Whether a compound like MMV008138 could comprise a new and useful adjunct to other antimalarials will depend upon many factors, including pharmacokinetic parameters.

Structure-activity relationship (SAR) of MMV008138

The most notable structural features of MMV008138 are its pipecolic acid and tetrahydro-β-carboline moieties. A review of the 400 compounds in the Malaria Box revealed that only MMV008138 possessed both of these functionalities. One other tetrahydro-β-carboline, (MMV019690), and two related structures (MMV396719, and MMV396715, Figure 3.6) were identified among the 400 compounds with only MMV019690 possessing the 1-aryl substituent present in MMV008138. Since none of the three other related structures possessed anti-apicoplast activity, we conclude that the appropriate 1-aryl group and 3-carboxylic acid (i.e., pipecolic acid) moiety contribute to anti-apicoplast activity. Interestingly, the clinical candidate, NITD609, has a very similar scaffold structure to MMV008138 and is currently in human clinical trials as a monotherapy for malaria (*44-47*).

In addition to possessing the 1-aryl-tetrahydro-β-carboline, this potential antimalarial features a

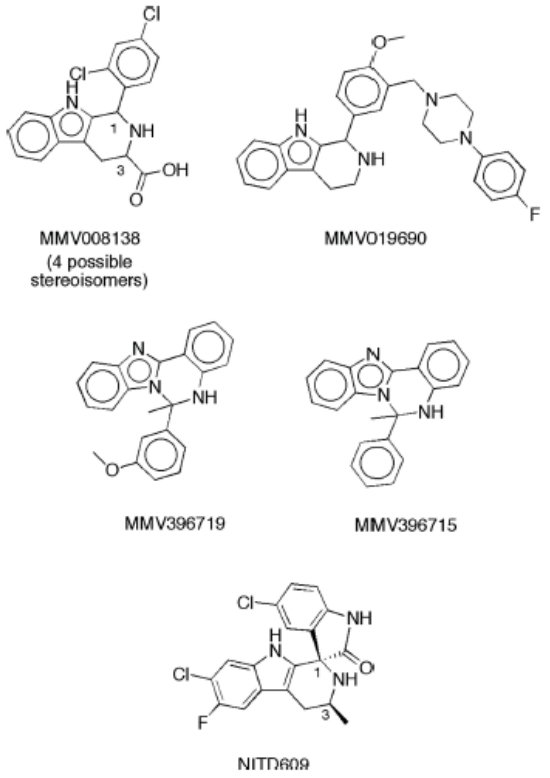

Figure 3. 6. Structures of MMV008138, three other tetrahydro-β-carbolines or close analogs in the Malaria Box, and clinical candidate NITD609.

transposed pipecolic acid moiety in the form of a spiro-amide and a methyl group in place of the carboxy group of MMV008138 (Figure 3.6). It should be noted that MMV008138 is present in the Malaria Box as an unspecified mixture of four stereoisomers that differ in their configurations at C1 and C3.

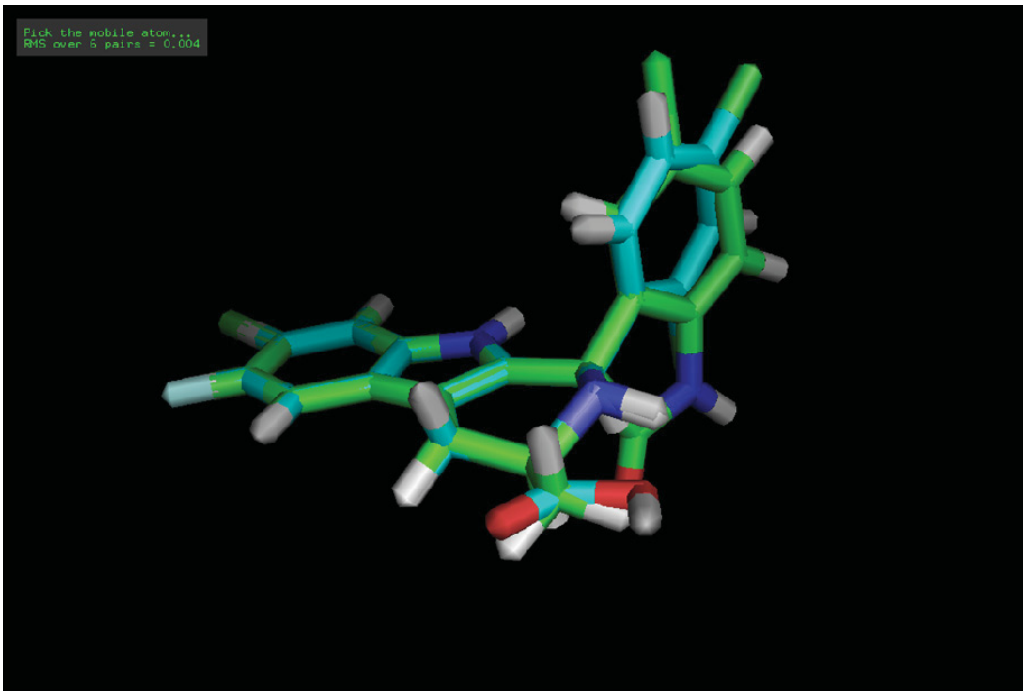

Figure 3. 7. Overly of minimum energy structure of (1*R*,3*R*)-MMV008138 and NITD609 (cyan and green sticks, respectively; MMFF94 optimization).

After we confirmed that MMV008138 was specifically targeting the apicoplast, MMV008138 was purchased from Sigma-Aldrich (again, an unspecified mixture of stereoisomers) and the re-assay results matched those of the MMV sample. Of these possible stereoisomers, the (1*R*,3*R*)-stereoisomer of MMV008138 coincidentally provides a very close structural mimic of NITD609 (Figure 3.7). NITD609 targets PfATPase4, a plasma membrane Na^+ efflux pump (*44*), and is active against gametocyte stages (*45*). Is the (1*R*,3*R*)-stereoisomer of MMV008138 present in the Malaria Box, and if so, does it have activity similar to that of NITD609? At this point, we cannot address this question, since, as mentioned, the low gametocytocidal activity of MMV008138 may be due to poor transport in late-stage gametocytes.

It is also too early to know what off-target activities MMV08138 might possess. Tetrahydro β-carbolines comprise a large group of natural and synthetic indole alkaloids. These compounds are of great interest due to their diverse biological activities and possess a broad

spectrum of pharmacological properties including sedative, anxiolytic, hypnotic, anticonvulsant, antitumor, antiviral, and antiparasitic as well as antimicrobial activities (*48*). Additionally, their molecular targets span from inhibition of topoisomerase, monoamine oxidase, and cyclic nucleotide phosphodiesterases to interaction with benzodiazepine receptors and 5-hydroxy serotonin receptors. However, to the best of our knowledge, MMV008138 has no other biological or enzymatic activity reported beyond its antimalarial activity in asexual intraerythrocytic stages (*29-31*).

New potential leads for transmission-blocking development

Currently, primaquine is the only drug active against late stage gametocytes and only a small set of new transmission-blocking drugs are in clinical trials (*49*), supporting the urgent need for new leads against late-stage gametocytes. Therefore, we decided to interrogate the Malaria Box against late stage gametocytes not only as a complementary assay to study their mechanisms of action, but also to identify new gametocytocidal leads. Twelve compounds with IC_{50} values below 1 μM against late-stage gametocytes were identified. Three compounds MMV000248, MMV006172, and MMV019555 showed mid-nanomolar IC_{50} values in late-stage gametocytes and low-nanomolar IC_{50} values in asexual stages (Table 3.2).

Among these three compounds, two basic pharmacophores were identified: the benzimidazole imine scaffold and the 9-aminoacridine/9-aminotetrahydroacridine scaffold.

MMV000248 (Figure 3.8) is a promising drug-like compound that showed the best overall potency in late-stage gametocytes and asexual stages (Table 3.2). It possesses the bicyclic

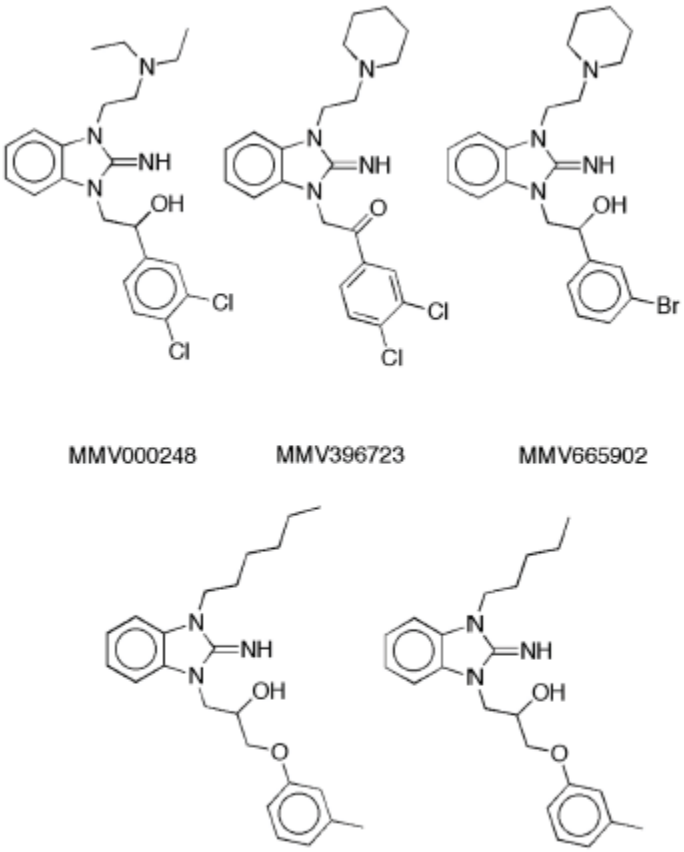

Figure 3. 8. MMV000248 and related benzimidazole imine structures in the Malaria Box. The IC_{50} values for MMV396723 (~1.25 μM), MMV665902 (~1 μM), MMV000445 (~1.135 μM), and MMV000444 (~1.25 μM) in asexual intraerythrocytic stages were previously reported and can be found in the ChEMBL database (https://www.ebi.ac.uk/chemblntd).

guanidine or benzimidazole imine scaffold, which is also present in four other compounds in the Malaria Box (Figure 3.8). Similar to MMV000248, both MMV396723 and MMV665902 contain pendant tertiary amine moieties. Three of the four compounds (MMV665902, MMV000445, and MMV000444) also resemble MMV000248 in bearing a secondary alcohol embedded in a two- to four-atom linker connecting the endocyclic nitrogen of the imidazole imine to an aromatic ring. The lack of confirmed gametocytocidal activity of these four compounds, combined with 10- to 20-fold increases in their previously reported asexual stage IC_{50} values (*2*) is quite striking. Overall, these data indicate strict structural requirements for both gametocytocidal and asexual

stage activity within this scaffold (Figure 3.8).

MV006172 and MMV019555 possess the 9-aminoacridine and 9-amino-tetrahydroacridine scaffolds, respectively, known to be antimalarial pharmacophores (*50*). MV006172 was shown to have moderate activity against the liver-stage of *P. yoelii* (*30*) and this compound was also found to bind to the recombinant human α-2C adrenergic receptor (*51*). MMV019555 is a dimeric molecule that was originally explored as an acetylcholinesterase inhibitor (*52*). A search of the Malaria Box revealed three other 9-aminoacridines (MMV000304, MMV000448, and MMV006513) and no additional 9-aminotetrahydroacridines (Figure 3.9).

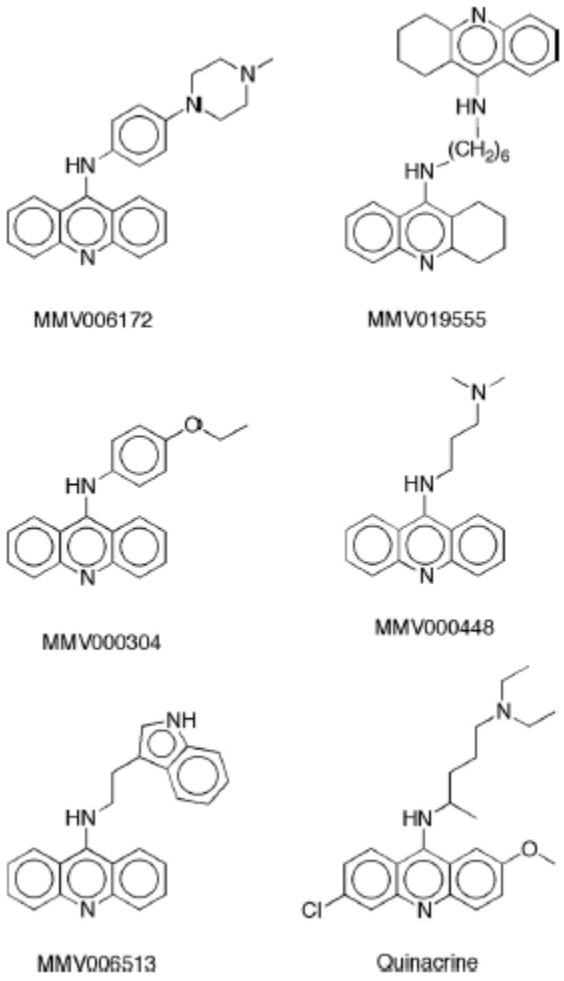

Figure 3. 9. MMV006172, MMV019555, three related 9-aminoacridines in the Malaria Box, and quinacrine.

Interestingly, MMV006172 bears a close resemblance to the three other 9-aminoacridines and quinacrine, which is a known potent antimalarial active against intraerythrocytic asexual stages of chloroquine-resistant *P. falciparum* Dd2 strain (*53*) and inactive against *P. falciparum* gametocytes (*54, 55*). The asexual stage potency of MMV006172, MMV019555, and MMV000448 (Table 3.2) may stem from their structural resemblance to quinacrine (IC_{50} = 5-10 nM, (*53*)). Like quinacrine, both of these compounds feature a five- to seven-atom tether to a basic amine moiety. The three other 9-aminoacridines in Figure 3.8 either feature a shorter tether or lack a pendant basic amine. However, since quinacrine is inactive against *P. falciparum* gametocytes, this structural motif is clearly not sufficient for gametocytocidal activity.

In conclusion, we identified one promising drug-like compound, MMV000248, showing activity against both asexual and sexual intraerythrocytic stages at low and mid-nanomolar values, respectively, and is a potential multistage lead that could be developed to both cure malaria and stop its transmission.

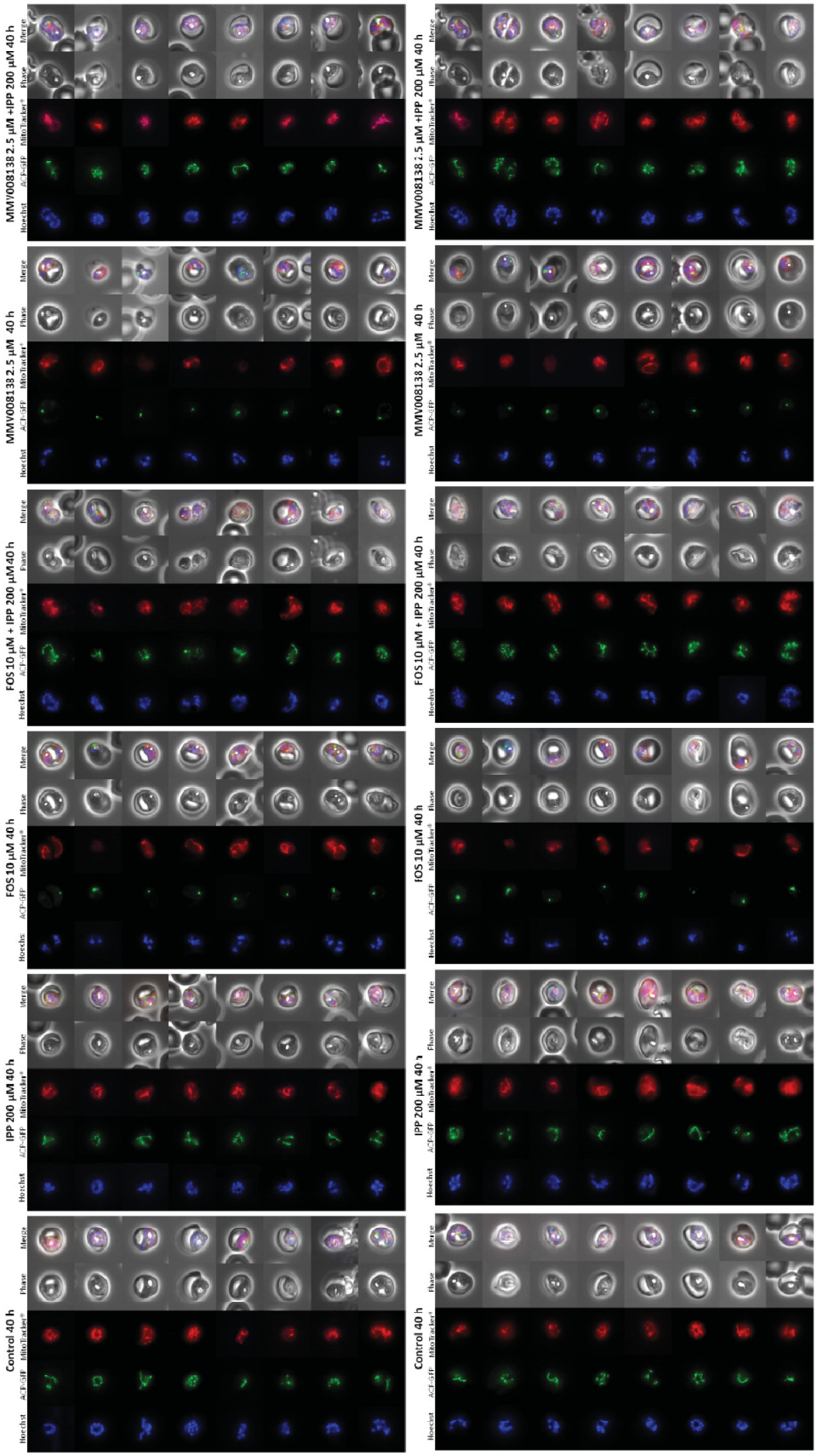

Figure 3. 10. Widefield Epifluorescence Microscopy of parasites treated with MMV008138 10 µM at 40 h. The two panels above show widefield epifluorescence microscopy for the nucleus (Hoechst), apicoplast (ACP-GFP), and mitochondria (MitoTracker®), comparing several microscopic fields of schizonts from each indicated condition. D10-ACP_L parasites in the ring stage were cultured at 4% parasitemia for 40 h in the absence or presence of each drug and in the absence or presence of 200 µM IPP. All conditions were also supplemented with 0.1 µM pyrimethamine.

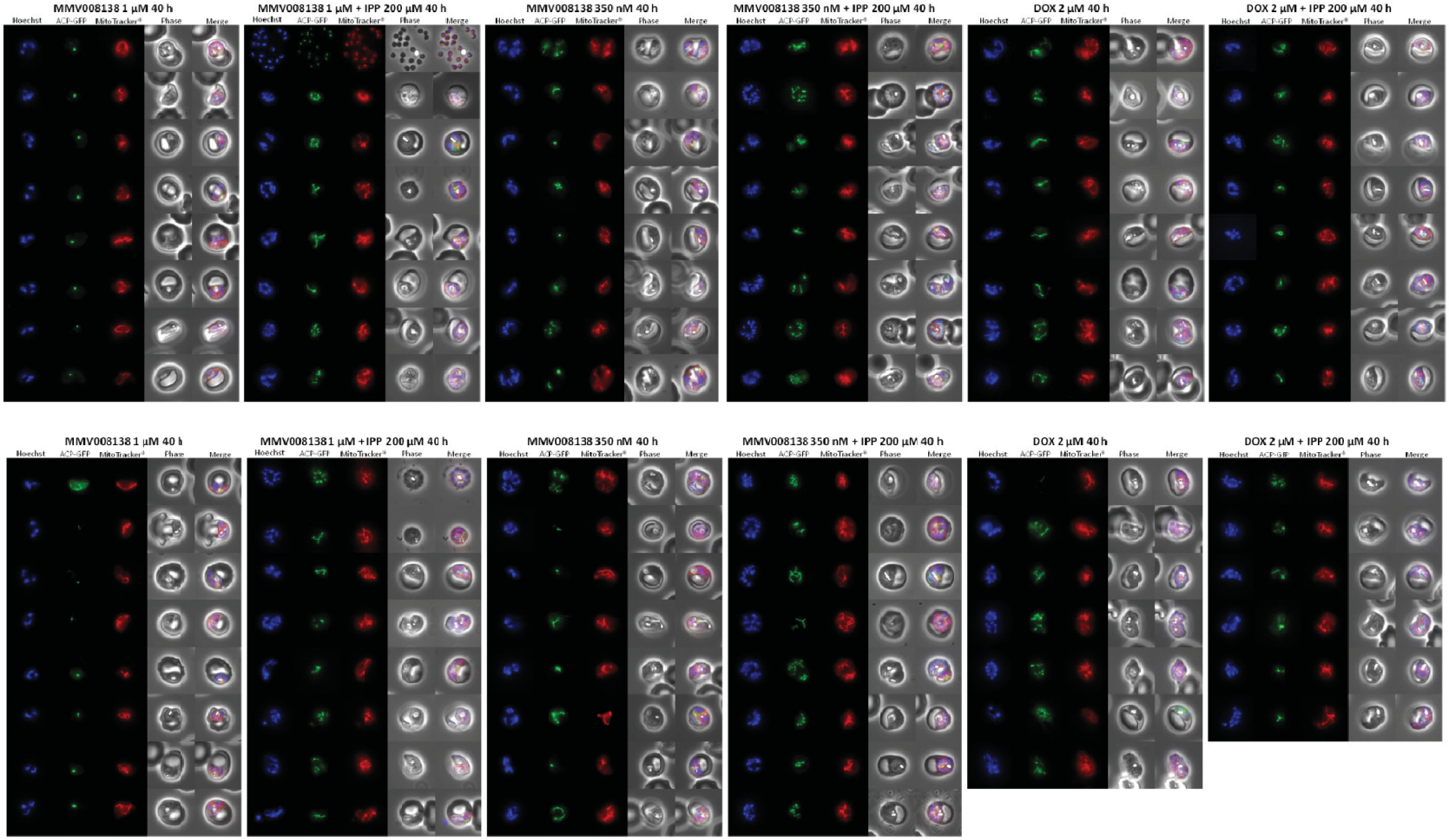
MMV008138 1 µM 40 h
MMV008138 1 µM + IPP 200 µM 40 h
MMV008138 350 nM 40 h
MMV008138 350 nM + IPP 200 µM 40 h
DOX 2 µM 40 h
DOX 2 µM + IPP 200 µM 40 h
Hoechst
ACP-GFP
MitoTracker®
Phase
Merge

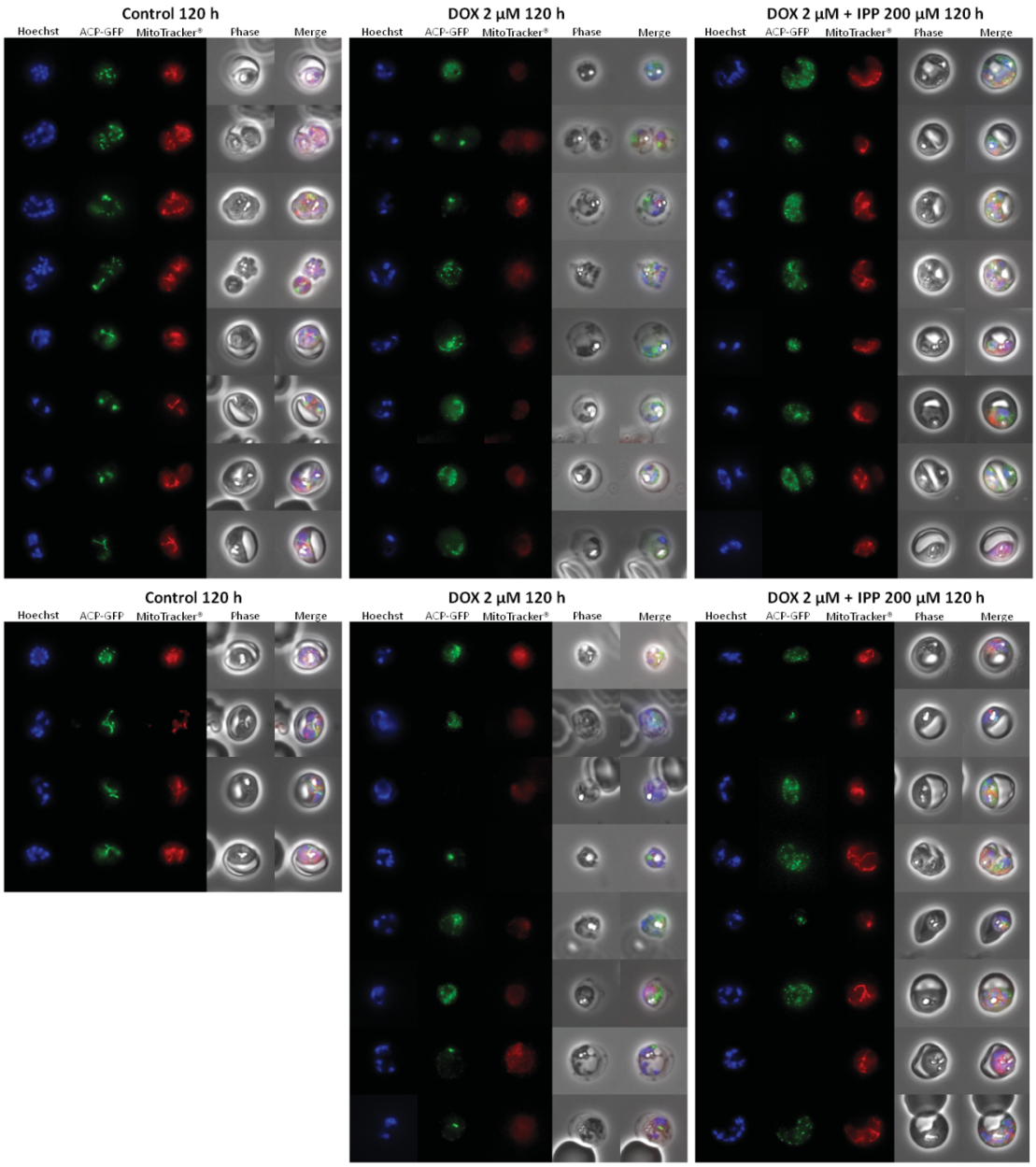

Figure 3. 12. Widefield Epifluorescence Microscopy of parasites treated with DOX 2 µM at 120 h. The two panels above show widefield epifluorescence microscopy for the nucleus (Hoechst), apicoplast (ACP-GFP), and mitochondria (MitoTracker®), comparing several microscopic fields of schizonts from each indicated condition. D10-ACP_L parasites starting in the ring stage were cultured at 4% parasitemia for 120 h in the absence or presence of 2 µM DOX, and 2 µM DOX and 200 µM IPP. All conditions were supplemented with 0.1 µM pyrimethamine. Media was changed every 24 h for all conditions. After 72 h, parasitemia was reduced by half in the control culture (no drug added) to maintain healthy parasites.

Data Set S1 A. This file contains the list of percentage for *growth inhibition* at 5 µM of inhibitor of the 400 compounds from the Malaria Box. MMV008138 is highlighted in yellow.

Compound #	% Inhibition @ 5 µM	Plate Designation	Well #	HEOS_COMPOUND_ID	Set
FOS	96				
1	94	A	A02	MMV019066	Drug-like
2	100	A	A03	MMV665941	Probe-like
3	100	A	A04	MMV396680	Probe-like
4	100	A	A05	MMV666601	Probe-like
5	100	A	A06	MMV008294	Probe-like
6	100	A	A07	MMV011259	Drug-like
7	100	A	A08	MMV019406	Probe-like
8	88	A	A09	MMV006278	Drug-like
9	93	A	A10	MMV666688	Probe-like
10	95	A	A11	MMV019110	Drug-like
11	100	A	B02	MMV006427	Drug-like
12	100	A	B03	MMV666062	Probe-like
13	100	A	B04	MMV020885	Probe-like
14	100	A	B05	MMV000570	Probe-like
15	100	A	B06	MMV020439	Drug-like
16	94	A	B07	MMV396672	Drug-like
17	100	A	B08	MMV019871	Drug-like
18	100	A	B09	MMV085583	Probe-like
19	91	A	B10	MMV008416	Probe-like
20	100	A	B11	MMV665874	Drug-like
21	100	A	C02	MMV006203	Probe-like
22	100	A	C03	MMV665977	Probe-like
23	96	A	C04	MMV020549	Drug-like
24	100	A	C05	MMV001246	Drug-like
25	100	A	C06	MMV666607	Probe-like
26	100	A	C07	MMV665915	Drug-like
27	100	A	C08	MMV007695	Probe-like
28	100	A	C09	MMV000448	Probe-like
29	100	A	C10	MMV020500	Drug-like
30	100	A	C11	MMV665878	Drug-like
31	100	A	D02	MMV666101	Probe-like
32	100	A	D03	MMV666596	Probe-like
33	100	A	D04	MMV396679	Probe-like
34	100	A	D05	MMV396797	Drug-like
35	100	A	D06	MMV008138	Drug-like
36	97	A	D07	MMV665916	Drug-like
37	100	A	D08	MMV020788	Probe-like
38	100	A	D09	MMV666691	Probe-like

39	100	A	D10	MMV665785	Probe-like
40	100	A	D11	MMV665831	Probe-like
41	100	A	E02	MMV011099	Drug-like
42	100	A	E03	MMV000642	Probe-like
43	93	A	E04	MMV666600	Probe-like
44	100	A	E05	MMV006172	Probe-like
45	86	A	E06	MMV006309	Probe-like
46	100	A	E07	MMV006087	Drug-like
47	97	A	E08	MMV020492	Drug-like
48	100	A	E09	MMV006455	Drug-like
49	100	A	E10	MMV665782	Drug-like
50	100	A	E11	MMV665876	Drug-like
51	100	A	F02	MMV666023	Probe-like
52	100	A	F03	MMV009063	Drug-like
53	100	A	F04	MMV006558	Probe-like
54	100	A	F05	MMV007160	Probe-like
55	100	A	F06	MMV006429	Drug-like
56	100	A	F07	MMV396703	Drug-like
57	100	A	F08	MMV006937	Drug-like
58	100	A	F09	MMV085203	Probe-like
59	100	A	F10	MMV665820	Drug-like
60	100	A	F11	MMV665841	Probe-like
61	100	A	G02	MMV007116	Drug-like
62	100	A	G03	MMV007384	Probe-like
63	96	A	G04	MMV020548	Drug-like
64	100	A	G05	MMV019258	Drug-like
65	39	A	G06	MMV007686	Probe-like
66	100	A	G07	MMV011256	Drug-like
67	100	A	G08	MMV666693	Drug-like
68	100	A	G09	MMV008956	Drug-like
69	100	A	G10	MMV665827	Probe-like
70	100	A	G11	MMV001038	Drug-like
71	100	A	H02	MMV007839	Drug-like
72	100	A	H03	MMV000662	Drug-like
73	100	A	H04	MMV396678	Probe-like
74	98	A	H05	MMV006861	Probe-like
75	100	A	H06	MMV006457	Probe-like
76	100	A	H07	MMV396693	Probe-like
77	100	A	H08	MMV011567	Drug-like
78	96	A	H09	MMV007907	Drug-like
79	100	A	H10	MMV665805	Drug-like
80	100	A	H11	MMV666021	Probe-like
81	97	B	A02	MMV665800	Drug-like

82	97	B	A03	MMV000634	Drug-like
83	95	B	A04	MMV666103	Drug-like
84	98	B	A05	MMV666057	Drug-like
85	100	B	A06	MMV007564	Drug-like
86	9	B	A07	MMV001255	Drug-like
87	61	B	A08	MMV665917	Drug-like
88	100	B	A09	MMV000563	Drug-like
89	49	B	A10	MMV665850	Drug-like
90	89	B	A11	MMV665817	Drug-like
91	64	B	B02	MMV665979	Drug-like
92	83	B	B03	MMV665928	Drug-like
93	74	B	B04	MMV666105	Drug-like
94	78	B	B05	MMV666072	Drug-like
95	90	B	B06	MMV000653	Drug-like
96	90	B	B07	MMV000620	Drug-like
97	68	B	B08	MMV665909	Drug-like
98	94	B	B09	MMV665940	Drug-like
99	82	B	B10	MMV665891	Drug-like
100	32	B	B11	MMV665899	Drug-like
101	83	B	C02	MMV665961	Drug-like
102	97	B	C03	MMV665929	Drug-like
103	92	B	C04	MMV666108	Drug-like
104	91	B	C05	MMV665948	Drug-like
105	91	B	C06	MMV006188	Drug-like
106	27	B	C07	MMV001230	Drug-like
107	93	B	C08	MMV665918	Drug-like
108	82	B	C09	MMV665799	Drug-like
109	92	B	C10	MMV665826	Drug-like
110	91	B	C11	MMV665807	Drug-like
111	86	B	D02	MMV665946	Drug-like
112	89	B	D03	MMV665935	Drug-like
113	88	B	D04	MMV666102	Drug-like
114	90	B	D05	MMV666061	Drug-like
115	89	B	D06	MMV008149	Drug-like
116	98	B	D07	MMV019074	Drug-like
117	31	B	D08	MMV665914	Drug-like
118	39	B	D09	MMV665798	Drug-like
119	96	B	D10	MMV665902	Drug-like
120	97	B	D11	MMV665888	Drug-like
121	86	B	E02	MMV666067	Drug-like
122	91	B	E03	MMV665939	Drug-like
123	94	B	E04	MMV009060	Drug-like
124	58	B	E05	MMV666110	Drug-like

125	75	B	E06	MMV019758	Drug-like
126	68	B	E07	MMV000498	Drug-like
127	49	B	E08	MMV665913	Drug-like
128	100	B	E09	MMV665789	Drug-like
129	21	B	E10	MMV665901	Drug-like
130	100	B	E11	MMV666069	Drug-like
131	96	B	F02	MMV666080	Drug-like
132	97	B	F03	MMV666081	Drug-like
133	42	B	F04	MMV666009	Drug-like
134	91	B	F05	MMV019313	Drug-like
135	46	B	F06	MMV019746	Drug-like
136	75	B	F07	MMV019064	Drug-like
137	76	B	F08	MMV011944	Drug-like
138	100	B	F09	MMV665803	Drug-like
139	98	B	F10	MMV665857	Drug-like
140	81	B	F11	MMV666071	Drug-like
141	100	B	G02	MMV019780	Drug-like
142	81	B	G03	MMV666093	Drug-like
143	96	B	G04	MMV665953	Drug-like
144	100	B	G05	MMV000648	Drug-like
145	97	B	G06	MMV019662	Drug-like
146	96	B	G07	MMV007571	Drug-like
147	98	B	G08	MMV007617	Drug-like
148	96	B	G09	MMV665796	Drug-like
149	94	B	G10	MMV665906	Drug-like
150	48	B	G11	MMV665954	Drug-like
151	94	B	H02	MMV019738	Drug-like
152	42	B	H03	MMV666075	Drug-like
153	81	B	H04	MMV666070	Drug-like
154	46	B	H05	MMV142383	Drug-like
155	97	B	H06	MMV000788	Drug-like
156	80	B	H07	MMV000561	Drug-like
157	97	B	H08	MMV000248	Drug-like
158	56	B	H09	MMV665879	Drug-like
159	95	B	H10	MMV665890	Drug-like
160	94	B	H11	MMV666116	Drug-like
161	84	C	A02	MMV006913	Drug-like
162	48	C	A03	MMV008127	Drug-like
163	52	C	A04	MMV403679	Drug-like
164	92	C	A05	MMV305841	Drug-like
165	91	C	A06	MMV019700	Drug-like
166	89	C	A07	MMV019670	Drug-like
167	84	C	A08	MMV001344	Drug-like

168	96	C	A09	MMV011795	Drug-like
169	51	C	A10	MMV019124	Drug-like
170	59	C	A11	MMV006767	Drug-like
171	80	C	B02	MMV007808	Drug-like
172	96	C	B03	MMV019017	Drug-like
173	53	C	B04	MMV396681	Drug-like
174	98	C	B05	MMV006587	Drug-like
175	57	C	B06	MMV019202	Drug-like
176	100	C	B07	MMV000848	Drug-like
177	54	C	B08	MMV020275	Drug-like
178	88	C	B09	MMV019918	Drug-like
179	42	C	B10	MMV075490	Drug-like
180	94	C	B11	MMV396633	Drug-like
181	77	C	C02	MMV007374	Drug-like
182	100	C	C03	MMV396719	Drug-like
183	30	C	C04	MMV396744	Drug-like
184	65	C	C05	MMV006706	Drug-like
185	97	C	C06	MMV009108	Drug-like
186	98	C	C07	MMV020700	Drug-like
187	96	C	C08	MMV007906	Drug-like
188	89	C	C09	MMV008270	Drug-like
189	99	C	C10	MMV019127	Drug-like
190	94	C	C11	MMV396794	Drug-like
191	84	C	D02	MMV396736	Drug-like
192	92	C	D03	MMV306025	Drug-like
193	21	C	D04	MMV056726	Drug-like
194	78	C	D05	MMV274073	Drug-like
195	98	C	D06	MMV018984	Drug-like
196	96	C	D07	MMV000911	Drug-like
197	99	C	D08	MMV007430	Drug-like
198	99	C	D09	MMV007977	Drug-like
199	98	C	D10	MMV020654	Drug-like
200	28	C	D11	MMV665883	Drug-like
201	99	C	E02	MMV084940	Drug-like
202	100	C	E03	MMV396715	Drug-like
203	96	C	E04	MMV000963	Drug-like
204	73	C	E05	MMV006319	Drug-like
205	76	C	E06	MMV000972	Drug-like
206	54	C	E07	MMV020490	Drug-like
207	98	C	E08	MMV001318	Drug-like
208	100	C	E09	MMV007978	Drug-like
209	100	C	E10	MMV020660	Drug-like
210	86	C	E11	MMV665904	Drug-like

211	96	C	F02	MMV396632	Drug-like
212	76	C	F03	MMV007875	Drug-like
213	95	C	F04	MMV006820	Drug-like
214	100	C	F05	MMV396749	Drug-like
215	99	C	F06	MMV011576	Drug-like
216	69	C	F07	MMV020651	Drug-like
217	100	C	F08	MMV000483	Drug-like
218	98	C	F09	MMV019266	Drug-like
219	100	C	F10	MMV001049	Drug-like
220	98	C	F11	MMV665806	Drug-like
221	25	C	G02	MMV667487	Drug-like
222	99	C	G03	MMV000356	Drug-like
223	97	C	G04	MMV396705	Drug-like
224	100	C	G05	MMV006704	Drug-like
225	100	C	G06	MMV000760	Drug-like
226	99	C	G07	MMV007881	Drug-like
227	99	C	G08	MMV008212	Drug-like
228	100	C	G09	MMV007363	Drug-like
229	17	C	G10	MMV007791	Drug-like
230	89	C	G11	MMV665843	Drug-like
231	98	C	H02	MMV396595	Drug-like
232	96	C	H03	MMV396669	Drug-like
233	98	C	H04	MMV396704	Drug-like
234	45	C	H05	MMV019762	Drug-like
235	89	C	H06	MMV020505	Drug-like
236	20	C	H07	MMV020942	Drug-like
237	99	C	H08	MMV000839	Drug-like
238	97	C	H09	MMV666599	Drug-like
239	18	C	H10	MMV000481	Drug-like
240	0	C	H11	MMV665897	Drug-like
241	93	D	A02	MMV665908	Probe-like
242	80	D	A03	MMV665924	Probe-like
243	98	D	A04	MMV665944	Probe-like
244	99	D	A05	MMV666054	Probe-like
245	57	D	A06	MMV008474	Probe-like
246	95	D	A07	MMV000445	Probe-like
247	97	D	A08	MMV006882	Probe-like
248	96	D	A09	MMV007127	Probe-like
249	77	D	A10	MMV666123	Probe-like
250	96	D	A11	MMV006389	Probe-like
251	97	D	B02	MMV665949	Probe-like
252	99	D	B03	MMV665934	Probe-like
253	96	D	B04	MMV665994	Probe-like

254	99	D	B05	MMV665980	Probe-like
255	91	D	B06	MMV007577	Probe-like
256	100	D	B07	MMV019995	Probe-like
257	100	D	B08	MMV007208	Probe-like
258	100	D	B09	MMV000442	Probe-like
259	95	D	B10	MMV666124	Probe-like
260	90	D	B11	MMV000444	Probe-like
261	93	D	C02	MMV666109	Probe-like
262	60	D	C03	MMV665936	Probe-like
263	94	D	C04	MMV666020	Probe-like
264	100	D	C05	MMV665971	Probe-like
265	25	D	C06	MMV001241	Probe-like
266	100	D	C07	MMV000720	Probe-like
267	79	D	C08	MMV000619	Probe-like
268	94	D	C09	MMV006753	Probe-like
269	97	D	C10	MMV006787	Probe-like
270	94	D	C11	MMV665794	Probe-like
271	100	D	D02	MMV000917	Probe-like
272	100	D	D03	MMV666125	Probe-like
273	100	D	D04	MMV665987	Probe-like
274	100	D	D05	MMV007574	Probe-like
275	100	D	D06	MMV000326	Probe-like
276	98	D	D07	MMV000604	Probe-like
277	84	D	D08	MMV007557	Probe-like
278	88	D	D09	MMV000699	Probe-like
279	0	D	D10	MMV009127	Probe-like
280	79	D	D11	MMV665786	Probe-like
281	98	D	E02	MMV006250	Probe-like
282	100	D	E03	MMV666079	Probe-like
283	100	D	E04	MMV665969	Probe-like
284	96	D	E05	MMV000304	Probe-like
285	97	D	E06	MMV000443	Probe-like
286	100	D	E07	MMV666604	Probe-like
287	100	D	E08	MMV008455	Probe-like
288	100	D	E09	MMV007199	Probe-like
289	21	D	E10	MMV085471	Probe-like
290	100	D	E11	MMV665797	Probe-like
291	100	D	F02	MMV006513	Probe-like
292	100	D	F03	MMV666095	Probe-like
293	100	D	F04	MMV665943	Probe-like
294	100	D	F05	MMV019555	Probe-like
295	100	D	F06	MMV019741	Probe-like
296	100	D	F07	MMV019690	Probe-like

297	77	D	F08	MMV000621	Probe-like
298	98	D	F09	MMV008173	Probe-like
299	91	D	F10	MMV019241	Probe-like
300	33	D	F11	MMV665783	Probe-like
301	100	D	G02	MMV000787	Probe-like
302	91	D	G03	MMV666106	Probe-like
303	100	D	G04	MMV666022	Probe-like
304	96	D	G05	MMV498479	Probe-like
305	98	D	G06	MMV007396	Probe-like
306	70	D	G07	MMV000617	Probe-like
307	100	D	G08	MMV006764	Probe-like
308	100	D	G09	MMV007275	Probe-like
309	100	D	G10	MMV007273	Probe-like
310	100	D	G11	MMV666026	Probe-like
311	0	D	H02	MMV665923	Probe-like
312	97	D	H03	MMV666025	Probe-like
313	100	D	H04	MMV666060	Probe-like
314	60	D	H05	MMV666597	Probe-like
315	100	D	H06	MMV007224	Probe-like
316	100	D	H07	MMV020912	Probe-like
317	100	D	H08	MMV007181	Probe-like
318	39	D	H09	MMV007113	Probe-like
319	97	D	H10	MMV007228	Probe-like
320	91	D	H11	MMV665972	Probe-like
321	97	E	A02	MMV073843	Probe-like
322	99	E	A03	MMV006303	Probe-like
323	96	E	A04	MMV667490	Probe-like
324	99	E	A05	MMV667492	Probe-like
325	98	E	A06	MMV019881	Probe-like
326	99	E	A07	MMV000478	Probe-like
327	41	E	A08	MMV020403	Probe-like
328	47	E	A09	MMV007764	Probe-like
329	91	E	A10	MMV665830	Probe-like
330	91	E	A11	MMV665886	Probe-like
331	89	E	B02	MMV396664	Probe-like
332	12	E	B03	MMV001239	Probe-like
333	99	E	B04	MMV667491	Probe-like
334	94	E	B05	MMV006169	Probe-like
335	99	E	B06	MMV086103	Probe-like
336	92	E	B07	MMV084434	Probe-like
337	98	E	B08	MMV666692	Probe-like
338	94	E	B09	MMV665836	Probe-like
339	54	E	B10	MMV665881	Probe-like

340	72	E	B11	MMV665875	Probe-like
341	100	E	C02	MMV007020	Probe-like
342	100	E	C03	MMV006656	Probe-like
343	98	E	C04	MMV396726	Probe-like
344	97	E	C05	MMV006522	Probe-like
345	100	E	C06	MMV666686	Probe-like
346	100	E	C07	MMV007474	Probe-like
347	97	E	C08	MMV006962	Probe-like
348	47	E	C09	MMV665813	Probe-like
349	47	E	C10	MMV080034	Probe-like
350	98	E	C11	MMV019199	Probe-like
351	99	E	D02	MMV396652	Probe-like
352	100	E	D03	MMV000704	Probe-like
353	62	E	D04	MMV396635	Probe-like
354	100	E	D05	MMV000986	Probe-like
355	60	E	D06	MMV008160	Probe-like
356	100	E	D07	MMV000753	Probe-like
357	100	E	D08	MMV011436	Probe-like
358	100	E	D09	MMV665882	Probe-like
359	99	E	D10	MMV665809	Probe-like
360	100	E	D11	MMV665810	Probe-like
361	98	E	E02	MMV665927	Probe-like
362	18	E	E03	MMV667486	Probe-like
363	85	E	E04	MMV667488	Probe-like
364	66	E	E05	MMV006825	Probe-like
365	100	E	E06	MMV009085	Probe-like
366	73	E	E07	MMV007591	Probe-like
367	98	E	E08	MMV128432	Probe-like
368	90	E	E09	MMV665852	Probe-like
369	79	E	E10	MMV396717	Probe-like
370	12	E	E11	MMV638723	Probe-like
371	100	E	F02	MMV396594	Probe-like
372	89	E	F03	MMV396665	Probe-like
373	100	E	F04	MMV396723	Probe-like
374	100	E	F05	MMV007654	Probe-like
375	86	E	F06	MMV011832	Probe-like
376	100	E	F07	MMV020750	Probe-like
377	100	E	F08	MMV007092	Probe-like
378	82	E	F09	MMV665898	Probe-like
379	100	E	F10	MMV665864	Probe-like
380	100	E	F11	MMV665814	Probe-like
381	81	E	G02	MMV007285	Probe-like
382	100	E	G03	MMV396663	Probe-like

383	94	E	G04	MMV007041	Probe-like
384	52	E	G05	MMV000340	Probe-like
385	100	E	G06	MMV666687	Probe-like
386	98	E	G07	MMV645672	Probe-like
387	100	E	G08	MMV011438	Probe-like
388	74	E	G09	MMV665840	Probe-like
389	66	E	G10	MMV665894	Probe-like
390	79	E	G11	MMV011522	Probe-like
391	98	E	H02	MMV020243	Probe-like
392	42	E	H03	MMV667489	Probe-like
393	90	E	H04	MMV396770	Probe-like
394	96	E	H05	MMV009015	Probe-like
395	83	E	H06	MMV008829	Probe-like
396	100	E	H07	MMV011895	Probe-like
397	100	E	H08	MMV666689	Probe-like
398	22	E	H09	MMV665824	Probe-like
399	99	E	H10	MMV665812	Probe-like
400	88	E	H11	MMV001041	Probe-like

Data Set S1 B. List of percentage of *growth recovery* at 5 µM of inhibitor and 200 µM IPP of the 400 compounds from the Malaria Box. MMV008138 is highlighted in yellow.

Compound #	% IPP Recovery	Plate Designation	Well #	HEOS_COMPOUND_ID	Set
FOS	100				
1	7	A	A02	MMV019066	Drug-like
2	0	A	A03	MMV665941	Probe-like
3	0	A	A04	MMV396680	Probe-like
4	1	A	A05	MMV666601	Probe-like
5	0	A	A06	MMV008294	Probe-like
6	0	A	A07	MMV011259	Drug-like
7	0	A	A08	MMV019406	Probe-like
8	15	A	A09	MMV006278	Drug-like
9	8	A	A10	MMV666688	Probe-like
10	2	A	A11	MMV019110	Drug-like
11	0	A	B02	MMV006427	Drug-like
12	0	A	B03	MMV666062	Probe-like
13	0	A	B04	MMV020885	Probe-like
14	0	A	B05	MMV000570	Probe-like
15	0	A	B06	MMV020439	Drug-like
16	7	A	B07	MMV396672	Drug-like
17	0	A	B08	MMV019871	Drug-like
18	0	A	B09	MMV085583	Probe-like
19	15	A	B10	MMV008416	Probe-like
20	0	A	B11	MMV665874	Drug-like
21	1	A	C02	MMV006203	Probe-like
22	0	A	C03	MMV665977	Probe-like
23	7	A	C04	MMV020549	Drug-like
24	0	A	C05	MMV001246	Drug-like
25	7	A	C06	MMV666607	Probe-like
26	0	A	C07	MMV665915	Drug-like
27	0	A	C08	MMV007695	Probe-like
28	0	A	C09	MMV000448	Probe-like
29	0	A	C10	MMV020500	Drug-like
30	0	A	C11	MMV665878	Drug-like
31	0	A	D02	MMV666101	Probe-like
32	0	A	D03	MMV666596	Probe-like
33	0	A	D04	MMV396679	Probe-like
34	0	A	D05	MMV396797	Drug-like
35	63	A	D06	MMV008138	Drug-like
36	8	A	D07	MMV665916	Drug-like
37	0	A	D08	MMV020788	Probe-like

38	0	A	D09	MMV666691	Probe-like
39	0	A	D10	MMV665785	Probe-like
40	0	A	D11	MMV665831	Probe-like
41	0	A	E02	MMV011099	Drug-like
42	0	A	E03	MMV000642	Probe-like
43	6	A	E04	MMV666600	Probe-like
44	0	A	E05	MMV006172	Probe-like
45	26	A	E06	MMV006309	Probe-like
46	0	A	E07	MMV006087	Drug-like
47	1	A	E08	MMV020492	Drug-like
48	0	A	E09	MMV006455	Drug-like
49	0	A	E10	MMV665782	Drug-like
50	0	A	E11	MMV665876	Drug-like
51	0	A	F02	MMV666023	Probe-like
52	0	A	F03	MMV009063	Drug-like
53	0	A	F04	MMV006558	Probe-like
54	0	A	F05	MMV007160	Probe-like
55	0	A	F06	MMV006429	Drug-like
56	0	A	F07	MMV396703	Drug-like
57	0	A	F08	MMV006937	Drug-like
58	0	A	F09	MMV085203	Probe-like
59	0	A	F10	MMV665820	Drug-like
60	0	A	F11	MMV665841	Probe-like
61	0	A	G02	MMV007116	Drug-like
62	0	A	G03	MMV007384	Probe-like
63	12	A	G04	MMV020548	Drug-like
64	0	A	G05	MMV019258	Drug-like
65	72	A	G06	MMV007686	Probe-like
66	0	A	G07	MMV011256	Drug-like
67	0	A	G08	MMV666693	Drug-like
68	0	A	G09	MMV008956	Drug-like
69	0	A	G10	MMV665827	Probe-like
70	2	A	G11	MMV001038	Drug-like
71	0	A	H02	MMV007839	Drug-like
72	0	A	H03	MMV000662	Drug-like
73	1	A	H04	MMV396678	Probe-like
74	2	A	H05	MMV006861	Probe-like
75	0	A	H06	MMV006457	Probe-like
76	0	A	H07	MMV396693	Probe-like
77	0	A	H08	MMV011567	Drug-like
78	3	A	H09	MMV007907	Drug-like
79	0	A	H10	MMV665805	Drug-like
80	0	A	H11	MMV666021	Probe-like

81	27	B	A02	MMV665800	Drug-like
82	34	B	A03	MMV000634	Drug-like
83	12	B	A04	MMV666103	Drug-like
84	35	B	A05	MMV666057	Drug-like
85	32	B	A06	MMV007564	Drug-like
86	93	B	A07	MMV001255	Drug-like
87	111	B	A08	MMV665917	Drug-like
88	34	B	A09	MMV000563	Drug-like
89	66	B	A10	MMV665850	Drug-like
90	32	B	A11	MMV665817	Drug-like
91	46	B	B02	MMV665979	Drug-like
92	29	B	B03	MMV665928	Drug-like
93	30	B	B04	MMV666105	Drug-like
94	32	B	B05	MMV666072	Drug-like
95	26	B	B06	MMV000653	Drug-like
96	26	B	B07	MMV000620	Drug-like
97	31	B	B08	MMV665909	Drug-like
98	27	B	B09	MMV665940	Drug-like
99	30	B	B10	MMV665891	Drug-like
100	64	B	B11	MMV665899	Drug-like
101	52	B	C02	MMV665961	Drug-like
102	31	B	C03	MMV665929	Drug-like
103	29	B	C04	MMV666108	Drug-like
104	34	B	C05	MMV665948	Drug-like
105	36	B	C06	MMV006188	Drug-like
106	49	B	C07	MMV001230	Drug-like
107	26	B	C08	MMV665918	Drug-like
108	25	B	C09	MMV665799	Drug-like
109	25	B	C10	MMV665826	Drug-like
110	27	B	C11	MMV665807	Drug-like
111	34	B	D02	MMV665946	Drug-like
112	23	B	D03	MMV665935	Drug-like
113	23	B	D04	MMV666102	Drug-like
114	24	B	D05	MMV666061	Drug-like
115	28	B	D06	MMV008149	Drug-like
116	22	B	D07	MMV019074	Drug-like
117	67	B	D08	MMV665914	Drug-like
118	68	B	D09	MMV665798	Drug-like
119	31	B	D10	MMV665902	Drug-like
120	28	B	D11	MMV665888	Drug-like
121	32	B	E02	MMV666067	Drug-like
122	24	B	E03	MMV665939	Drug-like
123	28	B	E04	MMV009060	Drug-like

124	56	B	E05	MMV666110	Drug-like
125	36	B	E06	MMV019758	Drug-like
126	37	B	E07	MMV000498	Drug-like
127	58	B	E08	MMV665913	Drug-like
128	22	B	E09	MMV665789	Drug-like
129	98	B	E10	MMV665901	Drug-like
130	27	B	E11	MMV666069	Drug-like
131	24	B	F02	MMV666080	Drug-like
132	25	B	F03	MMV666081	Drug-like
133	68	B	F04	MMV666009	Drug-like
134	39	B	F05	MMV019313	Drug-like
135	109	B	F06	MMV019746	Drug-like
136	41	B	F07	MMV019064	Drug-like
137	35	B	F08	MMV011944	Drug-like
138	24	B	F09	MMV665803	Drug-like
139	22	B	F10	MMV665857	Drug-like
140	34	B	F11	MMV666071	Drug-like
141	24	B	G02	MMV019780	Drug-like
142	39	B	G03	MMV666093	Drug-like
143	26	B	G04	MMV665953	Drug-like
144	26	B	G05	MMV000648	Drug-like
145	22	B	G06	MMV019662	Drug-like
146	23	B	G07	MMV007571	Drug-like
147	24	B	G08	MMV007617	Drug-like
148	24	B	G09	MMV665796	Drug-like
149	27	B	G10	MMV665906	Drug-like
150	58	B	G11	MMV665954	Drug-like
151	31	B	H02	MMV019738	Drug-like
152	73	B	H03	MMV666075	Drug-like
153	33	B	H04	MMV666070	Drug-like
154	59	B	H05	MMV142383	Drug-like
155	22	B	H06	MMV000788	Drug-like
156	44	B	H07	MMV000561	Drug-like
157	26	B	H08	MMV000248	Drug-like
158	50	B	H09	MMV665879	Drug-like
159	21	B	H10	MMV665890	Drug-like
160	20	B	H11	MMV666116	Drug-like
161	34	C	A02	MMV006913	Drug-like
162	71	C	A03	MMV008127	Drug-like
163	50	C	A04	MMV403679	Drug-like
164	28	C	A05	MMV305841	Drug-like
165	31	C	A06	MMV019700	Drug-like
166	37	C	A07	MMV019670	Drug-like

167	41	C	A08	MMV001344	Drug-like
168	36	C	A09	MMV011795	Drug-like
169	68	C	A10	MMV019124	Drug-like
170	58	C	A11	MMV006767	Drug-like
171	38	C	B02	MMV007808	Drug-like
172	22	C	B03	MMV019017	Drug-like
173	70	C	B04	MMV396681	Drug-like
174	26	C	B05	MMV006587	Drug-like
175	67	C	B06	MMV019202	Drug-like
176	26	C	B07	MMV000848	Drug-like
177	69	C	B08	MMV020275	Drug-like
178	34	C	B09	MMV019918	Drug-like
179	85	C	B10	MMV075490	Drug-like
180	23	C	B11	MMV396633	Drug-like
181	38	C	C02	MMV007374	Drug-like
182	24	C	C03	MMV396719	Drug-like
183	84	C	C04	MMV396744	Drug-like
184	54	C	C05	MMV006706	Drug-like
185	22	C	C06	MMV009108	Drug-like
186	26	C	C07	MMV020700	Drug-like
187	26	C	C08	MMV007906	Drug-like
188	29	C	C09	MMV008270	Drug-like
189	24	C	C10	MMV019127	Drug-like
190	25	C	C11	MMV396794	Drug-like
191	19	C	D02	MMV396736	Drug-like
192	23	C	D03	MMV306025	Drug-like
193	79	C	D04	MMV056726	Drug-like
194	30	C	D05	MMV274073	Drug-like
195	21	C	D06	MMV018984	Drug-like
196	19	C	D07	MMV000911	Drug-like
197	22	C	D08	MMV007430	Drug-like
198	20	C	D09	MMV007977	Drug-like
199	19	C	D10	MMV020654	Drug-like
200	64	C	D11	MMV665883	Drug-like
201	20	C	E02	MMV084940	Drug-like
202	17	C	E03	MMV396715	Drug-like
203	24	C	E04	MMV000963	Drug-like
204	44	C	E05	MMV006319	Drug-like
205	37	C	E06	MMV000972	Drug-like
206	58	C	E07	MMV020490	Drug-like
207	21	C	E08	MMV001318	Drug-like
208	20	C	E09	MMV007978	Drug-like
209	19	C	E10	MMV020660	Drug-like

210	22	C	E11	MMV665904	Drug-like
211	19	C	F02	MMV396632	Drug-like
212	39	C	F03	MMV007875	Drug-like
213	20	C	F04	MMV006820	Drug-like
214	19	C	F05	MMV396749	Drug-like
215	16	C	F06	MMV011576	Drug-like
216	48	C	F07	MMV020651	Drug-like
217	19	C	F08	MMV000483	Drug-like
218	21	C	F09	MMV019266	Drug-like
219	19	C	F10	MMV001049	Drug-like
220	20	C	F11	MMV665806	Drug-like
221	75	C	G02	MMV667487	Drug-like
222	19	C	G03	MMV000356	Drug-like
223	20	C	G04	MMV396705	Drug-like
224	19	C	G05	MMV006704	Drug-like
225	18	C	G06	MMV000760	Drug-like
226	28	C	G07	MMV007881	Drug-like
227	28	C	G08	MMV008212	Drug-like
228	22	C	G09	MMV007363	Drug-like
229	86	C	G10	MMV007791	Drug-like
230	31	C	G11	MMV665843	Drug-like
231	19	C	H02	MMV396595	Drug-like
232	39	C	H03	MMV396669	Drug-like
233	21	C	H04	MMV396704	Drug-like
234	63	C	H05	MMV019762	Drug-like
235	31	C	H06	MMV020505	Drug-like
236	93	C	H07	MMV020942	Drug-like
237	22	C	H08	MMV000839	Drug-like
238	25	C	H09	MMV666599	Drug-like
239	92	C	H10	MMV000481	Drug-like
240	71	C	H11	MMV665897	Drug-like
241	36	D	A02	MMV665908	Probe-like
242	68	D	A03	MMV665924	Probe-like
243	29	D	A04	MMV665944	Probe-like
244	23	D	A05	MMV666054	Probe-like
245	73	D	A06	MMV008474	Probe-like
246	10	D	A07	MMV000445	Probe-like
247	34	D	A08	MMV006882	Probe-like
248	34	D	A09	MMV007127	Probe-like
249	47	D	A10	MMV666123	Probe-like
250	42	D	A11	MMV006389	Probe-like
251	32	D	B02	MMV665949	Probe-like
252	28	D	B03	MMV665934	Probe-like

253	32	D	B04	MMV665994	Probe-like
254	29	D	B05	MMV665980	Probe-like
255	40	D	B06	MMV007577	Probe-like
256	29	D	B07	MMV019995	Probe-like
257	30	D	B08	MMV007208	Probe-like
258	31	D	B09	MMV000442	Probe-like
259	32	D	B10	MMV666124	Probe-like
260	32	D	B11	MMV000444	Probe-like
261	26	D	C02	MMV666109	Probe-like
262	60	D	C03	MMV665936	Probe-like
263	25	D	C04	MMV666020	Probe-like
264	25	D	C05	MMV665971	Probe-like
265	76	D	C06	MMV001241	Probe-like
266	20	D	C07	MMV000720	Probe-like
267	37	D	C08	MMV000619	Probe-like
268	27	D	C09	MMV006753	Probe-like
269	26	D	C10	MMV006787	Probe-like
270	27	D	C11	MMV665794	Probe-like
271	23	D	D02	MMV000917	Probe-like
272	17	D	D03	MMV666125	Probe-like
273	19	D	D04	MMV665987	Probe-like
274	23	D	D05	MMV007574	Probe-like
275	19	D	D06	MMV000326	Probe-like
276	20	D	D07	MMV000604	Probe-like
277	27	D	D08	MMV007557	Probe-like
278	21	D	D09	MMV000699	Probe-like
279	185	D	D10	MMV009127	Probe-like
280	57	D	D11	MMV665786	Probe-like
281	28	D	E02	MMV006250	Probe-like
282	19	D	E03	MMV666079	Probe-like
283	18	D	E04	MMV665969	Probe-like
284	20	D	E05	MMV000304	Probe-like
285	22	D	E06	MMV000443	Probe-like
286	23	D	E07	MMV666604	Probe-like
287	25	D	E08	MMV008455	Probe-like
288	27	D	E09	MMV007199	Probe-like
289	85	D	E10	MMV085471	Probe-like
290	34	D	E11	MMV665797	Probe-like
291	24	D	F02	MMV006513	Probe-like
292	22	D	F03	MMV666095	Probe-like
293	17	D	F04	MMV665943	Probe-like
294	21	D	F05	MMV019555	Probe-like
295	23	D	F06	MMV019741	Probe-like

296	22	D	F07	MMV019690	Probe-like
297	43	D	F08	MMV000621	Probe-like
298	37	D	F09	MMV008173	Probe-like
299	29	D	F10	MMV019241	Probe-like
300	78	D	F11	MMV665783	Probe-like
301	20	D	G02	MMV000787	Probe-like
302	27	D	G03	MMV666106	Probe-like
303	13	D	G04	MMV666022	Probe-like
304	21	D	G05	MMV498479	Probe-like
305	23	D	G06	MMV007396	Probe-like
306	39	D	G07	MMV000617	Probe-like
307	21	D	G08	MMV006764	Probe-like
308	23	D	G09	MMV007275	Probe-like
309	25	D	G10	MMV007273	Probe-like
310	27	D	G11	MMV666026	Probe-like
311	30	D	H02	MMV665923	Probe-like
312	28	D	H03	MMV666025	Probe-like
313	23	D	H04	MMV666060	Probe-like
314	67	D	H05	MMV666597	Probe-like
315	23	D	H06	MMV007224	Probe-like
316	26	D	H07	MMV020912	Probe-like
317	27	D	H08	MMV007181	Probe-like
318	85	D	H09	MMV007113	Probe-like
319	33	D	H10	MMV007228	Probe-like
320	44	D	H11	MMV665972	Probe-like
321	30	E	A02	MMV073843	Probe-like
322	29	E	A03	MMV006303	Probe-like
323	12	E	A04	MMV667490	Probe-like
324	27	E	A05	MMV667492	Probe-like
325	25	E	A06	MMV019881	Probe-like
326	11	E	A07	MMV000478	Probe-like
327	27	E	A08	MMV020403	Probe-like
328	73	E	A09	MMV007764	Probe-like
329	30	E	A10	MMV665830	Probe-like
330	29	E	A11	MMV665886	Probe-like
331	30	E	B02	MMV396664	Probe-like
332	85	E	B03	MMV001239	Probe-like
333	26	E	B04	MMV667491	Probe-like
334	26	E	B05	MMV006169	Probe-like
335	29	E	B06	MMV086103	Probe-like
336	35	E	B07	MMV084434	Probe-like
337	22	E	B08	MMV666692	Probe-like
338	29	E	B09	MMV665836	Probe-like

339	53	E	B10	MMV665881	Probe-like
340	42	E	B11	MMV665875	Probe-like
341	25	E	C02	MMV007020	Probe-like
342	23	E	C03	MMV006656	Probe-like
343	25	E	C04	MMV396726	Probe-like
344	40	E	C05	MMV006522	Probe-like
345	20	E	C06	MMV666686	Probe-like
346	24	E	C07	MMV007474	Probe-like
347	24	E	C08	MMV006962	Probe-like
348	61	E	C09	MMV665813	Probe-like
349	22	E	C10	MMV080034	Probe-like
350	24	E	C11	MMV019199	Probe-like
351	23	E	D02	MMV396652	Probe-like
352	19	E	D03	MMV000704	Probe-like
353	55	E	D04	MMV396635	Probe-like
354	21	E	D05	MMV000986	Probe-like
355	49	E	D06	MMV008160	Probe-like
356	19	E	D07	MMV000753	Probe-like
357	19	E	D08	MMV011436	Probe-like
358	20	E	D09	MMV665882	Probe-like
359	20	E	D10	MMV665809	Probe-like
360	24	E	D11	MMV665810	Probe-like
361	30	E	E02	MMV665927	Probe-like
362	85	E	E03	MMV667486	Probe-like
363	35	E	E04	MMV667488	Probe-like
364	50	E	E05	MMV006825	Probe-like
365	22	E	E06	MMV009085	Probe-like
366	42	E	E07	MMV007591	Probe-like
367	29	E	E08	MMV128432	Probe-like
368	24	E	E09	MMV665852	Probe-like
369	21	E	E10	MMV396717	Probe-like
370	91	E	E11	MMV638723	Probe-like
371	26	E	F02	MMV396594	Probe-like
372	57	E	F03	MMV396665	Probe-like
373	18	E	F04	MMV396723	Probe-like
374	30	E	F05	MMV007654	Probe-like
375	59	E	F06	MMV011832	Probe-like
376	21	E	F07	MMV020750	Probe-like
377	21	E	F08	MMV007092	Probe-like
378	66	E	F09	MMV665898	Probe-like
379	27	E	F10	MMV665864	Probe-like
380	30	E	F11	MMV665814	Probe-like
381	30	E	G02	MMV007285	Probe-like

382	20	E	G03	MMV396663	Probe-like
383	28	E	G04	MMV007041	Probe-like
384	64	E	G05	MMV000340	Probe-like
385	12	E	G06	MMV666687	Probe-like
386	16	E	G07	MMV645672	Probe-like
387	18	E	G08	MMV011438	Probe-like
388	43	E	G09	MMV665840	Probe-like
389	49	E	G10	MMV665894	Probe-like
390	32	E	G11	MMV011522	Probe-like
391	22	E	H02	MMV020243	Probe-like
392	75	E	H03	MMV667489	Probe-like
393	24	E	H04	MMV396770	Probe-like
394	29	E	H05	MMV009015	Probe-like
395	29	E	H06	MMV008829	Probe-like
396	18	E	H07	MMV011895	Probe-like
397	23	E	H08	MMV666689	Probe-like
398	88	E	H09	MMV665824	Probe-like
399	30	E	H10	MMV665812	Probe-like
400	39	E	H11	MMV001041	Probe-like

Data Set S1 C. List of percentage of *gametocytocidal activity* measured as gametocyte mitochondrial activity at 5 µM of inhibitor of the 400 compounds from the Malaria Box.

Compound #	% Late stage Gametocyte Inhibition	Plate Designation	Well #	HEOS_COMPOUND_ID	Set
FOS (10 µM)	8				
epoxomicin (60 nM)	100				
1	32	A	A02	MMV019066	Drug-like
2	86	A	A03	MMV665941	Probe-like
3	33	A	A04	MMV396680	Probe-like
4	9	A	A05	MMV666601	Probe-like
5	22	A	A06	MMV008294	Probe-like
6	22	A	A07	MMV011259	Drug-like
7	83	A	A08	MMV019406	Probe-like
8	28	A	A09	MMV006278	Drug-like
9	2	A	A10	MMV666688	Probe-like
10	23	A	A11	MMV019110	Drug-like
11	80	A	B02	MMV006427	Drug-like
12	38	A	B03	MMV666062	Probe-like
13	41	A	B04	MMV020885	Probe-like
14	66	A	B05	MMV000570	Probe-like
15	47	A	B06	MMV020439	Drug-like
16	27	A	B07	MMV396672	Drug-like
17	27	A	B08	MMV019871	Drug-like
18	91	A	B09	MMV085583	Probe-like
19	39	A	B10	MMV008416	Probe-like
20	11	A	B11	MMV665874	Drug-like
21	80	A	C02	MMV006203	Probe-like
22	43	A	C03	MMV665977	Probe-like
23	64	A	C04	MMV020549	Drug-like
24	73	A	C05	MMV001246	Drug-like
25	0	A	C06	MMV666607	Probe-like
26	41	A	C07	MMV665915	Drug-like
27	48	A	C08	MMV007695	Probe-like
28	95	A	C09	MMV000448	Probe-like
29	36	A	C10	MMV020500	Drug-like
30	73	A	C11	MMV665878	Drug-like
31	39	A	D02	MMV666101	Probe-like
32	39	A	D03	MMV666596	Probe-like
33	28	A	D04	MMV396679	Probe-like
34	90	A	D05	MMV396797	Drug-like
35	20	A	D06	MMV008138	Drug-like

36	30	A	D07	MMV665916	Drug-like
37	82	A	D08	MMV020788	Probe-like
38	55	A	D09	MMV666691	Probe-like
39	77	A	D10	MMV665785	Probe-like
40	56	A	D11	MMV665831	Probe-like
41	15	A	E02	MMV011099	Drug-like
42	80	A	E03	MMV000642	Probe-like
43	0	A	E04	MMV666600	Probe-like
44	87	A	E05	MMV006172	Probe-like
45	46	A	E06	MMV006309	Probe-like
46	42	A	E07	MMV006087	Drug-like
47	70	A	E08	MMV020492	Drug-like
48	82	A	E09	MMV006455	Drug-like
49	83	A	E10	MMV665782	Drug-like
50	34	A	E11	MMV665876	Drug-like
51	88	A	F02	MMV666023	Probe-like
52	86	A	F03	MMV009063	Drug-like
53	68	A	F04	MMV006558	Probe-like
54	39	A	F05	MMV007160	Probe-like
55	75	A	F06	MMV006429	Drug-like
56	29	A	F07	MMV396703	Drug-like
57	35	A	F08	MMV006937	Drug-like
58	57	A	F09	MMV085203	Probe-like
59	98	A	F10	MMV665820	Drug-like
60	65	A	F11	MMV665841	Probe-like
61	40	A	G02	MMV007116	Drug-like
62	94	A	G03	MMV007384	Probe-like
63	0	A	G04	MMV020548	Drug-like
64	19	A	G05	MMV019258	Drug-like
65	26	A	G06	MMV007686	Probe-like
66	16	A	G07	MMV011256	Drug-like
67	95	A	G08	MMV666693	Drug-like
68	71	A	G09	MMV008956	Drug-like
69	41	A	G10	MMV665827	Probe-like
70	44	A	G11	MMV001038	Drug-like
71	15	A	H02	MMV007839	Drug-like
72	71	A	H03	MMV000662	Drug-like
73	0	A	H04	MMV396678	Probe-like
74	24	A	H05	MMV006861	Probe-like
75	48	A	H06	MMV006457	Probe-like
76	77	A	H07	MMV396693	Probe-like
77	80	A	H08	MMV011567	Drug-like
78	67	A	H09	MMV007907	Drug-like

79	72	A	H10	MMV665805	Drug-like
80	58	A	H11	MMV666021	Probe-like
81	22	B	A02	MMV665800	Drug-like
82	57	B	A03	MMV000634	Drug-like
83	4	B	A04	MMV666103	Drug-like
84	21	B	A05	MMV666057	Drug-like
85	53	B	A06	MMV007564	Drug-like
86	0	B	A07	MMV001255	Drug-like
87	3	B	A08	MMV665917	Drug-like
88	18	B	A09	MMV000563	Drug-like
89	6	B	A10	MMV665850	Drug-like
90	70	B	A11	MMV665817	Drug-like
91	36	B	B02	MMV665979	Drug-like
92	79	B	B03	MMV665928	Drug-like
93	33	B	B04	MMV666105	Drug-like
94	33	B	B05	MMV666072	Drug-like
95	36	B	B06	MMV000653	Drug-like
96	63	B	B07	MMV000620	Drug-like
97	64	B	B08	MMV665909	Drug-like
98	72	B	B09	MMV665940	Drug-like
99	57	B	B10	MMV665891	Drug-like
100	27	B	B11	MMV665899	Drug-like
101	40	B	C02	MMV665961	Drug-like
102	82	B	C03	MMV665929	Drug-like
103	64	B	C04	MMV666108	Drug-like
104	54	B	C05	MMV665948	Drug-like
105	41	B	C06	MMV006188	Drug-like
106	40	B	C07	MMV001230	Drug-like
107	60	B	C08	MMV665918	Drug-like
108	54	B	C09	MMV665799	Drug-like
109	71	B	C10	MMV665826	Drug-like
110	87	B	C11	MMV665807	Drug-like
111	57	B	D02	MMV665946	Drug-like
112	60	B	D03	MMV665935	Drug-like
113	34	B	D04	MMV666102	Drug-like
114	88	B	D05	MMV666061	Drug-like
115	38	B	D06	MMV008149	Drug-like
116	27	B	D07	MMV019074	Drug-like
117	33	B	D08	MMV665914	Drug-like
118	8	B	D09	MMV665798	Drug-like
119	91	B	D10	MMV665902	Drug-like
120	48	B	D11	MMV665888	Drug-like
121	44	B	E02	MMV666067	Drug-like

122	44	B	E03	MMV665939	Drug-like
123	46	B	E04	MMV009060	Drug-like
124	60	B	E05	MMV666110	Drug-like
125	56	B	E06	MMV019758	Drug-like
126	47	B	E07	MMV000498	Drug-like
127	62	B	E08	MMV665913	Drug-like
128	98	B	E09	MMV665789	Drug-like
129	64	B	E10	MMV665901	Drug-like
130	89	B	E11	MMV666069	Drug-like
131	81	B	F02	MMV666080	Drug-like
132	70	B	F03	MMV666081	Drug-like
133	58	B	F04	MMV666009	Drug-like
134	77	B	F05	MMV019313	Drug-like
135	81	B	F06	MMV019746	Drug-like
136	58	B	F07	MMV019064	Drug-like
137	65	B	F08	MMV011944	Drug-like
138	80	B	F09	MMV665803	Drug-like
139	78	B	F10	MMV665857	Drug-like
140	56	B	F11	MMV666071	Drug-like
141	94	B	G02	MMV019780	Drug-like
142	57	B	G03	MMV666093	Drug-like
143	98	B	G04	MMV665953	Drug-like
144	60	B	G05	MMV000648	Drug-like
145	65	B	G06	MMV019662	Drug-like
146	65	B	G07	MMV007571	Drug-like
147	67	B	G08	MMV007617	Drug-like
148	78	B	G09	MMV665796	Drug-like
149	65	B	G10	MMV665906	Drug-like
150	64	B	G11	MMV665954	Drug-like
151	23	B	H02	MMV019738	Drug-like
152	25	B	H03	MMV666075	Drug-like
153	48	B	H04	MMV666070	Drug-like
154	0	B	H05	MMV142383	Drug-like
155	61	B	H06	MMV000788	Drug-like
156	41	B	H07	MMV000561	Drug-like
157	100	B	H08	MMV000248	Drug-like
158	63	B	H09	MMV665879	Drug-like
159	52	B	H10	MMV665890	Drug-like
160	92	B	H11	MMV666116	Drug-like
161	32	C	A02	MMV006913	Drug-like
162	3	C	A03	MMV008127	Drug-like
163	37	C	A04	MMV403679	Drug-like
164	38	C	A05	MMV305841	Drug-like

165	37	C	A06	MMV019700	Drug-like
166	0	C	A07	MMV019670	Drug-like
167	14	C	A08	MMV001344	Drug-like
168	100	C	A09	MMV011795	Drug-like
169	24	C	A10	MMV019124	Drug-like
170	7	C	A11	MMV006767	Drug-like
171	17	C	B02	MMV007808	Drug-like
172	100	C	B03	MMV019017	Drug-like
173	16	C	B04	MMV396681	Drug-like
174	42	C	B05	MMV006587	Drug-like
175	28	C	B06	MMV019202	Drug-like
176	100	C	B07	MMV000848	Drug-like
177	46	C	B08	MMV020275	Drug-like
178	100	C	B09	MMV019918	Drug-like
179	0	C	B10	MMV075490	Drug-like
180	96	C	B11	MMV396633	Drug-like
181	36	C	C02	MMV007374	Drug-like
182	86	C	C03	MMV396719	Drug-like
183	24	C	C04	MMV396744	Drug-like
184	37	C	C05	MMV006706	Drug-like
185	0	C	C06	MMV009108	Drug-like
186	38	C	C07	MMV020700	Drug-like
187	42	C	C08	MMV007906	Drug-like
188	49	C	C09	MMV008270	Drug-like
189	100	C	C10	MMV019127	Drug-like
190	100	C	C11	MMV396794	Drug-like
191	100	C	D02	MMV396736	Drug-like
192	100	C	D03	MMV306025	Drug-like
193	33	C	D04	MMV056726	Drug-like
194	30	C	D05	MMV274073	Drug-like
195	39	C	D06	MMV018984	Drug-like
196	0	C	D07	MMV000911	Drug-like
197	34	C	D08	MMV007430	Drug-like
198	100	C	D09	MMV007977	Drug-like
199	99	C	D10	MMV020654	Drug-like
200	54	C	D11	MMV665883	Drug-like
201	100	C	E02	MMV084940	Drug-like
202	100	C	E03	MMV396715	Drug-like
203	100	C	E04	MMV000963	Drug-like
204	79	C	E05	MMV006319	Drug-like
205	77	C	E06	MMV000972	Drug-like
206	91	C	E07	MMV020490	Drug-like
207	72	C	E08	MMV001318	Drug-like

208	100	C	E09	MMV007978	Drug-like
209	100	C	E10	MMV020660	Drug-like
210	100	C	E11	MMV665904	Drug-like
211	100	C	F02	MMV396632	Drug-like
212	96	C	F03	MMV007875	Drug-like
213	96	C	F04	MMV006820	Drug-like
214	100	C	F05	MMV396749	Drug-like
215	100	C	F06	MMV011576	Drug-like
216	74	C	F07	MMV020651	Drug-like
217	100	C	F08	MMV000483	Drug-like
218	100	C	F09	MMV019266	Drug-like
219	100	C	F10	MMV001049	Drug-like
220	100	C	F11	MMV665806	Drug-like
221	79	C	G02	MMV667487	Drug-like
222	100	C	G03	MMV000356	Drug-like
223	90	C	G04	MMV396705	Drug-like
224	89	C	G05	MMV006704	Drug-like
225	100	C	G06	MMV000760	Drug-like
226	86	C	G07	MMV007881	Drug-like
227	91	C	G08	MMV008212	Drug-like
228	85	C	G09	MMV007363	Drug-like
229	81	C	G10	MMV007791	Drug-like
230	89	C	G11	MMV665843	Drug-like
231	40	C	H02	MMV396595	Drug-like
232	21	C	H03	MMV396669	Drug-like
233	27	C	H04	MMV396704	Drug-like
234	36	C	H05	MMV019762	Drug-like
235	100	C	H06	MMV020505	Drug-like
236	28	C	H07	MMV020942	Drug-like
237	100	C	H08	MMV000839	Drug-like
238	100	C	H09	MMV666599	Drug-like
239	47	C	H10	MMV000481	Drug-like
240	29	C	H11	MMV665897	Drug-like
241	0	D	A02	MMV665908	Probe-like
242	0	D	A03	MMV665924	Probe-like
243	31	D	A04	MMV665944	Probe-like
244	34	D	A05	MMV666054	Probe-like
245	0	D	A06	MMV008474	Probe-like
246	87	D	A07	MMV000445	Probe-like
247	0	D	A08	MMV006882	Probe-like
248	0	D	A09	MMV007127	Probe-like
249	0	D	A10	MMV666123	Probe-like
250	0	D	A11	MMV006389	Probe-like

251	0	D	B02	MMV665949	Probe-like
252	0	D	B03	MMV665934	Probe-like
253	17	D	B04	MMV665994	Probe-like
254	27	D	B05	MMV665980	Probe-like
255	0	D	B06	MMV007577	Probe-like
256	40	D	B07	MMV019995	Probe-like
257	47	D	B08	MMV007208	Probe-like
258	72	D	B09	MMV000442	Probe-like
259	8	D	B10	MMV666124	Probe-like
260	77	D	B11	MMV000444	Probe-like
261	55	D	C02	MMV666109	Probe-like
262	0	D	C03	MMV665936	Probe-like
263	18	D	C04	MMV666020	Probe-like
264	73	D	C05	MMV665971	Probe-like
265	8	D	C06	MMV001241	Probe-like
266	62	D	C07	MMV000720	Probe-like
267	24	D	C08	MMV000619	Probe-like
268	15	D	C09	MMV006753	Probe-like
269	92	D	C10	MMV006787	Probe-like
270	100	D	C11	MMV665794	Probe-like
271	65	D	D02	MMV000917	Probe-like
272	100	D	D03	MMV666125	Probe-like
273	64	D	D04	MMV665987	Probe-like
274	25	D	D05	MMV007574	Probe-like
275	30	D	D06	MMV000326	Probe-like
276	67	D	D07	MMV000604	Probe-like
277	22	D	D08	MMV007557	Probe-like
278	0	D	D09	MMV000699	Probe-like
279	49	D	D10	MMV009127	Probe-like
280	4	D	D11	MMV665786	Probe-like
281	47	D	E02	MMV006250	Probe-like
282	100	D	E03	MMV666079	Probe-like
283	67	D	E04	MMV665969	Probe-like
284	51	D	E05	MMV000304	Probe-like
285	95	D	E06	MMV000443	Probe-like
286	74	D	E07	MMV666604	Probe-like
287	84	D	E08	MMV008455	Probe-like
288	54	D	E09	MMV007199	Probe-like
289	52	D	E10	MMV085471	Probe-like
290	80	D	E11	MMV665797	Probe-like
291	100	D	F02	MMV006513	Probe-like
292	64	D	F03	MMV666095	Probe-like
293	100	D	F04	MMV665943	Probe-like

294	100	D	F05	MMV019555	Probe-like
295	92	D	F06	MMV019741	Probe-like
296	100	D	F07	MMV019690	Probe-like
297	65	D	F08	MMV000621	Probe-like
298	50	D	F09	MMV008173	Probe-like
299	55	D	F10	MMV019241	Probe-like
300	42	D	F11	MMV665783	Probe-like
301	78	D	G02	MMV000787	Probe-like
302	57	D	G03	MMV666106	Probe-like
303	72	D	G04	MMV666022	Probe-like
304	68	D	G05	MMV498479	Probe-like
305	62	D	G06	MMV007396	Probe-like
306	50	D	G07	MMV000617	Probe-like
307	88	D	G08	MMV006764	Probe-like
308	78	D	G09	MMV007275	Probe-like
309	55	D	G10	MMV007273	Probe-like
310	89	D	G11	MMV666026	Probe-like
311	0	D	H02	MMV665923	Probe-like
312	50	D	H03	MMV666025	Probe-like
313	94	D	H04	MMV666060	Probe-like
314	74	D	H05	MMV666597	Probe-like
315	100	D	H06	MMV007224	Probe-like
316	85	D	H07	MMV020912	Probe-like
317	89	D	H08	MMV007181	Probe-like
318	52	D	H09	MMV007113	Probe-like
319	52	D	H10	MMV007228	Probe-like
320	47	D	H11	MMV665972	Probe-like
321	39	E	A02	MMV073843	Probe-like
322	3	E	A03	MMV006303	Probe-like
323	48	E	A04	MMV667490	Probe-like
324	25	E	A05	MMV667492	Probe-like
325	76	E	A06	MMV019881	Probe-like
326	47	E	A07	MMV000478	Probe-like
327	0	E	A08	MMV020403	Probe-like
328	1	E	A09	MMV007764	Probe-like
329	78	E	A10	MMV665830	Probe-like
330	0	E	A11	MMV665886	Probe-like
331	0	E	B02	MMV396664	Probe-like
332	0	E	B03	MMV001239	Probe-like
333	91	E	B04	MMV667491	Probe-like
334	34	E	B05	MMV006169	Probe-like
335	0	E	B06	MMV086103	Probe-like
336	5	E	B07	MMV084434	Probe-like

337	29	E	B08	MMV666692	Probe-like
338	3	E	B09	MMV665836	Probe-like
339	11	E	B10	MMV665881	Probe-like
340	12	E	B11	MMV665875	Probe-like
341	25	E	C02	MMV007020	Probe-like
342	69	E	C03	MMV006656	Probe-like
343	30	E	C04	MMV396726	Probe-like
344	50	E	C05	MMV006522	Probe-like
345	100	E	C06	MMV666686	Probe-like
346	64	E	C07	MMV007474	Probe-like
347	94	E	C08	MMV006962	Probe-like
348	36	E	C09	MMV665813	Probe-like
349	44	E	C10	MMV080034	Probe-like
350	15	E	C11	MMV019199	Probe-like
351	52	E	D02	MMV396652	Probe-like
352	39	E	D03	MMV000704	Probe-like
353	42	E	D04	MMV396635	Probe-like
354	22	E	D05	MMV000986	Probe-like
355	25	E	D06	MMV008160	Probe-like
356	50	E	D07	MMV000753	Probe-like
357	65	E	D08	MMV011436	Probe-like
358	92	E	D09	MMV665882	Probe-like
359	67	E	D10	MMV665809	Probe-like
360	23	E	D11	MMV665810	Probe-like
361	66	E	E02	MMV665927	Probe-like
362	55	E	E03	MMV667486	Probe-like
363	71	E	E04	MMV667488	Probe-like
364	63	E	E05	MMV006825	Probe-like
365	89	E	E06	MMV009085	Probe-like
366	100	E	E07	MMV007591	Probe-like
367	70	E	E08	MMV128432	Probe-like
368	87	E	E09	MMV665852	Probe-like
369	69	E	E10	MMV396717	Probe-like
370	60	E	E11	MMV638723	Probe-like
371	48	E	F02	MMV396594	Probe-like
372	45	E	F03	MMV396665	Probe-like
373	96	E	F04	MMV396723	Probe-like
374	40	E	F05	MMV007654	Probe-like
375	67	E	F06	MMV011832	Probe-like
376	42	E	F07	MMV020750	Probe-like
377	100	E	F08	MMV007092	Probe-like
378	56	E	F09	MMV665898	Probe-like
379	81	E	F10	MMV665864	Probe-like

380	89	E	F11	MMV665814	Probe-like
381	44	E	G02	MMV007285	Probe-like
382	86	E	G03	MMV396663	Probe-like
383	80	E	G04	MMV007041	Probe-like
384	56	E	G05	MMV000340	Probe-like
385	100	E	G06	MMV666687	Probe-like
386	62	E	G07	MMV645672	Probe-like
387	100	E	G08	MMV011438	Probe-like
388	64	E	G09	MMV665840	Probe-like
389	45	E	G10	MMV665894	Probe-like
390	50	E	G11	MMV011522	Probe-like
391	0	E	H02	MMV020243	Probe-like
392	0	E	H03	MMV667489	Probe-like
393	15	E	H04	MMV396770	Probe-like
394	89	E	H05	MMV009015	Probe-like
395	31	E	H06	MMV008829	Probe-like
396	38	E	H07	MMV011895	Probe-like
397	37	E	H08	MMV666689	Probe-like
398	29	E	H09	MMV665824	Probe-like
399	68	E	H10	MMV665812	Probe-like
400	44	E	H11	MMV001041	Probe-like

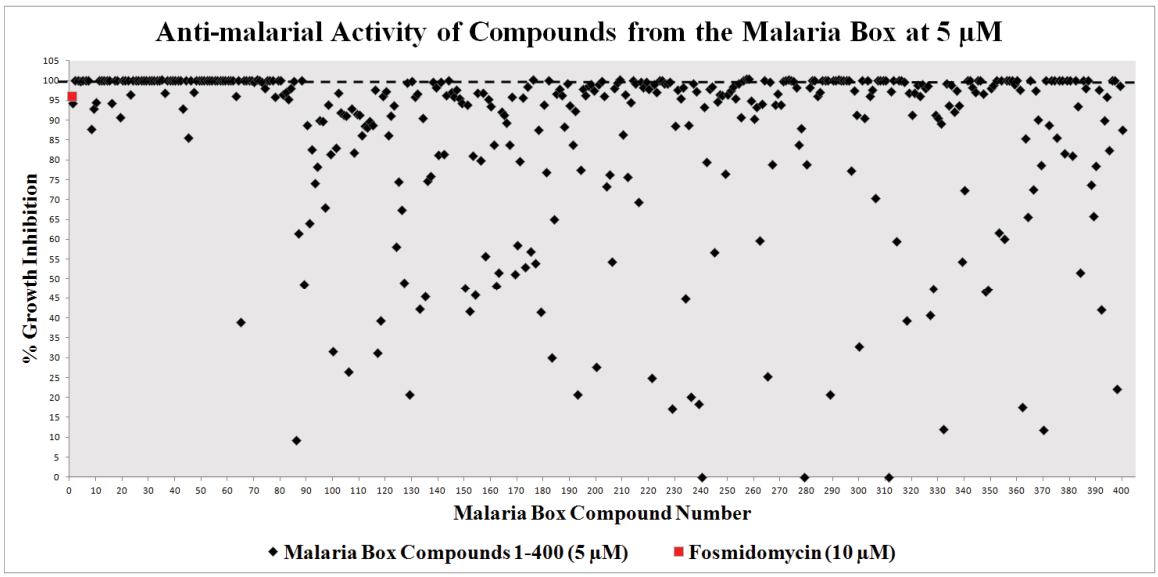

Data Set S1 D. Scatter plot reflecting the anti-malarial activity of compounds from the Malaria Box at 5 µM and summarizing Data Set S1 A. A large number of compounds achieved 100% growth inhibition against *P. falciparum*. Fosmidomycin was used as a positive control.

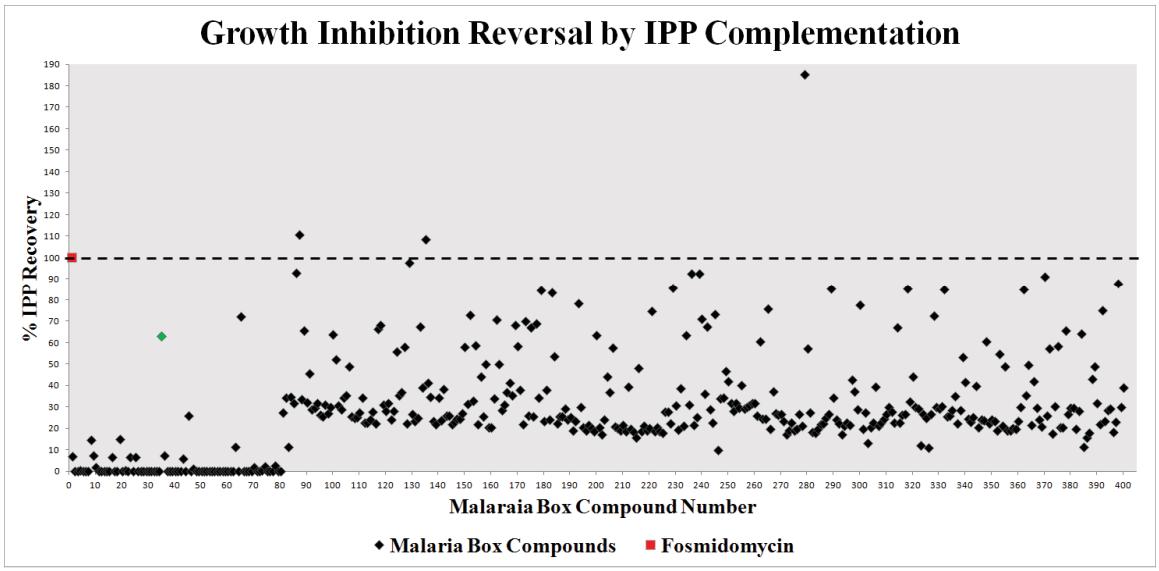

Data Set S1 E. Scatter plot reflecting the reversal of growth inhibition with IPP and summarizing Data Set S1 B. IPP complementation reversed killing effect of several compounds, however MMV008138 (green diamond) was the only "drug-like" compound found to be targeting the apicoplast. Other potential compounds were "probe-like" and not investigated further in this study.

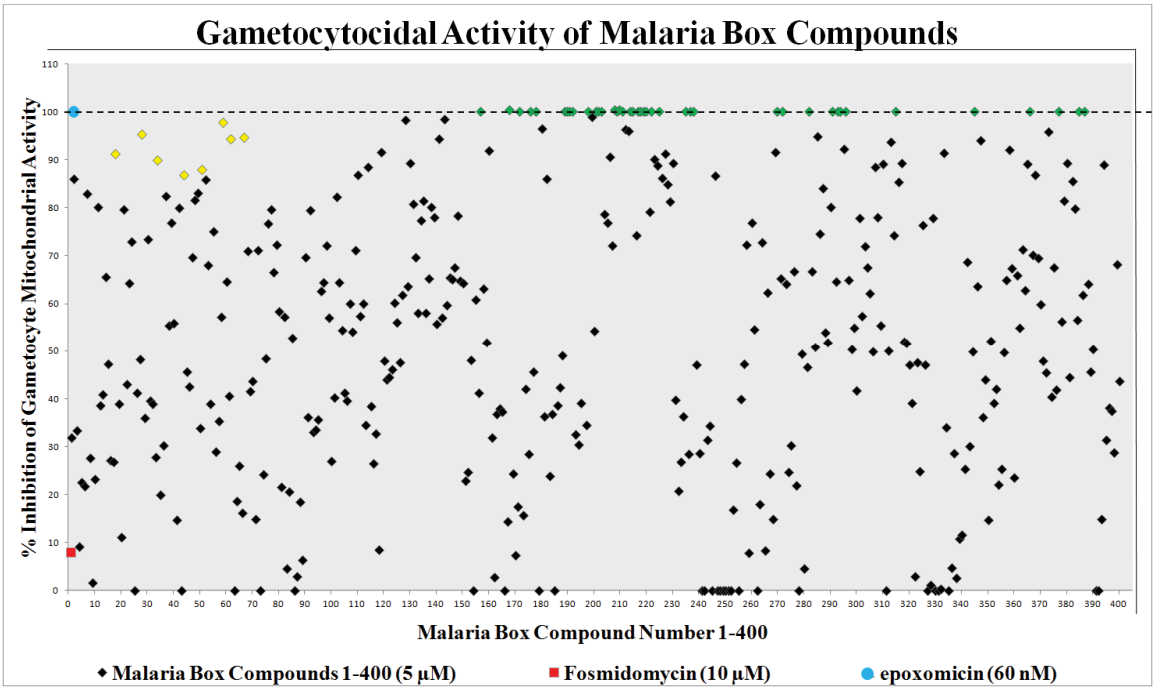

Data Set S1 F. Scatter plot reflecting gametocytocidal activity of malaria box compounds and summarizing Data Set S1 C. Epoxomicin and fosmidomycin were used as positive and negative controls, respectively. Compounds from plate A that exhibited the greatest gametocytocidal activity (yellow diamonds) were focused on in this study. Compound from plates B-E that exhibited gametocytocidal activity greater than or equal to epoxomicin (green diamonds) were focused on in this study.

Acknowledgments

This work was supported by funds from the Fralin Life Science Institute, the Jeffress Memorial Trust of Virginia (J-1058), and the Virginia Commonwealth Health Research Board (208-03-12) (to M.B.C.). J.D.B. is a recipient of a scholarship from the National Science Foundation S-STEM project (DUE-0850198). B.S. is a GRA distinguished investigator and his work on the apicoplast is supported by the National Institutes of Health (AI64671 and AI084415). We would like to thank Dr. Michael Klemba and Priscilla Krai for assistance with fluorescence microscopy and valuable discussions.

References

1. J. N. Burrows, Antimalarial drug discovery: where next? *Future Med Chem* **4**, 2233-2235 (2012).
2. T. Spangenberg, J. N. Burrows, P. Kowalczyk, S. McDonald, T. N. C. Wells, P. Willis, The Open Access Malaria Box: A Drug Discovery Catalyst for Neglected Diseases. *PLoS One* **8**, e62906 (2013).
3. W. A. Guiguemde, A. A. Shelat, J. F. Garcia-Bustos, T. T. Diagana, F. J. Gamo, R. K. Guy, Global phenotypic screening for antimalarials. *Chem Biol* **19**, 116-129 (2012).
4. C. D. Goodman, G. I. McFadden, Targeting apicoplasts in malaria parasites. *Expert Opin Ther Targets* **17**, 167-177 (2013).
5. G. G. van Dooren, B. Striepen, The algal past and parasite present of the apicoplast. *Annu Rev Microbiol* **67**, 271-289 (2013).
6. A. R. Odom, W. C. Van Voorhis, Functional genetic analysis of the *Plasmodium falciparum* deoxyxylulose 5-phosphate reductoisomerase gene. *Mol Biochem Parasitol* **170**, 108-111 (2010).
7. S. C. Nair, C. F. Brooks, C. D. Goodman, A. Sturm, G. I. McFadden, S. Sundriyal, J. L. Anglin, Y. Song, S. N. Moreno, B. Striepen, Apicoplast isoprenoid precursor synthesis and the molecular basis of fosmidomycin resistance in *Toxoplasma gondii*. *J Exp Med* **208**, 1547-1559 (2011).
8. E. Yeh, J. L. DeRisi, Chemical rescue of malaria parasites lacking an apicoplast defines organelle function in blood-stage *Plasmodium falciparum*. *PLoS Biol* **9**, e1001138 (2011).
9. S. Wittlin, E. Ekland, J. C. Craft, J. Lotharius, I. Bathurst, D. A. Fidock, P. Fernandes, In vitro and in vivo activity of solithromycin (CEM-101) against Plasmodium species. *Antimicrob Agents Chemother* **56**, 703-707 (2012).
10. E. L. Dahl, P. J. Rosenthal, Multiple antibiotics exert delayed effects against the *Plasmodium falciparum* apicoplast. *Antimicrob Agents Chemother* **51**, 3485-3490 (2007).
11. E. L. Dahl, J. L. Shock, B. R. Shenai, J. Gut, J. L. DeRisi, P. J. Rosenthal, Tetracyclines specifically target the apicoplast of the malaria parasite *Plasmodium falciparum*. *Antimicrob Agents Chemother* **50**, 3124-3131 (2006).

12. C. D. Goodman, V. Su, G. I. McFadden, The effects of anti-bacterials on the malaria parasite Plasmodium falciparum. *Mol Biochem Parasitol* **152**, 181-191 (2007).
13. M. N. Aminake, S. Schoof, L. Sologub, M. Leubner, M. Kirschner, H. D. Arndt, G. Pradel, Thiostrepton and derivatives exhibit antimalarial and gametocytocidal activity by dually targeting parasite proteasome and apicoplast. *Antimicrob Agents Chemother* **55**, 1338-1348 (2011).
14. S. Rathore, D. Sinha, M. Asad, T. Bottcher, F. Afrin, V. S. Chauhan, D. Gupta, S. A. Sieber, A. Mohmmed, A cyanobacterial serine protease of *Plasmodium falciparum* is targeted to the apicoplast and plays an important role in its growth and development. *Molecular microbiology*, (2010).
15. M. E. Fichera, D. S. Roos, A plastid organelle as a drug target in apicomplexan parasites. *Nature* **390**, 407-409 (1997).
16. E. L. Dahl, P. J. Rosenthal, Apicoplast translation, transcription and genome replication: targets for antimalarial antibiotics. *Trends Parasitol* **24**, 279-284 (2008).
17. M. B. Cassera, F. C. Gozzo, F. L. D'Alexandri, E. F. Merino, H. A. del Portillo, V. J. Peres, I. C. Almeida, M. N. Eberlin, G. Wunderlich, J. Wiesner, H. Jomaa, E. A. Kimura, A. M. Katzin, The methylerythritol phosphate pathway is functionally active in all intraerythrocytic stages of *Plasmodium falciparum*. *J Biol Chem* **279**, 51749-51759 (2004).
18. H. Jomaa, J. Wiesner, S. Sanderbrand, B. Altincicek, C. Weidemeyer, M. Hintz, I. Turbachova, M. Eberl, J. Zeidler, H. K. Lichtenthaler, D. Soldati, E. Beck, Inhibitors of the nonmevalonate pathway of isoprenoid biosynthesis as antimalarial drugs. *Science* **285**, 1573-1576 (1999).
19. M. Delves, D. Plouffe, C. Scheurer, S. Meister, S. Wittlin, E. A. Winzeler, R. E. Sinden, D. Leroy, The activities of current antimalarial drugs on the life cycle stages of Plasmodium: a comparative study with human and rodent parasites. *PLoS Med* **9**, e1001169 (2012).
20. C. L. Peatey, D. Leroy, D. L. Gardiner, K. R. Trenholme, Anti-malarial drugs: how effective are they against *Plasmodium falciparum* gametocytes? *Malar J* **11**, 34 (2012).

21. R. F. Waller, M. B. Reed, A. F. Cowman, G. I. McFadden, Protein trafficking to the plastid of *Plasmodium falciparum* is via the secretory pathway. *EMBO J* **19**, 1794-1802 (2000).

22. N. V. Dharia, A. B. Sidhu, M. B. Cassera, S. J. Westenberger, S. E. Bopp, R. T. Eastman, D. Plouffe, S. Batalov, D. J. Park, S. K. Volkman, D. F. Wirth, Y. Zhou, D. A. Fidock, E. A. Winzeler, Use of high-density tiling microarrays to identify mutations globally and elucidate mechanisms of drug resistance in *Plasmodium falciparum*. *Genome Biol* **10**, R21 (2009).

23. L. Harinantenaina, J. D. Bowman, P. J. Brodie, C. Slebodnick, M. W. Callmander, E. Rakotobe, R. Randrianaivo, V. E. Rasamison, A. Gorka, P. D. Roepe, M. B. Cassera, D. G. Kingston, Antiproliferative and Antiplasmodial Dimeric Phloroglucinols from Mallotus oppositifolius from the Madagascar Dry Forest. *J Nat Prod*, (2013.

24. M. Smilkstein, N. Sriwilaijaroen, J. X. Kelly, P. Wilairat, M. Riscoe, Simple and inexpensive fluorescence-based technique for high-throughput antimalarial drug screening. *Antimicrob Agents Chemother* **48**, 1803-1806 (2004).

25. M. J. Gubbels, C. Li, B. Striepen, High-throughput growth assay for *Toxoplasma gondii* using yellow fluorescent protein. *Antimicrob Agents Chemother* **47**, 309-316 (2003)

26. J. I. MacRae, M. W. Dixon, M. K. Dearnley, H. H. Chua, J. M. Chambers, S. Kenny, I. Bottova, L. Tilley, M. J. McConville, Mitochondrial metabolism of sexual and asexual blood stages of the malaria parasite Plasmodium falciparum. *BMC biology* **11**, 67 (2013).

27. T. Q. Tanaka, K. C. Williamson, A malaria gametocytocidal assay using oxidoreduction indicator, alamarBlue. *Mol Biochem Parasitol* **177**, 160-163 (2011).

28. B. Czesny, S. Goshu, J. L. Cook, K. C. Williamson, The proteasome inhibitor epoxomicin has potent *Plasmodium falciparum* gametocytocidal activity. *Antimicrob Agents Chemother* **53**, 4080-4085 (2009).

29. F. J. Gamo, L. M. Sanz, J. Vidal, C. de Cozar, E. Alvarez, J. L. Lavandera, D. E. Vanderwall, D. V. Green, V. Kumar, S. Hasan, J. R. Brown, C. E. Peishoff, L. R. Cardon, J. F. Garcia-Bustos, Thousands of chemical starting points for antimalarial lead identification. *Nature* **465**, 305-310 (2010).

30. S. Meister, D. M. Plouffe, K. L. Kuhen, G. M. Bonamy, T. Wu, S. W. Barnes, S. E. Bopp, R. Borboa, A. T. Bright, J. Che, S. Cohen, N. V. Dharia, K. Gagaring, M.

Gettayacamin, P. Gordon, T. Groessl, N. Kato, M. C. Lee, C. W. McNamara, D. A. Fidock, A. Nagle, T. G. Nam, W. Richmond, J. Roland, M. Rottmann, B. Zhou, P. Froissard, R. J. Glynne, D. Mazier, J. Sattabongkot, P. G. Schultz, T. Tuntland, J. R. Walker, Y. Zhou, A. Chatterjee, T. T. Diagana, E. A. Winzeler, Imaging of Plasmodium liver stages to drive next-generation antimalarial drug discovery. *Science* **334**, 1372-1377 (2011).

31. D. Plouffe, A. Brinker, C. McNamara, K. Henson, N. Kato, K. Kuhen, A. Nagle, F. Adrian, J. T. Matzen, P. Anderson, T. G. Nam, N. S. Gray, A. Chatterjee, J. Janes, S. F. Yan, R. Trager, J. S. Caldwell, P. G. Schultz, Y. Zhou, E. A. Winzeler, In silico activity profiling reveals the mechanism of action of antimalarials discovered in a high-throughput screen. *Proc Natl Acad Sci U S A* **105**, 9059-9064 (2008).

32. M. B. Cassera, E. F. Merino, V. J. Peres, E. A. Kimura, G. Wunderlich, A. M. Katzin, Effect of fosmidomycin on metabolic and transcript profiles of the methylerythritol phosphate pathway in *Plasmodium falciparum*. *Memorias do Instituto Oswaldo Cruz* **102**, 377-383 (2007).

33. S. A. Ralph, G. G. Van Dooren, R. F. Waller, M. J. Crawford, M. J. Fraunholz, B. J. Foth, C. J. Tonkin, D. S. Roos, G. I. McFadden, Tropical infectious diseases: Metabolic maps and functions of the *Plasmodium falciparum* apicoplast. *Nat Rev Microbiol* **2**, 203-216 (2004).

34. L. Lim, G. I. McFadden, The evolution, metabolism and functions of the apicoplast. *Philosophical transactions of the Royal Society of London. Series B, Biological sciences* **365**, 749-763 (2010).

35. J. Y. van der Meer, A. K. Hirsch, The isoprenoid-precursor dependence of Plasmodium spp. *Nat Prod Rep* **29**, 721-728 (2012).

36. N. Okamoto, T. P. Spurck, C. D. Goodman, G. I. McFadden, Apicoplast and mitochondrion in gametocytogenesis of *Plasmodium falciparum*. *Eukaryot Cell* **8**, 128-132 (2009).

37. M. A. Missinou, S. Borrmann, A. Schindler, S. Issifou, A. A. Adegnika, P. B. Matsiegui, R. Binder, B. Lell, J. Wiesner, T. Baranek, H. Jomaa, P. G. Kremsner, Fosmidomycin for malaria. *Lancet* **360**, 1941-1942 (2002).

38. J. Wiesner, S. Borrmann, H. Jomaa, Fosmidomycin for the treatment of malaria. *Parasitol Res* **90 Suppl 2**, S71-76 (2003).
39. J. Wiesner, D. Henschker, D. B. Hutchinson, E. Beck, H. Jomaa, *In vitro* and *in vivo* synergy of fosmidomycin, a novel antimalarial drug, with clindamycin. *Antimicrob Agents Chemother* **46**, 2889-2894 (2002).
40. S. Borrmann, A. A. Adegnika, P. B. Matsiegui, S. Issifou, A. Schindler, D. P. Mawili-Mboumba, T. Baranek, J. Wiesner, H. Jomaa, P. G. Kremsner, Fosmidomycin-clindamycin for *Plasmodium falciparum* Infections in African children. *Journal of Infectious Diseases* **189**, 901-908 (2004).
41. S. Borrmann, A. A. Adegnika, F. Moussavou, S. Oyakhirome, G. Esser, P. B. Matsiegui, M. Ramharter, I. Lundgren, M. Kombila, S. Issifou, D. Hutchinson, J. Wiesner, H. Jomaa, P. G. Kremsner, Short-course regimens of artesunate-fosmidomycin in treatment of uncomplicated *Plasmodium falciparum* malaria. *Antimicrob Agents Chemother* **49**, 3749-3754 (2005).
42. S. Borrmann, S. Issifou, G. Esser, A. A. Adegnika, M. Ramharter, P. B. Matsiegui, S. Oyakhirome, D. P. Mawili-Mboumba, M. A. Missinou, J. F. Kun, H. Jomaa, P. G. Kremsner, Fosmidomycin-clindamycin for the treatment of *Plasmodium falciparum* malaria. *Journal of Infectious Diseases* **190**, 1534-1540 (2004).
43. K. Na-Bangchang, R. Ruengweerayut, J. Karbwang, A. Chauemung, D. Hutchinson, Pharmacokinetics and pharmacodynamics of fosmidomycin monotherapy and combination therapy with clindamycin in the treatment of multidrug resistant falciparum malaria. *Malar J* **6**, 70 (2007).
44. N. J. Spillman, R. J. Allen, C. W. McNamara, B. K. Yeung, E. A. Winzeler, T. T. Diagana, K. Kirk, Na(+) regulation in the malaria parasite *Plasmodium falciparum* involves the cation ATPase PfATP4 and is a target of the spiroindolone antimalarials. *Cell Host Microbe* **13**, 227-237 (2013).
45. J. C. van Pelt-Koops, H. E. Pett, W. Graumans, M. van der Vegte-Bolmer, G. J. van Gemert, M. Rottmann, B. K. Yeung, T. T. Diagana, R. W. Sauerwein, The spiroindolone drug candidate NITD609 potently inhibits gametocytogenesis and blocks *Plasmodium falciparum* transmission to anopheles mosquito vector. *Antimicrob Agents Chemother* **56**, 3544-3548 (2012).

46. M. Rottmann, C. McNamara, B. K. Yeung, M. C. Lee, B. Zou, B. Russell, P. Seitz, D. M. Plouffe, N. V. Dharia, J. Tan, S. B. Cohen, K. R. Spencer, G. E. Gonzalez-Paez, S. B. Lakshminarayana, A. Goh, R. Suwanarusk, T. Jegla, E. K. Schmitt, H. P. Beck, R. Brun, F. Nosten, L. Renia, V. Dartois, T. H. Keller, D. A. Fidock, E. A. Winzeler, T. T. Diagana, Spiroindolones, a potent compound class for the treatment of malaria. *Science* **329**, 1175-1180 (2010).

47. B. K. Yeung, B. Zou, M. Rottmann, S. B. Lakshminarayana, S. H. Ang, S. Y. Leong, J. Tan, J. Wong, S. Keller-Maerki, C. Fischli, A. Goh, E. K. Schmitt, P. Krastel, E. Francotte, K. Kuhen, D. Plouffe, K. Henson, T. Wagner, E. A. Winzeler, F. Petersen, R. Brun, V. Dartois, T. T. Diagana, T. H. Keller, Spirotetrahydro beta-carbolines (spiroindolones): a new class of potent and orally efficacious compounds for the treatment of malaria. *J Med Chem* **53**, 5155-5164 (2010).

48. R. Cao, W. Peng, Z. Wang, A. Xu, beta-Carboline alkaloids: biochemical and pharmacological functions. *Curr Med Chem* **14**, 479-500 (2007).

49. O. Dechy-Cabaret, F. Benoit-Vical, Effects of antimalarial molecules on the gametocyte stage of *Plasmodium falciparum*: the debate. *Journal of medicinal chemistry* **55**, 10328-10344 (2012).

50. A. F. Valdes, Acridine and acridinones: old and new structures with antimalarial activity. *Open Med Chem J* **5**, 11-20 (2011).

51. I. P. Hoglund, S. Silver, M. T. Engstrom, H. Salo, A. Tauber, H. K. Kyyronen, P. Saarenketo, A. M. Hoffren, K. Kokko, K. Pohjanoksa, J. Sallinen, J. M. Savola, S. Wurster, O. A. Kallatsa, Structure-activity relationship of quinoline derivatives as potent and selective alpha(2C)-adrenoceptor antagonists. *Journal of medicinal chemistry* **49**, 6351-6363 (2006).

52. P. R. Carlier, Y. F. Han, E. S. Chow, C. P. Li, H. Wang, T. X. Lieu, H. S. Wong, Y. P. Pang, Evaluation of short-tether bis-THA AChE inhibitors. A further test of the dual binding site hypothesis. *Bioorg Med Chem* **7**, 351-357 (1999).

53. S. Pou, R. W. Winter, A. Nilsen, J. X. Kelly, Y. Li, J. S. Doggett, E. W. Riscoe, K. W. Wegmann, D. J. Hinrichs, M. K. Riscoe, Sontochin as a guide to the development of drugs against chloroquine-resistant malaria. *Antimicrob Agents Chemother* **56**, 3475-3480 (2012).

54. G. Covell, G. R. Coatney, J. W. Field, J. Singh, Chemotherapy of malaria. *Monogr Ser World Health Organ* **27**, 1-123 (1955).

55. R. D. Powell, W. D. Tigertt, Drug resistance of parasites causing human malaria. *Annu Rev Med* **19**, 81-102 (1968).

CHAPTER 4: CONCLUSION

Malaria remains a significant global health burden that is transmitted by *Anopheles* mosquitoes. Understanding the essential role of the apicoplast during sexual development of the malaria parasite will aid the development of novel strategies to control and potentially eliminate malaria transmission. Additionally, identifying new antimalarials with novel mechanism of actions is crucial, as drug resistance remains an increasing problem in this field.

The apicoplast is an essential organelle in the malaria parasite (*1, 2*), which must be maternally inherited and cannot be generated *de novo* (*1-3*) and its discovery opened a new avenue for drug discovery and development due to its unusual and non-mammalian metabolism (*4, 5*). The role of the apicoplast during the asexual intraerythrocytic stages of the malaria parasite has been extensively investigated (*2, 3, 6-8*). However, the role of the apicoplast during gametocytogenesis was not previously studied. In the presented work, we have demonstrated that the apicoplast is essential for gametocytogenesis and isoprenoid biosynthesis is its main function during these stages, validating isoprenoid biosynthesis as potential drug targets to develop novel transmission-blocking inhibitors.

In addition, mature gametocytes are not affected by current schizonticides. We screened compounds from the Malaria Box against mature gametocytes to assess their gametocytocidal potential (*9*), and several compounds were identified. In the same work, we identified one compound from the Malaria Box that specifically targets the apicoplast using reversal of growth inhibition by isopentenyl diphosphate (IPP) supplementation in asexual intraerythrocytic stages, therefore, identifying its mechanism of action (*9*). Because still new antimalarial compounds are urgently needed against the asexual stages, where the onset of the disease occurs, in collaboration with Dr. Kingston laboratory several novel antimalarial compounds were identified from natural sources that may serve as starting points for development of new therapies (*10-13*). The work performed to identify new potential antimalarials from natural products can be found in appendices A-D. Altogether, our work has demonstrated that the apicoplast is still remains a rich source of drug targets during both asexual and sexual intraerythrocytic stages.

References

1. B. J. Foth, G. I. McFadden, *The apicoplast: A plastid in Plasmodium falciparum and other apicomplexan parasites*. W. J. Kwang, Ed., International Review of Cytology (Academic Press, 2003), vol. Volume 224, pp. 57-110.
2. M. Kalanon, G. I. McFadden, Malaria, *Plasmodium falciparum* and its apicoplast. *Biochemical Society transactions* **38**, 775-782 (2010)10.1042/BST0380775).
3. C. Y. Botté, F. Dubar, G. I. MacFadden, E. Marechal, C. Biot, *Plasmodium falciparum* Apicoplast Drugs: Targets or Off-Targets? *Chemical reviews* **112**, 1269-1283 (2012).
4. G. I. McFadden, M. E. Reith, J. Munholland, N. Lang-Unnasch, Plastid in human parasites. *Nature* **381**, 482 (1996).
5. G. I. McFadden, D. S. Roos, Apicomplexan plastids as drug targets. *Trends Microbiol* **7**, 328-333 (1999).
6. S. A. Ralph, G. G. Van Dooren, R. F. Waller, M. J. Crawford, M. J. Fraunholz, B. J. Foth, C. J. Tonkin, D. S. Roos, G. I. McFadden, Tropical infectious diseases: Metabolic maps and functions of the *Plasmodium falciparum* apicoplast. *Nat Rev Microbiol* **2**, 203-216 (2004).
7. J. Y. van der Meer, A. K. Hirsch, The isoprenoid-precursor dependence of Plasmodium spp. *Nat Prod Rep* **29**, 721-728 (2012).
8. C. D. Goodman, G. I. McFadden, Fatty Acid Biosynthesis as a Drug Target in Apicomplexan Parasites. *Current Drug Targets* **8**, 15-30 (2007).
9. J. D. Bowman, E. F. Merino, C. F. Brooks, B. Striepen, P. R. Carlier, M. B. Cassera, Antiapicoplast and Gametocytocidal Screening To Identify the Mechanisms of Action of Compounds within the Malaria Box. *Antimicrob Agents Chemother* **58**, 811-819 (2014).
10. Y. Dai, L. Harinantenaina, J. D. Bowman, I. O. Da Fonseca, P. J. Brodie, M. Goetz, M. B. Cassera, D. G. I. Kingston, Isolation of antiplasmodial anthraquinones from *Kniphofia ensifolia*, and synthesis and structure–activity relationships of related compounds. *Bioorganic & Medicinal Chemistry* **22**, 269-276 (2014).
11. A. L. Eaton, L. Harinantenaina, P. J. Brodie, M. B. Cassera, J. D. Bowman, M. W. Callmander, R. Randrianaivo, R. Rakotondrajaona, E. Rakotobe, V. E. Rasamison, D. G. Kingston, A new bioactive diterpene glycoside from *Molinaea retusa* from the Madagascar dry forest. *Natural product communications* **8**, 1201-1203 (2013).

12. L. Harinantenaina, J. D. Bowman, P. J. Brodie, C. Slebodnick, M. W. Callmander, E. Rakotobe, R. Randrianaivo, V. E. Rasamison, A. Gorka, P. D. Roepe, M. B. Cassera, D. G. Kingston, Antiproliferative and antiplasmodial dimeric phloroglucinols from *Mallotus oppositifolius* from the Madagascar dry forest. *Journal of Natural Products* **76**, 388-393 (2013).
13. Y. Liu, L. Harinantenaina, P. J. Brodie, J. D. Bowman, M. B. Cassera, C. Slebodnick, M. W. Callmander, R. Randrianaivo, E. Rakotobe, V. E. Rasamison, W. Applequist, C. Birkinshaw, G. P. Lewis, D. G. Kingston, Bioactive compounds from *Stuhlmannia moavi* from the Madagascar dry forest. *Bioorg Med Chem* **21**, 7591-7594 (2013).

APPENDIX A: ISOLATION OF ANTIPLASMODIAL ANTHRAQUINONES FROM *KNIPHOFIA ENSIFOLIA*, AND SYNTHESIS AND STRUCTURE-ACTIVITY RELATIONSHIP OF RELATED COMPOUNDS

Yumin, Dai, Liva Harinantenaina, Jessica D. Bowman, Isabel Osorio Da Fonseca, Peggy J. Brodie, Michael Goetz, Maria B. Cassera, and David G. I. Kingston

Manuscript published – Reprinted with permission from Bioorganic & Medicinal Chemistry

ABSTRACT

Bioassay-guided separation of the South African plant *Kniphofia ensifolia* for antiplasmodial activity led to the isolation of two new anthraquinones, named kniphofiones A and B (**3, 4**), together with three known bioactive anthraquinone monomers (**1**, **2** and **5**), and four known bisanthraquinones (**6 - 9**). The structures of the two new compounds were elucidated based on analyses of their 1D and 2D NMR spectra and mass spectrometric data. The dimeric compounds **6** and **7** displayed the strongest antiplasmodial activity among all the isolated compounds, with IC_{50} values of 0.4 ± 0.1 and 0.2 ± 0.1 μM, respectively. The two new compounds displayed modest activities, with IC_{50} values of 26 ± 4 and 9 ± 1 μM, respectively. Due to the synthetic accessibility of the new compounds and the increased activity shown by the dimeric compounds, a structure-activity relationship study was conducted. As a result, one analogue of kniphofione B (**4**), the caffeic acid derivative of aloe-emodin, was found to have the highest activity among all the aloe-emodin derivatives, with an IC_{50} value of 1.3 ± 0.2 μM.

Introduction

Malaria remains one of the major infectious diseases that threaten human lives. According to the latest available estimates from the World Health Organization (WHO), there were about 219 million cases of malaria and an estimated 660,000 deaths from malaria in 2010, with about 90% of all of these deaths occurring in sub-Saharan Africa (*1*). Although current anti-malarial therapies, including mefloquinone and its analogues (*2*) and artemisinin combination therapy combined with insecticide-treated bed nets (*3*) have achieved significant success in controlling the spread of the disease, malaria still remains a burden to humanity due to increasing drug resistance and the lack of multistage therapies to target the complex life cycle of the parasites. The recent emergence of resistance to artemisinin in the Cambodia–Thailand border area is particularly troubling (*4*). A continuing search for new anti-malarial drugs is thus important to the overall goal of eradicating this scourge of mankind.

As part of a collaborative research project established between Virginia Tech and the Institute for Hepatitis and Virus Research (IHVR) and its the Natural Products Discovery Institute (NPDI) (*5*), we are searching for antiproliferative and antimalarial natural products in the plant extract library of the NPDI. An investigation for antiproliferative compounds from this library yielded several homoisoflavonones and bufadienolides with strong antiproliferative activity(*6*), and the present work reports the first results from our investigation of extracts with antimalarial activity.

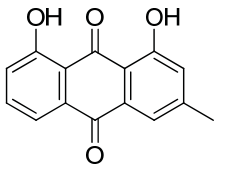

1

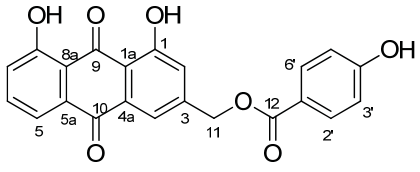

3

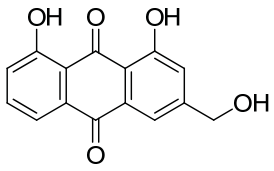

2

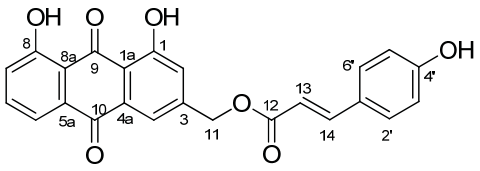

4

Screening of over 6,900 extracts from the NPDI collection led to the identification of a dichloromethane extract of *Kniphofia ensifolia* Baker (Asphodelaceae) (*7*) as an extract with promising antiplasmodial activity against the drug-resistant Dd2 strain of *Plasmodium*

falciparum, with an IC_{50} value of ~ 6 µg/mL. Members of the Asphodelaceae family are widely distributed in Africa, central and western Europe, the Mediterranean basin, Central Asia, and Australia (*8*). The genus *Kniphofia* is a rich source of anthraquinones, flavonoids and alkaloids, which are well-known for their broad range of bioactivities, including anticancer and antimalarial activities (*9-11*). Although the genus *Kniphofia* has been well explored, the phytochemistry of *K. ensifolia* has not previously been investigated, and its extract of was thus selected for bioassay-guided fractionation to isolate its bioactive components.

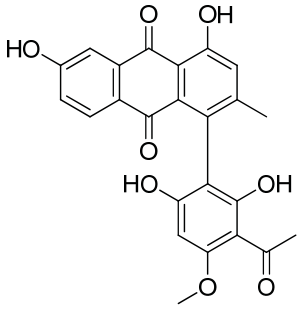

5

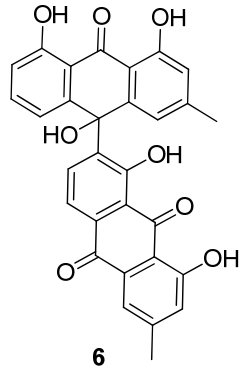

6

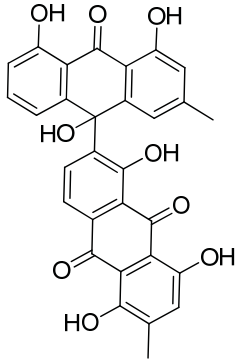

7

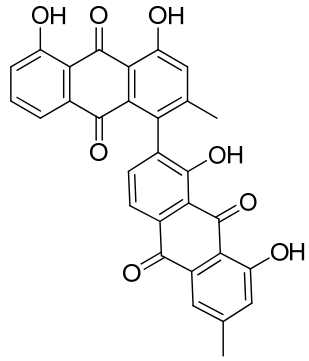

8

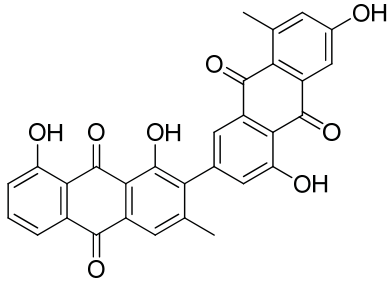

9

Results and Discussion

Isolation and structure elucidation of bioactive anthra-quinones

An EtOH extract of the whole plant of *K. ensifolia* was subjected to liquid-liquid partitioning to give an antiplasmodial CH_2Cl_2 fraction (IC_{50} = ~ 6.0 µg/mL). Bioassay-guided separation of the CH_2Cl_2 fraction, including Sephadex LH-20 size-exclusion chromatography, normal-phase silica gel chromatography, and C_{18} reverse-phase HPLC, yielded two new anthraquinones, named kniphofiones A and B (**3**, **4**), two known strongly active anthraquinones (**6**, **7**), and five other known anthraquinones (**1**, **2**, **5**, **8**, **9**). The structure elucidation of the new compounds is reported herein.

Compounds **1**, **2** and **5-9** were identified as chrysophanol (**1**) (*12*), aloe-emodin (**2**) (*13*), knipholone (**5**) (*14*), 10-(chrysophanol-7'-yl)-10-hydroxychrysophanol-9-anthrone (**6**) (*10*), chryslandicin (**7**) (*15*), asphodeline (**8**) (*16*), and microcarpin (**9**) (*17*) respectively, by comparison of their experimental and reported physical and spectroscopic data with literature data.

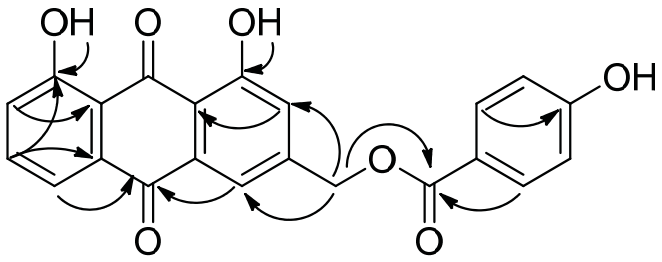

Figure A. 1. HMBC correlations of compound 3**.**

Kniphofione A (**3**) was isolated as a yellow-orange powder. Its negative ion HR-ESI-MS revealed a peak for a deprotonated molecular ion at *m/z* 389.0688 $[M-H]^-$, corresponding to a molecular formula of $C_{22}H_{14}O_7$. Its IR spectrum exhibited absorption bands at 3390 and 1673 cm^{-1}, indicating the presence of hydroxy and conjugated carbonyl groups. The presence of two chelated hydroxy groups was further confirmed by two singlet signals located at δ_H 12.09 and 12.12 in the ^1H NMR spectrum (Table A 1). In addition, a set of three coupled aromatic protons in the ABC-type spin system [δ_H 7.90 (1H, dd, *J* = 7.9, 1.6 Hz), 7.73 (1H, dd, *J* = 8.0, 7.9 Hz) and 7.39 (1H, dd, *J* = 8.0, 1.6 Hz)], two *meta*-coupled doublets located at δ_H 7.87 and 7.34 (both, 1H, *J* = 1.6), as well as methylene protons on an oxygen-bearing carbon at δ_H 5.44 (2H, singlet), were similar to the corresponding signals of aloe-emodin (**2**) and of aloe-emodin-type

anthraquinones (*13, 18*). The observation of two carbonyl carbon resonances located at δ_C 192.7 and 181.6, as well as a methylene carbon signal at δ_C 64.9 (C-11) in the ^{13}C NMR spectrum, corroborated its structure as an aloe-emodin derivative. The basic skeleton of 1,8-dihydroxy-3-(hydroxymethyl)anthracene-9,10-dione was confirmed by the HMBC correlations between H-2 and C-1a, H-4 and C-10, H-6 and C-8, H-7 and C-8a, and H-11 and C-2 (Figure A 1).

Table A. 1. NMR Spectroscopic Data for 3 and 4 in $CDCl_3$ (500 MHz)

	3		**4**	
posn	δ_H (*J* in Hz)	δ_C, type	δ_H (*J* in Hz)	δ_C, type
1	-	162.9, C	-	162.8, C
1a	-	115.3, C	-	115.2, C
2	7.87 d (1.6)	118.6, CH	7.87 d (1.6)	118.5, CH
3	-	147.0, C	-	146.9, C
4	7.34 d (1.6)	122.4, CH	7.36 d (1.6)	122.4, CH
4a	-	133.6, C	-	133.6, C
5	7.90 dd (7.9, 1.6)	120.2, CH	7.87 dd (7.9, 1.6)	120.2, CH
5a	-	134.1, C	-	133.9, C
6	7.73 dd (8.0, 7.9)	137.4, CH	7.73 dd (8.0, 7.9)	137.3, CH
7	7.39 dd (8.0, 1.6)	124.8, CH	7.35 dd (8.0, 1.6)	124.8, CH
8	-	162.7, C	-	162.8, C
8a	-	115.9, C	-	115.8, C
9	-	192.7, C	-	192.7, C
10	-	181.6, C	-	181.6, C
11	5.44 s	64.9, CH_2	5.35 s	64.6, CH_2
12	-	165.8, C	-	166.7, C
13	-	-	6.43 d (15.9)	114.4, CH
14	-	-	7.75 d (15.9)	145.8, CH
1'	-	121.8, C	-	126.9, C
2'	8.07 brd (8.8)	132.0, CH	7.50 brd (8.5)	130.0, CH
3'	6.92 brd (8.8)	113.9, CH	6.88 brd (8.5)	114.4, CH
4'	-	159.6, C	-	159.5, C
5'	6.92 brd (8.8)	113.9, CH	6.88 brd (8.5)	114.4, CH
6'	8.07 brd (8.8)	132.0, CH	7.50 brd (8.5)	130.0, CH
1-OH	12.12 s	-	12.11 s	-
8-OH	12.09 s	-	12.09 s	-

Furthermore, the presence of a *para*-hydroxybenzoate group was suggested by the presence of two doublets at δ_H 8.07 and 6.92 (2H each, J = 8.8 Hz) in the ^1H NMR spectrum, and a set of five carbon signals at δ_C 165.8 (C-12), 159.6 (C-4'), 132.0 (C-2'/6'), 122.4 (C-

1'),and 113.9 (C-3'/5'), in the ^{13}C NMR spectrum.(*19*) The structure of the *para*-hydroxybenzoate group and its connection to C-11 was further confirmed by the HMBC correlations between H-2'/H-6' and C-12, H-6'/H-2' and C-4', and H_2-11 and C-12. Hence, the structure of compound **3** was assigned as (1,8-dihydroxy-9,10-dioxo-9,10-dihydroanthracen-3-yl)methyl-4-hydroxybenzoate.

Kniphofione B (**4**) was obtained as a light yellow oil. Its molecular formula was deduced to be $C_{24}H_{16}O_7$, based on its protonated molecular ion peak at *m/z* 417.0986 $[M+H]^+$ and a sodiated molecular ion peak at *m/z* 439.0806 $[M+Na]^+$ in its positive ion HR-ESI-MS. The ^1H-NMR spectrum of compound **4** displayed splitting patterns in the aromatic region similar to that of compound **3**, suggesting they have related structures. Comparison of the ^{13}C NMR spectroscopic data of **4** with those of **3** (Table A 1) indicated that both compounds shared the same aloe-emodin-type anthraquinone skeleton, but differed in the acyl group attached to C-11. The presence of a *trans para*-hydroxycinnamate group in **4**, as opposed to the *para*-hydroxybenzoate group in **3**, was indicated by the presence of two doublets at δ_H 7.50 and 6.88 (2H each, J = 8.8 Hz) in the ^1H NMR spectrum, a set of five carbon signals at δ_C 166.7 (C-12), 159.5 (C-4'), 130.0 (C-2'/6'), 126.9 (C-1'),and 114.4 (C-3'/5') in the ^{13}C NMR spectrum, and *trans*-coupled doublet proton signals at δ_H 6.43 and 7.75 (both, 1H, J = 15.9 Hz). The latter signals corresponded by HMQC to the two methine carbon resonances at δ_C 114.4 (C-13) and 145.8 (C-14) (*20*). The two carbons of the carbon-carbon double bond in the cinnamate group were assigned to C-13 and C-14, based on the HMBC crosspeaks between H-13 and C-1', H-6' and C-14, and H-14 and C-12 (Figure A 2).

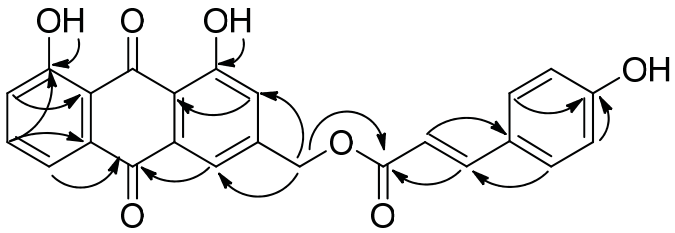

Figure A. 2 HMBC correlations of compound 4**.**

The structure of compound **4** was thus determined as (*E*)-(1,8-dihydroxy-9,10-dioxo-9,10- dihydroanthracen-3-yl)-methyl-3-(4-hydroxyphenyl) acrylate.

Biological activities and structure-activity relationships

All the isolated compounds were tested for antiproliferative activity against the A2780 ovarian cancer cell line and for antiplasmodial activity against the Dd2 chloroquine-resistant strain of *P. falciparum*. As listed in Table 2, the known dimeric compounds (**6** and **7**) displayed the highest antiplasmodial activity, with IC_{50} values of 0.4 ± 0.1 and 0.2 ± 0.1 μM, respectively. In addition, both of these dimeric compounds showed modest antiproliferative activity against the A2780 human ovarian cancer cell line, with IC_{50} values of 6 ± 1 and 4 ± 1 μM, respectively. However, their antiproliferative activity and lack of synthetic accessibility decreased their appeal as lead compounds for potential new antimalarial agents.

Table A. 2. Bioactivities of the isolated anthraquinones (1-9**).**

	Compound				
	1	**2**	**3**	**4**	**5**
Dd2 IC_{50} (μM)	58	55	26 ± 4	9 ± 1	1.1± 0.2
A2780 IC_{50} (μM)	> 60	26 ± 2	> 60	> 60	8 ± 2
	6	**7**	**8**	**9**	Artemisinin
Dd2 IC_{50} (μM)	0.4 ± 0.1	0.2 ± 0.1	10 ± 2	10 ± 2	0.007
A2780 IC_{50} (μM)	6 ± 1	4 ± 1	>60	>60	ND

For these reasons, the two modestly active new compounds (**3** and **4**, IC_{50} = 26 ± 4 and 9 ± 1 μM, respectively) were more attractive for a study of structure-activity relationships due to their low cytotoxicities (IC_{50} > 60 μM to the A2780 ovarian cancer cell line) and synthetic accessibility. Both compounds are C-11 acylated derivatives of aloe-emodin (**2**), and so a number of C-11 acylated aloe-emodin derivatives were prepared by standard methods to determine the feasibility of developing derivatives with improved antiplasmodial activity.

Antiplasmodial activity data on the isolated natural products showed that compound **4**, the *para*-hydroxy cinnamate derivative of aloe-emodin (**2**), is about six times more potent than **2**, and this compound was thus selected as the lead compound for the present SAR study. Various acyl derivatives of aloe-emodin were then prepared by reaction of the commercially available natural product aloe-emodin (**2**) with a variety of organic acids, with 1-ethyl-3-(3-dimethylaminopropyl) carbodiimide (EDCI) as the coupling reagent. The reaction products were purified by column chromatography and their structures were confirmed by ^{1}H and ^{13}C NMR spectroscopy, as well as by HR-ESI-MS. The resulting compounds and their antiplasmodial activities are listed in Table 3. All the compounds were also tested for antiproliferative activity

against A2780 cells, but none of them had IC_{50} values less than 60 μM. Inspection of the results of this study led to the following conclusions:

(i) Acetylation of the primary alcohol of aloe-emodin slightly increased antiplasmodial activity, while acetylation of the hydrogen-bonded hydroxy group had the reverse effect.

The C-11 monoacetate (**10**, IC_{50} = ~ 42 μM) displayed slightly better antiplasmodial activity than aloe-emodin (IC_{50} = ~ 55 μM), while the mixture of the C-1, C-11 and C-8, C-11 diacetates (**11**, IC_{50} = ~ 60 μM) was slightly less potent than aloe-emodin. This result suggested that the presence of the hydrogen-bonded hydroxy groups might be important for antiplasmodial activity, and so acylation of the primary alcohol (C-11) of aloe-emodin was selected as the modification of choice for investigation.

(ii) The phenyl group and the non-aromatic carbon-carbon double bond are both important functional groups for increasing the antiplasmodial activity.

To explore whether acylation of the primary alcohol might increase potency, the C-11 crotonate, benzoate, phenylpropionate and cinnamate derivatives were synthesized. Cinnamate **15** (IC_{50} = 18.4 ± 2.4 μM) displayed the highest activity among the four; benzoate **12** (IC_{50} = 31.5 ± 1.5 μM), phenylpropionate **14** (IC_{50} = ~ 36 μM), and crotonate **13**, (IC_{50} = ~ 45 μM) were all less potent. Although cinnamate **15** displayed the highest activity among all four acylated derivatives, it was only approximately half as potent as the 4-hydroxy-cinnamate **4** (kniphofione B), indicating that the hydroxy group at the C-4' of the phenyl group is a contributor to the higher activity.

(iii) The position and number of oxygenations on the phenyl group influences antiplasmodial activity.

The influence of the type of oxygenation at C-4' of the phenyl ring on antiplasmodial activity was investigated by the synthesis of 4-methoxybenzoate **16** (IC_{50} = 22 ± 2 μM), 4-methoxycinnamate **17** (IC_{50} = 5 ± 1 μM), 4-acetoxycinnamate **18** (IC_{50} = 12 ± 2 μM), and 4-acetoxybenzoate **19** (IC_{50} = 30 ± 2 μM). 4-Methoxycinnamate derivative **17** was more potent than kniphofione B (**4**) and **18**, with hydroxycinnamate and acetoxycinnamate groups, respectively. Similar results were observed for the corresponding benzoate derivatives. The methoxy group is thus important for activity and was selected as the oxygenated moiety for further study.

Compounds **22** and **23** were then synthesized to investigate the influence of the number of methoxy groups on the phenyl ring of the cinnamate on potency. The 3,4-dimethoxycinnamate **22** (IC_{50} = 1.3 ± 0.2 μM) was more potent than both the 4-methoxycinnamate **17** (IC_{50} = 5 ± 1 μM) and the 3,4,5-trimethoxy-cinnamate **23** (IC_{50} = 2.7 ± 0.4 μM), suggesting that two methoxy groups on the cinnamate provides the best potency.

Finally, to understand what effect the positions of the methoxy groups on the cinnamate phenyl ring might have, 2,3-dimethoxy-cinnamate (**26**), 2,4- dimethoxy-cinnamate (**25**), 2,5-dimethoxy-cinnamate (**27**), and 3,5-dimethoxy-cinnamate (**24**) were synthesized and evaluated. 3,4-Dimethoxy-cinnamate (**22**) was the most potent of these compounds, and a similar response was observed from 3,4-methylenedioxy-cinnamate **28** (IC_{50} = 1.9 ± 0.3 μM), suggesting that alkylation on the 3' and 4' positions of the phenyl group favorably influences antiplasmodial activity.

In summary, this SAR study showed that esterification of the primary hydroxyl group of aloe-emodin (**2**) with various carboxylic acids increased its antiplasmodial activity, with the most potent analogue being the 3,4-dimethylcaffeic acid derivative (**22**), with an IC_{50} value of 1.3 ± 0.2 μM (Table 3). This analogue displays approximately 7 and 20 times the potency of the two new natural products **3** and **4**, and over 40 times than that of aloe-emodin (**2**).

Although aloe-emodin (**2**) has previously been identified as an anticancer agent (*21, 22*), and might thus be thought to have little potential for development as an antiplasmodial agent, our bioassay data indicated that acylation of the primary alcohol of aloe-emodin resulted in the increase of antiplasmodial activity (Dd2 assay), accompanied by a decrease of antiproliferative activity (A2780 assay). As an example, acylation of the C-11 hydroxyl group of aloe-emodin to give the *p*-coumaroyl derivative **4** increases its antiplasmodial activity sixfold while decreasing its antiproliferative activity to the A2780 cell line at least twofold. This observation indicates that further modifications of the C-11 hydroxyl group of aloe-emodin have the potential to yield antiplasmodial agents with little or no antiproliferative activity.

Table A. 3. Antiplasmodial activity of natural and synthetic aloe-emodin derivatives

Cmpd	Structure	IC_{50} (μM)	Cmpd	Structure	IC_{50} (μM)
1	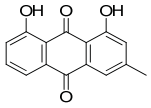	~ 58	**18**	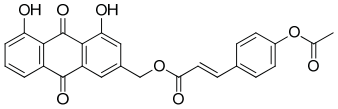	12 ± 2
2	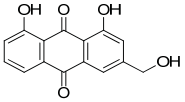	~ 55	**19**	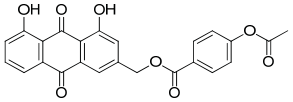	30 ± 2
3	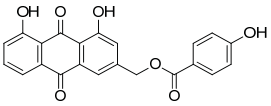	26 ± 4	**20**	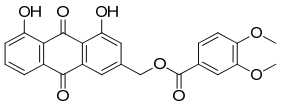	14 ± 2
4	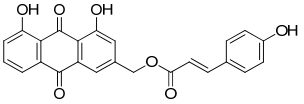	9 ± 1	**21**	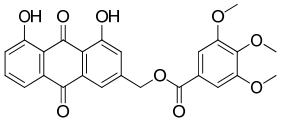	16 ± 2
10	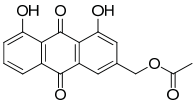	~ 42	**22**	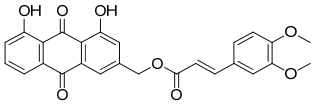	1.3 ± 0.2
11	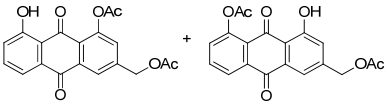	~ 60	**23**	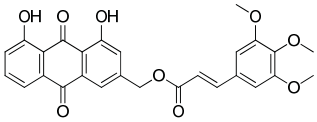	2.7 ± 0.4
12	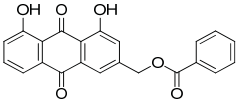	31 ± 2	**24**	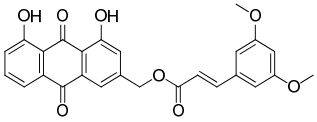	2.5 ± 0.9
13	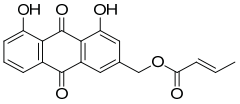	~ 45	**25**	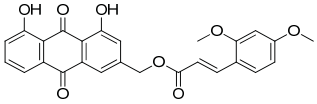	6 ± 2
14	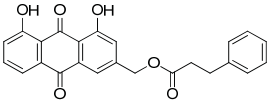	~ 36	**26**	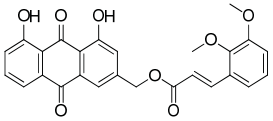	8 ± 2
15	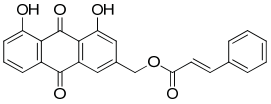	18 ± 2	**27**	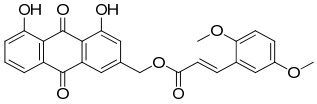	9 ± 2
16	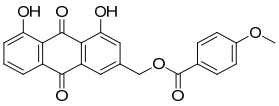	22 ± 2	**28**	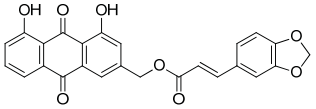	1.9 ± 0.3
17	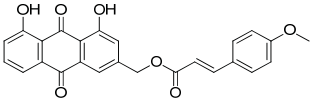	5 ± 1			

Experimental Section

General Experimental Procedures

UV and IR spectroscopic data were measured on a Shimadzu UV-1201 spectrophotometer and a MIDAC M-series FTIR spectrophotometer, respectively. NMR spectra were recorded in $CDCl_3$ on Bruker Avance 500 or 600 spectrometers. The chemical shifts are given in δ (ppm), and coupling constants (*J*) are reported in Hz. Mass spectra were obtained on an Agilent 6220 LC-TOF-MS in the positive and negative ion mode.

Antiproliferative Bioassays (A2780 assay)

Antiproliferative activities were obtained at Virginia Tech against the drug-sensitive A2780 human ovarian cancer cell line as previously described (*23*).

Antiplasmodial Bioassays (Dd2 assay)

The effect of each fraction and pure compound on parasite growth of the *P. falciparum* Dd2 strain was measured in a 72 h growth assay in the presence of drug as described previously with minor modifications (*24-26*). Briefly, ring stage parasite cultures (200 μL per well, with 1% hematocrit and 1% parasitemia) were then grown for 72 h in the presence of increasing concentrations of the drug in a 5.05% CO_2, 4.93% O_2, and 90.2% N_2 gas mixture at 37 °C. After 72 h in culture, parasite viability was determined by DNA quantitation using SYBR Green I (50 μL of SYBR Green I in lysis buffer at 0.4 μL of SYBR Green I/mL of lysis buffer). The half-maximum inhibitory concentration (IC_{50}) calculation was performed with GraFit software using nonlinear regression curve fitting. IC_{50} values are the average of three independent determinations with each determination in duplicate and are expressed ± SEM.

Plant Material

Plant collection of *K. ensifolia* Baker (Asphodelaceae) was made in April 1999 on top of Mariepskop in the Pilgrims Rest district, State of Mpumalanga, South Africa, by Prof. P. C. Zietsman under the auspices of the New York Botanical Garden, accession number Z03796a. A voucher specimen is deposited in the New York Botanical Garden and also at BLFU (Bloemfontein Free University, South Africa).

Extraction and Isolation

The dried and powdered whole plant (100 g) of *Kniphofia ensifolia* was exhaustively extracted with EtOH (2 × 1 L) in two 24-hour percolation steps; successive partition of the concentrated extract with hexanes and CH_2Cl_2 gave an active CH_2Cl_2 fraction. A 0.75 g sample of the original EtOH extract, designated 60031-9D, was shipped to Virginia Tech for bioassay-guided isolation. A 0.60 g portion of this sample (IC_{50} = ~ 6.0 μg/mL against *P. falciparum* strain Dd2) was suspended in aqueous MeOH (MeOH-H_2O 9:1, 100 mL), and extracted with hexanes (3 × 100 mL). The aqueous layer was diluted to 60% MeOH (v/v) with H_2O and extracted with CH_2Cl_2 (3 × 150 mL). The hexanes fraction was evaporated in vacuo to leave 107.7 mg of material with an IC_{50} value of 5 ~ 10 μg/mL. The residue from the CH_2Cl_2 fraction (20.7 mg) was the most active fraction with an IC_{50} value of 2.5 ~ 5 μg/mL. The remaining aqueous MeOH fraction had an IC_{50} value of greater than 10 μg/mL. The hexanes and CH_2Cl_2 fractions were combined due to the similarity of their TLC patterns.

The combined hexanes and CH_2Cl_2 fractions were divided into five fractions by Sephadex LH-20 size exclusion open column chromatography. The most active fraction (F4, 28.6 mg) had an IC_{50} value of 2.5 μg/mL. Fraction F4 was then applied to a silica gel column eluted with hexanes: EtOAc = 7:3 to give six fractions. Fraction 4-1 was evaporated to give compound **1** (0.3 mg, IC_{50} = ~ 58 μM) and fractions 4-5 were evaporated to give compound **5** (2.6 mg, IC_{50} = 1.1 ± 0.2 μM). The most active fraction 4-2 (1.8 mg, IC_{50} = 0.27 μg/mL), was subjected to HPLC on a C_{18} column using a MeCN and H_2O gradient as the solvent system to yield the four known active compounds **6** (0.3 mg, IC_{50} = 0.43 ± 0.14 μM), **7** (0.9 mg, IC_{50} = 0.20 ± 0.08 μM), **8** (0.3 mg, IC_{50} = 10.2 ± 1.6 μM) and **9** (0.3 mg, IC_{50} = 9.6 ± 1.8 μM), with retention times of 21.3, 26.0, 28.5 and 31.2 min, respectively. HPLC of fraction 4-3 (2.2 mg, IC_{50} = 4.3 μg/mL) on a C_{18} column gave compounds **2** (0.5 mg, IC_{50} = ~ 55 μM) **3** (0.7 mg, IC_{50} = 25.6 ± 3.6 μM) and **4** (1.0 mg, IC_{50} = 8.9 ± 1.2 μM), with retention times of 8.5, 18.0 and 21.2 min, respectively.

(1,8-dihydroxy-9,10-dioxo-9,10-dihydroanthracen-3-yl)methyl-4-hydroxybenzoate (3, kniphofione A):

Yellow-orange powder. UV (MeOH) λ_{max} (ε) 257 (1.6), 289 (0.5), 432 (0.5); IR ν_{max} cm^{-1}: 3390, 2915, 2343, 1673, 1621, 1450, 1277, 1110 cm^{-1}; ^1H NMR (600 MHz, $CDCl_3$), and ^{13}C

NMR (150 MHz, $CDCl_3$), see Table 1; HR-ESI-MS *m/z* 389.0688 $[M-H]^-$ (calcd for $C_{22}H_{13}O_7$, 389.0667).

(*E*)-(1,8-dihydroxy-9,10-dioxo-9,10-dihydroanthracen-3-yl)methyl-3-(4-hydroxyphenyl) acrylate (4, kniphofione B):

Yellow-orange powder. UV (MeOH) λ_{max} (ε) 259 (1.2), 289 (1.4), 310 (0.9), 433 (0.6); IR ν_{max} cm^{-1}: 3390, 2916, 2362, 1706, 1627, 1603, 1450, 1268, 1161 cm^{-1}; ^1H NMR (600 MHz, $CDCl_3$), and ^{13}C NMR (150 MHz, $CDCl_3$), see Table 1; HR-ESI-MS *m/z* 439.0806 $[M+Na]^+$ (calcd for $C_{24}H_{16}NaO_7$, 439.0788) and 417.0986 $[M+H]^+$ (calcd for $C_{24}H_{17}O_7$, 417.0969).

General procedure for synthesis of ester derivatives of aloe-emodin (*27*)

Substituted benzoic acids or cinnamic acids (0.1 mmol) in dry CH_2Cl_2 (0.2 mL) were treated with 1-ethyl-3-(3-dimethylaminopropyl) carbodiimide (EDCI, 20.6 mg, 0.1 mmol) and DMAP (1.0 mg, 0.006 mmol). The mixtures were stirred at room temperature for 5 minutes. Aloe-emodin (**2**, 5.4 mg, 0.02 mmol) was added, and stirring was continued at room temperature until the starting compound was consumed. The resulting solution was diluted with EtOAc (10 mL) and concentrated on a rotary evaporator. The final benzoate and cinnamate derivatives of aloe-emodin were purified by using preparative TLC (silica gel, 500 m; hexane/EtOAc, 4:1).

(1,8-dihydroxy-9,10-dioxo-9,10-dihydroanthracen-3-yl)methyl acetate (10):

Yellow-orange powder; HR-ESI-MS *m/z* 313.0711 $[M+H]^+$ (calcd for $C_{17}H_{13}O_6$, 313.0707); ^1H NMR (500 MHz, $CDCl_3$) δ_H 12.01 (s, 1H), 11.98 (s, 1H), 7.78 (dd, *J* = 7.5, 1.1 Hz, 1H), 7.72 (d, *J* = 1.6 Hz, 1H), 7.63 (dd, *J* = 8.2, 7.6 Hz, 1H), 7.25 (dd, *J* = 8.4, 1.1 Hz, 1H), 7.20 (d, *J* = 1.6 Hz, 1H), 5.12 (s, 2H), 2.12 (s, 3H); ^{13}C NMR (126 MHz, $CDCl_3$) δ_C 192.7, 181.5, 170.5, 162.8, 162.6, 146.4, 137.3, 133.9, 133.51, 124.8, 122.4, 120.2, 118.5, 115.8, 115.3, 64.7, 20.8.

Mixture of (1-acetoxy-8-hydroxy-9,10-dioxo-9,10-dihydroanthracen-3-yl)methyl acetate and (8-acetoxy-1-hydroxy-9,10-dioxo-9,10-dihydroanthracen-3-yl)methyl acetate (11):

Yellow-orange powder; HR-ESI-MS *m/z* 355.0815 $[M+H]^+$ (calcd for $C_{19}H_{15}O_7$, 355.0812); ^1H NMR (500 MHz, $CDCl_3$) δ_H 12.57 (s, 1H), 12.55 (s, 1H), 8.28 (dd, *J* = 7.8, 1.3

Hz, 1H), 8.22 (d, *J* = 1.0 Hz, 1H), 7.82 (dd, *J* = 8.0, 7.9 Hz, 1H), 7.81 (dd, *J* = 7.5, 1.2 Hz, 1H), 7.75(d, *J* = 1.6 Hz, 1H), 7.66 (dd, *J* = 8.3, 7.6 Hz, 1H), 7.43 (dd, *J* = 8.0, 1.3 Hz, 1H), 7.40 (d, *J* = 1.8 Hz, 1H), 7.26 (d, *J* =1.0 Hz, 1H), 5.24 (s, 2H), 5.17 (s, 2H), 2.48 (s, 3H), 2.48 (s, 3H), 2.19 (s, 3H), 2.18 (s, 3H).

(1,8-dihydroxy-9,10-dioxo-9,10-dihydroanthracen-3-yl)methyl benzoate (12):

Yellow-orange powder; HR-ESI-MS *m/z* 375.0866 $[M+H]^+$ (calcd for $C_{22}H_{15}O_6$, 375.0863); ^{1}H NMR (500 MHz, $CDCl_3$) δ_H 12.11 (s, 1H), 12.06 (s, 1H), 8.12 (dd, *J* = 8.4, 1.3 Hz, 2H), 7.89 (d, *J* = 1.6 Hz, 1H), 7.85 (dd, *J* = 7.5, 1.1 Hz, 1H), 7.71 (dd, *J* = 8.2, 7.6 Hz, 1H), 7.61 (tt, *J* = 7.5, 1.3 Hz, 1H), 7.49 (t, *J* = 7.8, 2H), 7.32 (dd, *J* = 8.4, 1.0 Hz, 1H),, 5.46 (s, 2H); ^{13}C NMR (125 MHz, $CDCl_3$) δ_C 192.7, 181.5, 166.0, 162.8, 162.6, 146.6, 137.3, 133.9, 133.8, 133.5, 130.1, 129.8, 128.6, 124.8, 122.4, 120.2, 118.5, 115.8, 115.3, 65.1.

(*E*)-(1,8-dihydroxy-9,10-dioxo-9,10-dihydroanthracen-3-yl)methyl-but-2-enoate (13):

Yellow-orange powder; HR-ESI-MS *m/z* 339.0865 $[M+H]^+$ (calcd for $C_{19}H_{15}O_6$, 339.0863); ^{1}H NMR (500 MHz, $CDCl_3$) δ_H 12.09 (s, 1H), 12.07 (s, 1H), 7.85 (dd, *J* = 7.6, 1.1 Hz, 1H), 7.80 (d, *J* = 1.6 Hz, 1H), 7.70 (dd, *J* = 8.2, 7.8 Hz, 1H), 7.32 (dd, *J* = 8.4, 1.1 Hz, 1H), 7.29 (d, *J* = 1.6 Hz, 1H), 7.10 (dd, *J* = 15.5, 7.0 Hz, 1H), 5.96 (dd, *J* = 15.6, 1.6 Hz, 1H), 1.94 (dd, *J* = 6.9, 1.6 Hz, 3H); ^{13}C NMR (125 MHz, $CDCl_3$) δ_C 192.7, 181.6, 166.4, 162.8, 162.6, 146.8, 146.4, 137.3, 133.8, 133.6, 124.8, 122.3, 121.9, 120.2, 118.4, 115.8, 115.2, 64.4, 18.2.

(1,8-dihydroxy-9,10-dioxo-9,10-dihydroanthracen-3-yl)methyl-3-phenylpropanoate (14):

Yellow-orange powder; HR-ESI-MS *m/z* 403.1146 $[M+H]^+$ (calcd for $C_{24}H_{19}O_6$, 403.1176); ^{1}H NMR (500 MHz, $CDCl_3$) δ_H 12.07 (s, 1H), 12.06 (s, 1H), 7.85 (dd, *J* = 7.6, 1.1 Hz, 1H), 7.76 (d, *J* = 1.6 Hz, 1H), 7.70 (dd, *J* = 8.3, 7.8 Hz, 1H), 7.32 (dd, *J* = 8.4, 1.1 Hz, 1H), 7.29 (d, *J* = 1.6 Hz, 1H), 7.28 (m, 2H), 7.21 (m, 3H), 5.18 (s, 2H), 3.01 (d, *J* = 7.8 Hz, 2H), 2.77 (d, *J* = 7.8 Hz, 2H); ^{13}C NMR (125 MHz, $CDCl_3$) δ_C 192.7, 181.5, 172.4, 162.8, 162.6, 146.4, 140.1, 137.3, 133.9, 133.5, 128.6, 128.3, 126.4, 124.8, 122.5, 120.2, 118.6, 115.8, 115.3, 64.7, 35.7, 30.9.

(1,8-dihydroxy-9,10-dioxo-9,10-dihydroanthracen-3-yl)methyl cinnamate (15):

Yellow-orange powder; HR-ESI-MS *m/z* 401.1031 $[M+H]^+$ (calcd for $C_{24}H_{17}O_6$, 401.1020); ^{1}H NMR (500 MHz, $CDCl_3$) δ_H 12.03 (s, 1H), 12.00 (s, 1H), 7.79 (dd, *J* = 7.5, 1.1

Hz, 1H), 7.79 (d, *J* = 1.6 Hz, 1H), 7.73 (d, *J* = 16.0 Hz, 1H), 7.64 (dd, *J* = 8.3, 7.6 Hz, 1H), 7.50 (m, 2H), 7.35 (m, 3H), 7.27 (d, *J* = 1.6 Hz, 1H), 7.25 (dd, *J* = 8.4, 1.1 Hz, 1H), 6.48 (d, *J* = 16.0 Hz, 1H), 5.27 (s, 2H); ^{13}C NMR (125 MHz, $CDCl_3$) δ_C 192.7, 181.6, 166.4, 162.8, 162.6, 146.7, 146.2, 137.3, 134.1, 133.9, 133.6, 130.6, 129.0, 128.3, 124.8, 122.4, 120.2, 118.6, 117.0, 115.4, 115.3, 64.7.

(1,8-dihydroxy-9,10-dioxo-9,10-dihydroanthracen-3-yl)methyl-4-methoxybenzoate (16):

Yellow-orange powder; HR-ESI-MS *m/z* 405.0971 $[M+H]^+$ (calcd for $C_{23}H_{17}O_7$, 405.0969); ^{1}H NMR (500 MHz, $CDCl_3$) δ_H 12.10 (s, 1H), 12.07 (s, 1H), 8.08 (d, *J* = 8.9 Hz, 2H), 7.88 (d, *J* = 1.5 Hz, 1H), 7.85 (dd, *J* = 7.5, 1.0 Hz, 1H), 7.70 (dd, *J* = 8.1, 7.8 Hz, 1H), 7.37 (d, *J* = 1.5 Hz, 1H), 7.32 (dd, *J* = 8.4, 1.0 Hz, 1H), 6.96 (d, *J* = 8.9 Hz, 2H), 5.42 (s, 2H), 3.88 (s, 3H); ^{13}C NMR (125 MHz, $CDCl_3$) δ_C 192.7, 181.6, 165.7, 164. 9, 162.8, 162.6, 146.9, 137.3, 134.1, 133.6, 131.9, 124.8, 122.3, 121.7, 120.2, 118.5, 115.8, 115.3, 113.8, 64.8, 55.5.

(*E*)-(1,8-dihydroxy-9,10-dioxo-9,10-dihydroanthracen-3-yl)methyl-3-(4-methoxyphenyl) acrylate (17):

Yellow-orange powder; HR-ESI-MS *m/z* 431.1133 $[M+H]^+$ (calcd for $C_{25}H_{19}O_7$, 431.1125); ^{1}H NMR (500 MHz, $CDCl_3$) δ_H 12.02 (s, 1H), 12.00 (s, 1H), 7.79 (dd, *J* = 7.4, 1.1 Hz, 1H), 7.78 (d, *J* = 1.6 Hz, 1H), 7.68 (d, *J* = 16.0 Hz, 1H), 7.63 (dd, *J* = 8.3, 7.7 Hz, 1H), 7.45 (d, *J* = 8.8 Hz, 2H), 7.27 (d, *J* = 1.6 Hz, 1H), 7.25 (dd, *J* = 8.4, 1.1 Hz, 1H), 6.86 (d, *J* = 8.8 Hz, 2H), 6.34 (d, *J* = 16.0 Hz, 1H), 5.26 (s, 2H), 3.78 (s, 3H); ^{13}C NMR (125 MHz, $CDCl_3$) δ_C 192.7, 181.6, 166.7, 162.8, 161.7, 159.8, 146.9, 145.8, 137.3, 133.9, 133.6, 130.0, 126.9, 124.8, 122.4, 120.2, 118.5, 118.2, 115.8, 115.3, 114.4, 64.6, 55.5.

(*E*)-(1,8-dihydroxy-9,10-dioxo-9,10-dihydroanthracen-3-yl)methyl -3-(4-acetoxy phenyl)acrylate (18):

Yellow-orange powder; HR-ESI-MS *m/z* 459.1079 $[M+H]^+$ (calcd for $C_{26}H_{19}O_8$, 459.1074); ^{1}H NMR (600 MHz, $CDCl_3$) δ_H 12.09 (s, 1H), 12.06 (s, 1H), 7.86 (dd, *J* = 7.4, 1.1 Hz, 1H), 7.85 (d, *J* = 1.6 Hz, 1H), 7.76 (d, *J* = 16.0 Hz, 1H), 7.70 (dd, *J* = 8.3, 7.7 Hz, 1H), 7.58

(d, J = 8.7 Hz, 2H), 7.35 (d, J = 1.6 Hz, 1H), 7.32 (dd, J = 8.4, 1.1 Hz, 1H), 7.15 (d, J = 8.6 Hz, 2H), 6.50 (d, J = 16.0 Hz, 1H), 5.33 (s, 2H), 2.32 (s, 3H); ^{13}C NMR (150 MHz, $CDCl_3$) δ_C 192.8, 181.6, 169.2, 166.3, 162.9, 162.7, 152.5, 146.7, 145.1, 137.4, 134.0, 133.7, 132.0, 129.5, 124.9, 122.6, 122.3, 120.3, 118.7, 117.3, 115.9, 115.4, 64.9, 21.2.

(1,8-dihydroxy-9,10-dioxo-9,10-dihydroanthracen-3-yl)methyl 4-acetoxybenzoate (19):

Yellow-orange powder; HR-ESI-MS *m/z* 433.0935 $[M+H]^+$ (calcd for $C_{24}H_{17}O_8$, 433.0918); ^{1}H NMR (600 MHz, $CDCl_3$) δ_H 12.09 (s, 1H), 12.05 (s, 1H), 8.15 (d, J = 8.9 Hz, 2H), 7.87 (d, J = 1.6 Hz, 1H), 7.85 (dd, J = 7.5, 1.0 Hz, 1H), 7.70 (dd, J = 8.1, 7.8 Hz, 1H), 7.36 (d, J = 1.6 Hz, 1H), 7.32 (dd, J = 8.4, 1.0 Hz, 1H), 7.22 (d, J = 8.9 Hz, 2H), 5.44 (s, 2H), 2.33 (s, 3H); ^{13}C NMR (150 MHz, $CDCl_3$) δ_C 192.7, 181.6, 167.7, 164.3, 162.8, 162.6, 158.4, 143.5, 137.4, 134.1, 133.5, 131.5, 127.0, 124.9, 122.5, 121.9, 120.3, 118.6, 115.7, 115.3, 65.3, 21.3.

(1,8-dihydroxy-9,10-dioxo-9,10-dihydroanthracen-3-yl)methyl 3,4-dimethoxybenzoate (20):

Yellow-orange powder; HR-ESI-MS *m/z* 435.1084 $[M+H]^+$ (calcd for $C_{24}H_{19}O_8$, 435.1074); ^{1}H NMR (500 MHz, $CDCl_3$) δ_H 12.10 (s, 1H), 12.06 (s, 1H), 7.89 (d, J = 1.6 Hz, 1H), 7.85 (dd, J = 7.5, 1.1 Hz, 1H), 7.78 (dd, J = 8.4, 2.0 Hz, 1H), 7.77 (dd, J = 8.2, 7.8 Hz, 1H), 7.60 (d, J = 2.0 Hz, 1H), 7.36 (d, J = 1.6 Hz, 1H), 7.32 (dd, J = 8.4, 1.1 Hz, 1H), 6.93 (d, J = 8.5 Hz, 1H), 5.43 (s, 2H), 3.96 (s, 6H) ^{13}C NMR (125 MHz, $CDCl_3$) δ_C 192.7, 181.6, 165.8, 162.8, 162.6, 153.4, 148.8, 146.9, 137.3, 133.91, 133.5, 124.8, 124.0, 122.4, 121.8, 120.2, 118.5, 115.8, 115.3, 112.1, 110.4, 65.0, 56.1.

(1,8-dihydroxy-9,10-dioxo-9,10-dihydroanthracen-3-yl)methyl-3,4,5-trimethoxybenzo ate (21):

Yellow-orange powder; HR-ESI-MS *m/z* 465.1187 $[M+H]^+$ (calcd for $C_{25}H_{21}O_9$, 465.1180); ^{1}H NMR (500 MHz, $CDCl_3$) δ_H 12.09 (s, 1H), 12.05 (s, 1H), 7.89 (d, J = 1.6 Hz, 1H), 7.85 (dd, J = 7.5, 1.1 Hz, 1H), 7.70 (dd, J = 8.2, 7.7 Hz, 1H), 7.35 (s, 2H), 7.33 (d, J = 1.6 Hz, 1H), 7.32 (dd, J = 8.4, 1.1 Hz, 1H), 5.44 (s, 2H), 3.93 (s, 9H); ^{13}C NMR (125 MHz, $CDCl_3$) δ_C 192.7, 181.5, 165.7, 162.8, 162.6, 159.8, 153.1, 146.6, 137.4, 134.0, 133.5, 124.8, 124.3, 122.5, 120.2, 118.5, 115.8, 115.4, 107.1, 65.2, 61.0, 56.3.

(*E*)-(1,8-dihydroxy-9,10-dioxo-9,10-dihydroanthracen-3-yl)methyl-3-(3,4-dimethoxy phenyl)acrylate (22):

Yellow-orange powder; HR-ESI-MS *m/z* 461.1245 $[M+H]^+$ (calcd for $C_{26}H_{21}O_8$, 461.1231); ^{1}H NMR (500 MHz, $CDCl_3$) δ_H 12.02 (s, 1H), 11.99 (s, 1H), 7.78 (d, *J* = 1.6 Hz, 1H), 7.78 (dd, *J* = 7.6, 1.1 Hz, 1H), 7.66 (d, *J* = 15.9 Hz, 1H), 7.63 (dd, *J* = 8.3, 7.6 Hz, 1H), 7.27 (d, *J* = 1.6 Hz, 1H), 7.25 (dd, *J* = 8.4, 1.1 Hz, 1H), 7.07 (dd, *J* = 8.3, 1.9 Hz, 1H), 7.02 (d, *J* = 1.9 Hz, 1H), 6.82 (d, *J* = 8.3 Hz, 1H), 6.35 (d, *J* = 15.9 Hz, 1H), 5.26 (s, 2H), 3.87 (s, 3H), 3.86 (s, 3H). ^{13}C NMR (125 MHz, $CDCl_3$) δ_C 192.7, 181.7, 166.7, 162.8, 162.7, 151.4, 149.3, 146.9, 146.1, 137.3, 133.9, 133.6, 127.1, 124.8, 123.0, 122.4, 120.2, 118.5, 115.8, 115.3, 114.6, 111.0, 109.6, 64.6, 56.0, 55.9.

(*E*)-(1,8-dihydroxy-9,10-dioxo-9,10-dihydroanthracen-3-yl)methyl-3-(3,4,5-trimethoxy phenyl)acrylate (23):

Yellow-orange powder; HR-ESI-MS *m/z* 491.1352 $[M+H]^+$ (calcd for $C_{27}H_{23}O_9$, 491.1337);. ^{1}H NMR (500 MHz, $CDCl_3$) δ_H 12.04 (s, 1H), 11.99 (s, 1H), 7.80 (d, *J* = 1.6 Hz, 1H), 7.79 (dd, *J* = 7.6, 1.1 Hz, 1H), 7.64 (dd, *J* = 8.3, 7.6 Hz, 1H), 7.63 (d, *J* = 15.9 Hz, 1H), 7.28 (d, *J* = 1.6 Hz, 1H), 7.26 (dd, *J* = 8.4, 1.1 Hz, 1H), 6.73 (s, 2H), 6.39 (d, *J* = 15.9 Hz, 1H), 5.27 (s, 2H), 3.84 (s, 6H), 3.83 (s, 3H); ^{13}C NMR (125 MHz, $CDCl_3$) δ_C 192.7, 181.6, 166.3, 162.8, 162.6, 153.5, 146.7, 146.1, 140.4, 137.3, 133.9, 133.5, 129.6, 124.8, 122.4, 120.2, 118.5, 116.2, 115.8, 115.3, 105.4, 64.7, 61.0, 56.2.

(*E*)-(1,8-dihydroxy-9,10-dioxo-9,10-dihydroanthracen-3-yl)methyl-3-(3,5-dimethoxy phenyl)acrylate (24):

Yellow-orange powder; HR-ESI-MS *m/z* 461.1224 $[M+H]^+$ (calcd for $C_{26}H_{21}O_8$, 461.1231); ^{1}H NMR (600 MHz, $CDCl_3$) δ_H 12.09 (s, 1H), 12.06 (s, 1H), 7.86 (dd, *J* = 7.6, 1.1 Hz, 1H), 7.85 (d, *J* = 1.6 Hz, 1H), 7.70 (dd, *J* = 8.3, 7.6 Hz, 1H), 7.70 (d, *J* = 15.9 Hz, 1H), 7.33 (d, *J* = 1.6 Hz, 1H), 7.32(dd, *J* = 8.4, 1.1 Hz, 1H), 6.70 (d, *J* = 2.2 Hz, 2H), 6.52 (t, *J* = 2.3 Hz, 1H), 6.51(d, *J* = 15.9 Hz, 1H), 5.33 (s, 2H), 3.83 (s, 6H); ^{13}C NMR (150 MHz, $CDCl_3$) δ_C 192.8, 181.7, 166.4, 162.7, 161.2, 146.8, 146.3, 137.5, 136.1, 134.1, 133.7, 124.9, 122.6, 120.3, 118.7, 117.7, 116.0, 115.5, 106.2, 103.2, 77.2, 64.9, 55.5.

(*E*)-(1,8-dihydroxy-9,10-dioxo-9,10-dihydroanthracen-3-yl)methyl-3-(2,4-dimethoxy phenyl)acrylate (25):

Yellow-orange powder; HR-ESI-MS *m/z* 461.1212 $[M+H]^+$ (calcd for $C_{26}H_{21}O_8$, 461.1231); ^{1}H NMR (600 MHz, $CDCl_3$) δ_H 12.08 (s, 1H), 12.07 (s, 1H), 8.01 (d, *J* = 16.1 Hz, 1H), 7.85 (dd, *J* = 7.7, 1.1 Hz, 1H), 7.85 (d, *J* = 1.6 Hz, 1H), 7.70 (dd, *J* = 8.2, 7.7 Hz, 1H), 7.47 (d, *J* = 8.6 Hz, 1H), 7.34 (d, *J* = 2.3 Hz, 1H), 7.32 (dd, *J* = 8.4, 1.1 Hz, 1H), 6.54 (d, *J* = 16.1 Hz, 1H), 6.53, 6.53, 6.52 (dd, *J* = 8.6, 2.3 Hz, 1H), 6.47 (d, *J* = 2.3 Hz, 1H), 5.32 (s, 2H), 3.89 (s, 3H), 3.85 (s, 3H); ^{13}C NMR (150 MHz, $CDCl_3$) δ_C 192.7, 181.6, 167.3, 163.0, 162.6, 160.1, 147.2, 146.8, 141.6, 137.2, 133.8, 133.6, 130.9, 124.7, 122.4, 120.1, 118.6, 118.3, 116.4, 115.9, 114.8, 105.3, 98.5, 64.4, 55.5.

(*E*)-(1,8-dihydroxy-9,10-dioxo-9,10-dihydroanthracen-3-yl)methyl-3-(2,3-dimethoxy phenyl)acrylate (26):

Yellow-orange powder; HR-ESI-MS *m/z* 461.1242 $[M+H]^+$ (calcd for $C_{26}H_{21}O_8$, 461.1231);. ^{1}H NMR (600MHz, $CDCl_3$) δ_H 12.08 (s, 1H), 12.06 (s, 1H), 8.12 (d, *J* = 16.2 Hz, 1H), 7.86 (d, *J* = 1.6 Hz, 1H), 7.85 (dd, *J* = 7.4, 1.1 Hz, 1H), 7.70 (dd, *J* = 8.3, 7.6 Hz, 1H), 7.34 (d, *J* = 1.6 Hz, 1H), 7.32 (dd, *J* = 8.4, 1.1 Hz, 1H), 7.20 (dd, *J* = 7.9, 1.2 Hz, 1H), 7.08 (t, *J* = 8.0 Hz, 1H), 6.97 (dd, *J* = 8.1, 1.3 Hz, 1H), 6.59 (d, *J* = 16.2 Hz, 1H), 5.34 (s, 2H), 3.89 (s, 6H); ^{13}C NMR (150 MHz, $CDCl_3$) δ_C 192.7, 181.5, 166.6, 162.8, 162.6, 153.2, 148.7, 146.8, 141.0, 137.3, 133.9, 133.6, 128.3, 124.7, 124.2, 122.4, 120.2, 119.4, 118.5, 118.3, 115.8, 115.3, 114.3, 64.7, 61.4.

(*E*)-(1,8-dihydroxy-9,10-dioxo-9,10-dihydroanthracen-3-yl)methyl-3-(2,5-dimethoxy phenyl)acrylate (27):

Yellow-orange powder; HR-ESI-MS *m/z* 461.1211 $[M+H]^+$ (calcd for $C_{26}H_{21}O_8$, 461.1231); ^{1}H NMR (600 MHz, $CDCl_3$) δ 12.07 (s, 1H), 12.06 (s, 1H), 8.07 (d, *J* = 16.1 Hz, 1H), 7.86 (d, *J* = 1.6 Hz, 1H), 7.85 (dd, *J* = 7.4, 1.1 Hz, 1H), 7.70 (dd, *J* = 8.3, 7.6 Hz, 1H), 7.34 (d, *J* = 1.6 Hz, 1H), 7.32 (dd, *J* = 8.4, 1.1 Hz, 1H), 7.07 (d, *J* = 3.0 Hz, 1H), 6.93 (dd, *J* = 9.0, 3.0 Hz, 1H), 6.87 (d, *J* = 9.0 Hz, 1H), 6.62 (d, *J* = 16.1 Hz, 1H), 5.33 (s, 2H), 3.86 (s, 3H), 3.81 (s, 3H); ^{13}C NMR (150 MHz, $CDCl_3$) δ_C 192.8, 181.7, 166.9, 163.0, 162.7, 153.7, 153.2, 147.1, 141.6,

137.4, 134.1, 133.7, 124.9, 123.8, 122.6, 120.3, 118.7, 117.8, 116.0, 115.4, 113.5, 112.7, 77.2, 64.8, 56.2.

(*E*)-(1,8-dihydroxy-9,10-dioxo-9,10-dihydroanthracen-3-yl)methy-3-(3,4-methylene dioxyphenyl)acrylate (28):

Yellow-orange powder; HR-ESI-MS *m/z* 445.0912 $[M+H]^+$ (calcd for $C_{25}H_{17}O_8$, 445.0918); H NMR (500 MHz, $CDCl_3$) H NMR (500 MHz, $CDCl_3$) δ_H 12.09 (s, 1H), 12.07 (s, 1H), 7.86 (d, J = 1.6 Hz, 1H), 7.85 (dd, J = 7.4, 1.1 Hz, 1H), 7.70 (dd, J = 8.3, 7.6 Hz, 1H), 7.69 (d, J = 15.9 Hz, 1H), 7.33 (d, J = 1.6 Hz, 1H), 7.32 (dd, J = 8.4, 1.1 Hz, 1H), 7.07 (d, J = 1.7 Hz, 1H), 7.04 (dd, J = 8.0, 1.7 Hz, 1H), 6.83 (d, J = 8.0 Hz, 1H), 6.37 (d, J = 15.9 Hz, 1H), 6.02 (s, 2H), 5.32 (s, 2H); ^{13}C NMR (125 MHz, $CDCl_3$) δ_C 192.8, 181.7, 166.7, 163.0, 162.8, 150.1, 148.6, 147.0, 141.6, 137.5, 134.0, 133.7, 128.7, 125.0, 124.9, 122.6, 120.3, 118.7, 116.0, 115.4, 115.1, 108.8, 106.8, 101.8, 64.8.

Notes

The authors declare that there are no competing financial interest.

Acknowledgments

This project was supported by the National Center for Complementary and Alternative Medicine under award 3U01TW000313-19S1 as a supplement to Cooperative Agreement U01 TW000313-19 from the Fogarty International Center, the National Cancer Institute, the National Science Foundation, the National Heart, Lung and Blood Institute, the National Institute of Mental Health, the Office of Dietary Supplements, and the Office of the Director of NIH, with the International Cooperative Biodiversity Groups. This work was also supported by The Jeffress Memorial Trust of Virginia (J-1058). These supports are gratefully acknowledged. This work was also supported by the National Science Foundation under Grant no. CHE-0619382 for purchase of the Bruker Avance 500 NMR spectrometer and Grant no. CHE-0722638 for the purchase of the Agilent 6220 mass spectrometer. We thank Mr. Bill Bebout for obtaining the mass spectra. We gratefully acknowledge Dr. Dennis Stevenson and Daniel Atha of the New York Botanical Garden and Dr. P. C. Zietsman of the National Museum (Bloemfontein, South Africa) for the provision of plant material. J.D.B. is a recipient of a scholarship from the National Science Foundation S-STEM project (DUE-0850198).

References

1. WHO, *World Malaria Report 2012*. (World Health Organization, Geneva, Switzerland, 2012).
2. E. F. Boudreau, L. W. Pang, S. Chaikummao, C. Witayarut, Comparison of mefloquine, chloroquine plus pyrimethamine-sulfadoxine (Fansidar), and chloroquine as malarial prophylaxis in eastern Thailand. *Southeast Asian J. Trop. Med. Public Health* **22**, 183-189 (1991).
3. A. Bhattarai, A. S. Ali, S. P. Kachur, A. Mårtensson, A. K. Abbas, R. Khatib, A.-W. Al-Mafazy, M. Ramsan, G. Rotllant, J. F. Gerstenmaier, F. Molteni, S. Abdulla, S. M. Montgomery, A. Kaneko, A. Björkman, Impact of Artemisinin-Based Combination Therapy and Insecticide-Treated Nets on Malaria Burden in Zanzibar. *PLoS Med* **4**, e309 (2007).
4. A. M. Dondorp, R. M. Fairhurst, L. Slutsker, J. R. MacArthur, J. G. Breman, P. J. Guerin, T. E. Wellems, P. Ringwald, R. D. Newman, C. V. Plowe, The threat of artemisinin-resistant malaria. *N. Engl. J. Med.* **365**, 1073 (2011).
5. L. Jarvis, Marketing Mother Nature's Molecules. *Chem. Eng. News* **90 (8)**, 30 (2012).
6. Y. Dai, L. Harinantenaina, P. J. Brodie, M. Goetz, Y. Shen, K. TenDyke, D. G. I. Kingston, Antiproliferative Homoisoflavonoids and Bufatrienolides from Urginea depressa. *J. Nat. Prod.*, (2013).
7. V. R. Clark, N. P. Barker, L. Mucina, The Sneeuberg: A new centre of floristic endemism on the Great Escarpment, South Africa. *S. Afr. J. Bot.* **75**, 196-238 (2009).
8. M. W. Chase, A. Y. De Bruijn, A. V. Cox, G. Reeves, P. J. Rudall, M. A. T. Johnson, L. E. Eguiarte, Phylogenetics of Asphodelaceae (Asparagales): An Analysis of Plastid rbcL and trnL-F DNA Sequences. *Ann. Bot. (Oxford, U. K.)* **86**, 935-951 (2000).
9. S. Habtemariam, Knipholone anthrone from *Kniphofia foliosa* induces a rapid onset of necrotic cell death in cancer cells. *Fitoterapia* **81**, 1013-1019 (2010).
10. A. A. Wube, F. Bucar, K. Asres, S. Gibbons, L. Rattray, S. L. Croft, Antimalarial compounds from *Kniphofia foliosa* roots. *Phytother. Res.* **19**, 472-476 (2005).
11. T. Blitzke, A. Porzel, M. Masaoud, J. Schmidt, A chlorinated amide and piperidine alkaloids from Aloe sabaea. *Phytochemistry* **55**, 979-982 (2000).

12. K. García-Sosa, N. Villarreal-Alvarez, P. Lübben, L. M. Peña-Rodríguez, Chrysophanol, an Antimicrobial Anthraquinone from the Root Extract of *Colubrina greggii*. *J. Mex. Chem. Soc.* **50**, 76-78 (2006).
13. K. Danielsen, D. W. Aksnes, G. W. Francis, NMR study of some anthraquinones from rhubarb. *Magn. Reson. Chem.* **30**, 359-360 (1992).
14. E. Dagne, W. Steglich, Knipholone: a unique anthraquinone derivative from *Kniphofia foliosa*. *Phytochemistry* **23**, 1729-1731 (1984).
15. E. Dagne, E. Berhanu, W. Steglich, New bianthraquinone pigments from *Kniphofia species*. *Bull. Chem. Soc. Ethiop.*, 32-35 (1987).
16. B.-E. Van Wyk, A. Yenesew, E. Dagne, The chemotaxonomic significance of root anthraquinones and pre-anthraquinones in the genus Lomatophyllum (asphodelaceae). *Biochem. Syst. Ecol.* **23**, 805-808 (1995).
17. N. Fujitake, T. Suzuki, M. Fukumoto, Y. Oji, Predomination of Dimers over Naturally Occurring Anthraquinones in Soil. *J. Nat. Prod.* **61**, 189-192 (1998).
18. J. M. Conner, A. I. Gray, T. Reynolds, P. G. Waterman, Anthracene and chromone derivatives in the exudate of Aloe rabaiensis. *Phytochemistry* **28**, 3551-3553 (1989).
19. C.-L. Chang, L.-J. Zhang, R. Y. Chen, L.-M. Y. Kuo, J.-P. Huang, H.-C. Huang, K.-H. Lee, Y.-C. Wu, Y.-H. Kuo, Antioxidant and Anti-inflammatory Phenylpropanoid Derivatives from *Calamus quiquesetinervius*. *J. Nat. Prod.* **73**, 1482-1488 (2010).
20. M. Hosny, J. P. N. Rosazza, Novel Isoflavone, Cinnamic Acid, and Triterpenoid Glycosides in Soybean Molasses. *J. Nat. Prod.* **62**, 853-858 (1999).
21. T. Pecere, M. V. Gazzola, C. Mucignat, C. Parolin, F. D. Vecchia, A. Cavaggioni, G. Basso, A. Diaspro, B. Salvato, M. Carli, G. Palù, Aloe-emodin Is a New Type of Anticancer Agent with Selective Activity against Neuroectodermal Tumors. *Cancer Res.* **60**, 2800-2804 (2000).
22. G. Srinivas, S. Babykutty, P. P. Sathiadevan, P. Srinivas, Molecular mechanism of emodin action: Transition from laxative ingredient to an antitumor agent. *Med. Res. Rev.* **27**, 591-608 (2007).
23. E. Pan, L. Harinantenaina, P. J. Brodie, M. Callmander, S. Rakotonandrasana, E. Rakotobe, V. E. Rasamison, K. TenDyke, Y. Shen, E. M. Suh, D. G. I. Kingston,

Cardenolides of *Leptadenia madagascariensis* from the Madagascar dry forest. *Bioorg. Med. Chem.* **19**, 4224-4428 (2011).

24. T. N. Bennett, M. Paguio, B. Gligorijevic, C. Seudieu, A. D. Kosar, E. Davidson, P. D. Roepe, Novel, rapid, and inexpensive cell-based quantification of antimalarial drug efficacy. *Antimicrob. Agents Chemother.* **48**, 1807-1810 (2004).
25. M. Smilkstein, N. Sriwilaijaroen, J. X. Kelly, P. Wilairat, M. Riscoe, Simple and inexpensive fluorescence-based technique for high-throughput antimalarial drug screening. *Antimicrob. Agents Chemother.* **48**, 1803-1806 (2004).
26. L. Harinantenaina, J. D. Bowman, P. J. Brodie, C. Slebodnick, M. W. Callmander, E. Rakotobe, R. Randrianaivo, V. E. Rasamison, A. Gorka, P. D. Roepe, M. B. Cassera, D. G. I. Kingston, Antiproliferative and Antiplasmodial Dimeric Phloroglucinols from *Mallotus oppositifolius* from the Madagascar Dry Forest. *J. Nat. Prod.* **76**, 388-393 (2013).
27. B. Rivero-Cruz, I. Rivero-Cruz, R. Rodríguez-Sotres, R. Mata, Effect of natural and synthetic benzyl benzoates on calmodulin. *Phytochemistry* **68**, 1147-1155 (2007).

APPENDIX B: BIOACTIVE COMPOUNDS FROM *STUHLMANNIA MOAVI* FROM THE MADAGASCAR DRY FOREST

Yixi Liu, Liva Harinantenaina, Peggy J. Brodie, Jessica D. Bowman, Maria B. Cassera, Carla Slebodnick, Martin W. Callmander, Richard Randrianaivo, Etienne Rakotobe, Vincent E. Rasamison, Wendy Applequist, Chris Birkinshaw, Gwilym P. Lewis, and David G. I. Kingston

Manuscript published – Reprinted with permission from Bioorganic & Medicinal Chemistry

ABSTRACT

Bioassay-directed fractionation of the leaf and root extracts of the antiproliferative Madagascar plant *Stuhlmannia moavi* afforded 6-acetyl-5,8-dihydroxy-2-methoxy-7-methyl-1,4-naphthoquinone (stuhlmoavin, **1**) as the most active compound, with an IC_{50} value of 8.1 μM against the A2780 human ovarian cancer cell line, as well as the known homoisoflavonoid bonducellin (**2**) and the stilbenoids 3,4,5'-trihydroxy-3'-methoxy-trans-stilbene (**3**), piceatannol (**4**), resveratrol (**5**), rhapontigenin (**6**), and isorhapontigenin (**7**). The structure elucidation of all compounds was based on NMR and mass spectroscopic data, and the structure of **1** was confirmed by a single crystal X-ray analysis. Compounds **2**–**5** showed weak A2780 activities, with IC50 values of 10.6, 54.0, 41.0, and 74.0 μM, respectively. Compounds **1**–**3** also showed weak antimalarial activity against Plasmodium falciparum with IC_{50} values of 23, 26, and 27 μM, respectively.

Introduction

As a part of the Madagascar International Cooperative Biodiversity Group (ICBG) program (*1, 2*), an ethanol extract of the leaves of a plant initially identified as an *Eligmocarpus* sp. was selected for evaluation as a possible source of new antiproliferative agents based on its activity against the A2780 ovarian cancer cell line. The final identification of the plant proved to be a botanical challenge. Although it was initially identified in the field as a species of *Eligmocarpus*, it was then reidentified as *Bussea sakalava* Du Puy & R. Rabev., and was finally classified as *Stuhlmannia moavi* Taub. (synonym: *Caesalpinia insolita* (Harms) Brenan & J.B. Gillett) (Leguminosae) (*3*).

The largely tropical genus *Caesalpinia,* a member of the informal Caesalpinia group (*4*) in the Leguminosae family, traditionally comprises up to 150 species, although *Caesalpinia* sensu stricto is now considered to comprise only about a dozen species (*5*). Seventeen species of the genus *Caesalpinia*, as circumscribed in its broadest sense, have been found in China, and some of them have been used for the treatment of rheumatism and inflammatory diseases in Chinese traditional medicine (*6*). Triterpenes, flavonoids and other compounds have been isolated from plants of the genus *Caesalpinia* sensu lato (*7, 8*), and 5-hydroxy-1,4-naphthoquinone has been isolated from the Asian species *C. sappan* (*9*). The genus is also a rich source of cassane-type diterpenes (*10, 11*), which have been reported to have significant antimalarial (*12*), antibacterial (*13*), antihelmintic (*14*), antiproliferative and antineoplasmic activities (*15, 16*). *Caesalpinia* is one of 21 genera included in the Caesalpinia group of legumes (*4*), a group of genera that includes the East African and Madagascan monospecifc genus *Stuhlmannia* (*17, 18*). The only previous chemical studies on the genus *Stuhlmannia* led to the isolation of some antimicrobial furanoid diterpenes (*19*).

We describe herein the isolation and structure elucidation of the new bioactive 1,4-naphthoquinone stuhlmoavin (1) and several other bioactive compounds (Figure B 1). Bioassay-guided isolation of the root extract of *S. moavi* furnished the known isoflavonoid bonducellin (**2**), together with the five known stilbenoids 3,4,5'-trihydroxy-3'-methoxy-trans-stilbene (**3**) (*20*), piceatannol (**4**) (*21, 22*), resveratrol (**5**) (*23*), rhapontigenin (**6**) (*24*), and isorhapontigenin (**7**) (*24*). The structures of compounds **2 -7** were determined by comparison of their ^{1}H NMR and mass spectra with literature data. Compound **1** showed moderate A2780 activity, compounds **2**–**5**

showed weak A2780 activities, and compounds **1**– **3** also showed weak antimalarial activities against the Dd2 drug-resistant strain of *Plasmodium falciparum*.

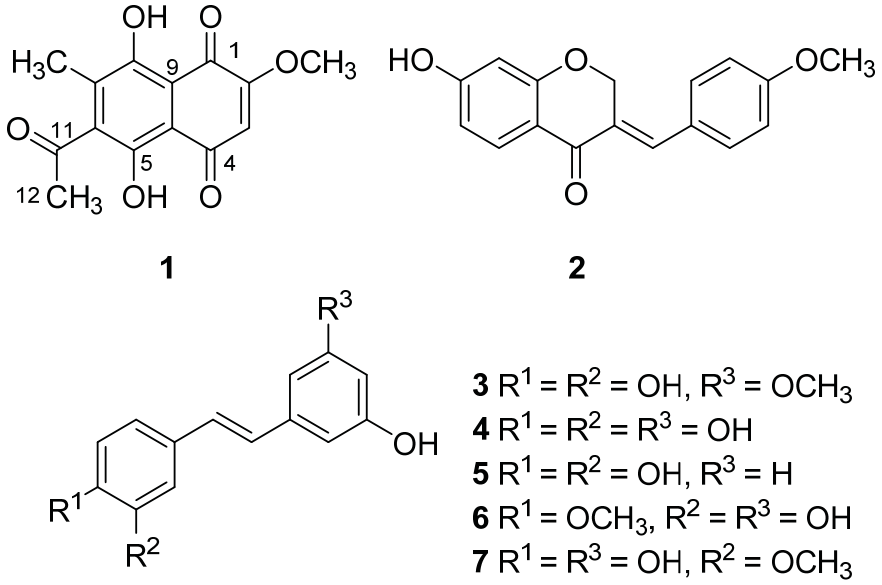

Figure B. 1. Structures of compounds from *Stuhlmannia moavi*..

Results and Discussion

Compound **1** (red needles) had the molecular formula $C_{14}H_{12}O_6$, as indicated by high-resolution ESIMS analysis (*m/z* 277.0729 [M+H]+, calcd. 277.0712). The IR spectrum showed absorptions characteristic of ketone (1708 cm^{-1}) and chelated hydroxyl (3384 cm^{-1}) functions as well as quinone carbonyl groups (1609 and 1564 cm-1) (*25, 26*). The ^1H NMR data (Table B 1) displayed resonances due to aromatic methyl (δ_H 2.22, s, 3H), acetyl methyl (δ_H 2.57, s, 3H), methoxy (δ_H 3.95, s, 3H), and aromatic methine (δ_H 6.19, s, 1H) groups. Two additional deshielded broad singlets at δ_H 12.63 (s, 1H) and δ_H 12.90 (s, 1H) indicated the presence of two hydrogen bonded hydroxyl groups in **1**. The ^1H NMR signals, taken in conjunction with the UV absorption spectrum, suggested that **1** had a 1,4-naphthoquinone skeleton with two peri-substituted hydroxyl groups.(*26, 27*) The ^{13}C NMR spectrum of **1** (Table B 1) exhibited 14 carbon signals, and the ^{13}C DEPT NMR spectrum showed signals due to two methyl groups (δ_C 12.7, δ_C 31.8), one methoxy group (δ_C 56.9), and one methine (δ_C 110.7).

Table B. 1. ^1H and ^{13}C NMR Data (δ, ppm) for compound 1 (500 and 125 MHz)[a]

position	δ_H	δ_C (DEPT)
1		186.7 (C)[b]
2		160.8 (C)
3	6.19 s	110.3 (CH)
4		181.3 (C)[b]
5		154.5 (C)
6		142.1 (C)
7		135.5 (C)
8		158.9 (C)
9		110.7 (C)
10		108.9 (C)
11		202.0 (C)
12	2.57 s	31.8 (CH_3)
2-OCH_3	3.95 s	56.9 (CH_3)
7-CH_3	2.22 s	12.7 (CH_3)
5-OH	12.90 s	
8-OH	12.63 s	

[a]In $CDCl_3$. Assignments based on HMBC

[b]These signals may be exchanged

The 10 remaining quaternary carbon signals in the ^{13}C NMR spectrum corresponded to an acetyl carbonyl group (δ_C 202.0), two quinone carbonyl groups (δ_C 186.7 and 181.3), three oxygen bearing aromatic carbons at δ_C 158.9, 154.5, and 160.8, and four signals for more shielded carbons at δ_C 110.3, 135.5, 108.9, and 110.7, corresponding to an aromatic methine, a methylated aromatic carbon, and the two bridgehead carbons of the naphthoquinone skeleton. In the HMBC experiment (Figure B 2), the correlations between δ_H 12.63 (OH-8) and δ_C 158.9, and δ_H 12.90 (OH-5) and δ_C 154.5, suggested that the two carbons were at the 8 and 5 positions, respectively.

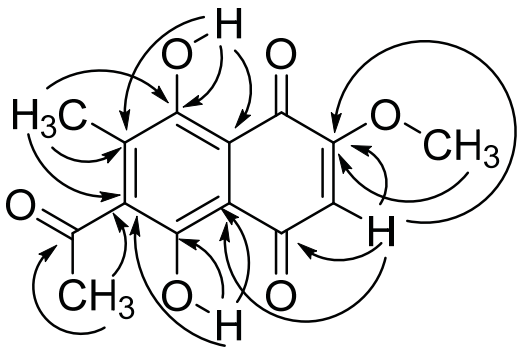

Figure B. 2. Key HMBC correlations of 1.

The HMBC correlations between the proton signals of the methyl group at δ_H 2.57 (CH_3-12) with both the carbonyl carbon at δ_C 202.0 (C-11) and the aromatic carbon at δ_C 142.1 (C-6), together with the long range HMBC correlation between δ_H 12.90 (OH-5) and δ_C 142.1 (C-6), indicated the attachment of an acetyl group at the C-6 position. In addition, the methyl group was assigned to C-7 based on the long-range correlations (Figure B 2) observed between the signal at δ_H 2.22 and δ_C 142.1 (C-6), δ_C 135.5 (C-7), and δ_C 158.9 (C-8). Furthermore, the signals for the deshielded hydroxyl groups OH-1 and OH-4 also correlated with carbon signals at δ_C 110.7 and δ_C 108.9, which were assigned to the two bridgehead carbons at C-9 and C-10, respectively. In the same manner, the methine group at the C-3 position was confirmed by observation of the HMBC long range correlation between δ_H 6.19 (H-3) and C-10 (δ_C 108.9). Moreover, the signal at H-3 correlated with both of the two quinone carbonyl groups at δ_C 181.3 and δ_C 186.7, which were assigned to C-4 and C-1. The methoxy group was assigned to C-2 (δC 160.8), which agrees with the correlation between δ_H 3.95 and δ_C 160.8 in the HMBC experiment. Compound **1** was thus deduced to be 6-acetyl-2-methoxy-7-methyl-1,4-naphthoquinone and has been named

stuhlmoavin. The proposed structure of **1** was confirmed by single-crystal X-ray diffraction analysis (Figure B 3).

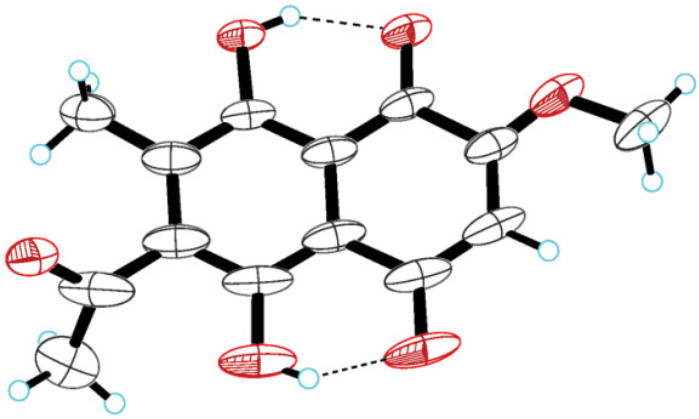

Figure B. 3. Anisotropic displacement ellipsoid drawing (50% probability) of compound 1.

Compounds **1**–**5** showed antiproliferative activity against the A2780 human ovarian cancer cell line. Among the seven compounds isolated, **1** showed moderate activity with an IC_{50} value of 8.1 ± 0.4 μM. Compounds **2**–**5** showed weaker activities with IC_{50} values of 10.6 ± 0.4 μM, 54 ± 1 μM, 41 ± 1 μM, and 74 ± 1 μM, respectively. Compounds **1**–**5** were also evaluated for antimalarial activity against *Plasmodium falciparum* Dd2 (a chloroquine/mefloquine-resistant strain), and compounds **1**–**3** showed moderate activities with IC_{50} values of 24 ± 7, 26 ± 3, and 27 ± 2 μM, respectively.

Experimental

General experimental procedures

IR and UV spectra were measured on MIDAC M-series FTIR and Shimadzu UV-1201 spectrophotometers, respectively. ^{1}H and ^{13}C NMR spectra were recorded on a Bruker Avance 500 spectrometer in $CDCl_3$ with TMS as internal standard. Mass spectra were obtained on an Agilent 6220 mass spectrometer. Open column chromatography was performed using Sephadex LH-20 and silica gel (230-400 mesh, Silicycle Co. USA). Flash chromatography was performed on a Biotage Horizon flash chromatograph using a C18 column (Phenomenex, 150 x 12 mm, 11 g). Semi-preparative HPLC was performed using Shimadzu LC-10AT pumps coupled with a semipreparative Phenomenex C18 column (5 μm, 250 × 10 mm), a Shimadzu SPD M10A diode array detector, and a SCL-10A system controller. All isolated compounds were purified to 95% purity or better, as judged by HPLC and by NMR (both UV and ELSD detection) before determining bioactivity. The HPLC chromatograms and NMR spectra can be found in the Supplementary Data.

Plant material

Leaves and roots of *Stuhlmannia moavi* Taub. (*28*) Brenan and Gillett (*3*) collected in dry forest 3 km north of Tsaratanana in the Sava locality, Daraina, in northern Madagascar The sample was from a tree 12 m high, 30 cm DBH, with yellow flowers and orange anthers. The tree is common in this location. It was identified as *Stuhlmannia moavi* Taub. (synonyms: C. insolita (Harms) Brenan & J.B. Gillett, from Madagascar and *Caesalpinia dalei* Brenan & J.B. Gillett, from East Africa) by comparison with the literature (*3, 28*), and by matching photographs taken in the field with herbarium specimens housed in the collections of the Royal Botanic Gardens, Kew.

Antiproliferative bioassay

The A2780 ovarian cancer cell line antiproliferative bioassay was performed at Virginia Tech as previously reported (*29*). The A2780 cell line is a drug-sensitive ovarian cancer cell line (*30*). Paclitaxel was used as the positive control; it had an IC_{50} value of 0.024 μM.

Antimalarial bioassay

The effect of each compound on parasite growth of the Dd2 strain of *P. falciparum* was measured in a 72 h growth assay in the presence of compound as described previously with minor modifications (*31, 32*). Briefly, ring stage parasite cultures (200 μL per well, with 1% hematocrit and 1% parasitemia) were grown for 72 h in the presence of increasing concentrations of the drug in a 5.05% CO_2, 4.93% O_2, and 90.2% N_2 gas mixture at 37 °C. After 72 h in culture, parasite viability was determined by DNA quantitation using SYBR Green I (50 μL of SYBR Green I in lysis buffer at 0.4 μL of SYBR Green I/mL of lysis buffer) (*32*). The half-maximum inhibitory concentration (IC_{50}) calculation was performed with GraFit software using a nonlinear regression curve fitting. IC_{50} values are the average of three independent determinations with each determination in duplicate and are expressed ± SEM. Artemisinin was used as the positive control; it had an IC_{50} value of 7 nM.

Extraction and isolation

A ground sample of *Stuhlmannia moavi* leaves (309 g) was extracted with EtOH at room temperature to yield 27.9 g of crude EtOH extract designated MG 4425. A total of 5.64 g of this extract was made available to Virginia Tech. The crude EtOH extract (2.0 g) was dissolved in 90% aq. MeOH (300 mL), and extracted with hexanes (3 × 200 mL). Evaporation of the hexane-soluble fraction afforded 285 mg of residue. The 90% aq. MeOH layer was then evaporated, suspended in H_2O (300 mL), and extracted with EtOAc (3 × 200 mL) to yield 600 mg of EtOAc-soluble fraction. The aqueous layer was concentrated to give 1.1 g of brown residue. The hexanes fraction was found to be cytotoxic with an IC_{50} value of 13 μg/mL and was subjected to Sephadex LH-20 open column chromatography (CH_2Cl_2:MeOH, 1:1) to give 7 fractions. Further purification of the most active fraction (IC_{50} 3.2 μg/mL) furnished the major and most active compound **1** (5.8 mg) with an IC_{50} of 2.6 μg/mL.

A ground sample of *S. moavi* roots (335 g) was extracted with EtOH at room temperature to yield 19.6 g of crude EtOH extract designated MG 4423. A total of 4.36 g of this extract was made available to Virginia Tech. A part of the crude EtOH extract (2.0 g) was dissolved in 90% aq. MeOH (300 mL) and extracted with hexanes (3 × 200 mL). Evaporation of the hexanes-soluble fraction yielded 508 mg of residue. The 90% aq. MeOH layer was then evaporated, suspended in H_2O (300 mL), and extracted with EtOAc (3 × 200 mL) to yield 1.106 mg of

EtOAc-soluble fraction. The aqueous layer was concentrated to give 256 mg of brown residue. The EtOAc fraction was found to be weakly cytotoxic with an IC_{50} value of 18 µg/mL and was subjected to Sephadex LH-20 open column chromatography (CH_2Cl_2: MeOH = 1:1) to give 7 fractions. Compound **2** (10.1 mg) was crystallized from MeOH from the second fraction. The third fraction from the Sephadex column (IC_{50} 13 µg/mL) was further fractionated using a C18 flash chromatograph column to yield 5 fractions. The third subfraction was subjected to HPLC on a C-18 column with a solvent gradient from H_2O:MeOH, 55:45 (for 30 min), to 40:60 from 30 to 35 min, to 0:100 from 35 to 40 min, and ending with 100% MeOH to 55 min. This process yielded compounds **4** (2.5 mg, t_R 14 min), **5** (3.2 mg, t_R 23.8 min), **6** (2.4 mg, t_R 26.5 min), **7** (1.2 mg, t_R 32 min) and **3** (4.5 mg, t_R 41.5 min).

6-Acetyl-5,8-dihydroxy-2-methoxy-7-methyl-1,4-naphthoquinone (stuhlmoavin, 1)

Red crystals; mp 185 °C; UV λ_{max} (MeOH) nm (log ε): 217 (4.11), 296 (3.54), 492 (3.27); IR ν_{max} cm-1: 3384, 1708, 1609 and 1564; ^1H and ^{13}C NMR data, see Table B 1; positive ion HRESIMS *m/z*: 277.0729 $[M+H]^+$ (calcd for $C_{14}H_{13}O_6$, 277.0712).

X-ray crystallography of 1

A red needle (0.01 x 0.04 x 0.62 mm^3) was centered on the goniometer of an Agilent SuperNova A diffractometer operating with CuKα radiation. The data collection routine, unit cell refinement, and data processing were carried out with the program CrysAlisPro.(*33*) The Laue symmetry and systematic absences were consistent with the monoclinic space group $P2_1/n$. The structure was solved using SHELXS-97 (*34*) and refined using SHELXL-97 via OLEX2 (*35*). The final refinement model involved anisotropic displacement parameters for non-hydrogen atoms and a riding model for all hydrogen atoms. A 2-position disorder model was used for the ketone oxygen with relative occupancies that refined to 0.490(13) and 0.510(13). The relatively poor refinement statistics and elongated displacement parameters are attributed to the small size and high mosaicity of the crystal. Crystal data: $C_{14}H_{12}O_6$, M_r =276.24, monoclinic, $P2_1/n$, a = 4.9896(3) Å, b = 23.446(3) Å, c = 10.5394(7) Å, α = 90°, β = 100.893(6)°, γ = 90°, V = 1210.73(18) $Å^3$, 9071 reflections, 196 parameters; crystal size 0.62 x 0.04 x 0.01 mm^3. The final indices were R_1 = 0.0803, wR_2 = 0.2080 [I>2σ(I)]. Crystallographic data for compound **1**

have been deposited as Supporting Information at the Cambridge Crystallographic Data Centre (deposition no. CCDC 919140) (*36*).

Acknowledgments

This project was supported by the Fogarty International Center, the National Cancer Institute, the National Institute of Allergy and Infectious Diseases, the National Institute of Mental Health, the National Institute on Drug Abuse, the National Heart Lung and Blood Institute, the National Center for Complementary and Alternative Medicine, the Office of Dietary Supplements, the National Institute of General Medical Sciences, the Biological Sciences Directorate of the National Science Foundation, and the Office of Biological and Environmental Research of the U.S. Department of Energy under Cooperative Agreement U01 TW00313 with the International Cooperative Biodiversity Groups. This project was also supported by the National Research Initiative of the Cooperative State Research, Education and Extension Service, USDA, Grant #2008-35621-04732. These supports are gratefully acknowledged. Work at Virginia Tech was supported by the National Science Foundation under Grant CHE-0722638 for the purchase of the Agilent 6220 mass spectrometer. We thank Mr. B. Bebout for obtaining the mass spectra. Fieldwork essential for this project was conducted under a collaborative agreement between the Missouri Botanical Garden and the Parc Botanique et Zoologique de Tsimbazaza and a multilateral agreement between the ICBG partners, including the Centre National d'Application des Recherches Pharmaceutiques. We thank S. Rakotonandrasana, R. Guittou, V. Benjara, C. Claude & A. Amady for assistance with plant collection, and we gratefully acknowledge courtesies extended by the Government of Madagascar (Ministère des Eaux et Forêts). paper or to the reference listing at the end.

Supplementary data

Supplementary data associated with this article, consisting of HPLC chromatograms and ^{1}H NMR spectra for all isolated products and the ^{13}C NMR spectrum of **1**, can be found, in the online version, at http://dx.doi.org/10.1016/j.bmcl.2013 .xx.

References

1. S. Cao, D. G. I. Kingston, Biodiversity conservation and drug discovery: Can they be combined? The Suriname and Madagascar experiences. *Pharm. Biol.* **47**, 809 – 823 (2009).
2. D. G. I. Kingston, Modern Natural Products Drug Discovery and Its Relevance to Biodiversity Conservation. *J. Nat. Prod.* **74**, 496–511 (2011).
3. J. P. M. Brenan, Notes on African Caesalpinioïdeae. *Kew Bull.* **17**, 197-218 (1963).
4. G. Lewis, in *Legumes of the World,* G. Lewis, B. Schrire, B. Mackinder , M. Lock, Eds. (Royal Botanic Gardens, Kew, UK, 2005), pp. 127-161.
5. E. Gagnon, G. P. Lewis, J. Solange Sotuyo, C. E. Hughes, A. Bruneau, A molecular phylogeny of *Caesalpinia* sensu lato: Increased sampling reveals new insights and more genera than expected. *S. Afr. J. Bot.*, in press (2013).
6. M. Wu, Y. F. Wang, M. L. Zhang, C. H. Huo, M. Dong, Q. W. Shi, H. Kiyota, Chemical Constituents of Plants from the Genus *Caesalpinia*. *Chem Biodivers* **8**, 1370-1399 (2011).
7. G. M. Woldemichael, M. P. Singh, W. M. Maiese, B. N. Timmermann, Constituents of antibacterial extract of *Caesalpinia paraguariensis* Burk. *Zeitschrift fur Naturforschung. C, Journal of biosciences* **58**, 70-75 (2003).
8. K. V. N. S. Srinivas, R. Y. Koteswara, I. Mahender, B. Das, K. K. V. S. Rama, K. K. Hara, U. S. N. Murty, Flavanoids from *Caesalpinia pulcherrima*. *Phytochemistry* **63**, 789-793 (2003).
9. M.-Y. Lim, J.-H. Jeon, E.-Y. Jeong, C.-H. Lee, H.-S. Lee, Antimicrobial activity of 5-hydroxy-1,4-naphthoquinone isolated from *Caesalpinia sappan* toward intestinal bacteria. *Food Chem.* **100**, 1254-1258 (2006).
10. J. Cheng, J. S. Roach, S. McLean, W. F. Reynolds, W. F. Tinto, Three new cassane diterpenes from *Caesalpinia pulcherrima*. *Nat. Prod. Commun.* **3**, 1751-1754 (2008).
11. W. Pranithanchai, C. Karalai, C. Ponglimanont, S. Subhadhirasakul, K. Chantrapromma, Cassane diterpenoids from the stem of *Caesalpinia pulcherrima*. *Phytochemistry* **70**, 300-304 (2009).
12. S. K. Kalauni, S. Awale, Y. Tezuka, A. H. Banskota, T. Z. Linn, P. B. S. Asih, D. Syafruddin, S. Kadota, Antimalarial activity of cassane- and norcassane-type diterpenes

from *Caesalpinia crista* and their structure-activity relationship. *Biol. Pharm. Bull.* **29**, 1050-1052 (2006).

13. R. A. Dickson, P. J. Houghton, P. J. Hylands, Antibacterial and antioxidant cassane diterpenoids from *Caesalpinia benthamiana*. *Phytochemistry* **68**, 1436-1441 (2007).
14. A. Jabbar, M. A. Zaman, Z. Iqbal, M. Yaseen, A. Shamim, Anthelmintic activity of *Chenopodium album* (L.) and *Caesalpinia crista* (L.) against trichostrongylid nematodes of sheep. *J. Ethnopharmacol.* **114**, 86-91 (2007).
15. Y. Hou, S. Cao, P. Brodie, J. S. Miller, C. Birkinshaw, F. Ratovoson, R. Rakotondrajaona, R. Andriantsiferana, V. E. Rasamison, D. G. I. Kingston, Antiproliferative cassane diterpenoids of *Cordyla madagascariensis* ssp. *madagascariensis* from the Madagascar rainforest. *J. Nat. Prod.* **71**, 150-152 (2008).
16. P. P. Yadav, R. Maurya, J. Sarkar, A. Arora, S. Kanojiya, S. Sinha, M. N. Srivastava, R. Raghubir, Cassane Diterpenes from *Caesalpinia bonduc*. *Phytochemistry* **70**, 256-261 (2009).
17. G. P. Lewis, Notes on *Stuhlmannia* Taub. and the correct placement of *Caesalpinia insolita* (Harms) Brenan & Gillett (Leguminosae: Caesalpinioideae: Casalpinieae). *Kew Bull.* **51**, 377-379 (1996).
18. G. Lewis, in *Legumes of the World,* G. Lewis, B. Schrire, B. MacKinder , M. Lock, Eds. (Royal Botanical Gardens, Kew, UK, 2005), pp. 136.
19. J. O. Odalo, C. C. Joseph, M. H. H. Nkunya, I. Sattler, C. Lange, H.-M. Dahse, U. Moellman, Cytotoxic, anti-proliferative and antimicrobial furanoditerpenoids from *Stuhlmannia moavi*. *Phytochemistry* **70**, 2047-2052 (2009).
20. S. Prakash, M. A. Khan, K. Z. Khan, A. Zaman, Stilbenes of *Gnetum-Ula*. *Phytochemistry* **24**, 622-624 (1985).
21. J. H. Hart, Role of phytostilbenes in decay and disease resistance. *Ann. Rev. Phytopathol.* **19**, 437-458 (1981).
22. M. L. Cardona, M. I. Fernandez, M. B. Garcia, J. R. Pedro, Synthesis of natural polyhydroxystilbenes. *Tetrahedron* **42**, 2725-2730 (1986).
23. K. Nakajima, H. Taguchi, T. Endo, I. Yosioka, The constituents of *Scirpus fluviatilis* (Torr.) A. Gray. I. The structures of two new hydroxystilbene dimers, scirpusin A and B. *Chem. Pharm. Bull.* **26**, 3050-3057 (1978).

24. A. Silayo, B. T. Ngadjui, B. M. Abegaz, Homoisoflavonoids and stilbenes from the bulbs of *Scilla nervosa* subsp. *rigidifolia*. *Phytochemistry* **52**, 947-955 (1999).
25. N. N. Gerber, B. Wieclawek, The Structures of Two Naphthoquinone Pigments from an Actinomycete. *J. Org. Chem.* **31**, 1496-1498 (1966).
26. T. Hanumaiah, B. K. Rao, C. P. Rao, G. S. R. Rao, J. U. M. Rao, K. V. J. Rao, D. S. Marshall, R. H. Thomson, Naphthalenes and Naphthoquinones from *Ventilago* Species. *Phytochemistry* **24**, 1811-1815 (1985).
27. S. Natori, Y. Kumada, H. Nishikawa, The structure of mompain, a naphthoquinone from *Helicobasidium mompa* Tanaka, and its relation to spinochrome A (M). *Chem. Pharm. Bull.* **13**, 633-635 (1965).
28. G. Lewis, in *Legumes of the World,* G. Lewis, B. Schrire, B. MacKinder , M. Lock, Eds. (Royal Botanical Gardens, Kew, UK, 2005), pp. 140.
29. S. Cao, P. J. Brodie, J. S. Miller, R. Randrianaivo, F. Ratovoson, C. Birkinshaw, R. Andriantsiferana, V. E. Rasamison, D. G. I. Kingston, Antiproliferative Xanthones of *Terminalia calcicola* from the Madagascar Rain Forest. *J. Nat. Prod.* **70**, 679-681 (2007).
30. K. G. Louie, B. C. Behrens, T. J. Kinsella, T. C. Hamilton, K. R. Grotzinger, W. M. McKoy, M. A. Winker, R. F. Ozols, Radiation survival parameters of antineoplastic drug-sensitive and -resistant human ovarian cancer cell lines and their modification by buthionine sulfoximine. *Cancer Res.* **45**, 2110-2115 (1985).
31. T. N. Bennett, M. Paguio, B. Gligorijevic, C. Seudieu, A. D. Kosar, E. Davidson, P. D. Roepe, Novel, rapid, and inexpensive cell-based quantification of antimalarial drug efficacy. *Antimicrob. Agents Chemother.* **48**, 1807-1810 (2004).
32. M. Smilkstein, N. Sriwilaijaroen, J. X. Kelly, P. Wilairat, M. Riscoe, Simple and inexpensive fluorescence-based technique for high-throughput antimalarial drug screening. *Antimicrob. Agents Chemother.* **48**, 1803-1806 (2004).
33. H. M. Berman, J. Westbrook, Z. Feng, G. Gilliland, T. N. Bhat, H. Weissig, I. N. Shindyalov, P. E. Bourne, The Protein Data Bank. *Nucleic Acids Research* **28**, 235-242 (2000).
34. G. M. Sheldrick, A short history of SHELX. *Acta Crystallogr., Sect. A: Found. Crystallogr.* **A64**, 112-122 (2008).

35. O. V. Dolomanov, L. J. Bourhis, R. J. Gildea, J. A. K. Howard, H. Puschmann, OLEX2: a complete structure solution, refinement and analysis program. *J. Appl. Crystallogr.* **42**, 339-341 (2009).

36. M. A. Marti-Renom, A. C. Stuart, A. Fiser, R. Sanchez, F. Melo, A. Sali, COMPARATIVE PROTEIN STRUCTURE MODELING OF GENES AND GENOMES. *Annual Review of Biophysics & Biomolecular Structure* **29**, 291 (2000).

APPENDIX C: ANTIPROLIFERATIVE AND ANTIPLASMODIAL DIMERIC PHLOROGLUSINOLC FROM *MALLOTUS OPPOSITIFOLIUS* FROM THE MADAGASCAR DRY FOREST

Liva Harinantenaina, Jessica D. Bowman, Peggy J. Brodie, Carla Slebodnick, Martin W. Callmander, Etienne Rakotobe, Richard Randrianaivo, Vincent E. Rasamison, Alexander Gorka, Paul D. Roepe, Maria B. Cassera, and David G. I. Kingston

Manuscript published – Reprinted with permission the Journal of Natural Products

ABSTRACT

Bioassay-guided fractionation of an ethanol extract of the leaves and inflorescence of *Mallotus oppositifolius* collected in Madagascar led to the isolation of the two new bioactive dimeric phloroglucinols, mallotojaponins B (**1**) and C (**2**), together with the known mallotophenone (**3**). The structures of the new compounds were determined on the basis of spectroscopic evidence, including their 1- and 2D-NMR spectra, mass spectrometry, and an X-ray crystal structure. Compounds **1** and **2** showed potent antimalarial activity against chloroquine-resistant *Plasmodium falciparum,* with IC_{50} values of 0.75 ± 0.30 and 0.14 ± 0.04 μM, while **3** was inactive in this assay. Compounds **1**–**3** also displayed strong antiproliferative activity against the A2780 human ovarian cancer cell line (IC_{50} 1.10 ± 0.05, 1.3 ± 0.1 and 6.3 ± 0.4 μM, respectively).

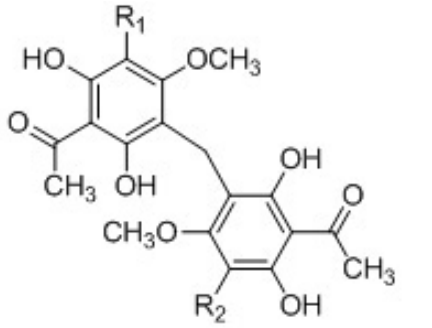

1 $R_1 = CH_3$, $R_2 = CH_2CH{=}C(CH_3)_2$
2 $R_1 = R_2 = CH_2CH{=}C(CH_3)_2$
3 $R_1 = R_2 = CH_3$

Introduction

The tropical genus *Mallotus*, a member of the family Euphorbiaceae, contains about 150 species of trees and shrubs (*1*). It shares membership in the tribe Acalypheae with the genus *Macaranga* (*1*), a genus that has afforded several promising bioactive compounds (*2, 3*). *Mallotus philippinensis* is the source of rottlerin, a natural product which first appears to have been isolated in 1855 (*4*), and has been the subject of numerous biological investigations (*5-7*).

Our ongoing screening of extracts from plants collected in Madagascar as part of the Madagascar International Cooperative Biodiversity Group (ICBG) program for antiproliferative activity towards the A2780 ovarian cancer cell line (*8*) has recently been supplemented with screening for antiplasmodial activity against the malaria parasite *Plasmodium falciparum.* An ethanol extract of *Mallotus oppositifolius* (Geiseler) Müll. Arg. (Euphorbiaceae) was found to display strong activity against *P. falciparum* as well as antiproliferative activity against the A2780 cell line, and this extract was thus selected for further investigation to isolate the active metabolite(s) responsible for the observed activities. *M. oppositifolius* has been used as a chewing stick in Nigeria (*9*), and its aqueous and ethanol extracts have been reported to have antifungal activity (*10*), but no previous work on its constituents has been reported.

Results and Discussion

Isolation of Bioactive Constituents. Initial dereplication studies using size-exclusion chromatography and HPLC on a small amount of an active hexanes-soluble fraction obtained from the liquid-liquid partition of the active extract indicated the presence of unknown antiproliferative phloroglucinols. Scale up of the isolation to 1 g of extract yielded an antiproliferative hexanes fraction (IC_{50} 6.7 μg/mL), which was subjected to another size-exclusion column chromatography (Sephadex LH-20) to furnish two active fractions with IC_{50} values of 1.6 and 2.3 μg/mL, and the known phloroglucinol mallotophenone (**3**, IC_{50} 6.3 ± 0.4 μM). The most active fractions were subjected to HPLC and silica gel column chromatography to yield the two new bioactive phloroglucinols **1** and **2**.

Structure Elucidation. Mallotophenone (**3**) was identified by single-crystal X-ray analysis and by comparison of its spectroscopic data with values reported in the literature (*11*).

Table C. 1. ^{1}H NMR Data for Compounds 1-3 (500 MHz, $CDCl_3$)

Position	1	2	3
1a	3.68 s	3.68 s	3.66 s
8	2.71 s	2.70 s	2.70 s
9	2.13 s	3.31 d (6.3)	2.11 s
8'	2.71 s	2.70 s	2.70 s
9'	3.31 d (6.5)	3.31 d (6.3)	2.11 s
OCH_3	3.98 s	3.98 s	3.97 s
	3.98 s	3.98 s	3.97 s
1"	5.21 (tq, 6.5, 1.4)	5.21 (br t, 6.0)	
3"	1.68 s	1.68 s	
4"	1.77 s	1.77 s	
1"'		5.21 (br t, 6.0)	
3"'		1.68 s	
4"'		1.77 s	
OH	8.97 s	9.05s	8.99
	13.64 s	13.48 s	13.66

Compound **1** was obtained as yellowish crystals and gave the molecular formula $C_{25}H_{30}O_8$ as indicated by high-resolution ESIMS analysis, which gave a protonated molecular ion peak at *m/z* 459.1963 $[M+H]^+$. Its IR spectrum showed an absorption characteristic of a conjugated hydrogen bonded carbonyl group (1620 cm^{-1}). The UV spectrum of **1** was very similar to that of **3**, suggesting that the two compounds share the same chromophore.

Table C. 2. ^{13}C NMR Data for Compounds 1-3 (125 MHz, $CDCl_3$)

Carbon	1	2	3
1	108.3	108.5	108.4
1a	18.1	17.9	18.1
2	157.2	157.5	157.1
3	109.2	114.2	109.1
4	162.9	162.8	163.0
5	110.0	109.2	110.2
6	159.8	159.6	159.9
7	205.4	205.4	205.6
8	33.8	33.8	34.1
9	8.9	22.9	9.2
1'	108.5	108.5	108.4
2'	157.7	157.5	157.1
3'	114.2	114.2	109.1
4'	162.9	162.8	163.0
5'	109.2	109.2	110.2
6'	159.6	159.6	159.9
7'	205.4	205.4	205.6
8'	33.8	33.8	34.1
9'	22.9	22.9	9.2
OCH_3	62.1	63.0	62.2
	63.0	63.0	62.2
1"	122.7	122.7	
2"	132.2	132.2	
3"	18.0	17.9	
4"	25.8	25.8	
1"'		122.7	
2"'		132.2	
3"'		17.9	
4"'		25.8	

The ^1H NMR spectroscopic data of **1** (Table C 1) displayed resonances due to an aromatic methyl (δ2.13, s, 3H), a 3,3-dimethylallyl group (δ1.68, s, 3H and 1.77, s, 3H), δ5.21 (tq, J = 6.5, 1.4 Hz, 1H) and δ3.31 (d, J = 6.5 Hz, 2H), two methoxy groups (δ3.98, bs, 6H), two acyl methyl groups (δ2.71, bs, 6H), and one methylene group at δ3.68 (s, 2H), together with signals for two hydroxy groups, one of which was hydrogen bonded (δ8.97, s, 1H and 13.64, s, 1H).

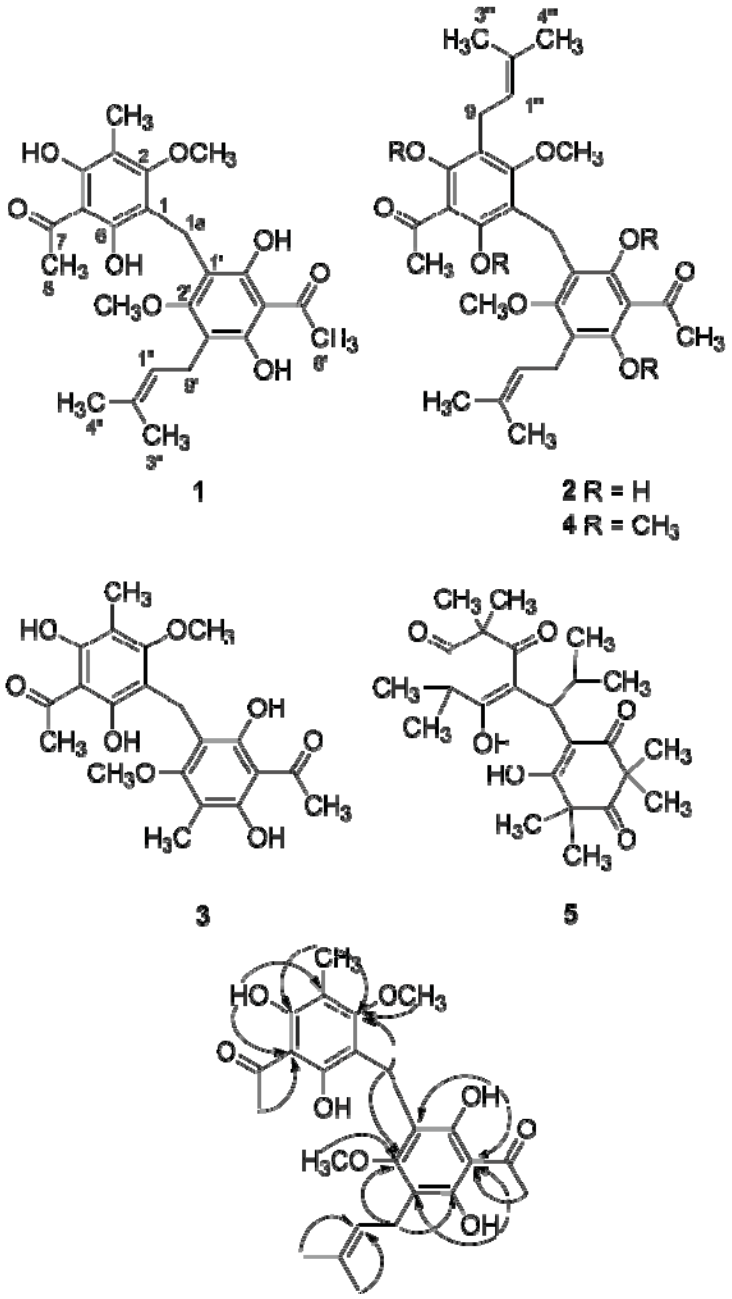

Figure C. 1. Important HMBC correlations observed in 1.

The ^{13}C NMR data of **1** (Table C 1) exhibited 25 carbon signals that were identical with those of

3 except for the replacement of the signal of an aromatic methyl carbon with signals for the carbons of a 3,3-dimethylallyl unit (δ18.0, 22.9, 25.8, 122.7, 132.2). On comparison of the ^{13}C NMR data of **1** with those of **3**, the deshielding of the signal for C-3' (δ114.2 instead of 109.1 in **3**) suggested that the 3,3-dimethylallyl group is attached at this position, which is methylated in **3** (*12*). The locations of the methyl, methoxy, methylene, carboxyl, hydroxy and the 3,3-dimethylallyl groups were confirmed by interpretation of the 1D- and 2D-NMR spectroscopic data of **1**, including COSY, HSQC, HMBC, and nuclear Overhauser effect spectroscopy experiments. The attachment of the 3,3-dimethylallyl group at C-3' was confirmed by the observation of the HMBC long-range correlation between the two geminal methyls at δ1.68 and 1.77 to C-1" (δ122.7), and from the methine proton at δ5.21 to C-3' (δ114.2). The methoxy groups were assigned to C-2 and C-2' due to the long-range correlations (Figure C 1) observed between the signals at δ3.98 and those at δ157.2 (C-2) and 157.7 (C-2'), between the C-1a methylene proton signal (δ3.68) and C-2 and C-2', as well as those observed between the aromatic methyl protons at δ2.13 and C-2 and between the methylene protons signals at δ3.31 and C-2'. In the same manner, the acyl group was assigned to C-5 and C-5' from the HMBC cross peaks between the methyl protons at δ2.71 (CH_3-8 and 8') and C-5 and C-5'. The two hydroxy groups must be located at C-4, C-4', and C-6, C-6', as indicated by the presence of two hydrogen-bonded hydroxy protons and the HMBC long-range correlations between the hydroxy group at δ8.97 and C-3, C-3', C-5 and C-5'. Moreover, NOESY correlations were observed between the methoxy protons and H-1", H-1a, and CH_3-9.

The structure of **1** was confirmed by single-crystal X-ray diffraction (Figure C 2). Compound **1** was thus assigned as 3'-(3,3-dimethylallyl)-1'-(5-acetyl-6-hydroxy-3-methyl-2-methoxybenzyl)-2'-methoxyphloraceto-phenone, and has been named mallotojaponin B based on its relationship to mallotojaponin A (*13*).

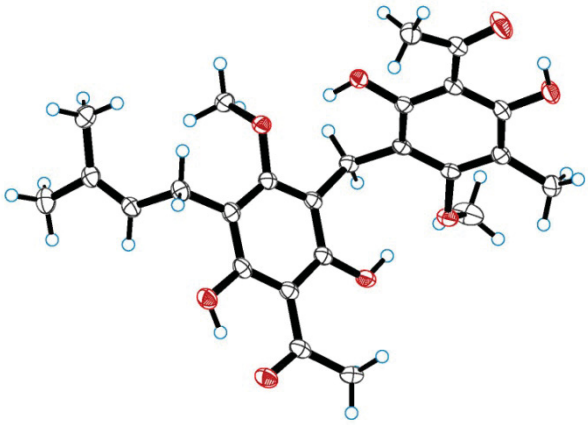

Figure C. 2. Anisotropic displacement ellipsoid drawing (50%) of 1.

Compound **2**, named mallotojaponin C, gave the molecular formula $C_{29}H_{36}O_8$ as determined by positive ion HRESIMS (*m/z* 513.2499, $[M+H]^+$, requires for $C_{29}H_{37}O_8$, 513.2488). Similarly to **1**, the IR and UV spectra of **2** were indicative of the presence of a prenylated phloroglucinol. The ^1H and ^{13}C NMR spectroscopic data of **2** were superposable upon those of **1** (Tables C 1 and C 2), except for the replacement of the signal due to the aromatic methyl group with the signals for a second 3,3-dimethylallyl group. Thus, the signal due to the methine of the 3,3-dimethylallyl group (δ5.21, brt, J = 6.0 Hz) integrated for two protons (H-1" and H-1'") while the signal at δ3.68 (s, H_2-1a) integrated for two protons. In addition, the broad triplet observed for the ^1H NMR signal of the methine protons at δ5.21 suggested the presence of two overlapping signals (H-1" and H-1'"). These data coupled with the high-resolution mass spectra allowed the conclusion to be made that compound **2** was a symmetrical dimer with two 3,3-dimethylallyl units, one each at C-3 and C-3'. This was also confirmed by the observation of the base peak at *m/z* 263 (Figure C 3).

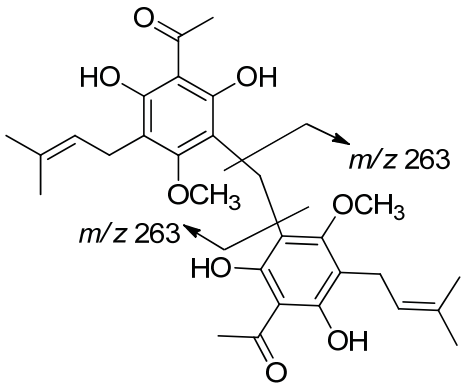

Figure C. 3. Mass fragmentation observed for 2.

Comparison of the ^{13}C NMR spectroscopic data of **2** with those of **1** demonstrated that the methyl group at C-3 of **1** is replaced by a 3,3-dimethylallyl unit in **2**. Also, HMBC long-range correlations were observed from H-1" and H-1'" to C-3 and C-3', respectively, and from H-9 and H-9' to C-2, C-4 and to C-2' and C-4', respectively. The locations of the hydroxy groups at C-4 (C-4') and C-6 (C-6'), the methoxyl groups at C-2 (C-2'), the acetyl group at C-5 (C-5'), and the methylene at C-1 (C-1') were elucidated in the same manner as for **1**. These data led to the assignment of the structure of **2** as 1-methylene-*bis*-4-methoxy-6-hydroxy-3-(3,3-dimethylallyl)-2-methoxyacetophenone.

Biological Activities. Compounds **1-3** were evaluated for their activity against *P. falciparum* Dd2 (a chloroquine/mefloquine-resistant strain). Compounds **1** and **2** showed submicromolar activity with half-maximum inhibitory concentration (IC_{50}) values of 0.76 ± 0.30 and 0.14 ± 0.04 μM, respectively, while compound **3** was not active. In addition to their cytostatic activity in inhibiting the growth of *P. falciparum*, compounds **1** and **2** also showed cytocidal activity vs. *P. falciparum*. Using a newly developed rapid assay for determination of cytocidal activity (*14*), compound **1** was found to have median lethal dose (LD_{50}) values of 14.6 ± 0.7 and 6.7 ± 0.2 μM vs. the drug-sensitive HB3 strain and the drug-resistant Dd2 strain, respectively, while compound **2** had LD_{50} values of 0.81 ± 0.05 and 0.80 ± 0.02 μM vs the same two strains. In these same assays, chloroquine exhibited LD_{50} values of 0.10 ± 0.01 and 15.3 ± 0.9 μM (HB3 vs. Dd2), so for the drug-resistant Dd2 strain, compound **2** in particular is significantly more cytocidally potent than chloroquine.

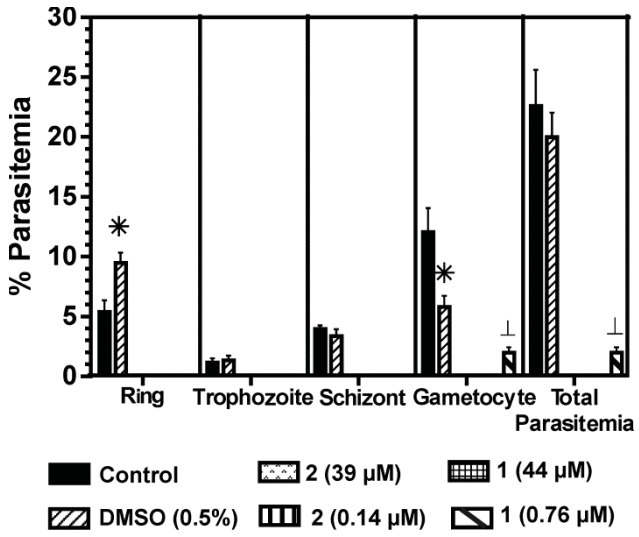

Figure C. 4. *P. falciparum* blood stage distribution after 13 days of treatment at the indicated concentrations to assess antimalarial activity against early stage gametocytes. The control is untreated parasites. DMSO (drug vehicle at 0.5%) was included as a second control since it affects the blood-stages distribution but does not affect the total parasitemia. No parasite growth was observed at doses of 2 of 0.14 and 39 µM and of 1 at 44 µM. Results are presented as means of two independent experiments ± S.E.M., (*) $p \leq 0.02$ and (⊥) $p \leq 0.005$ compared with the control group.

Compounds **1** and **2** were further evaluated for their gametocytocidal activity against late stage gametocytes (the stage responsible for malaria transmission) using the chloroquine-sensitive NF54 strain to generate gametocytes. This strain was used because it forms gametocytes in culture much better than the chloroquine-sensitive HB3 strain. Only compound **2** showed gametocytocidal activity with an IC_{50} value of 3.6 ± 0.2 µM. This activity is comparable to the current antimalarial drug artesunate (IC_{50} value of 2.3 µM) and to NPC1161B, an antimalarial drug currently in the development pipeline (IC_{50} value of 3.8 µM).(*15, 16*) The IC_{50} value determined for compound **2** against asexual stages in the NF54 strain was 0.07 ± 0.01 µM.

In order to address if compounds **1** and **2** were able also to prevent gametocytogenesis (generation of the malaria transmission stages), *P. falciparum* in vitro cultures were treated with 0.76 µM (~IC_{50}) or 44 µM (~IC_{100}) of compound **1** and 0.14 µM (~IC_{50}) or 39 µM (~IC_{100}) of compound **2** for 13 days, as described in the Experimental Section. On day 13, cultures were recovered and smeared for microscopic examination. Neither asexual intraerythrocytic stages nor gametocytes were observed in cultures treated with 0.14 µM of compound **2** (Figure C 4). Compound **1** cleared asexual intraerythrocytic stages in vitro at 0.76 µM, and the presence of mature gametocytes was reduced 80% as compared to untreated parasites (control). The

gametocytes observed in the presence of compound **1** did not appear healthy by microscopy, however, a gametocyte viability assay (measuring exflagellation) would be needed to confirm this finding. This is the first report on mallotojaponin derivatives showing antimalarial activity.

Compounds **1** and **2** also displayed strong antiproliferative activity against the A2780 human ovarian cancer cell line with IC_{50} values of 1.10 ± 0.05 and 1.3 ± 0.1 μM, respectively. Since mallotophenone (**3**) showed weaker activity (IC_{50} 6.3 ± 0.4 μM), it appears that the presence of the 3,3-dimethylallyl group in the molecule enhances the activity; however, this effect was more pronounced in the malaria parasite. Phloroglucinols have been reported to have a wide range of biological activities (*13, 17-21*). Previous investigation showed that 3'-(3,3-dimethylallyl)-1'-(5-acetyl-6-hydroxy-3-methyl-2-methoxybenzyl)-2'-hydroxyphloracetophenone, a 2'-hydroxylated derivative of mallotojaponin B (**1**), displayed cytotoxic activities against KB and mouse leukemia L-5178Y (ED_{50} 0.58 and 0.74 μg/mL, respectively) (*11*).

The discovery of the strong antimalarial and gametocytocidal activities of compound **2** raised the question of its possible mechanism of action. It has been proposed that acylphloroglucinols can function as antimalarial agents by acting as radical-generating species or by inhibiting hemozoin formation (*22*). The latter may occur through binding to pre-crystalline forms of heme via π-π interactions (given their electron rich structures) and/or coordination with the Fe^{3+} center of hematin (such as an Fe—O interaction with the phenolic moiety of **2**) (*22*). As a test of the importance of the phenolic hydroxy groups of **2**, the compound was converted to its tetramethyl ether **4** by treatment with potassium carbonate and excess methyl iodide. Compound **4** was active against *P. falciparum,* with an IC_{50} value of 2.2 ± 0.5 μM and 2.5 ± 0.5 μM to the drug-sensitive NF54 cell line and the drug-resistant Dd2 cell line, respectively, and was thus fifteen times less potent than its parent compound **2**. It thus appears that the phenolic hydroxy groups of **2** are important for its antimalarial activity, supporting the idea that coordination to Fe^{3+} and/or radical generation plays an important role in the antimalarial activity of the phloroglucinols in general and of compound **2** in particular. This conclusion is also supported by the recent report of the modest antiplasmodial activity of watsonianone A (**5**), a related compound lacking phenolic hydroxyl groups isolated from the Australian tree *Corymbia watsonian* (*23*).

Bioactive phloroglucinols have been detected in the Aspidiaceae, Cannabinaceae, Clusiaceae, Compositae, Crassulaceae, Euphorbiaceae, Fagaceae, Guttiferae, Lauraceae, Myrtaceae, Rosaceae and Rutaceae families (*17*). From the present study, we may be concluded that *Mallotus japonicus* and *M. oppositifolius* are two Euphorbiaceous species that produce dimeric phloroglucinols such as mallotophenone (**3**) and related compounds (*11, 24, 25*). It is also noteworthy that an extract of *Mallotus japonicus* inhibited production of pro-inflammatory cytokines during macrophage activation, and mallotojaponin was one of the bioactive phloroglucinol derivatives isolated from this extract that showed this effect (*26*). Mallotojaponin was also shown to inhibit HIV-reverse transcriptase activity (*27*).

Experimental Section

General Experimental Procedures. Optical rotations were recorded on a JASCO P-2000 polarimeter. IR and UV spectra were measured on MIDAC M-series FTIR and Shimadzu UV-1201 spectrophotometers, respectively. ^{1}H and ^{13}C NMR spectra were recorded on a JEOL Eclipse 500 spectrometer in $CDCl_3$ with TMS as internal standard. Mass spectra were obtained on JEOL JMS-HX-110, Agilent 6220 LC-TOF-MS. Preparative HPLC was performed using Shimadzu LC-10AT pumps coupled with a semipreparative Varian Dynamax C_{18} column (5 μm, 250x10 mm), a Shimadzu SPD M10A diode array detector (DAD), and a SCL-10A system controller.

Plant Material. Leaves and inflorescences of *Mallotus oppositifolius* (Geiseler) Müll. Arg. (collection: Richard Randrianaivo & et al. 1425) were collected at an elevation of 137 m in December 2006 near the village of Befarafara in the dry forest of Solanampilana, 35 km north of Daraina, Antsiranana, Sava region, 13°05'42"S 049°34'57"E, northern Madagascar. The sample collected was from a shrub 3 m tall, with white flowers. The plant taxonomy was determined by Dr. Gordon McPherson (Missouri Botanical Garden). Duplicate voucher specimens were deposited at the Centre National d'Application des Recherches Pharmaceutiques (CNARP), the Herbarium of the Parc Botanique et Zoologique de Tsimbazaza, Antananarivo, Madagascar (TAN), the Missouri Botanical Garden, St. Louis, Missouri (MO), and the Museum National d'Histoire Naturelle in Paris, France (P).

Antiproliferative Bioassay. The A2780 ovarian cancer cell line assay was performed at Virginia Polytechnic Institute and State University as previously reported (*28*). The A2780 cell line is a drug-sensitive ovarian cancer cell line (*29*).

Intraerythrocytic Stages Antimalarial Bioassay. The effect of each fraction and pure compound on parasite growth of Dd2 strain was measured in a 72 h growth assay in the presence of drug as described previously with minor modifications (*30, 31*). Briefly, ring stage parasite cultures (200 μL per well, with 1% hematocrit and 1% parasitemia) were then grown for 72 h in the presence of increasing concentrations of the drug in a 5.05% CO_2, 4.93% O_2 and 90.2% N_2

gas mixture at 37 ^{o}C. After 72 h in culture, parasite viability was determined by DNA quantitation using SYBR Green I (50 μL of SYBR Green I in lysis buffer at 0.4 μL of SYBR Green I/mL of lysis buffer) (*31*). The half-maximum inhibitory concentration (IC_{50}) calculation was performed with GraFit software using a nonlinear regression curve fitting. IC_{50} values are the average of three independent determinations with each determination in duplicate, and are expressed ± S.E.M.

Intraerythrocytic Stages Cytocidal Antimalarial Bioassay. The effectiveness of compounds **1** and **2** at killing intraerythrocytic stages of the chloroquine-sensitive HB3 and chloroquine-resistant Dd2 strains of *P. falciparum* was performed as previously reported (*14*). LD_{50} values are the average of three replicate determinations and are expressed ± S.E.M.

Late Gametocyte Stage Antimalarial Bioassay. To test compounds for their effectiveness in killing late stage (stage V) gametocytes, late stage gametocytes were generated using a combination of established methods (*15, 32*). Initial gametocyte cultures were developed from the *P. falciparum* NF54 strain (chloroquine-sensitive strain). All cultures were maintained in 75 cm^2 culture flasks in a reduced oxygen environment (5% O_2, 5% CO_2, 95% N_2) at 37 ˚C. Parasitemia was calculated by counting the percentage of infected RBCs by Giemsa staining of thin smears and light microscopy. Asexual stages were synchronized by sorbitol treatment at least two days before setting gametocyte cultures (*33*). Thin blood smears were made and stained with Giemsa to check parasite development on days 4, 8, 12, and 13 after the initial subculture. On day nine of the gametocyte cultures, parasites were treated with 5% sorbitol for 10 min at 37 ˚C to start removing asexual stages. Sorbitol treatment was performed for four consecutive days, which effectively removes >99% of asexual parasites. Gametocyte recovery and concentration was achieved on day 13 using a NycoPrep™ 1.077 cushion (*15*) and the number of gametocytes was calculated using a Neubauer chamber and 30,000 to 50,000 gametocytes per well were added to the black flat-bottom half-area 96-well plates containing drug candidates in a 100 μL final volume. The plate was incubated in a humidified chamber at 37 ˚C and low oxygen conditions (5% O_2, 5% CO_2, 95% N_2) for 72 h. AlamarBlue® was added on day 16 post-induction at 10% of the well volume (*32*). The plate was returned to the chamber for an additional 24 h and then was read in a microplate reader at 585 nm after excitation at 540 nm.

IC_{50} values were calculated using a dose-response curve fitting with GraFit. IC_{50} values are the average of two independent determinations, each determination in duplicate and are expressed ± S.E.M.

Early Gametocyte Stage Antimalarial Bioassay. To test efficacy in preventing gametocytogenesis, 24-well plates were set at 0.75% parasitemia (NF54 strain) and 1% hematocrit and cultured for 13 days with or without the presence of compound **1** and **2**. The plate was incubated in a humidified chamber at 37˚C and low oxygen conditions for the duration of the experiment. Medium or medium supplemented with drug was replaced on days 4, 6, 8, and 9-12. On day 13, each well was recovered and the parasitaemia (both asexual and sexual) was calculated from Giemsa stained smears.

Extraction and Isolation. A ground sample of *M. oppositifolius* leaves and inflorescences (137 g) was extracted with ethanol at room temperature to yield 6.0 g of crude ethanol extract, designated MG 4129. A total of 1.8 g of this extract was made available to Virginia Polytechnic Institute and State University. In order to locate the biological activity and to have an idea about the types of metabolites responsible for the activity of the active fraction, 100 mg of the crude ethanol extract of *A. alnifolia* were subjected to a liquid-liquid partition using hexanes, EtOAc and H_2O to afford 42.5 mg of an active hexanes fraction (IC_{50} 6.7 μg/mL). Size-exclusion chromatography on Sephadex LH-20 of the hexanes fraction eluted with MeOH-CH_2Cl_2 gave mallotophenone (**3**, IC_{50} 6.3 ± 0.4μM) and two active fractions (Fr. 3, 13 mg; IC_{50} 2.3 μg/mL and Fr. 4, 8.4 mg; IC_{50} 1.6 μg/mL). High-performance liquid chromatography (HPLC) on a C_{18} column with a solvent gradient from water-MeOH (system I): 40:60 to 30:70 for 10 min, to 20:80 from 10 to 15 min, to 15:85 from 15 to 20 min, keep 15:85 for 5 min, to 10:90 from 25 to 30 min, and to 0:100 from 30 min to 35 min, ending with 100% MeOH to 50 min of fractions 3 and 4 showed the presence of two major and active phloroglucinols (t_R: 39.79 min; IC_{50} 0.5 mg/mL and t_R: 44.15 min; IC_{50} 0.61 mg/mL). To isolate more compounds for structure elucidation and for activity evaluations, the isolation was scaled up by starting with 1 g of ethanol extract. Liquid-liquid partion (hexanes, 3 x 200 mL) followed by Sephadex LH-20 of the hexanes fraction (407 mg) afforded two active fractions (Fr.3, 125.2 mg; IC_{50} 2.4 μg/mL and Fr.4, 137.1 mg; IC_{50} 2.2 μg/mL). Mallotophenone (**3**) was obtained from fractions 3 and 4 by

precipitation. The mother liquid of fraction 3 was subjected to silica gel column chromatography to give compounds **1** (8.3 mg), and **2** (6 mg). Also, HPLC of the mother liquid of fraction 4 on a C_{18} column using isocratic 100% MeOH gave two active peaks (t_R: 39.79 min and 44.15 min), which were purified by silica gel CC to yield compounds **1** (3.1 mg) and **2** (5 mg).

Mallotojaponin B (1): Colorless prism (EtOAc-hexane), mp 175 ± 1 °C; UV (MeOH) λ_{max} (log ε): 283 (4.06) nm; IR (film) ν_{max} 3450, 3223, 1620, 1596, 1405, 1283, 1128 cm^{-1}; ^1H NMR and ^{13}C NMR data, see Tables 1 and 2; positive HRESIMS *m/z* 459.2023 $[M+H]^+$ (calcd for $C_{25}H_{31}O_8$, 459.2019).

X-ray Crystallography of 1. A colorless prism of **1** (0.13 x 0.15 x 0.41 mm^3) was centered on the goniometer of an Oxford Diffraction SuperNova A diffractometer operating with CuKα radiation. The data collection routine, unit cell refinement, and data processing were carried out with the program CrysAlisPro.(*34*) The Laue symmetry and systematic absences were consistent with the monoclinic space group $P2_1/c$. The structure was solved using SHELXS-97(*35*) and refined using SHELXL-97(*35*) via OLEX2.(*36*) The final refinement model involved anisotropic displacement parameters for non-hydrogen atoms. A riding model was used for the aromatic and alkyl hydrogens. The –OH hydrogen positions were located from the residual electron density map and refined independently.

Crystal Data: Colorless prism; $C_{25}H_{30}O_8$, *Mr* = 458.49, monoclinic, $P2_1$, *a* = 12.88614(12) Å, *b* = 12.34409(7) Å, *c* = 14.84644(13) Å, β = 110.4761(10)°, V = 2212.38(3) $Å^3$, 37837 reflections, 317 parameters; crystal size: 0.4149 x 0.1458 x 0.1287 mm^3. The final indices were R_1 = 0.0367, wR_2 = 0.0973 [$I > 2\sigma(I)$]. Crystallographic data for compound **1** have been deposited as supplementary material at the Cambridge Crystallographic Data Centre (Deposition No. CCDC 874720) (*37*).

Mallotojaponin B (2): Amorphous powder; UV (MeOH) λ_{max} (log ε) 283 (4.12) nm; IR (film) ν_{max} 3440, 3220, 1620, 1595, 1434, 1405, 1280, 1121 cm^{-1}; ^1H NMR and ^{13}C NMR data, see Table 1; positive HRESIMS *m/z* 513.2499 $[M+H]^+$ (calcd for $C_{29}H_{37}O_8$, 513.2488).

Mallotophenone (3): The structure of **3** was identified by single crystal X-ray analysis and by comparison of its spectroscopic data with values reported in the literature (*11*). Crystallographic data for compound **3** has been deposited as supplementary material at the Cambridge Crystallographic Data Centre (Deposition No. CCDC 874719) (*37*).

Methylation of Mallotojaponin B (2): Compound **2** (0.9 mg) was dissolved in acetone (1.5 mL) and treated with K_2CO_3 (120 mg) and methyl iodide (100 μL). The mixture was stirred at room temperature for 17 hours. The reaction mixture was evaporated, dissolved in water and extracted with EtOAc to give compound **4** (1 mg). The structure of **4** was confirmed by interpretation of its ^{1}H NMR spectrum and by HRESIMS (see Supporting Information).

Supporting Information

^{1}H and ^{13}C NMR spectra of compounds **1** and **2** and ^{1}H NMR spectrum of **4**, and an ORTEP drawing of **3**. This information is available free of charge via the Internet at http://pubs.acs.org.

Acknowledgments

This project was supported by the Fogarty International Center, the National Cancer Institute, the National Science Foundation, the National Heart, Lung and Blood Institute, the National Institute of Mental Health, the Office of Dietary Supplements, and the Office of the Director of NIH, under Cooperative Agreement U01 TW000313 with the International Cooperative Biodiversity Groups. This project was also supported by the National Research Initiative of the Cooperative State Research, Education and Extension Service, USDA, Grant #2008-35621-04732, and by the National Center for Complementary and Alternative Medicine under Cooperative Agreement U01 TW000313-19S1. This work was also supported by the National Science Foundation under Grant no. CHE-0619382 for purchase of the Bruker Avance 600 NMR spectrometer and Grant no. CHE-0722638 for the purchase of the Agilent 6220 mass spectrometer. We thank Mr. B. Bebout for obtaining the mass spectra and Dr. Hugo Azurmendi for assistance with the NMR spectra. Field work essential for this project was conducted under a collaborative agreement between the Missouri Botanical Garden and the Parc Botanique et Zoologique de Tsimbazaza and a multilateral agreement between the ICBG partners, including the Centre National d'Applications des Recherches Pharmaceutiques. We gratefully acknowledge courtesies extended by the Government of Madagascar (Ministère des Eaux et Forêts). All support is gratefully acknowledged.

References

1. A. Radcliffe-Smith, *Genera Euphorbiacearum.*, (Royal Botanic Gardens, Kew, UK, 2001), pp. 464.
2. B. J. Yoder, S. Cao, A. Norris, J. S. Miller, F. Ratovoson, J. Razafitsalama, R. Andriantsiferana, V. E. Rasamison, D. G. I. Kingston, Antiproliferative Prenylated Stilbenes and Flavonoids from *Macaranga alnifolia* from the Madagascar Rain Forest. *J. Nat. Prod.* **70**, 342-346 (2007).
3. J. A. Beutler, R. H. Shoemaker, T. Johnson, M. R. Boyd, *J. Nat. Prod.* **61**, 1509-1512 (1998).
4. A. McGookin, F. P. Reed, A. Robertson, Rottlerin. I. *J. Chem. Soc.*, 748-755 (1937).
5. Y.-F. Liao, Y.-C. Hung, W.-H. Chang, G. J. Tsay, T.-C. Hour, H.-C. Hung, G.-Y. Liu, The PKC delta inhibitor, rottlerin, induces apoptosis of haematopoietic cell lines through mitochondrial membrane depolarization and caspases' cascade. *Life Sciences* **77**, 707-719 (2005).
6. V. Sharma, A polyphenolic compound rottlerin demonstrates significant in vitro cytotoxicity against human cancer cell lines: isolation and characterization from the fruits of Mallotus philippinensis. *Journal of Plant Biochemistry and Biotechnology* **20**, 190-195 (2011).
7. G. Valacchi, A. Pecorelli, C. Sticozzi, C. Torricelli, M. Muscettola, C. Aldinucci, E. Maioli, Rottlerin exhibits antiangiogenic effects in vitro. *Chem. Biol. Drug Des.* **77**, 460-470 (2011).
8. D. G. I. Kingston, Modern Natural Products Drug Discovery and Its Relevance to Biodiversity Conservation. *J. Nat. Prod.* **74**, 496–511 (2011).
9. A. A. Adekunle, A. M. Ikumapayi, Antifungal property and phytochemical screening of the crude extracts of Funtumia elastica and Mallotus oppositifolius. *West Indian Med. J.* **55**, 219-223 (2006).
10. D. E. Okwu, O. Ekei, Phytochemical screening and mineral composition of chewing sticks in South Eastern Nigeria. *Global J. Pure Appl. Sci.* **9**, 235-238 (2003).

11. M. Arisawa, A. Fujita, T. Hayashi, N. Morita, N. Kawano, S. Koshimura, Studies on cytotoxic constituents in pericarps of Mallotus japonicus, Part I. *J. Nat. Prod.* **48**, 455-459 (1985).
12. J. Zhang, D. S. Saleh, G. R. Wyatt, Juvenile hormone regulation of an insect gene: a specific transcription factor and a DNA response element. *Molecular and Cellular Endocrinology* **122**, 15-20 (1996).
13. M. Arisawa, A. Fujita, N. Morita, T. Okuyama, H. Nishino, Inhibition of tumor-promoter-enhanced ^{3}H-choline incorporation into cellular phospholipids by phloroglucinol derivatives from Mallotus japonicus. *J. Nat. Prod.* **54**, 1409-1412 (1991).
14. M. F. Paguio, K. L. Bogle, P. D. Roepe, *Mol. Biochem. Parasitol.* **178**, 1-6 (2011).
15. J. Lelievre, M. J. Almela, S. Lozano, C. Miguel, V. Franco, D. Leroy, E. Herreros, Activity of clinically relevant antimalarial drugs on Plasmodium falciparum mature gametocytes in an ATP bioluminescence "transmission blocking" assay. *PLoS One* **7**, e35019 (2012).
16. C. L. Peatey, D. Leroy, D. L. Gardiner, K. R. Trenholme, Anti-malarial drugs: how effective are they against *Plasmodium falciparum* gametocytes? *Malar. J.* **11**, 34-37 (2012).
17. I. P. Singh, S. B. Bharate, Phloroglucinol compounds of natural origin. *Nat. Prod. Rep.* **23**, 558–591 (2006).
18. E. S. Costa, C. A. Hiruma-Lima, E. O. Lima, G. C. Sucupira, A. O. Bertolin, S. F. Lolis, F. D. P. Andrade, W. Vilegas, A. R. M. Souza-Brito, Antimicrobial activity of some medicinal plants of the cerrado, Brazil. *Phytother. Res.* **22**, 705-707 (2008).
19. F. Cottiglia, L. Casu, M. Leonti, P. Caboni, C. Floris, B. Busonera, P. Farci, A. Ouhtit, G. Sanna, Cytotoxic Phloroglucinols from the Leaves of Myrtus communis. *J. Nat. Prod.* **75**, 225-229 (2012).
20. E. O. Farombi, O. O. Ogundipe, E. S. Uhunwangho, M. A. Adeyanju, J. O. Moody, Antioxidant Properties of Extracts from Alchornea laxiflora (Benth) Pax and Hoffman. *Phytother. Res.* **17**, 713-716 (2003).
21. H. Mavar-Manga, M. Haddad, L. Pieters, C. Baccelli, A. Penge, J. Quetin-Leclercq, Anti-inflammatory compounds from leaves and root bark of Alchornea cordifolia (Schumach. & Thonn.) Mull. Arg. *J. Ethnopharmacol.* **115**, 25-29 (2008).

22. L. Verotta, Are acylphloroglucinols lead structures for the treatment of degenerative diseases? *Phytochem. Rev.* **1**, 389-407 (2002).
23. A. R. Carroll, V. M. Avery, S. Duffy, P. I. Forster, G. P. Guymer, Watsonianone A-C, anti-plasmodial β-triketones from the Australian tree, *Corymbia watsoniana. Org. Biomol. Chem.* **11**, 453-458 (2013).
24. M. Arisawa, A. Fujita, T. Hayashi, K. Hayashi, H. Ochiai, N. Morita, Cytotoxic and antiherpetic activity of phloroglucinol derivatives from Mallotus japonicus (Euphorbiaceae). *Chem. Pharm. Bull.* **38**, 1624-1628 (1990).
25. M. Arisawa, A. Fujita, N. Morita, Studies on cytotoxic constituents in pericarps of *Mallotus japonicus*. Three new phloroglucinol derivatives, butyrylmallotochromanol, isobutyrylmallotochromanol, and mallotojaponol. *J. Nat. Prod.* **53**, 638-643 (1990).
26. R. Ishii, M. Horie, K. Saito, M. Arisawa, S. Kitanaka, Inhibition of lipopolysaccharide-induced pro-inflammatory cytokine expression via suppression of nuclear factor-KB activation by *Mallotus japonicus* phloroglucinol derivatives. *Biochim. Biophys. Acta* **1620**, 108-118 (2003).
27. H. Nakane, M. Arisawa, A. Fujita, S. Koshimura, K. Ono, Inhibition of HIV-reverse transcriptase activity. *FEBS Lett.* **286**, 83-85 (1991).
28. S. Cao, P. J. Brodie, J. S. Miller, R. Randrianaivo, F. Ratovoson, C. Birkinshaw, R. Andriantsiferana, V. E. Rasamison, D. G. I. Kingston, Antiproliferative Xanthones of *Terminalia calcicola* from the Madagascar Rain Forest. *J. Nat. Prod.* **70**, 679-681 (2007).
29. K. G. Louie, B. C. Behrens, T. J. Kinsella, T. C. Hamilton, K. R. Grotzinger, W. M. McKoy, M. A. Winker, R. F. Ozols, Radiation survival parameters of antineoplastic drug-sensitive and -resistant human ovarian cancer cell lines and their modification by buthionine sulfoximine. *Cancer Res.* **45**, 2110-2115 (1985).
30. T. N. Bennett, M. Paguio, B. Gligorijevic, C. Seudieu, A. D. Kosar, E. Davidson, P. D. Roepe, Novel, rapid, and inexpensive cell-based quantification of antimalarial drug efficacy. *Antimicrob. Agents Chemother.* **48**, 1807-1810 (2004).
31. M. Smilkstein, N. Sriwilaijaroen, J. X. Kelly, P. Wilairat, M. Riscoe, Simple and inexpensive fluorescence-based technique for high-throughput antimalarial drug screening. *Antimicrob. Agents Chemother.* **48**, 1803-1806 (2004).

32. T. Q. Tanaka, K. C. Williamson, A malaria gametocytocidal assay using oxidoreduction indicator, alamarBlue. *Mol. Biochem. Parasitol.* **177**, 160-163 (2011).
33. C. Lambros, J. P. Vanderberg, Synchronization of Plasmodium falciparum erythrocytic stages in culture. *J. Parasitol.* **65**, 418-420 (1979).
34. (Agilent Technologies UK Ltd, Oxford, UK,, 2011).
35. G. M. Sheldrick, A short history of SHELX. *Acta Cryst.* **A64**, 112-122 (2008).
36. O. V. Dolomanov, L. J. Bourhis, R. J. Gildea, J. A. K. Howard, H. Puschmann, *J. Appl. Cryst.* **42**, 339–341 (2009).
37. M. J. Sippl, Recognition of errors in three-dimensional structures of proteins. *Proteins: Structure, Function, and Bioinformatics* **17**, 355-362 (1993).

APPENDIX D: A STERIOD RECEPTOR COACTIVATOR ACTS AS THE DNA-BINDING PARTNER OF THE METHOPRENE-TOLERANT PROTEIN IN REGULATING JUVENILE HORMONE-RESPONSIVE GENES

Meng Li, Pengcheng Liu, Jessica D. Wiley, Reyaneh Ojani, David R. Bevan, Jianyong Li, Jinsong Zhu

Manuscript under review

ABSTRACT

Methoprene-tolerant (Met) protein, a basic helix-loop-helix Per-ARNT-Sim (bHLH-PAS) transcription factor, has been characterized as an intracellular receptor of juvenile hormone (JH) in insects. JH-bound Met forms a complex with another bHLH-PAS protein, FISC (βFTZ-F1 interacting steroid receptor coactivator), and together they regulate JH-responsive genes in mosquitoes. However, the exact mechanism by which the Met-FISC complex is recruited to the target promoters remains elusive. In this study, we demonstrated that FISC is the obligatory partner of Met for binding to JH-response elements (JHREs). Recombinant Met and FISC proteins were purified from bacteria and used in gel-shift assays. Met and FISC together were sufficient to bind a JHRE previously identified in the early trypsin gene, while Met or FISC alone could not do it. Mutagenesis analysis indicated that the basic regions adjacent to the HLH motif in both proteins were involved in DNA binding, suggesting that each protein recognized a portion of the hormone response element. Furthermore, employing an *in vitro* selection and amplification method, we identified an optimal DNA sequence recognized by Met and FISC. The core consensus sequence GCACGTG was similar to the JHREs that had been previously discovered in several JH target genes. While formation of the Met-FISC complex in mosquito cells was induced by JH, *in vitro* heterodimerization and DNA binding of the purified recombinant Met and FISC were JH-independent, implying that additional mosquito proteins were required to modulate the JH-binding activity and formation of the receptor complex.

Introduction

Juvenile hormone (JH) is one of the most enigmatic hormones in invertebrate endocrinology. In insects, it is secreted from corpora allata (CA), a pair of endocrine glands connected to the brain (*1*). JH plays crucial roles in many aspects of insect life, including development, reproduction, diapause, caste differentiation, migratory behavior and longevity (*2-4*). JH is most known for its anti-metamorphic effect on immature stages of insects. Molting and metamorphosis in insects are under the control of two hormones, the steroid 20-hydroxyecdysone (20E) and JH (*5*). While 20E is responsible for initiating molting, the nature of the molt is governed by JH. During larval development, 20E causes larval-larval molts when JH is present in the hemolymph. After the corpora allata stop secreting JH in the final larval instar, insect tissues change their commitment and 20E triggers the larval-pupal and pupal-adult molts (*5*).

Juvenile hormone is also a key regulator of vitellogenesis and oocyte maturation in insects (*6*). In the yellow fever mosquito *Aedes aegypti*, female adults need a vertebrate blood meal to obtain nutrients for egg production. An elevated JH titer after adult eclosion is essential for primary follicles to grow and differentiate in the first 2-3 days and to reach the resting stage where a blood meal is required for further development of the follicles (*7, 8*). In the newly emerged adult mosquitoes, JH induces proliferation of biosynthetic organelles in the fat body trophocyte cells and makes the fat body responsive to 20E (*9-11*). In an *in vitro* culture system, fat body tissues dissected from newly emerged female mosquitoes cannot synthesize vitellogenin in response to 20E in the medium (*12*). However, expression of the vitellogenin gene is readily induced by 20E if the fat body tissues from the newly emerged mosquitoes are cultured with JH prior to the 20E treatment (*13*).

Many functions of JH are mediated by the Methoprene-tolerant (Met) protein, an intracellular receptor of JH. Fruit flies carrying a null allele of Met show resistance to both the toxic and morphogenetic effects of JH and its mimic methoprene (*14*). JH stimulated protein synthesis in male accessory glands of *Drosophila melanogaster* are clearly abated in *Met*$^{-}$ mutants, compared with wild-type flies (*15*). RNAi mediated depletion of Met in the red flour beetle, *Tribolium castaneum*, causes larvae to pupate prematurely before reaching their final instar (*16*). In newly emerged female *Ae. aegypti* mosquitoes, RNAi knockdown of Met stalls the growth of ovarian follicles, similar to the phenotypic effects of JH deprivation (*17*).

The Met protein belongs to the basic-helix-loop-helix Per-Arnt-Sim (bHLH-PAS) family of transcription factors (*18*). The basic region of the bHLH domain is comprised of 13 amino acids, rich in arginine and lysine residues. The HLH region contains two alpha-helices separated by a loop of variable length. The helices promote formation of homo- or heterodimers, which bring basic regions of two proteins together to bind to DNA with a hexanucleotide core called E-box (CANNTG) (*19*). The PAS domain functions as a protein dimerization motif and consists of two similar hydrophobic repeats, termed PAS-A and PAS-B, separated by a poorly conserved spacer (*20*). The PAS domains in signal transduction proteins serve as a versatile sensor to detect a wide variety of chemical and physical stimuli, and to regulate the activity of effector domains covalently linked to the PAS domains (*21*). Recent studies have demonstrated that *in vitro* synthesized Met binds JH with relatively high affinity through a binding pocket formed by the PAS-B domain (*22, 23*).

It has been shown in several insect species that Met is essential for the induced expression of JH-responsive genes (*24-26*). In newly emerged female *Ae. aegypti* mosquitoes, the post-eclosion activation of the Krüppel homolog 1 (AaKr-h1) gene and the early-trypsin (AaET) gene requires both AaMet and AaFISC, another bHLH-PAS transcription factor that has been previously identified as a coactivator of the ecdysteroid receptor complex (*27, 28*). AaMet and AaFISC form a heterodimer in the presence of JH. Both proteins are associated with the *AaET* promoter in the midgut when *AaET* is upregulated by the elevated JH titer in the hemolymph, indicating that AaMet and AaFISC act directly on the *AaET* promoter to activate its transcription (*27*). In transient transfection assays, AaMet and AaFISC activate the *AaET* promoter in the presence of JH. A juvenile hormone response element (JHRE) identified in the *AaET* promoter, which contains a*n asymmetric E-box* (CACGCG), is sufficient for the JH-induced transactivation by AaMet-AaFISC (*27*).

JH-induced expression of Kr-h1 in *Ae. aegypti*, *Bombyx mori* and *T. castaneum* all requires the functions of Met and the orthologs of FISC (*27, 29-31*). E-box-like sequences have been identified in the regulatory region of Kr-h1 gene in these three species (*29, 32*). A more recent study by Raikhel's lab found similar E-box-like sequences in 68 *Ae aegypti* genes, the expression of which are AaMet-dependent in adult female mosquitoes (*17*). Thus, transcriptional activation by recruiting the Met-FISC complex to the E-box-like sequences might be a conserved mechanism in JH action.

Although the Met-FISC complex is shown to activate expression of JH-responsive genes, many questions remain unanswered: Are Met and FISC loaded to the target promoters through direct DNA binding or protein-protein interaction? Is FISC the DNA binding partner of Met or a coactivator of the JH receptor? Does Met-FISC recognize other types of JH response elements? Here we report our *in vitro* DNA-binding assays using bacterially expressed recombinant AaMet and AaFISC proteins. The results indicated that AaMet and AaFISC are required and sufficient for binding to the JHRE identified from *AaET*. Both AaMet and AaFISC directly bound JHRE through their basic regions located in the bHLH domains. Furthermore, utilizing a selection and amplification protocol, we performed a comprehensive screening of sequences preferably bound by AaMet and AaFISC. A consensus sequence, GCACGTG, was found to bind AaMet and AaFISC with high affinity. Luciferase reporter assay and *in vitro* DNA-binding assay demonstrated that the consensus sequence was a *bona fide* functional JHRE. This study significantly advances our understanding of the JH-induced gene activation by Met and FISC in molecular details.

Experimental Procedures

Plasmids–pCMA, pCMA-GAD, pCMA-GBD, and UAS×4-188-cc-Luc were from Dr. Lucy Cherbas (*33*). The expression vectors pCMA-AaMet and pCMA-AaFISC have been described previously (*27*). To construct 4×JHRE1-luc, a chimeric DNA fragment was inserted into the pGL3 basic plasmid between restriction sites *Kpn* I and *Nco* I. The insert consisted of the four tandem repeats of JHRE1 (CCACACGCGAAG) from *AaET* and the minimal promoter of *AaET* (-77 to +61). 4×MFBS1-luc was constructed similarly, except that the *AaET* JHRE was replaced with MFBS (5'-GCCGCACGTGTC-3').

Expression and purification of recombinant proteins–The codon usage of AaMet cDNA was optimized for bacterial expression (see supplemental information 1 for the optimized sequence). A cDNA fragment coding for amino acid sequence 1-597 was cloned into expression vector pGEX-6P-1 (GE Healthcare) between restriction sites *Bam*H I and *Not* I, resulting in a expression plasmid for AaMet, pGEX-6P-1-Metn. BL21(DE3) strain transformed with the plasmid was cultured in LB medium at 37^{o}C to approach an OD_{600} of 0.6. The temperature was then lowered to 25^{o}C. When OD_{600} reached 0.8, IPTG was added to a final concentration of 0.5 mM. The culture was harvested 3 hours after IPTG induction. Cell pellets were resuspended in lysis buffer (20 mM sodium phosphate, pH 7.3, 150 mM NaCl, 2 mM DTT, 1 mM PMSF, and 1×Halt protease inhibitor cocktail (Thermo Scientific)). Cells were lysed using DeBEE high pressure homogenizer (BEE international) and debris was removed by centrifugation at 30,000 × g for 30 min. Proteins in the supernatant were affinity-purified using AKTA prime and GSTrap FF column (GE Healthcare) at 4^{o}C with binding buffer (20 mM sodium phosphate, pH 7.3, 150 mM NaCl, and 2 mM DTT) and elution buffer (50 mM Tris-HCl, pH8.0, 10 mM reduced glutathione, and 2 mM DTT). Purified GST-AaMet was dialyzed in PBS buffer containing 2 mM DTT and 10% glycerol, and was stored at -80^{o}C until use.

The cDNA region coding for amino acid sequence 1-609 of AaFISC was cloned into expression vector pRSET A (Invitrogen) between restriction sites *Bam*H I and *Kpn* I. Recombinant AaFISC was expressed as a His-tag fusion protein under the control of T7 promoter in *E. coli* BL21(DE3) pLysS strain. Bacterial cells were grown in LB medium at 37^{o}C. Temperature was lowered to 20^{o}C when OD_{600} reached 0.4. IPTG was added to a final concentration of 0.2 mM when OD_{600} reached 0.6. Cells were cultured for two more hours and were then collected by centrifugation. 6×His-AaFISC was purified using AKTA prime and

HisTrap FF column according to the standard protocol provided by GE Healthcare. Buffers used for FISC protein purification were: lysis buffer (20 mM sodium phosphate, pH 7.4, 0.5 mM NaCl, 20 mM imidazole, 2 mM DTT, 1 mM PMSF, and 1×Halt protease inhibitor cocktail); binding buffer (20 mM sodium phosphate, pH 7.4, 0.5 mM NaCl, 20 mM imidazole, and 2 mM DTT); elution buffer (20 mM sodium phosphate, pH 7.4, 0.5 mM NaCl, 0.5 M imidazole, and 2 mM DTT). Dialysis in PBS and protein storage was conducted as described above for GST-AaMet.

Gel-shift assay–Double-stranded DNA oligonucleotides were end-labeled by T4 Polynucleotide Kinase (New England Biolabs) and [γ-^{32}P] ATP (PerkinElmer), followed by purification with Bio-Spin 6 column (Bio-Rad). For DNA binding, 0.5 μg of purified Met, FISC, or both proteins was added to the binding buffer (20 mM sodium phosphate (pH 7.4), 50 mM NaCl, 1 mM $MgCl_2$, 5 mM DTT, 100ng/μl BSA, 50 ng/μl poly(dA-dT), and 10 μM JH III or DMSO carrier). After 10 min incubation at room temperature, 20 fmol of the labeled probe (~20,000 cpm) were added to make a total volume of 20 μl. The reactions were incubated for 20 more minutes followed by electrophoresis at 120V for 50 min with a 6% polyacrylamide DNA retardation gel (Invitrogen) in 0.5× TBE buffer. The gel was dried and the ^{32}P-labeled DNA was visualized by autoradiography. Competition experiments were performed by inclusion of a 50-fold molar excess of unlabeled specific or nonspecific competitor DNA in the binding reaction. In super-shift experiments, 3 μg of GST antibody (Santa Cruz), His tag antibody (Millipore) or mock IgG (Fisher) were added to the binding reactions 20 minutes after addition of the labeled probe, and the reactions were incubated for an additional 20 minutes before electrophoresis.

Site-directed mutagenesis–Site-directed mutagenesis was carried out as described (*34*). Primers used for mutagenesis are included in Supplementary Table S1. Primers containing point mutations were used in PCR to amplify the template plasmids. PCR products were cleaned up with PCR purification kit (Qiagen), followed by *Dpn* I digestion at 37^{o}C for 1 hour to remove the template plasmids. The DNA was purified again and about 200 ng of the DNA were used to transform *E. coli* NEB 10-beta competent cells (New England Biolabs) following the manufacturer's instructions. The mutations were all confirmed by DNA sequencing.

In vitro selection and amplification of DNA binding site–Screening for DNA-binding site was modified from a method described previously by Swanson *et al*.(*35*). A single-stranded DNA library, 5'-CCACCAACAACAACATCAGC-$(N)_{17}$-CTTCCGATGGATACTGGAGG-3',

was synthesized. It contained all possible 17-bp DNA sequences ($4^{17} \approx 1.7 \times 10^{10}$ different sequences) flanked by adaptor sequences. To generate double-stranded DNA, the single-stranded DNA library was annealed to a primer complementary to the 3' adaptor sequence, followed by DNA extension with Taq polymerase at 72°C for 30 min. The reaction products were resolved in 2.5% agarose gel and the double-stranded DNA was recovered. Purified DNA was end-labeled with [γ-^{32}P] ATP and T4 Polynucleotide Kinase, followed by purification with Bio-Spin 6 column (Bio-Rad).

Gel-shift assays were conducted by incubating 0.5 μg each of purified AaMet and AaFISC, 1 ng of the labeled DNA in 20 μl binding buffer (20 mM sodium phosphate, pH 7.4, 50 mM NaCl, 1 mM $MgCl_2$, 5 mM DTT, 100 ng/μl BSA, 100 ng of sonicated salmon sperm DNA (GE healthcare), and 10 μM JH III). After electrophoresis and autoradiography, shifted band was cut from the gel. The gel slice was placed in 200 μl water and kept in a shaker at 700 rpm at 4°C overnight. Forty microliters of the eluent were used as DNA template for PCR amplification to generate an enriched pool of selected oligonucleotides for the next round of selection. A total of ten rounds of selection were conducted. After the last selection, DNA was cloned into pCR2.1 TOPO TA cloning vectors (Invitrogen) and subjected to sequencing analysis. Consensus motifs were identified by the MEME algorithm (*36*).

Luciferase reporter assay–Transfection of L57 cells was carried out as described previously (*33*). For *Aedes aegypti* Aag2 cells, 5×10^5 cells were plated in each well of a 48-well plate. Transfection was carried out according to the manufacturer's instructions with 2 μl cellfectin (Invitrogen) and 320 ng of DNA (100 ng of firefly luciferase reporter plasmid, 100 ng of each expression vector for AaMet and AaFISC, and 20 ng of internal control plasmid pRL-CMV (Promega)). JH-III, methoprene and pyriproxyfen were purchased from Sigma Aldrich and dissolved in dimethyl sulfoxide (DMSO). Hormones were added to the culture medium at 24 hours after transfection. Cells were harvested at 48 hours after transfection and reporter activity was measured using Dual Luciferase Assay kit (Promega).

Measuring the dissociation constants for the binding of AaMet and AaFISC to JHRE–The apparent equilibrium dissociation constants (K_d) for the binding of Met and FISC to JHREs were measured as described (*37*). Gel-shift assays were carried out with a fixed amount of purified Met and FISC proteins (0.5 μg each) and increasing amounts of probes. Probes were used at six concentrations, 1 nM, 2.5 nM, 5 nM, 10 nM, 25 nM, and 50 nM. After gel

electrophoresis, the bound and free probe was quantitated with a phosphorimager (Molecular Dynamics). The data were used to calculate the apparent K_d with a Scatchard plot (*38*).

Protein structure modeling and ligand docking–Homology modeling was carried out as described by Pandini et al (*39*). The NMR structures of hypoxia-inducible factor 2α (HIF-2α) and the Aryl hydrocarbon receptor nuclear translocator (ARNT) PAS-B domains were chosen as the homologous templates for homology modeling. Their coordinate files were obtained from the Protein Data Bank (PDB): entries 1P97 for HIF-2α (*40*) and 1X0O for ARNT (*41*). A three-dimensional model of the AaMet PAS-B domain was generated using MODELLER version 9v7 (*42*). Energy minimization was performed to improve overall quality of the generated structures by using the GROMACS 4.0.7 package (*43*). Identification and characterization of surface pockets and internal cavities in the modeled PAS-B were carried out by using CASTp with default parameters (*44*). AutoDockTools (ADT) (*45*) and AutoDock 4 (*46*) were used to set up and perform the docking calculations. Images were prepared with Pymol (DeLano Scientific).

JH-Binding Assays–The ^{3}H-labeled JH III (10-20 Ci/mmol) was from Perkin-Elmer. Dextran-coated charcoal (DCC) assays were performed as described (*22, 23*). Wild-type and mutants of AaMet were synthesized *in vitro* using the TNT T7 Coupled Reticulocyte Lysate System (Promega). Non-specific binding will be determined in a parallel experiment, where TNT products will be incubated with increasing concentrations of [^{3}H] JH-III in the presence of an excess (10 μM) of unlabelled JH-III. The esterase inhibitor 3-octylthio-1,1,1-trifluoro-2-propanone (OTFP) was added to all the binding assays at a final concentration of 1 μM. Dissociation constants (K_d) were determined using the Scatchard method (*38*).

Results

Met and FISC bind to JHRE as a complex–To investigate whether Met and FISC proteins are sufficient for binding to JHRE, we carried out gel-shift assays using purified recombinant *Ae. aegypti* Met and FISC proteins. The bHLH-PAS domain of AaMet (amino acid 1-597) was expressed in *E. coli* as a fusion protein with an N-terminal GST tag. The bHLH-PAS domain of AaFISC (amino acid 1-609) was expressed with an N-terminal 6×His tag (Figure D 1A). After affinity purification, there was only one major protein band corresponding to the 6×His-FISC fusion. For GST-Met fusion, we have tried many different purification procedures and conditions, and still couldn't separate two major proteins with sizes of 93 kD and 60 kD (Figure D 1B). Mass spectrometry analysis showed that the 93-kD polypeptide was the expected GST-Met fusion, while the 60-kD protein was a derivative of GST-Met that lacked the C-terminal portion of the Met PAS domain. The mixture of the 93-kD and 60-kD proteins was used as GST-Met in subsequent DNA binding assays.

A 29-bp DNA fragment from the *AaET* promoter, containing a characterized JHRE (CCACACGCGAAG), was used as a probe in gel-shift assays. The purified GST-Met or 6×His-FISC alone was unable to bind the *AaET* JHRE (Figure D 1C, lanes 2, 3, 5 and 6). When GST-Met and 6×His-FISC together were incubated with the labeled JHRE, a stable DNA-protein complex was detected in the absence or presence of JH (Figure D 1C, lanes 4 and 7). Formation of the complex *in vitro* seemed to be JH-independent. The specificity of the Met-FISC-JHRE binding was demonstrated by competition experiments. The binding was abrogated by addition of unlabeled *AaET* JHRE1 at 50-fold molar excess relative to the probe, but not by 50-fold excess of unlabeled nonspecific competitor (Figure D 1C). To verify that both Met and FISC were present in the observed DNA-protein complex, we performed a super-shift experiment. Addition of either GST antibody (Lane 2) or His antibody (Lane 3) to the DNA binding reactions resulted in formation of a larger DNA-protein complex, while addition of non-specific IgG did not show similar effect (Figure D 1D). The gel-shift experiment thus demonstrated that the purified AaMet and AaFISC proteins bind JHRE as a complex and this *in vitro* binding does not require other mosquito proteins.

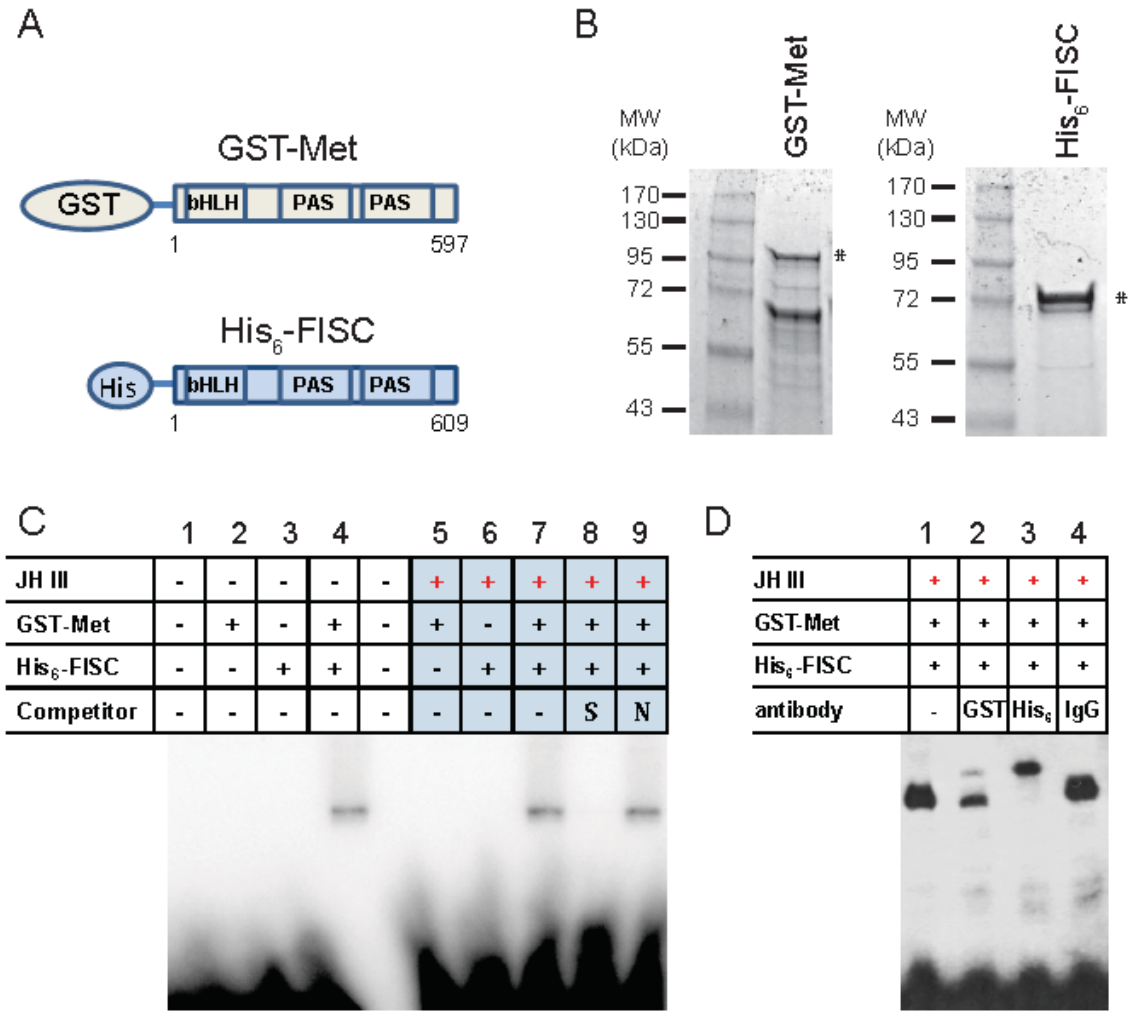

Figure D 1. Met and FISC are sufficient for *in vitro* binding of JHRE. A) Schematic diagram of *E. coli*-expressed N-terminal Met fused with GST tag and FISC with His tag. **B)** Coomassie staining of the purified recombinant Met and FISC. The asterisks (*) indicate protein bands with expected sizes. **C)** Gel-shift assay with the recombinant proteins. Met and FISC, or either protein alone, were incubated with the DNA probe (*AaET* JHRE1) in the presence or absence of 10^{-6} M JH-III for 20 min followed by electrophoresis. For competition, 50-fold molar excess of unlabeled specific (S) or non-specific (N) competitor DNA, was mixed with proteins for 20 min before addition of the probe. **D)** Super-shift assay. Antibodies for the GST tag (GST) or His tag (His) were included in the DNA-binding reactions. Non-specific rabbit immunoglobulin G (IgG) was used in parallel as a control.

The basic regions of both Met and FISC proteins are involved in DNA binding–The basic regions of bHLH proteins are usually involved in DNA binding, with the basic residues (arginine and lysine) often forming direct contacts with the major groove of the DNA (*47*). Seven and five basic residues exist in the basic regions of AaMet and AaFISC, respectively (Figure D 2A and E 2B). These residues are highly conserved among *Ae. aegypti*, *D. melanogaster*, *T. castaneum* and *B. mori*. To test whether the putative DNA binding domains of AaMet and AaFISC were required for their binding to JHRE, AaMet and AaFISC mutants were created by replacing the individual basic residues in the bHLH domains with glutamine, which is structurally similar to arginine and lysine but has no positive charge on its side chain. The mutants were then tested for their abilities to bind JHRE *in vitro* and their abilities to activate JH-inducible promoters in transient transfection assays.

We performed gel-shift assays with the affinity-purified wild-type and mutant proteins of AaMet and AaFISC that were expressed in *E. coli* (Figure D 2C and E 2D). The R122Q, R129Q, R130Q mutations in AaMet completely abolished the binding of Met and FISC to *AaET* JHRE1, while the R119Q, R124Q, K127Q and K132Q mutations in AaMet diminished the binding to a lesser extent (Figure D 2E). In AaFISC, the K117Q, R124Q and R125Q mutations also eliminated the DNA binding of AaMet-AaFISC (Figure D 2F). The results demonstrated that the binding of AaMet-AaFISC to JHRE requires the DNA-binding domains of both proteins, and implied that each partner perhaps binds to half of the *AaET* JHRE1.

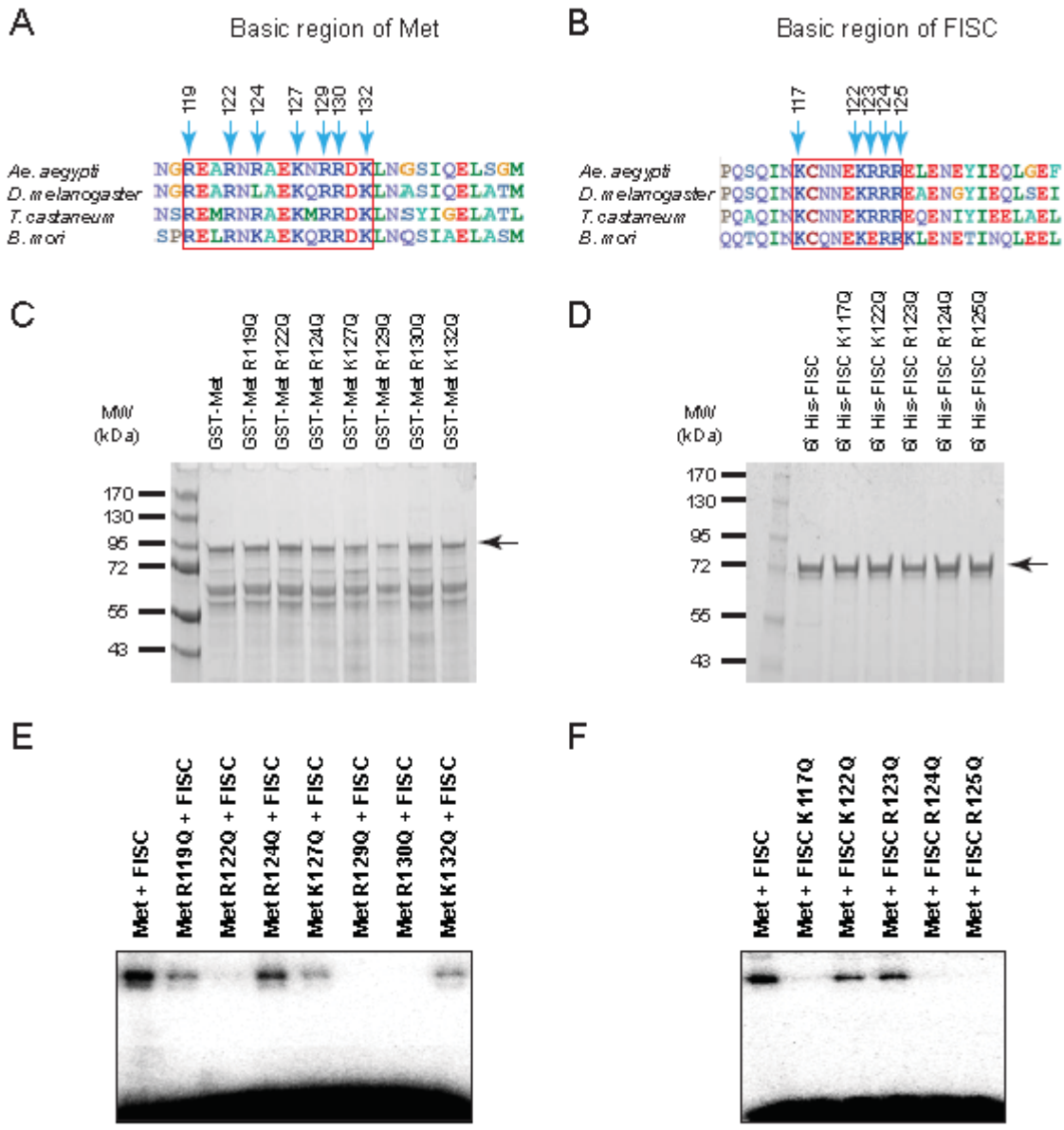

Figure D 2. The basic regions of Met and FISC are both involved in DNA binding. (A and B) Alignments of the first α-helix of the bHLH domain in the orthologs of Met **(A)** and FISC **(B)** from several insect species. The basic regions are highlighted in red rectangles. Numbers indicate positions of the basic residues in *Ae. aegypti* Met and FISC. **(C and D)** Coomassie staining of the partially purified recombinant Met, FISC, and their mutants. The arrows point to the protein bands with expected sizes. **(D and E)** Gel-shift assays with the recombinant Met and FISC that carry mutations in the basic regions. The *AaET* JHRE1 was used as the radiolabeled probe.

For the cell-based reporter assays, expression vectors for the wide-type or mutant AaMet and AaFISC were transfected into *Ae. aegypti* Aag2 cells together with a firefly luciferase reporter driven by four copies of the *AaET* JHRE1. The R122Q, R129Q, and R130Q mutations in AaMet all led to a dramatic decrease in the JH-induced expression of the reporter gene (Figure D 3A). Likewise, K117Q, R124Q, and R125Q mutations in AaFISC also displayed similar negative effect (Figure D 3A). There was a good correlation between the reporter assay and the *in vitro* DNA-binding assay. Mutations in Met and FISC that substantially reduced the JH-induced expression of 4×JHRE1-Luc in the reporter assay, such as Met^{R122Q}, Met^{R129Q}, Met^{R130Q}, $FISC^{K117Q}$, $FISC^{R124Q}$, and $FISC^{R125Q}$, also significantly weakened the binding of AaMet and AaFISC to the *AaET* JHRE1 (Figure D 2E and D 2F). To demonstrate that these mutations affect the DNA binding but not the dimerization or transactivation activity of AaMet and AaFISC, we carried out the reporter assay with some modifications. The wild-type AaMet and its mutants were expressed as fusions to the Gal4 DNA binding domain (GBD) and the firefly luciferase reporter gene was under the control of four copies of the GAL4 binding sites (UAS). In this system, we expected GBD-AaMet and AaFISC to form a heterodimer in the presence of JH and use the GBD domain to bind UAS of the reporter gene. GBD-AaMet and AaFISC indeed activated expression of the UAS-driven reporter gene when JH was added to the culture medium after transfection (Figure D 3B). None of the mutations of the basic residues in either AaMet or AaFISC showed significant negative impact on the JH-induced reporter expression (Figure D 3B), indicating that these basic residues are not essential for dimerization and transactivation activity of AaMet and AaFISC. Therefore, the gel-shift assay and these two reporter assays together suggested that the basic regions of both AaMet and AaFISC are required for binding of the AaMet-AaFISC complex to JHRE.

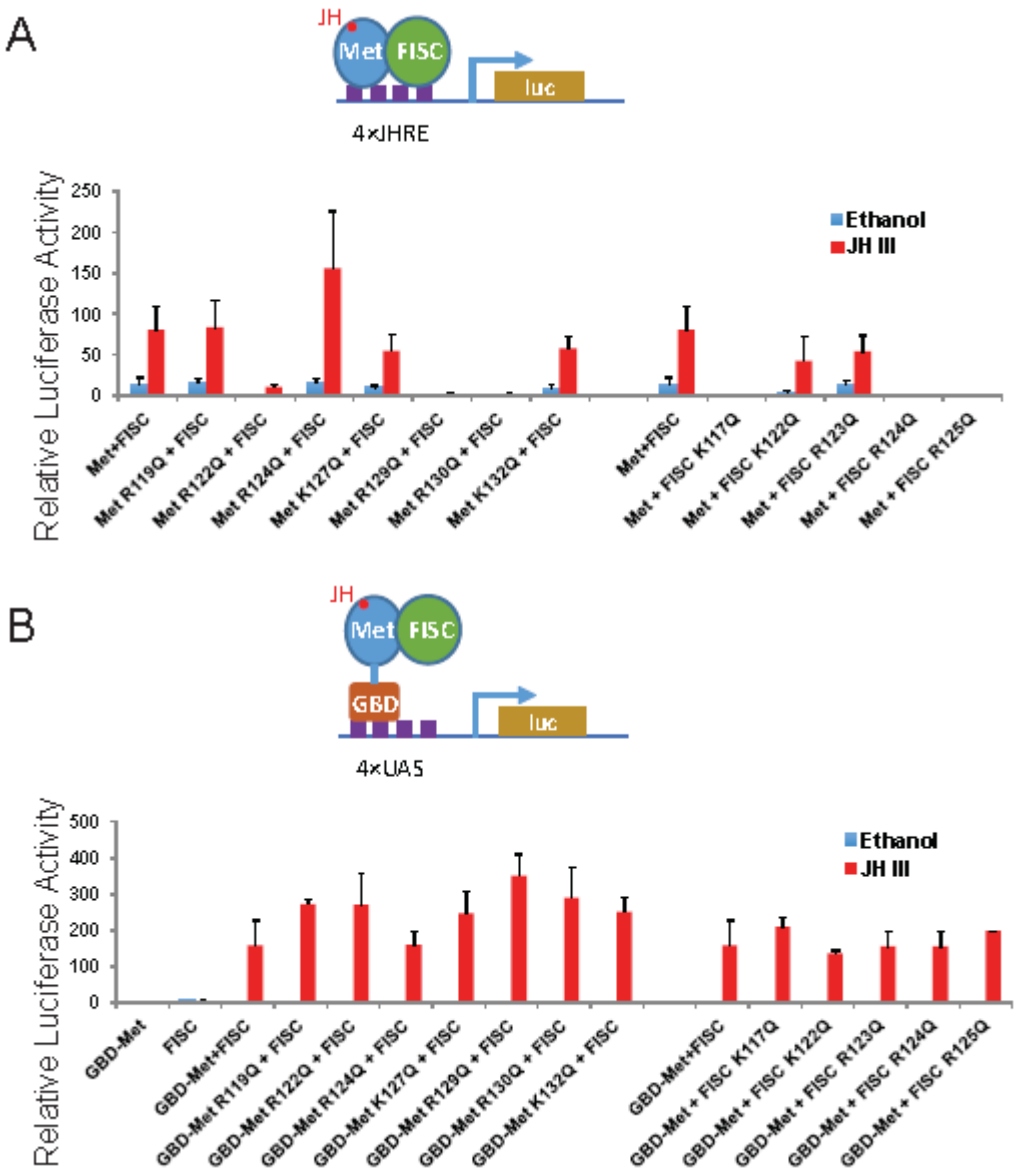

Figure D 3. The mutations in the basic regions primarily affect the DNA-binding properties of Met and FISC. (A) Transfection assay with a JHRE-driven luciferase reporter. Aag2 cells were transfected by the 4×JHRE1-luc reporter construct and expression vectors for the derivatives of Met and FISC. Transfected cells were treated with JH-III or ethanol. **(B)** Transfection assay with a UAS-driven luciferase reporter. Aag2 cells were transfected by the UAS×4-188-cc-Luc reporter construct and expression vectors for the derivatives of Met and FISC. All the Met derivatives were expressed as fusions to the Gal4 DNA-binding domain.

Identification of the consensus DNA sequence bound by the JH receptor complex–To identify the DNA sequence bound with high-affinity by the AaMet and AaFISC complex, we screened a random DNA library using multiple cycles of selection and amplification (*35*). The synthetic 57-nt DNA library used for selection contained a 17-nt random region flanked by PCR priming sequences. The double-stranded DNA was end-labeled with ^{32}P and incubated with JH-III and the purified GST-Met and 6×His-FISC in a gel-shift experiment. After electrophoresis and autoradiography, DNA was retrieved from the shifted band and amplified by PCR to get an enriched DNA pool for a second round of selection. After 10 rounds of selection, the enriched DNA was cloned and analyzed by DNA sequencing. Among the 70 sequences that we obtained, 34 were unique sequences. A consensus motif was identified by the MEME motif discovery algorithm. An E-box like sequence, GCACGTG, existed in 67 out of the total 70 sequences (Figure D 4A). For future reference, the consensus sequence was numbered from -4 to +3 as shown in Figure D 4B. The most abundant sequence, GGCCGCACGTGTCGTTG, was named MFBS1 (Met-FISC binding site 1) and used for further study.

The JHRE1 that we have previously identified in *AaET* shares some homology with the GCACGTG motif. A sequence downstream of the JHRE1 in the 5' regulatory region of *AaET* was found to harbor the exact consensus motif and named AaET_JHRE2. In addition, this motif was also discovered in the JH-inducible promoters of the *kr-h1* genes from *Ae. aegypti, B. mori*, *D. melanogaster* and *T. castaneum* (Figure D 4C). To validate the binding selectivity, gel-shift assay was conducted using the purified recombinant proteins of AaMet and AaFISC. As shown in Figure E 4D, AaMet and AaFISC were able to bind MFBS1 when JH was present. We went on introducing point mutations into the consensus motif and using the MFBS1 derivatives as probes in gel-shift assays. Individual point mutation at any position (-3, -2, -1, +1, +2 and +3) within the sequence CACGTG considerably decreased or abolished the DNA binding of AaMet-AaFISC (Figure D 4D). To examine the role of guanosine at -4 position in the DNA-protein interaction, we carried out a competition experiment. The guanosine at -4 position in MFBS1 was changed into adenine, cytosine or thymine to generate three new MFBS1 derivatives. The ^{32}P-labeled MFBS1 was incubated with the purified AaMet and AaFISC.

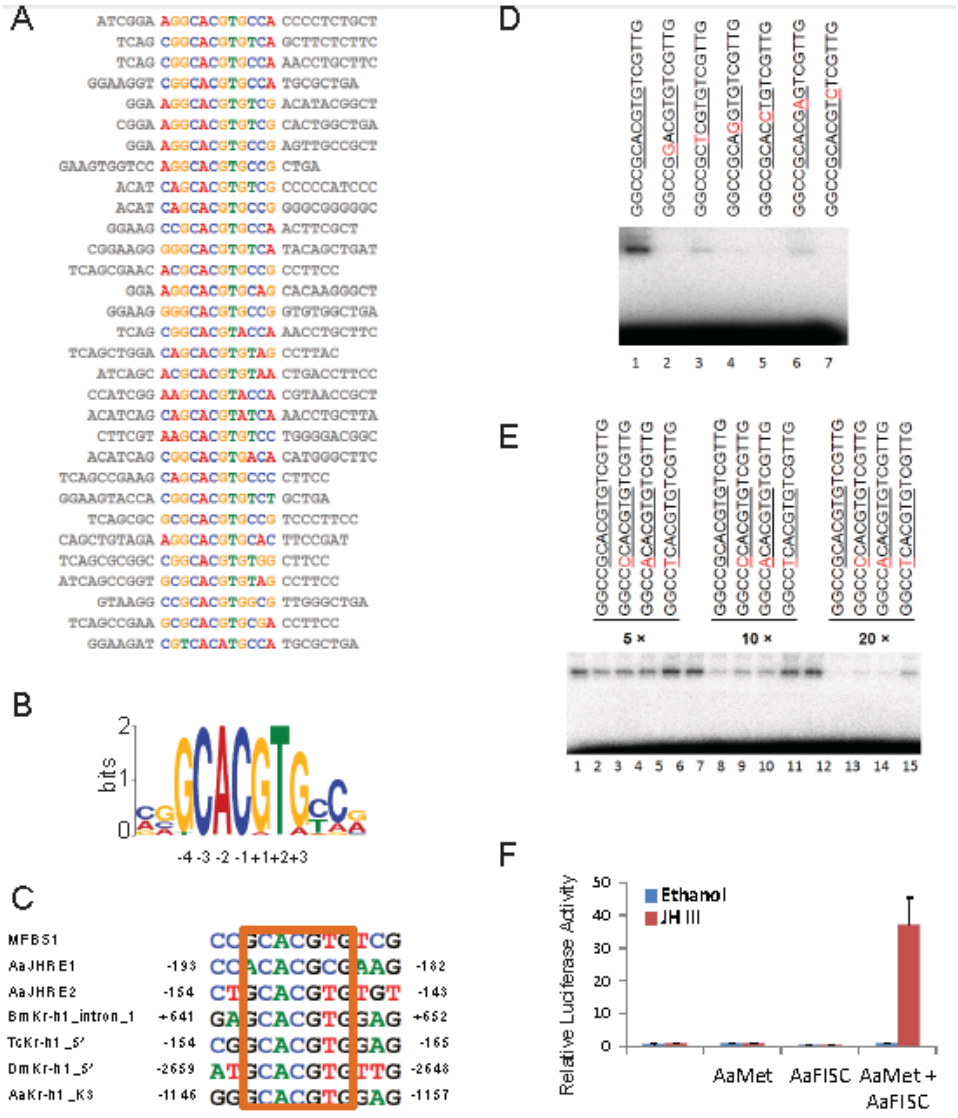

Figure D 4. *In vitro* selection of DNA sequences bound by Met and FISC. (A) 31 unique sequences after iterative cycles of enrichment and amplification were analyzed by the MEME algorithm. **(B)** The top-scoring motif generated by the MEME motif discovery algorithm. The common motif, GCACGTG, was numbered from -4 to +3. **(C)** Some previously identified JHREs contained the exact consensus sequence. The *AaET* JHRE1 was reported by Li et al. The regulatory regions of *Kr-h1* in *B. mori* (*Bm*), *T. castaneum* (*Tc*), *D. melanogaster* (*Dm*) and *Ae. aegypti* (*Aa*) were characterized by Dr. Shinoda's group and Dr. Raikhel's group. **(D)** Validation of the sequence-specific DNA binding. Gel-shift assays were conducted with purified Met and FISC proteins in the presence of 10^{-6} M JH-III. MFBS1 and its mutants were labeled individually and used as probes in the experiment. The consensus sequence was underlined and point mutations in the probe sequences were shown in red. **(E)** Guanosine is preferred at the -4 position in the consensus motif. MFBS1 was labeled as a probe. The indicated oligonucleotides with mutations at the -4 position were used as competitors in the gel-shift assay. The consensus sequence was underlined and point mutations were shown in red. **(F)** The consensus sequence is a functional JHRE. Aag2 cells were transfected with 4×MFBS1-luc and the expression vectors of AaMet and AaFISC. Transfected cells were treated with either 10^{-6} M JH-III or ethanol.

Unlabeled MFBS1 and the three derivatives were added at 5-, 10-, and 20-fold molar excess in the gel-shift assay. The unlabeled MFBS1 was the most effective one among the four competitors to inhibit the binding of AaMet-AaFISC to the labeled MFBS1. The *in vitro* binding assays demonstrated that the GCACGTG motif identified by our selection and amplification approach is a sequence-specific and high affinity binding site of AaMet-AaFISC.

To test whether MFBS1 actually functions as a juvenile hormone response element, we performed a reporter assay in Aag2 cells. A reporter plasmid (4×MFBS1-luc) was constructed such that the firefly luciferase expression was controlled by four copies of a shorter version of MFBS1, GCCGCACGTGTC. The reporter gene was readily induced by JH-III when AaMet and AaFISC were over-expressed in Aag2 cells, indicating that the consensus sequence functions as a JHRE that mediates the transcriptional activation by the AaMet-AaFISC complex (Figure D 4E).

Met and FISC bind the consensus sequence with high affinity–To compare the binding affinity of AaMet-AaFISC to MFBS1 and several naturally occurring E-box-like JHREs, we measured the apparent equilibrium dissociation constants (K_d). A series of gel-shift assays were performed with fixed amounts of the AaMet and AaFISC proteins and increasing amounts of DNA probes. The free and bound DNA probes were quantitated and the data were used to calculate the apparent K_d as shown in Figure D 5.

The AaMet-AaFISC complex showed the strongest binding to MFBS1, with a K_d of 5.8 nM (Figure D 5C). *AaET*_JHRE2 and the JHRE identified in the 5' regulatory region of *BmKr-h1* (BmKr-h1_5'_JHRE*)* each contain a GCACGTG motif with a *palindromic E-box*. Their binding affinities for the JH receptor complex were slightly weaker, with K_d values of 13.4 nM and 13.8 nM for *AaET*_JHRE2 and *BmKr-h1*_5'-JHRE, respectively. *AaET*_JHRE1 harbors a non-canonical E-box (CACGCG) and exhibited a much weaker affinity for the protein complex. Its K_d value was about 17-fold higher than that of MFBS1 (Figure D 5C).

To investigate whether the AaMet-AaFISC complex prefers the DNA sequence of CACGTG over the asymmetric CACGCG, we introduced point mutations to the abovementioned probes at the +2 position. The mutant probes were incubated with AaMet and AaFISC in gel-shift assays and their dissociation constants were measured in the presence of JH-III. When the *CACGTG* hexameric *core* was changed into CACGAG in MFBS1, the mutant probe

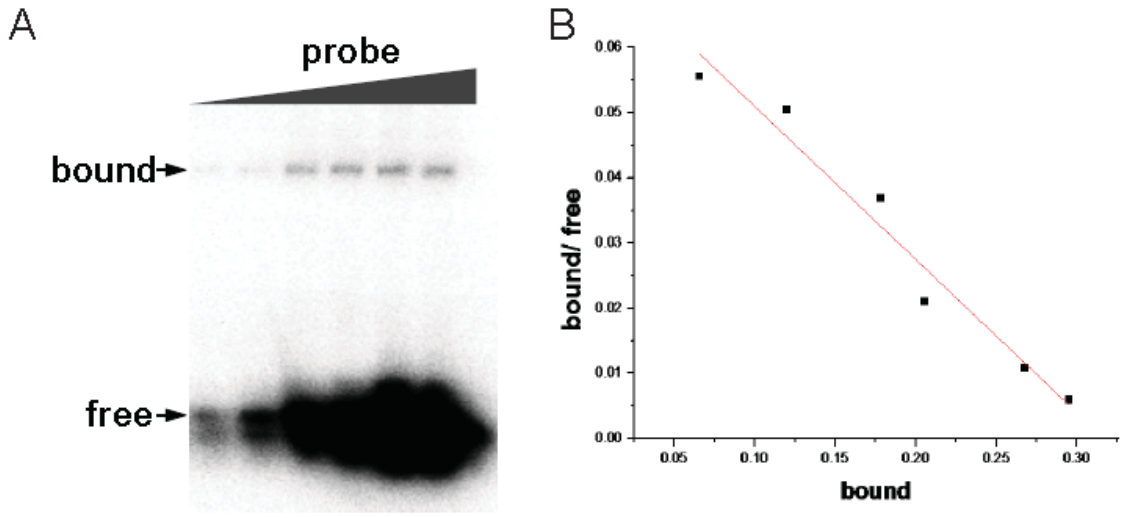

C

Probes	Sequences	K_d (nM)
MFBS1	GCCGCACGTGTCGTTGG	5.8 ± 2.0
MFBS1 T+2C	GCCGCACGCGTCGTTGG	ND
BmKr-h1_5'_JHRE	GCCTCCACGTGTCGAAC	13.8 ± 4.0
BmKr-h1_5'_JHRE T+2C	GCCTCCACGCGTCGAAC	ND
AaET_JHRE1	ATCCCACACGCGAAGAC	103.0 ± 28.0
AaET_JHRE1 C+2T	ATCCCACACGTGAAGAC	162.0 ± 24.0
AaET_JHRE2	ATCTGCACGTGTGTACC	13.4 ± 6.3
AaET_JHRE2 T+2C	ATCTGCACGCGTGTACC	ND

Figure D 5. The binding affinities of AaMet-AaFISC to various JHREs. (A) Dissociation constant (K_d) of the binding of Met/FISC to MFBS1 was measured by gel-shift assays. Details were described in the Experimental Procedures. **(B)** Scatchard analysis of the AaMet-AaFISC binding to MFBS1. The K_d value was calculated from the slope of the regression line. **(C)** Comparison of the binding affinities of AaMet-AaFISC to various JHREs. K_d was shown as mean±SD, n=3. ND, *Kd* was not determined because binding could not be detected.

completely lost the ability to bind the AaMet-AaFISC complex (Figure D 5C). Similarly, the thymine-to-cytosine mutation in *BmKr-h1*_5'_JHRE or *AaET*_JHRE2 all abolished the binding of AaMet-AaFISC. *AaET*_JHRE1 shares less homology with MFBS1 both in the hexameric core and in the flanking sequence. When the CACGAG hexamer in *AaET*_JHRE1 was replaced with CACGTG, the binding affinity nevertheless remained relatively weak (Figure D 5C). The results suggested that AaMet and AaFISC generally prefer a JHRE with a CACGTG core sequence, and the flanking sequences also contribute significantly to the overall binding affinity of the JHRE.

Generation of the JH-binding mutants of AaMet–The gel-shift experiment indicated that the purified AaMet and AaFISC bound to *AaET*_JHRE1 in a JH-independent manner. To examine whether the JH-binding capacity was compromised in the purified AaMet, we measured its dissociation constant. The recombinant AaMet purified from bacteria exhibited a K_d of 160.8 ± 27.6 nM for JH-III, while the AaMet protein produced in rabbit reticulocyte lysates showed a much stronger JH-III binding (K_d=4.4 ± 1.9 nM) (Figure D 6). A high background DNA-binding activity toward the *AaET* JHRE1 was observed in the unprogrammed reticulocyte lysate (data not shown), forbidding us from using this system to produce AaMet for gel-shift assays. To further investigate the effect of hormone binding on the DNA binding of AaMet-AaFISC, we employed homology modeling techniques to generate a three-dimensional model of the AaMet PAS-B domain and constructed several JH-binding mutants of AaMet based on the structural information.

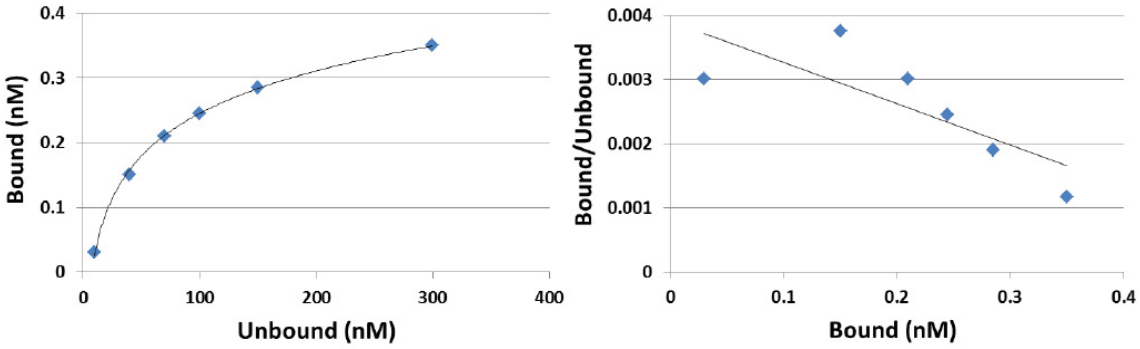

Figure D 6. Binding of [^{3}H] to recombinant AaMet. The binding of JH-III to purified AaMet was analyzed by the DCC assay method. Non-specific binding was determined by including a 100-fold excess of unlabelled JH-III in the binding reactions. Saturation curve and Scatchard plot analysis of specific binding data are shown. Data are an average of three independent experiments. The calculated K_d is 160.8 ± 27.6 nM.

Analysis of structural cavities indicated the presence of a buried cavity between the central anti-parallel β-sheet and several α-helices flanking the sheet (Figure D 7A). Side chains of 22 amino acids, which are conserved in the PAS-B domains of AaMet, DmMet and TcMet, were predicted to be internal to the cavity. Molecular docking calculations were performed to simulate JH-III binding to the PAS-B domain of AaMet. The following 14 residues were predicted to be in close contact with the docked JH-III: Thr403, His405, Ile411, Ile418, Val429, Phe437, Val446, Leu450, Ser463, Tyr465, Leu467, Thr479, Cys497 and Asn499.

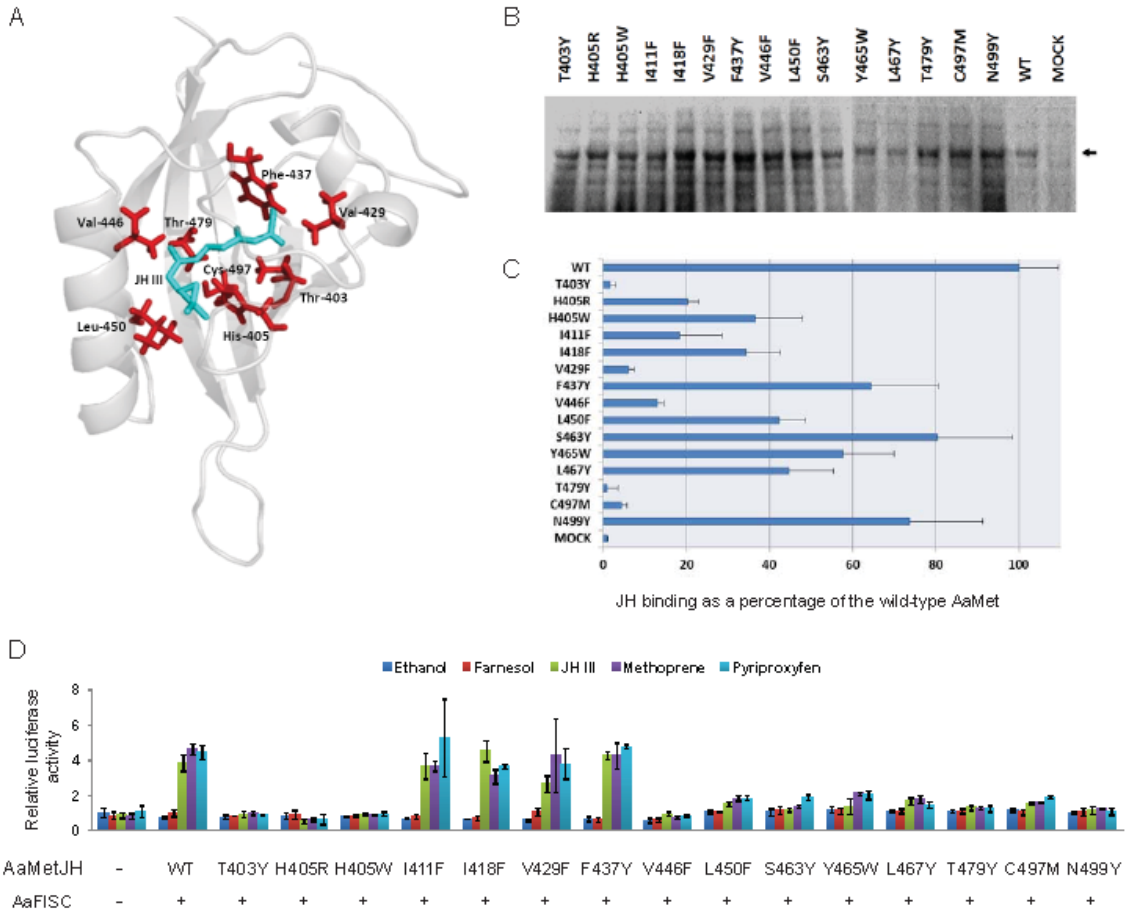

Figure D 7. Generation of JH-binding mutants of AaMet by structure-guided mutagenesis. (A) Cartoon representation of the modeled AaMet PAS-B domain with the lowest-energy docked conformation of JH-III (shown as green sticks). **(B)** Synthesis of the bHLH-PAS domain (aa. 1-597) of AaMet mutants by *in vitro* coupled transcription and translation reactions. The AaMet products were quantitatively measured after western blot analysis with an antibody against AaMet. The arrow indicates the band of the expected size. **(C)** Effect of mutations within the PAS-B domain of AaMet on the binding of [^{3}H]-labeled JH-III. The binding was normalized against the AaMet inputs measured in (B). **(D).** The JH-binding mutants reduce the JH-induced transactivation activity of AaMet-AaFISC. L57 cells were transfected by the 4×JHRE1-luc reporter plasmid and the expression vectors for AaFISC and the indicated AaMet derivatives. Transfected cells were treated with 1 μM of farnesol, JH-III, methoprene or pyriproxyfen. Ethanol was used as control. The mean and standard deviation from triplicate samples were indicated.

To validate this model, we performed site-directed mutagenesis of these selected residues and tested the effects of mutations on juvenile hormone binding. The bHLH-PAS domains of the wild-type and mutant AaMet were synthesized *in vitro* in coupled transcription/translation reactions (Figure D 7B). JH-III binding of AaMet was nearly abolished by the T403Y, V429F, T479Y and C497M mutations. H405R, I411F and V446F each reduced the JH-III binding to 10%-20% of that of the wild-type AaMet (Figure D 7C). The hormone binding assay

demonstrated that these residues are crucial for the high affinity binding of AaMet to JH-III. The corresponding residues in *T. castaneum* have been reported earlier to be essential for the binding of TcMet to JH-III (*22*), suggesting that the structure signatures of the JH-binding pocket in Met are highly conserved in insects. Furthermore, we carried out a transient transfection experiment to examine how these mutations in AaMet affect the transactivation activity of the AaMet-AaFISC complex. The JH-induced expression of the 4×JHRE1-luc reporter gene was substantially dampened when the 7 AaMet mutants (T403Y, H405R, I411F, V429F, V446F, T479Y and C497M) displaying considerably reduced JH-binding affinities were used in lieu of the wild-type AaMet, consistent with the predicted roles of those residues in binding of JH (Figure D 7D).

JH-independent interaction between the bacterially expressed Met and FISC– The T403Y, V429F and T479Y AaMet mutants were then compared with the wild-type AaMet in the *in vitro* DNA-binding assay. In the presence of JH and 6×His-AaFISC, the dissociate constants of the three mutants for MFBS1 were 6.1-7.3 nM, similar to 5.8 nM for the wild-type AaMet (Table D 1). In the absence of JH, the wild-type AaMet and AaFISC showed a slightly higher K_d value of 13.8 nM. Therefore, the results confirmed that the purified recombinant AaMet and AaFISC bound to JHRE in a JH-independent manner.

Table D. 1. Dissociation constants of AaMet-AaFISC for MFBS1.

Proteins	K_d (nM)	*p* -value (comparing to AaMet with JH)
AaMet + AaFISC +Ethanol	13.8±1.2	p<0.01
AaMet + AaFISC + JH-III	5.8±2.0	
AaMetT403Y + AaFISC + JH-III	6.1±2.0	p>0.05
AaMetV446F + AaFISC + JH-III	7.3±3.2	p>0.05
AaMetT479Y + AaFISC + JH-III	8.1±3.1	p>0.05

The purified AaMet derivatives were also compared for their protein-protein interaction with AaFISC. The GST-AaMet fusion protein was readily co-immunoprecipitated with 6×His-AaFISC regardless of the presence of JH. In this *in vitro* protein binding assay, the T403Y,

V429F or T479Y mutations showed no negative effect on the AaMet-AaFISC interaction when JH was present (Figure D 8A). In parallel, we performed a two-hybrid assay to test the protein interaction in Aag2 cells. AaMet was fused to the GAL4 DNA binding domain and AaFISC was expressed as a fusion to the activation domain of GAL4. Activation of the UAS reporter gene by the two fusion proteins was enhanced more than 20-fold when the transfected cells were treated with JH. The T403Y, V429F or T479Y mutations all eliminated the JH-induced expression of the reporter gene, confirming that the AaMet-AaFISC interaction in Aag2 cells is JH-dependent (Figure D 8B). The reason behind the divergent effects of JH on the Met-FISC interaction is presently unclear but may reflect an inhibitory mechanism in insect cells that prevents the un-liganded Met from binding to FISC.

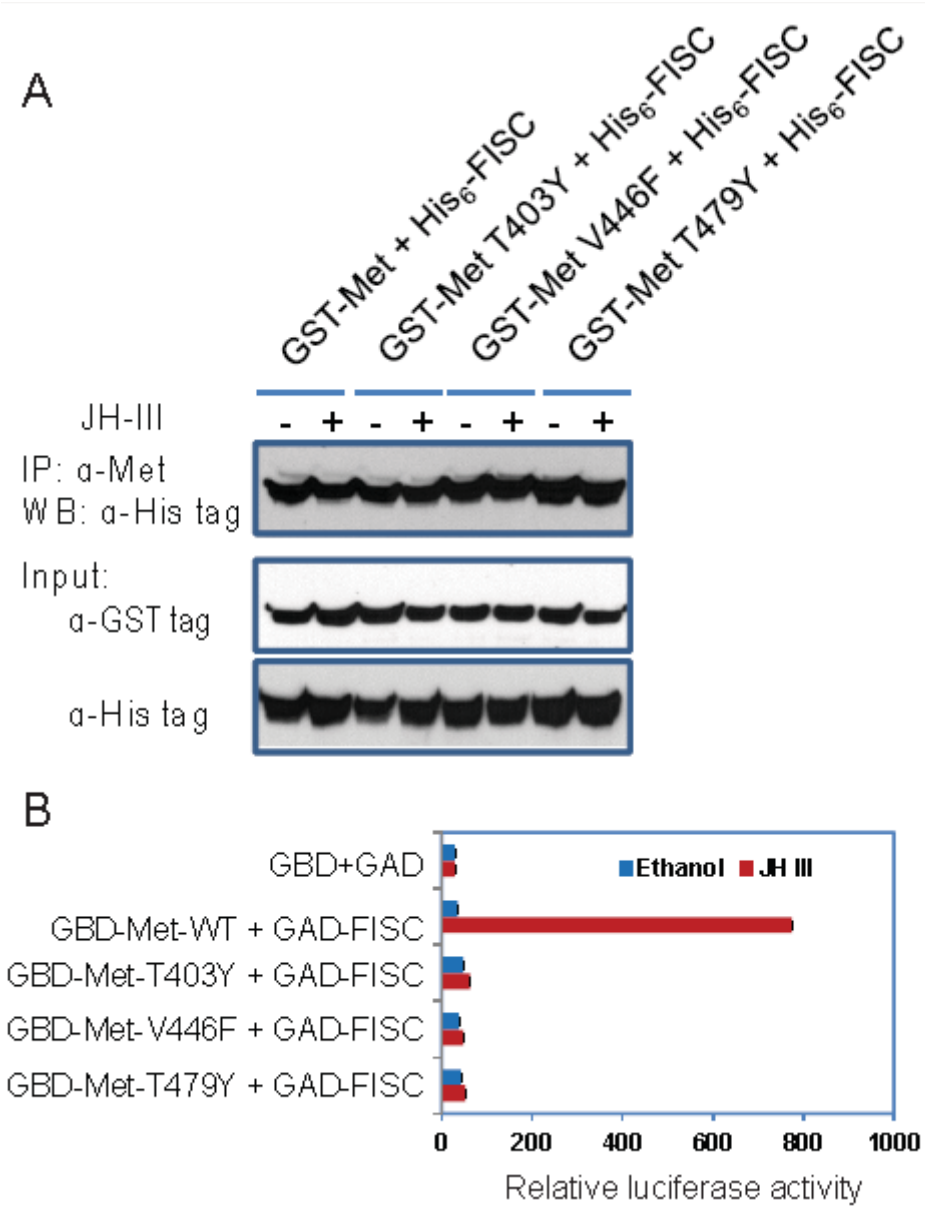

Figure D 8. The *in vitro* AaMet-AaFISC dimerization does not require JH. (A) Co-immunoprecipitation of the purified GST-Met and His_6-FISC. The proteins purified from bacteria were incubated in the absence or presence of 10 μM JH-III. The protein complexes were precipitated with the antibody against AaMet. The pellets were detected with the antibody against the His tag. **(B)** Interaction of AaMet and AaFISC in Aag2 cells. The cultured cells were transfected with the UAS×4-188-cc-Luc reporter plasmid and expression vectors for the indicated GAD and GBD fusion proteins. The transfected cells were treated with 1 μM JH-III or ethanol.

Discussion

Met and FISC are sufficient to bind JHRE–Our previous study of *Ae. aegypti* has shown that Met and FISC form a complex through their N-terminal bHLH-PAS domains in a JH-dependent manner (*27*). The protein complex occupies the promoter of *AaET* only when this gene is transcriptionally up-regulated by JH, indicating that these two transcriptional factors directly act on the JH-responsive promoter. The conclusion is supported by subsequent studies that both Met and FISC (or its ortholog) are required for expression of another JH-responsive gene, *kr-h1*, in *Ae. aegypti*, *T. castaneum*, and *B. mori* (*29, 31, 32*). Met and FISC regulate gene expression via recognition of short DNA sequences (JHRE) in the target genes (*27, 29*).

FISC and its *Drosophila* ortholog TAI have been previously characterized as a steroid receptor coactivator (SRC) of the p160 family. They function as a coactivator of the ecdysone receptor (EcR), enhancing gene expression induced by ecdysteroids (*28, 48*). Although possessing a putative DNA-binding domain, SRCs do not bind DNA by themselves. They interact with DNA-binding transcription factors and recruit downstream effectors including histone acetyltransferases and protein methyltransferases (*49*). Therefore, it is widely speculated that FISC acts as a coactivator of Met and that Met binds JHRE either alone or with a protein other than FISC.

To test this hypothesis, we first attempted to use cellular protein extracts or the rabbit reticulocyte lysate system for the *in vitro* binding assays. High levels of background binding were a huge problem because the *AaET* JHRE1 contained an E-box-like sequence which was recognized by many bHLH transcription factors. In this study, we used purified Met and FISC proteins in gel-shift assays to test their DNA binding properties. We demonstrated that Met or FISC alone was unable to bind the probe, but the two proteins together were able and sufficient to bind with specificity to JHRE1. To elucidate the molecular function of FISC in JH signaling, we explored whether the conserved basic helix-loop-helix region in FISC was a functional DNA-binding domain. Mutations in the basic region of FISC led to a dramatic decrease in the binding of Met and FISC to JHRE, consistent with the studies of other bHLH transcription factors showing that the basic regions contact DNA and determine DNA sequence specificity (*50*). Based on these evidence, we conclude that FISC functions as an obligatory DNA-binding partner of Met in mediating gene regulation by JH.

Some bHLH-PAS family proteins can function as either transcription factors or transcription cofactors, depending on the circumstances. The aryl hydrocarbon receptor nuclear translocator protein (ARNT) is such an example. ARNT and the aryl hydrocarbon receptor (AHR) are both bHLH-PAS domain proteins. Upon binding of environmental pollutants such as 2,3,7,8-tetrachlorodibenzo-p-dioxin, the AHR translocates from the cytoplasm to the nucleus where it binds ARNT and activates expression of proteins involved in xenobiotic metabolism. Both AHR and ARNT bind directly to the xenobiotic responsive element, T(C/T)GCGTG. AHR binds the 5'-T(C/T)GC half sites with high affinity while ARNT prefers the GTG-3' half-sites (*35*). ARNT can also serve as a coactivator of estrogen receptor (ER)-dependent transcription. It has been shown that ARNT is recruited to ER target gene promoters via physical interaction with ER (*51*). Here we show that FISC also function in similar way. Aside from it being a transcription coactivator of the ecdysone receptor, FISC is the DNA-binding partner of the JH receptor and directly bind to the JH-inducible promoters. Many studies have shown that JH can exert its functions by modulating the ecdysteroid signaling pathway (*52, 53*). It is intriguing to study whether FISC is involved in the crosstalk between the two pathways and whether EcR and Met compete for the binding of FISC when both JH and 20E are present.

DNA sequence heterogeneity in JHREs–The DNA binding sites of Met and FISC have been characterized so far in only a few JH-responsive genes (*27, 29*). It was not clear whether the E box-like sequence we have identified represents a typical binding site of Met-FISC. *In vitro* unbiased selection from random DNA library indicates that E-box-like sequences are indeed the DNA-binding sites of Met and FISC. Although the optimal binding site contains a core sequence of CACGTG, the flanking sequences also contribute significantly to the DNA binding affinity. For example, the *AaET* JHRE1 and JHRE2 differ in core sequence and flanking sequence (Figure D 5). After making a point mutation at the +2 position, the JHRE1 mutant (*AaET*_JHRE1_C+2T) and JHRE2 both harbor identical core sequence (CACGTG). However, the binding affinities of Met-FISC for the JHRE1 mutant and JHRE2 are 162.0 nM and 13.4 nM, respectively.

The upstream regulatory regions of *Kr-h1* from several insect species each contain several copies of the E-box-like sequences. Because of the DNA sequence heterogeneity, individual JHRE may exhibit a distinct binding affinity to the orthologs of Met and FISC. Copy

number and spacing of the multiple JHREs may define the expression pattern of the JH target genes, activating the regulated genes precisely at the proper concentration of JH.

DNA binding of the homodimer and heterodimer of Met–Met can form homodimer in the absence of JH (*54*). Met monomer or homodimer was not able to bind to AaET JHRE1 in our gel shift assy (Figure D 1). We have tried to use the amplification and selection protocol to identify the binding sites of Met. The experiment was performed without adding JH to the incubation. We were not able to enrich any specific DNA sequence after 10 rounds selection. The result does not support the hypothesis that the Met homodimer can bind to specific target genes.

Met is able to form a heterodimer in a JH-dependent manner with another bHLH-PAS protein, Cycle (CYC). The Met-CYC complex binds a JHRE found in *AaKr-h1* and the binding does not require FISC (*32*). In the newly emerged adult female mosquitoes, the expression of *AaKr-h1* is under the control of Met, FISC and CYC. It is not clear whether the three proteins are associated with the same promoter at the same time and whether the two heterodimers select the same JHREs or different JHREs. A 9-mer Met-binding motif, CACG(C)/TG(A)/G(T)/AG, has been identified from the mosquito genes that are regulated by Met in previtellogenic stage (*17*). It is similar to the GCACGTG motif that we report in this study. Identity of the transcriptional factors that recognize this Met-binding motif needs to be further investigated.

Effect of JH binding on the Met-FISC interaction–In the absence of ligands, the aryl hydrocarbon receptor is associated with several chaperone proteins, including the 90-kDa heat shock protein (Hsp90). The chaperones keeps AHR folded into a correct ligand-binding conformation (*55, 56*). The Hsp90 homolog in bacteria is unable to interact with AHR, and the bacterially expressed AHR fails to bind its specific ligand (*55*). In our experiment, the bacterially expressed AaMet displayed a much weaker binding affinity to JH-III, compared with the AaMet produced in rabbit reticulocyte lysates. We are currently examine whether Hsp90 and other chaperones are associated with AaMet *in vivo* and play a role in the JH binding of AaMet.

In our *in vitro* assays, the final concentration of JH-III was 10 μM, well above the equilibrium dissociation constant between the purified AaMet and JH-III (K_d=4.4 ± 1.9 nM). The protein interaction between AaMet and AaFISC and the binding of the complex to JHRE were all JH-independent. This conclusion was substantiated by further comparing the wild-type

AaMet and the JH-binding-deficient AaMet mutants in the *in vitro* assays. In contrast, two-hybrid assay indicated the AaMet-AaFISC interaction in *Drosophila* cells was considerably enhanced when JH was present. Similar to our results with the juvenile hormone receptor, ligand binding also does not affect the DNA-binding properties of AHR and ARNT that are expressed and purified from *E. coli* (*57*). In the absence of a ligand, AHR is associated with hsp90, co-chaperone protein p23, and several other proteins *in vivo*. These proteins serve to stabilize the ligand-binding conformation of the receptor and inhibit constitutive dimerization with ARNT. After ligand binding, these proteins are released from AHR (*58*). Studies have demonstrated that *in vitro* dissociation of the chaperone proteins from the unliganded AHR results in formation of the AHR-ARNT heterodimer in the absence of ligand (*56, 59*). The interaction between Met and hsp90 has been reported in *Helicoverpa armigera* (*60*). It will remain to be tested whether hsp90 has a similar inhibitory function in preventing the constitutive interaction between Met and FISC.

Acknowledgment

We thank Dr. Bruce Hammock for 3-octylthio-1,1,1-trifluoro-2-propanone (OTFP), Dr. Richard Helm for his help with mass spectrometry, and Ms. Anne Brown for helping with molecular docking. JDW is supported by a National Science Foundation S-STEM grant (DUE-0850198). This work was supported by NIH grant R01 AI099250 to JZ.

References

1. S. B. Tobe SS, in *Advances in Insect Physiology*. (1985), pp. 305-432.
2. T. Flatt, M. P. Tu, M. Tatar, Hormonal pleiotropy and the juvenile hormone regulation of Drosophila development and life history. *Bioessays* **27**, 999-1010 (2005).
3. C. M. Goodman WG, in *Insect Endocrinology* G. LI, Ed. (Elsevier, Amsterdam, The Netherlands, 2012), pp. 310-365.
4. H. F. Nijhout, *Insect Hormones*. (Princeton University Press, 1994).
5. L. M. Riddiford, K. Hiruma, X. F. Zhou, C. A. Nelson, Insights into the molecular basis of the hormonal control of molting and metamorphosis from Manduca sexta and Drosophila melanogaster. *Insect Biochemistry and Molecular Biology* **33**, 1327-1338 (2003).
6. A. Raikhel, Brown, MR, Belles, X, in *Comprehensive Molecular Insect Science,* L. Gilbert, Iatrou, K, Gill, SS, Ed. (Elsevier, Pergamon, 2005), vol. Vol.3: Endocrinology, pp. 433-491.
7. R. W. Gwadz, A. Spielman, Corpus allatum control of ovarian development in Aedes aegypti *J.Insect Physiol* **19**, 1441-1448 (1973).
8. H. H. Hagedorn, The endocrinology of the adult female mosquito. *Adv.Dis.Vect.Res.* **10**, 109-148 (1994).
9. F. Dittmann, P. H. Kogan, H. H. Hagedorn, Ploidy levels and DNA-synthesis in fat body cells of the adult mosquito, Aedes aegypti - the role of juvenile hormone. *Archives of Insect Biochemistry and Physiology* **12**, 133-143 (1989).
10. T. R. Flanagan, H. H. Hagedorn, Vitellogenin synthesis in mosquito - role of juvenile hormone in development of responsiveness to ecdysone. *Physiological Entomology* **2**, 173-178 (1977).
11. A. S. Raikhel, A. O. Lea, Juvenile hormone controls previtellogenic proliferation of ribosomal RNA in the mosquito fat body. *General and Comparative Endocrinology* **77**, 423-434 (1990).
12. M. Ma, J. Z. Zhang, H. Gong, R. Gwadz, Permissive action of juvenile-hormone on vitellogenin production by the mosquito, Aedes aegypti. . *Journal of Insect Physiology* **34**, 593-596 (1988).

13. J. Zhu, L. Chen, A. S. Raikhel, Posttranscriptional control of the competence factor betaFTZ-F1 by juvenile hormone in the mosquito Aedes aegypti. *Proc Natl Acad Sci U S A* **100**, 13338-13343 (2003).
14. T. G. Wilson, J. Fabian, A Drosophila melanogaster mutant resistant to a chemical analog of juvenile hormone. *Dev Biol* **118**, 190-201 (1986).
15. L. Shemshedini, M. Lanoue, T. G. Wilson, Evidence for a juvenile hormone receptor involved in protein synthesis in Drosophila melanogaster. *J Biol Chem* **265**, 1913-1918 (1990).
16. B. Konopova, M. Jindra, Juvenile hormone resistance gene Methoprene-tolerant controls entry into metamorphosis in the beetle Tribolium castaneum. *Proc Natl Acad Sci U S A* **104**, 10488-10493 (2007).
17. Z. Zou, T. T. Saha, S. Roy, S. W. Shin, T. W. Backman, T. Girke, K. P. White, A. S. Raikhel, Juvenile hormone and its receptor, methoprene-tolerant, control the dynamics of mosquito gene expression. *Proc Natl Acad Sci U S A* **110**, E2173-2181 (2013).
18. M. Ashok, C. Turner, T. G. Wilson, Insect juvenile hormone resistance gene homology with the bHLH-PAS family of transcriptional regulators. *Proc.Natl.Acad.Sci.U.S.A* **95**, 2761-2766 (1998).
19. J. K. Sailsbery, W. R. Atchley, R. A. Dean, Phylogenetic analysis and classification of the fungal bHLH domain. *Molecular Biology and Evolution* **29**, 1301-1318 (2012).
20. R. J. Kewley, M. L. Whitelaw, A. Chapman-Smith, The mammalian basic helix-loop-helix/PAS family of transcriptional regulators. *The International Journal of Biochemistry & Cell Biology* **36**, 189-204 (2004).
21. A. Moglich, R. A. Ayers, K. Moffat, Structure and signaling mechanism of Per-ARNT-Sim domains. *Structure* **17**, 1282-1294 (2009).
22. J. P. Charles, T. Iwema, V. C. Epa, K. Takaki, J. Rynes, M. Jindra, Ligand-binding properties of a juvenile hormone receptor, Methoprene-tolerant. *Proc Natl Acad Sci U S A* **108**, 21128-21133 (2011).
23. K. Miura, M. Oda, S. Makita, Y. Chinzei, Characterization of the Drosophila Methoprene -tolerant gene product. Juvenile hormone binding and ligand-dependent gene regulation. *FEBS J* **272**, 1169-1178 (2005).

24. C. Minakuchi, X. Zhou, L. M. Riddiford, Kruppel homolog 1 (Kr-h1) mediates juvenile hormone action during metamorphosis of Drosophila melanogaster. *Mech Dev* **125**, 91-105 (2008).
25. R. Parthasarathy, A. Tan, S. R. Palli, bHLH-PAS family transcription factor methoprene-tolerant plays a key role in JH action in preventing the premature development of adult structures during larval-pupal metamorphosis. *Mech Dev* **125**, 601-616 (2008).
26. J. Zhu, J. M. Busche, X. Zhang, Identification of juvenile hormone target genes in the adult female mosquitoes. *Insect Biochem Mol Biol* **40**, 23-29 (2010).
27. M. Li, E. A. Mead, J. Zhu, Heterodimer of two bHLH-PAS proteins mediates juvenile hormone-induced gene expression. *Proc Natl Acad Sci U S A* **108**, 638-643 (2011).
28. J. Zhu, L. Chen, G. Sun, A. S. Raikhel, The competence factor beta Ftz-F1 potentiates ecdysone receptor activity via recruiting a p160/SRC coactivator. *Molecular and cellular biology* **26**, 9402-9412 (2006).
29. T. Kayukawa, C. Minakuchi, T. Namiki, T. Togawa, M. Yoshiyama, M. Kamimura, K. Mita, S. Imanishi, M. Kiuchi, Y. Ishikawa, T. Shinoda, Transcriptional regulation of juvenile hormone-mediated induction of Kruppel homolog 1, a repressor of insect metamorphosis. *Proc Natl Acad Sci U S A* **109**, 11729-11734 (2012).
30. T. Kayukawa, K. Tateishi, T. Shinoda, Establishment of a versatile cell line for juvenile hormone signaling analysis in Tribolium castaneum. *Scientific reports* **3**, 1570 (2013).
31. Z. Zhang, J. Xu, Z. Sheng, Y. Sui, S. R. Palli, Steroid receptor co-activator is required for juvenile hormone signal transduction through a bHLH-PAS transcription factor, methoprene tolerant. *J Biol Chem* **286**, 8437-8447 (2011).
32. S. W. Shin, Z. Zou, T. T. Saha, A. S. Raikhel, bHLH-PAS heterodimer of methoprene-tolerant and Cycle mediates circadian expression of juvenile hormone-induced mosquito genes. *Proc Natl Acad Sci U S A* **109**, 16576-16581 (2012).
33. X. Hu, L. Cherbas, P. Cherbas, Transcription activation by the ecdysone receptor (EcR/USP): identification of activation functions. *Mol Endocrinol* **17**, 716-731 (2003).
34. P. Carrigan, P. Ballar, S. Tuzmen, in *Disease Gene Identification,* J. K. DiStefano, Ed. (Humana Press, 2011), vol. 700, chap. 8, pp. 107-124.
35. H. I. Swanson, W. K. Chan, C. A. Bradfield, DNA binding specificities and pairing rules of the Ah receptor, ARNT, and SIM proteins. *J Biol Chem* **270**, 26292-26302 (1995).

36. T. L. Bailey, M. Boden, F. A. Buske, M. Frith, C. E. Grant, L. Clementi, J. Ren, W. W. Li, W. S. Noble, MEME Suite: tools for motif discovery and searching. *Nucleic Acids Research* **37**, W202-W208 (2009).
37. J. L. Riechmann, M. Wang, E. M. Meyerowitz, DNA-binding properties of *Arabidopsis* MADS domain homeotic proteins APETALA1, APETALA3, PISTILLATA and AGAMOUS. *Nucleic Acids Research* **24**, 3134-3141 (1996).
38. G. Scatchard, The attractions of proteins for small molecules and ions. *Annals of the New York Academy of Sciences* **51**, 660-672 (1949).
39. A. Pandini, A. A. Soshilov, Y. Song, J. Zhao, L. Bonati, M. S. Denison, Detection of the TCDD binding-fingerprint within the Ah receptor ligand binding domain by structurally driven mutagenesis and functional analysis. *Biochemistry* **48**, 5972-5983 (2009).
40. P. J. Erbel, P. B. Card, O. Karakuzu, R. K. Bruick, K. H. Gardner, Structural basis for PAS domain heterodimerization in the basic helix--loop--helix-PAS transcription factor hypoxia-inducible factor. *Proc Natl Acad Sci U S A* **100**, 15504-15509 (2003).
41. P. B. Card, P. J. Erbel, K. H. Gardner, Structural basis of ARNT PAS-B dimerization: use of a common beta-sheet interface for hetero- and homodimerization. *J Mol Biol* **353**, 664-677 (2005).
42. A. Sali, T. L. Blundell, Comparative protein modelling by satisfaction of spatial restraints. *Journal of molecular biology* **234**, 779-815 (1993).
43. D. Van Der Spoel, E. Lindahl, B. Hess, G. Groenhof, A. E. Mark, H. J. Berendsen, GROMACS: fast, flexible, and free. *J Comput Chem* **26**, 1701-1718 (2005).
44. J. Dundas, Z. Ouyang, J. Tseng, A. Binkowski, Y. Turpaz, J. Liang, CASTp: computed atlas of surface topography of proteins with structural and topographical mapping of functionally annotated residues. *Nucleic Acids Res* **34**, W116-118 (2006).
45. M. F. Sanner, Python: a programming language for software integration and development. *Journal of molecular graphics & modelling* **17**, 57-61 (1999).
46. R. Huey, G. M. Morris, A. J. Olson, D. S. Goodsell, A semiempirical free energy force field with charge-based desolvation. *Journal of computational chemistry* **28**, 1145-1152 (2007).
47. S. Jones, An overview of the basic helix-loop-helix proteins. *Genome Biol* **5**, 226 (2004).

48. J. Bai, Y. Uehara, D. J. Montell, Regulation of invasive cell behavior by taiman, a Drosophila protein related to AIB1, a steroid receptor coactivator amplified in breast cancer. *Cell* **103**, 1047-1058 (2000).

49. J. Xu, R. C. Wu, B. W. O'Malley, Normal and cancer-related functions of the p160 steroid receptor co-activator (SRC) family. *Nature reviews. Cancer* **9**, 615-630 (2009).

50. T. Shimizu, A. Toumoto, K. Ihara, M. Shimizu, Y. Kyogoku, N. Ogawa, Y. Oshima, T. Hakoshima, Crystal structure of PHO4 bHLH domain-DNA complex: flanking base recognition. *EMBO J* **16**, 4689-4697 (1997).

51. S. Brunnberg, K. Pettersson, E. Rydin, J. Matthews, A. Hanberg, I. Pongratz, The basic helix-loop-helix-PAS protein ARNT functions as a potent coactivator of estrogen receptor-dependent transcription. *Proc Natl Acad Sci U S A* **100**, 6517-6522 (2003).

52. E. B. Dubrovsky, Hormonal cross talk in insect development. *Trends in endocrinology and metabolism: TEM* **16**, 6-11 (2005).

53. M. Jindra, S. R. Palli, L. M. Riddiford, The juvenile hormone signaling pathway in insect development. *Annu Rev Entomol* **58**, 181-204 (2013).

54. J. Godlewski, S. Wang, T. G. Wilson, Interaction of bHLH-PAS proteins involved in juvenile hormone reception in *Drosophila*. *Biochem Biophys Res Commun* **342**, 1305-1311 (2006).

55. P. Coumailleau, L. Poellinger, J. A. Gustafsson, M. L. Whitelaw, Definition of a minimal domain of the dioxin receptor that is associated with Hsp90 and maintains wild type ligand binding affinity and specificity. *J Biol Chem* **270**, 25291-25300 (1995).

56. I. Pongratz, G. G. Mason, L. Poellinger, Dual roles of the 90-kDa heat shock protein hsp90 in modulating functional activities of the dioxin receptor. Evidence that the dioxin receptor functionally belongs to a subclass of nuclear receptors which require hsp90 both for ligand binding activity and repression of intrinsic DNA binding activity. *J Biol Chem* **267**, 13728-13734 (1992).

57. Y. Kikuchi, S. Ohsawa, J. Mimura, M. Ema, C. Takasaki, K. Sogawa, Y. Fujii-Kuriyama, Heterodimers of bHLH-PAS protein fragments derived from AhR, AhRR, and Arnt prepared by co-expression in Escherichia coli: characterization of their DNA binding activity and preparation of a DNA complex. *J Biochem* **134**, 83-90 (2003).

58. T. V. Beischlag, J. Luis Morales, B. D. Hollingshead, G. H. Perdew, The aryl hydrocarbon receptor complex and the control of gene expression. *Critical reviews in eukaryotic gene expression* **18**, 207-250 (2008).

59. A. Kazlauskas, L. Poellinger, I. Pongratz, Evidence that the co-chaperone p23 regulates ligand responsiveness of the dioxin (Aryl hydrocarbon) receptor. *J Biol Chem* **274**, 13519-13524 (1999).

60. W. Liu, F. X. Zhang, M. J. Cai, W. L. Zhao, X. R. Li, J. X. Wang, X. F. Zhao, The hormone-dependent function of Hsp90 in the crosstalk between 20-hydroxyecdysone and juvenile hormone signaling pathways in insects is determined by differential phosphorylation and protein interactions. *Biochim Biophys Acta* **1830**, 5184-5192 (2013).